



# **An Active Unit Protection Scheme for Islanded Microgrids with Inverter-Interfaced Distributed Generation**

Md Asif Uddin Khan

A thesis submitted for the degree of Doctor of Philosophy to  
the Department of Electronic and Electrical Engineering  
University of Strathclyde  
Glasgow, United Kingdom

May 31, 2022

---

This thesis is the result of the author's original research. It has been composed by the author and has not been previously submitted for examination which has led to the award of a degree.

The copyright of this thesis belongs to the author under the terms of the United Kingdom Copyright Acts as qualified by University of Strathclyde Regulation 3.50. Due acknowledgement must always be made of the use of any material contained in, or derived from, this thesis.

Signed:

Date:

---

## Abstract

This thesis presents a solution to overcome challenges associated with the protection of microgrids that operate in islanded mode, and that are dominated by inverter-interfaced distributed generators (IIDGs). The solution is based around a unit protection scheme that does not require dedicated communications between the protection relays to coordinate and identify the faulted section in the microgrid. The research is justified through a detailed investigation and quantification of the issues and challenges associated with stability, control and protection of microgrids, along with a critical study and literature review of several control and protection schemes for microgrids with IIDGs, which shows the gaps in and shortcomings of other work which the solution outlined in this thesis addresses.

The design and operation of the proposed scheme is demonstrated, for a wide range of fault scenarios. A detailed model of a microgrid with a range of IIDGs (utilising a range of different controllers and control strategies to ensure the generic applicability of the solution) is implemented and extensive simulations conducted for an extensive range of conditions, using both Simulink and Hardware-in-the-Loop (HiL) simulation through real-time digital simulator (RTDS) and OPAL-RT. The behaviour of the microgrid systems under various scenarios is modelled, simulated and demonstrated, and this is used to both verify the problems and challenges that will exist in the near and longer-term future, as well as demonstrating and quantifying the capabilities of the developed protection solution. It is shown that the protection system is capable of correctly dealing with faults at all locations in the system, can successfully detect any fault within 100 ms of fault

---

inception, and is coordinated properly for all types of balanced and unbalanced faults, including operating correctly in backup modes where the failure of an element of the overall protection system is presumed. Furthermore, the protection scheme is shown to operate successfully for faults with a fault impedance of up to  $60 \Omega$  (in addition to any impedance to the fault) for three-phase to earth faults and  $20 \Omega$  for single-phase to earth faults. Moreover, it has been demonstrated and validated through simulation results that location of the IIDGs in the network does not have any adverse impact on the operation of the protection solution.

The thesis concludes with an overview of future work, which, in summary, should focus on the practical implementation of the solution as a prototype and validating its operation in a realistic microgrid model using actual inverter hardware to verify proposer operation and injection of harmonics for a variety of different fault situations.

---

## Acknowledgements

I would like to express my deepest gratitude to my supervisor, Professor Campbell Booth for his guidance on this thesis, showing me the path of conducting successful research and above all for always being there as a mentor. His suggestions drove me towards better ways of thinking, his positive thinking and his impressive technical knowledge have been a source of inspiration and motivation. I sincerely appreciate his continuous encouragement and without him this work would not have been completed.

I would like to offer my sincere thanks to Dr Adam Dyško and Dr Qiteng Hong for sharing their vast knowledge on the subject materials, and providing guidance to complete this research. I would also like to extend thanks to all my colleagues in the Advanced Electrical Systems group at University of Strathclyde, who have been really kind and helpful during this time, in particular Dr Rafael Peña-Alzola, Dr Dimitrios Tzelepis, Dr Agistí Egea-Álvarez, Madalitso Chikumbanje and Di Liu helped me a lot with their technical knowledge and support.

I am grateful to my beloved wife, Rumana for her love and support during the course of this degree, and also to my new born child, Aakif, who keep me awake for nights after nights providing distractions and encouragement to complete the degree. Finally, I would like to thank my parents, Md Mohi Uddin Khan and Khodeja Akter, to whom I will always be in debt for their sacrifices, and my siblings, Sharif, Asma and Helal, for their moral support. I dedicate this thesis to my Family.

---

## Abbreviations and Symbols

AC	Alternating Current
BESS	Battery Energy Storage System
BGR	Backward Group Relay
CB	Circuit Breaker
CC	Converter Controller
CCGT	Combined Cycle Gas Turbine
CT	Current Transformer
DC	Direct Current
DER	Distribution Energy Resource
DEMS	Decentralised Energy Management Systems
DFT	Discrete Fourier Transformation
DG	Distributed Generator
DNO	Distribution Network Operator
DWT	Discrete Wavelet Transformation
EU	European Union
EI	Extremely Inverse
FCL	Fault Current Limiter
FGR	Forward Group Relay
FFT	Fast Fourier Transformation
FRT	Fault Ride Through
GAST	Gas Turbine Governor for Synchronous Generator

---

GB	Great Britain
GFR	Grid Forming Inverter Control
GFL	Grid Following Inverter Control
GTAO	Giga-Transceiver Analogue Output
GTAI	Giga-Transceiver Analogue Input
GTDI	Giga-Transceiver Digital Input
HIF	High Impedance Fault
HiL	Hardware-in-the-Loop
HVDC	High Voltage Direct Current
IED	Intelligent Electronic Device
IDMT	Inverse Definite Minimum Time
IGBT	Insulated Gate Bipolar Thyristor
IIDG	Inverter-Interfaced Distributed Generator
LC	Load Controller
LOM	Loss of Mains
LV	Low Voltage
MCC	Microgrid Central Controller
MM	Melting Margin
MV	Medium Voltage
NG	National Grid
NGET	National Grid Electricity Transmission
OC	Overcurrent
OCGT	Open Cycle Gas Turbine

---

OCR	Overcurrent Relay
OT	Operating Time
PCC	Point of Common Coupling
PI	Proportional-Integral
PLL	Phase-Locked-Loop
POI	Point of Interconnection
PQ	Real and Reactive Power
PS	Plug Setting
PT	Potential Transformer
PSM	Plug Setting Multiplier
PV	Photovoltaic
PWM	Pulse Width Modulator
RoCoF	Rate of Change of Frequency
RTDS	Real-Time Digital Simulator
RMU	Ring Main Unit
SC	Synchronous Condenser
SCL	Short Circuit Level
SG	Synchronous Generator
SI	Standard Inverse
SLD	Single Line Diagram
SO	System Operator
SSE	Scottish and Southern Electricity
SP	Scottish Power

---

TC	Total Clearing
THD	Total Harmonic Distortion
TMS	Time Multiple Setting
TO	Transmission Owner
UK	United Kingdom
USA	United States of America
VI	Very Inverse
VT	Voltage Transformer
V/F	Voltage and Frequency
VSM	Virtual Synchronous Machine

# Contents

<b>Abstract</b>	<b>ii</b>
<b>Acknowledgements</b>	<b>iv</b>
<b>Abbreviations and Symbols</b>	<b>v</b>
<b>List of Figures</b>	<b>xii</b>
<b>List of Tables</b>	<b>xiv</b>
<b>1 Introduction</b>	<b>1</b>
1.1 Motivation and Objectives of Research . . . . .	1
1.2 Research Contributions . . . . .	7
1.3 Publications . . . . .	8
1.4 Overview of the Thesis . . . . .	10
References . . . . .	12
<b>2 The Evolution of Electrical Power Systems</b>	<b>15</b>
2.1 Power System Structure and Evolution . . . . .	16
2.2 Generation . . . . .	20
2.3 Transmission Network . . . . .	23
2.4 Distribution Network . . . . .	25
2.5 Integration of Distributed Generation . . . . .	28
2.6 Introduction to Microgrids . . . . .	30
2.6.1 Modes of Operation . . . . .	31
2.6.2 Advantages and Disadvantages of Microgrids . . . . .	34
2.7 Overview of Protection Schemes . . . . .	37
2.7.1 Differential Protection . . . . .	41
2.7.2 Distance Protection . . . . .	42
2.7.3 Overcurrent Protection . . . . .	45
2.7.4 Loss of Mains Protection . . . . .	48
2.8 Summary . . . . .	50
References . . . . .	50
<b>3 Literature Review: Microgrid Protection Challenges and Solutions</b>	<b>60</b>
3.1 Protection Issues due to Integration of Distributed Generation . . . . .	61

3.1.1	Sympathetic Tripping . . . . .	62
3.1.2	Blinding of Protection Relays . . . . .	65
3.1.3	Coordination Issues with Backup Protection . . . . .	66
3.1.4	Nuisance Tripping of Undervoltage Protection . . . . .	68
3.1.5	Out of Phase Reclose Issue . . . . .	69
3.1.6	Recloser and Fuse Coordination . . . . .	70
3.1.7	High Impedance Faults . . . . .	71
3.2	Critical Literature Review of Proposed Protection Solutions . . . . .	72
3.2.1	Adaptive Protection Scheme . . . . .	73
3.2.2	New Protection Algorithm . . . . .	78
3.2.3	Managing Fault Contribution from DGs . . . . .	91
3.3	Summary . . . . .	93
	References . . . . .	95
<b>4</b>	<b>Power Electronics Inverter Control in Microgrids and Analysis of their Dynamic Behaviour</b>	<b>103</b>
4.1	Classification of Inverter Controllers . . . . .	103
4.1.1	Grid-forming Inverter Control (GFR) . . . . .	106
4.1.2	Grid-following Inverter Control (GFL) . . . . .	113
4.2	Dynamic Behaviour Comparison between IIDG and Synchronous Machines . . . . .	117
4.2.1	Simulation Setup . . . . .	118
4.2.2	Studies of Short Circuit Faults . . . . .	119
4.2.3	Fault Ride Through (FRT) . . . . .	126
4.2.4	Voltage Steps . . . . .	128
4.3	Summary . . . . .	132
	References . . . . .	133
<b>5</b>	<b>Demonstration of Practical Challenges Associated with Overcurrent Protection and Proposed Protection Scheme</b>	<b>139</b>
5.1	Performance Analysis of Overcurrent Protection . . . . .	140
5.1.1	Simulation Model of Micorgrid and Overcurrent Relays . . . . .	140
5.1.2	Simulation Results with Demonstration of OC Relays Performance Under Different Scenarios . . . . .	142
5.2	Fundamental Principle of Operation of the Proposed Scheme . . . . .	149
5.3	IIDG Control Strategies . . . . .	150
5.4	Fault Detection Method by IIDG . . . . .	153
5.5	IIDG Injection of Harmonic Components . . . . .	154
5.6	Detection and Identification of Faulted Line Section by Relays . . . . .	155
5.7	Relay Coordination . . . . .	158
5.8	Protection Operation Example and Practical Consideration . . . . .	159
5.9	Summary . . . . .	162
	References . . . . .	163

<b>6</b>	<b>Demonstration and Validation of the Developed Protection Scheme and Analyses of Results</b>	<b>165</b>
6.1	Simulation based Performance Demonstration and Validation of the Proposed Scheme . . . . .	166
6.1.1	Overview of the Microgrid Model . . . . .	166
6.1.2	Selection of Harmonics . . . . .	168
6.1.3	Relay Settings . . . . .	168
6.1.4	Balanced Faults . . . . .	170
6.1.5	Unbalanced Faults . . . . .	176
6.1.6	High Impedance Faults (HIFs) . . . . .	177
6.1.7	Different Line Length/Impedance . . . . .	179
6.1.8	Different Combination of IIDG Locations . . . . .	179
6.1.9	Combination of IIDGs and Synchronus Generator (SG) . . . . .	180
6.2	Real Time Hardware-in-the-Loop (HiL) based Performance Demonstration and Validation of the Protection Scheme . . . . .	181
6.2.1	Overview of the Test Configuration . . . . .	181
6.2.2	Test Results for Three-Phase Balance Faults . . . . .	182
	References . . . . .	185
<b>7</b>	<b>Conclusions and Future Work</b>	<b>186</b>
7.1	Conclusions . . . . .	186
7.1.1	Analysis of the Dynamic Behaviours of IIDGs . . . . .	187
7.1.2	Protection Scheme . . . . .	187
7.2	Future Research Work . . . . .	189
	References . . . . .	190
<b>A</b>	<b>Relay Setting Calculation</b>	<b>191</b>
A.1	Calculation of Load Current . . . . .	192
A.2	Calculation of Fault Levels and Currents at Different Buses . . . . .	193
A.3	Relay Settings . . . . .	194
<b>B</b>	<b>SG and IIDG Parameters for Chapter 6</b>	<b>196</b>
B.1	Parameters for IIDGs . . . . .	196
B.2	Parameters for Synchronous Generator . . . . .	197
B.3	Parameters for Transformers . . . . .	198

# List of Figures

1.1	Timeline of challenges resulting from decreasing system inertia. . . . .	4
2.1	A typical electrical power system adapted from [7]. . . . .	18
2.2	Single line diagram of a typical power system. . . . .	19
2.3	Electricity energy consumption around the world between 1974 and 2018 [15]. . . . .	21
2.4	Electricity production by different types of generation units in 2020 at UK [22]. . . . .	24
2.5	UK transmission network owners by regions [23]. . . . .	26
2.6	Map of GB with DNOs and their operating regions as of September 2021 [31]. . . . .	27
2.7	Difference between traditional and future power system with the connection of DGs [32]. . . . .	29
2.8	A typical schematics of microgrid [44] . . . . .	32
2.9	Main components of power system protection. . . . .	39
2.10	Unit protection scheme. . . . .	40
2.11	Non-unit protection scheme. . . . .	40
2.12	One-relay differential protection scheme. . . . .	41
2.13	Double-relay differential protection scheme. . . . .	42
2.14	Distance protection relay's zones. . . . .	44
2.15	Boundary for each zone with Mho distance relay. . . . .	44
2.16	Protection with overcurrent relays. . . . .	47
2.17	Standard inverse IDMT characteristics of overcurrent relays shown in Figure 2.16. . . . .	47
2.18	Example of islanding . . . . .	48
3.1	An example of radial distribution network with multiple DG units contributing to a fault. . . . .	64
3.2	Example of protection blinding. . . . .	66
3.3	Instantaneous protection characteristic showing with and without DG fault current contribution [12]. . . . .	67
3.4	Coordination between fuse and recloser [18]. . . . .	70
3.5	Zonal division of distribution network according to [28]. . . . .	74
3.6	Three-layer architecture of the adaptive protection scheme suggested in [22]. . . . .	75
3.7	Flowchart of the adaptive scheme suggested in [25]. . . . .	77
3.8	Block diagram of the protection scheme proposed in [47]. . . . .	82

3.9	Proposed scheme in [48]. . . . .	83
3.10	Phase jump calculation in [36]. . . . .	84
3.11	Implementation of proposed differential scheme in [36]. . . . .	84
3.12	Fault detection algorithm proposed in [49]. . . . .	85
3.13	Proposed relay diagram in [50]. . . . .	86
3.14	Proposed algorithm in [51]. . . . .	88
4.1	Simplified diagram of a GFR. . . . .	104
4.2	Simplified diagram of a GFL. . . . .	105
4.3	Simplified diagram of a grid-supporting controller (a) when behaves like a GFR (b) when behaves like a GFL. . . . .	106
4.4	Basic control structure of a GFR. . . . .	107
4.5	Block diagram of different voltage formations, (a) general grid forming; (b) droop control; (c) inertia emulation with droop control; and (d) virtual impedance with inertia emulation and droop control. . . . .	109
4.6	Block diagram of the voltage control loop of a GFR. . . . .	111
4.7	Block diagram of the current control loop of a GFR. . . . .	113
4.8	Basic control structure of a GFL. . . . .	114
4.9	Block diagram of the PLL in a GFL. . . . .	115
4.10	Block diagram of the outer control of a GFL. . . . .	116
4.11	Simulation setup for dynamic behaviour study of IIDG and synchronous machines. . . . .	118
4.12	Schematic of the simulation model of SG and SC. . . . .	120
4.13	Grid voltage and current from all generation units during a three-phase fault. . . . .	122
4.14	Grid voltage and current from all generation units during a single-phase fault. . . . .	123
4.15	Grid voltage and current from all generation units during a phase to phase fault. . . . .	125
4.16	Simulation results for FRT. . . . .	127
4.17	Grid voltage, total and reactive power supplied by all generation units during voltage step to 0.3 pu simulation. . . . .	130
4.18	Grid voltage, total and reactive power supplied by all generation units during voltage step to 0.5 pu simulation. . . . .	131
4.19	Grid voltage, total and reactive power supplied by all generation units during voltage step to 0.85 pu simulation. . . . .	132
5.1	Designed microgrid to test the overcurrent relays. . . . .	141
5.2	IDMT characteristics for all three overcurrent relays used for simulations. . . . .	142
5.3	IDMT characteristic of $R_1$ with the instantaneous property. . . . .	144
5.4	Example of Miscoordination of the relays. . . . .	145
5.5	Miscoordination of relay $R_1$ due to fault $F_2$ with the instantaneous element. . . . .	146
5.6	Characteristics of relay $R_1$ with and without IIDG. . . . .	147

5.7	Microgrid protection challenge due to bidirectional power flow during fault. . . . .	148
5.8	Block Diagram of the Controllers of IIDGs including fault detection and harmonic injection process. . . . .	151
5.9	Fault detection algorithm. . . . .	157
5.10	Generic block diagram of the proposed scheme's relay . . . . .	157
5.11	Single section of a microgrid with two IIDGs. . . . .	159
5.12	Meshed network protection. . . . .	162
6.1	Model of the test microgrid used for demonstration and validation of the developed scheme's operation. . . . .	167
6.2	Harmonic and fundamental current measurements from the IIDGs for a fault, $F_3$ . . . . .	169
6.3	FGRs: fundamental current measurements, injected/measured harmonic output currents and tripping signals for a (non-cleared) three-phase balanced fault at $F_3$ . . . . .	171
6.4	BGRs: fundamental current measurements, injected/measured harmonic output currents and tripping signals for a (non-cleared) three-phase balanced fault at $F_3$ . . . . .	172
6.5	FGRs: fundamental current measurements, injected/measured harmonic output currents and tripping signals for a (non-cleared) three-phase balanced fault at $F_2$ . . . . .	173
6.6	BGRs: fundamental current measurements, injected/measured harmonic output currents and tripping signals for a (non-cleared) three-phase balanced fault at $F_2$ . . . . .	174
6.7	FGRs: fundamental current measurements, injected/measured harmonic output currents and tripping signals for a (non-cleared) three-phase balanced fault at $F_1$ . . . . .	175
6.8	BGRs: fundamental current measurements, injected/measured harmonic output currents and tripping signals for a (non-cleared) three-phase balanced fault at $F_1$ . . . . .	176
6.9	Simulation results for combination of IIDGs and SG. . . . .	180
6.10	HiL Testing Setup in the Laboratory. . . . .	181
6.11	HiL Test Results for a Fault at $F_1$ . . . . .	183
6.12	HiL Test Results for a Fault at $F_2$ . . . . .	184
6.13	HiL Test Results for a Fault at $F_3$ . . . . .	185
A.1	One-line diagram of the microgrid. . . . .	192

# List of Tables

2.1	Different types of power generation technologies [16]. . . . .	22
2.2	Definition of IDMT relay characteristics [61]. . . . .	46
3.1	Summary of the adaptive protection schemes. . . . .	78
3.2	Summary of the new protection algorithm-based schemes. . . . .	89
3.2	Summary of the new protection algorithm-based schemes. . . . .	90
3.2	Summary of the new protection algorithm-based schemes. . . . .	91
3.3	Comparison of the solutions . . . . .	94
4.1	Simulation and generators' parameters. . . . .	119
5.1	Settings of the relays used for the simulations. . . . .	142
5.2	Operating time (OT) of the relays during different faults with variation of grid fault level. . . . .	143
5.3	Operating time of the relays during islanded mode grid-connected operation modes. . . . .	148
6.1	Parameters for the microgrid model. . . . .	167
6.2	Injected harmonic components from IIDGs. . . . .	168
6.3	Relay settings. . . . .	170
6.4	Verification of the proposed solution under different fault simulations. . . . .	178
6.5	Results of Different Combination of IIDG Location With a Three- Phase Fault at $F_3$ . . . . .	179
A.1	Grid parameters . . . . .	191
A.2	Line parameters . . . . .	192
A.3	Load size and CT ratio. . . . .	193
A.4	Overcurrent relay settings . . . . .	195
B.1	Parameters for IIDG units . . . . .	196
B.2	Parameters for SG unit . . . . .	197
B.3	Parameters for transformers . . . . .	198

# Chapter 1

## Introduction

### 1.1 Motivation and Objectives of Research

In order to address recent and emerging environmental issues, modern electrical power systems and ‘Smart Grids’ are incorporating electricity production from renewable energy sources as a replacement for the bulk production of electricity from fossil fuels via large centralised power plants. For example, in the UK, electricity production from coal, oil, gas and nuclear power has decreased, whereas, generation from renewables has increased from 119.5 TWh (36.9%) to 134.6 TWh (43.1%) between 2019 to 2020 [1]. Presuming all hydro and solar generation are small-scale ( $\leq 50$  MW), the total electricity produced by small-scale renewable generation in the UK is 6% - 8% [2] and this is expected to increase significantly in the future due to enhance popularity of rooftop solar [2]. The closure and decommissioning of large centralised electrical power generation plants [3, 4] is causing the traditional configuration of power distribution network to change. There is a growing proliferation of power electronics devices in the network and the majority of renewable power sources are ultimately connected to the grid via some form of power electronics interface, and in this thesis, these will be referred collectively as inverter interfaced distributed generators (IIDGs). Furthermore, the

concept of microgrids has grown in popularity, particularly for developing nations and/or remote areas, and these are claimed to improve the quality, reliability and resilience of the power system network, while also providing an economical solution that improves accessibility and potentially reliability and economic costs of present and future power systems [5]. Thus, considering the economic benefits of the microgrid system, the developing countries around the world have received a better opportunity to improve availability of electricity in remote locations, where providing electrical power through traditional bulk transmission and distribution networks and centralised conventional generation would be very difficult to achieve from a number of technical and economic perspectives.

Microgrids are considered as promising solutions for future power distribution systems to interconnect numerous small-scale renewable (for example, wind, solar and storage) sources, situated relatively close to load centres, and provides the opportunity to operate autonomously without any connection or support from a central main grid. Avoiding catastrophic power outages due to various natural phenomena or cascading system failures is one of the main challenges for modern power systems and [6] provides seven recommendations to reduce the risks of the aforementioned outages or blackouts. Of the seven recommendations, one of them (number 3) states that, “Develop guidance and provide resources for states, territories, cities and localities to design community enclaves” - here, community enclave design approaches suggest implementation of microgrids that contain distributed energy resources (DERs) so that power system infrastructure can be made stronger and more stable. This recommendation can be achieved with the help of the proper design, management and operation of microgrids that combine distributed resources and energy storage, and that can be operated either in grid-connected or islanded mode. Moreover, according to the UK’s commitment towards the Paris agreement regarding climate change, a new target set by the UK is to achieve “net zero” greenhouse gas emission by 2050 [7], which will

present numerous challenges in the future if this objective is to be met. However, the technical analysis from [8, 9] approves the feasibility of this new target and makes a number of recommendations. Installation of a large number of renewable source-based generators is one of them and to integrate, operate and manage those sources microgrids may be considered as one feasible and suitable option – initially perhaps for the more remote locations in the UK, and perhaps over a longer timeframe a reduction of a transmission system for bulk power transfer (perhaps a system may be retained to provide some interconnection for use during emergency scenarios and peak demand) may be considered. Nevertheless, regardless of the future evolution, power systems exhibiting high penetrations of IIDGs, reduced inertia, relatively lower fault levels, bidirectional flow of power (in both healthy and faulted scenarios) and other characteristics that will present challenges to present-day protection solutions, will become more common in the future throughout the world.

All these developments and ambitious objectives have accompanying complications and this applies to microgrid systems. While in traditional power systems, the conventional arrangement using synchronous generators (SGs) provides relatively easy means of control and operation and possess attractive (from a protection perspective) characteristics of providing relatively high short-circuit level (SCL) and system inertia, a microgrid is typically dominated by numerous power electronics interfaced IIDGs and has almost no support from SGs (perhaps except from the grid connection, but even that could be compromised or reduced in future in terms of system “strength”). Even in the case of existing power systems, decommissioning of SGs is already causing overall SCL and inertia to decrease drastically and this is rendering the power system progressively weaker. It is expected that by 2025, in the GB’s electrical power system, inertia will reduce by 40% [10] and over some regions in the GB power network, the minimum SCL can decrease by more than 80% from previous levels [11]. Therefore, the addition

of renewable sources in the network could make the overall power system more vulnerable in terms of risks to control, stability, monitoring and protection [12]. Furthermore, in the case of microgrids, dual operation mode (grid-connected and islanded modes) means that the system could be more complicated to operate, and to protect (with potentially huge variations in fault level and system behaviour between grid-connected and islanded modes). The protection, control, stability and monitoring challenges are deeply correlated with each other and it is imperative to conduct research on all these aspects of the microgrid to ensure fully functional operation and protection of the system, in both operation modes.

The significant reduction in system inertia due to massive integration of converter interfaced renewable generation might cause several challenges. A timeline illustrating the historical high inertia power system transition to present-day and future very low inertia scenarios (along with key challenges in the context of the GB power system due to frequency control) is presented in Figure 1.1.

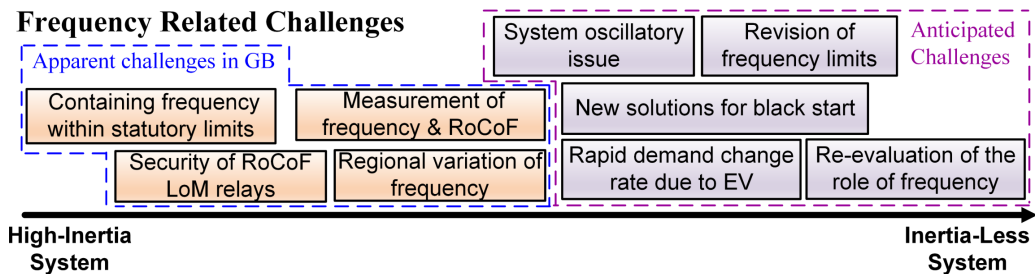


Figure 1.1: Timeline of challenges resulting from decreasing system inertia.

Due to low system inertia levels, microgrids may experience severe and rapid frequency excursions (which could be either increases or decreases in frequency) during an unexpected event that leads to a mismatch between generation and consumption. Furthermore, the behaviour of the converter interfaced generation can be significantly different than the conventional synchronous machine behaviour during frequency events.

The acute reduction in the SCL introduces several protection challenges for the

power system. Additionally, since microgrids can operate in islanded mode, SCL will be further reduced and therefore, detection of faults in the network through conventional protection strategies, typically based on time and current-graded overcurrent protection schemes, can be difficult, and in some cases, impossible, to achieve [13]. Limiting the fault currents supplied by inverter-interfaced generation is a critical requirement, as the semiconductor materials of the inverter cannot withstand large overcurrents. However, limiting fault currents to very low levels might lead to disruption, in terms of the ability to detect fault by the protection systems. Hence, effective limitation of fault current of inverter to a permissible level might be considered as one of the main protection challenges. In most cases the fault current limit of the inverter is assumed to be 1.2 to 2 times the nominal value [14, 15]. Furthermore, bidirectional power flows in the microgrid during both normal and fault condition makes the coordination of protection relays, as well as accurately locating the fault itself (even just to the feeder section that is faulted), very challenging in certain circumstances. In the context of this research, focussing on protection challenges and the identification of an effective solution, several questions must be addressed:

- What are the challenges that arise due to widespread addition of IIDGs without any support of SGs? Are the traditional control and protection schemes capable of tackling those challenges?
- How do microgrid-connected IIDGs behave during faults, when considering the multiple control strategies that may be applied to different inverters and the generally limited/reduced fault current provision from IIDGs compared to synchronous machine sources of similar capacity?
- Is it possible to overcome the protection challenges with the existing protection scheme, i.e. overcurrent protection where islanded microgrids are dominated with IIDGs?

- If overcurrent relays are not fit-for-purpose and need to be replaced, what are the most suitable and economical options to protect islanded microgrids (there is extensive research on this in the literature and this is reviewed later in the thesis)?
- Is it possible to suggest or propose a protection scheme that is integrated with the control strategies of the inverter-based distributed generators?
- Can the proposed protection scheme address all protection issues associated with microgrids? How efficient and practical will the proposed protection scheme be?

The main objective of this research is to analyse the protection issues that arise due to the extensive addition of IIDGs in microgrids and to suggest an effective, communications-free unit protection scheme that is integrated with and utilises the IIDG controllers for islanded microgrids that are presumed to be dominated by IIDGs. In order to achieve this primary objective, it is necessary to meet the following secondary objectives:

- Understanding the state-of-the-art of operation, control and monitoring of microgrids along with protection-related challenges and to conduct a critical review of the protection schemes proposed in the literature (and used in service) for microgrids and active distribution networks.
- Designing a realistic microgrid model with IIDGs equipped with suitable control scheme to emulate and accurately simulate and reproduce practical situations related to fault events.
- Determining efficient, reliable and effective combinations and integrations of control/protection strategies for IIDGs and microgrid to ensure proper and credible operation.

- Validating the developed IIDG control model by comparing the dynamic behaviours between IIDGs and synchronous machines and fully explore the capabilities of the IIDGs in terms of fault current contribution and fault ride through (FRT) capability.
- Investigating the effect of control techniques of the inverter on the protection schemes through characterising the fault behaviour and computing contribution from IIDGs during fault in order to show that traditional schemes are not suitable for all scenarios in systems with high penetrations of IIDGs working in grid-connected and islanded modes.
- Demonstrating the practical application and efficiency of the proposed protection scheme incorporated with a real-time model of the microgrid to enhance the credibility of the scheme design and its operation.
- Demonstrating and cross-validating the performance of the developed protection scheme using two different platforms – the real time digital simulation (RTDS) mentioned in the previous point, and a Matlab Simulink-based model. Both platforms are used to implement a realistic model of the microgrid under a range of fault conditions and include facilities for varying fault type, location and impedance.

## 1.2 Research Contributions

The novelty of this research and principal contribution to knowledge is summarised as follows:

The main contribution is in the form of a novel protection scheme, which is proposed, described and demonstrated and is able to overcome many of the challenges presented and addresses shortcomings that are apparent in many of the proposed solutions in the literature.

The scheme actively modifies the controller of the inverter after fault detection to inject signals into the system that the novel network protection system uses to establish the presence and location of faults. The proposed scheme does not require any communication equipment to detect and locate a fault and therefore, is comparatively cheaper and reliable than other communications-reliant or assisted protection schemes that are reviewed in the literature review section of the thesis. Also, the scheme provides effective solutions to many of the challenges presented in the literature.

There are a number of secondary contributions of this research, including -

- Investigation and demonstration of overcurrent relay performance in a microgrid for a range of fault scenarios - with varying fault levels, locations and resistance.
- Enhancing the understanding of fault behaviours in inverter-dominated systems by reviewing different existing inverter control strategies and analysing the impact of controller behaviour and strategy on fault response. Furthermore, a study is also presented to demonstrate the capability of IIDGs to remain connected and providing reactive power support during fault ride through and voltage step reduction scenarios, and comparing their performance with that of the conventional synchronous machines (SMs).

## 1.3 Publications

### Journal Papers:

1. Q. Hong, **M. A. U. Khan**, C. Henderson, A. E. Alvarez, D. Tzelepis and C. Booth, "Addressing Frequency Control Challenges in Future Low-Inertia

Power Systems: A Great Britain Perspective,” Engineering (2021), Accepted for publication.

2. **M. A. U. Khan**, Q. Hong, D. Liu, A. E. Alvarez, A. Dyško, C. Booth and D. Rostom, “Experimental Assessment and Validation of Inertial Behaviour of Virtual Synchronous Machines,” IET Renewable Power Generation (2022), Reviewed and resubmitted after minor revisions.
3. **M. A. U. Khan**, Q. Hong, A. E. Alvarez A. Dyško and C. Booth, “A Communication-Free Unit Protection Scheme for Islanded Microgrid,” International Journal of Electrical Power and Energy Systems (2022), Accepted for publication.

### Conference Papers:

1. **M. A. U. Khan**, Q. Hong, A. Dyško and C. Booth, “Review and Evaluation of Protection Issues and Solutions for Future Distribution Networks,” 54th International Universities Power Engineering Conference (UPEC), Bucharest, Romania, 2019, pp. 1-6, doi: 10.1109/UPEC.2019.8893528.
2. **M. A. U. Khan**, Q. Hong, A. Dyško, C. Booth, B. Wang and X. Dong, “Evaluation of Fault Characteristic in Microgrids Dominated by Inverter-Based Distributed Generators with Different Control Strategies, IEEE 8th International Conference on Advanced Power System Automation and Protection (APAP), Xi’an, China, 2019, pp. 846-849, doi: 10.1109/APAP-47170.2019.9224706.
3. J. Shi, L. Ji, Q. Hong, Y. Mi, Z. Cao, **A. Khan** and C. Booth, “A New Control Method for Three Phase Inverters Under Unsymmetrical Voltage Sag Conditions,” IEEE 8th International Conference on Advanced Power System

Automation and Protection (APAP), Xi'an, China, 2019, pp. 991-995, doi: 10.1109/APAP47170.2019.9224927.

4. **M. A. U. Khan**, Q. Hong, A. Dyško and C. Booth, “An Active Protection Scheme for Islanded Microgrids,” Conference on Development in Power system Protection (DPSP), Liverpool, UK, 2020.
5. **M. A. U. Khan**, Q. Hong, A. Dyško and C. Booth, “Performance Analysis of the Overcurrent Protection for the Renewable Distributed Generation Dominated Microgrids,” IEEE Region 10 Symposium (TENSymp), Dhaka, Bangladesh, 2020.
6. **M. A. U. Khan**, Q. Hong, D. Liu, A. E. Alvarez, A. Dyško, and C. Booth, D. Rostom, “Comparative Evaluation of Dynamic Performance of a Virtual Synchronous Machine and Synchronous Machines”, IET Conference Proceedings, 2021, p. 366-371, DOI: 10.1049/icp.2021.1362.

## Presentation and Webinars

1. **M. A. U. Khan**, “A Novel Protection Scheme for Active Distribution Network with Inverter Interfaced Distributed Generators,” Presented at the CIGRE UK Next Generation Network (NGN) Young Members Showcase Competition, Manchester, UK, 2020.
2. **M. A. U. Khan**, “An Active Protection Scheme for Islanded Microgrids,” Presented at the CIGRE UK Technical Webinar Series: Optimising Power Transmission and Distribution from Sky to the Sea, Online Webinar, 2020.

## 1.4 Overview of the Thesis

This thesis is organised as follows:

Chapter 2 describes the evolution of microgrids. A brief history of the traditional transmission and distribution power system network incorporating conventional protection schemes is presented and discussed. A review of and trends associated with the connection of renewable generation in the UK network are presented. Furthermore, the basic advantages and disadvantages of microgrids and their operation and management are described.

A critical review of the existing protection-related issues and several solutions that are discussed and proposed in the literature is presented in Chapter 3. Different protection challenges due to large-scale integration of distributed renewable resources are illustrated. The solutions that are suggested from the analysis of a range of different research publications and project are also explained and both positive and negative aspects are summarised and discussed. Finally, a mapping between the existing solutions, their features, their shortcomings, and how the proposed protection schemes developed through this research addresses the shortcomings are illustrated.

Chapter 4 provides detailed descriptions of the design and implementation of inverter-interfaced distributed generation. Different parameters of the inverter control are illustrated, with detailed analysis and descriptions being presented with the aid of figures and equations. Furthermore, to validate the implemented IIDG control models, a comparison between an IIDG and synchronous machines has been presented in respect to different grid situations in addition to balanced and unbalanced fault events.

Chapter 5 demonstrates the performance of a standard and conventional overcurrent protection scheme when presented with the protection of a microgrid and shows its response to challenges under a variety of fault events and scenarios. Furthermore, this chapter also presents the proposed new protection scheme and discusses the details of the implementation and development of the scheme.

Case studies, simulation results and validation of performance for developed

protection solution are presented in Chapter 6. The chapter also presents details of the microgrid model implemented in RTDS and Simulink along with the details of the HiL arrangement and configuration.

Finally, Chapter 7 presents the main conclusions associated with the research. Future work is also presented and discussed in this final chapter of the thesis. The appendices present different parameters of the generation units- Synchronous Generator (SG) and Inverter Interfaced Distributed Generator (IIDG) along with overcurrent protection relay settings that are used for the demonstration and verification purpose.

## References

- [1] Department for Business, Energy & Industrial Strategy, “UK Energy in Brief 2021,” Tech. Rep., 2021. [Online]. Available: [www.gov.uk/government/statistics/uk-energy-in-brief-2021](http://www.gov.uk/government/statistics/uk-energy-in-brief-2021)
- [2] F. Mitschke, “DIGEST of United Kingdom Energy Statistics 2020: Chapter 5 Electricity,” Digest of United Kingdom Energy Statistics (DUKES), London, Tech. Rep., 2019. [Online]. Available: [https://assets.publishing.service.gov.uk/government/uploads/system/uploads/attachment\\_data/file/904805/DUKES\\_2020\\_Chapter\\_5.pdf](https://assets.publishing.service.gov.uk/government/uploads/system/uploads/attachment_data/file/904805/DUKES_2020_Chapter_5.pdf)
- [3] T. Macalister, “Longannet power station closes ending coal power use in Scotland,” in *The Guardian*, 2016. [Online]. Available: <https://www.theguardian.com/environment/2016/mar/24/longannet-powerstation-%0Acloses-coal-power-scotland>
- [4] F. MacDonald, “Goodbye to Cockerzie power station, a cathedral to coal,” 2015. [Online]. Avail-

able: <https://www.theguardian.com/uk-news/scotland-blog/2015/sep/24/goodbye-tocockenzie-%0Apower-station-a-cathedral-to-coal>

- [5] R. H. Lasseter, “MicroGrids,” *2002 IEEE Power Engineering Society Winter Meeting, Vols 1 and 2, Conference Proceedings*, pp. 305–308, 2002.
- [6] The President’s National Infrastructure Advisory Council (NIAC), “Surviving a Catastrophic Power Outage,” United States.” Tech. Rep., 2018. [Online]. Available: [https://www.cisa.gov/sites/default/files/publications/NIACCatastrophicPowerOutageStudy\\_FINAL.pdf](https://www.cisa.gov/sites/default/files/publications/NIACCatastrophicPowerOutageStudy_FINAL.pdf)
- [7] R. Harrabin, “Climate change: UK government to commit to 2050 target.” [Online]. Available: <https://www.bbc.co.uk/news/science-environment-48596775>
- [8] Committee on Climate Change, “Net Zero: Technical Report,” London, United Kingdom, Tech. Rep., 2019. [Online]. Available: <https://www.theccc.org.uk/publication/net-zero-technical-report/>
- [9] —, “Net Zero: The UK’s contribution to stopping global warming,” London, United Kingdom, Tech. Rep., 2019. [Online]. Available: <https://www.theccc.org.uk/wp-content/uploads/2019/05/Net-Zero-The-UKs-contribution-to-stopping-global-warming.pdf>.
- [10] National Grid ESO, “Operating a Low Inertia System,” 2020. [Online]. Available: <https://www.nationalgrideso.com/document/164586/download>
- [11] National Grid, “System Operability Framework 2016,” no. November, 2016. [Online]. Available: <https://www.nationalgrideso.com/sites/eso/files/documents/8589937803-SOF2016-FullInteractiveDocument.pdf>

- [12] N. Hatziargyriou, H. Asano, R. Iravani, and C. Marnay, “Microgrids: An Overview of Ongoing Research, Development, and Demonstration Projects,” no. august, 2007.
- [13] V. Telukunta, S. Member, J. Pradhan, S. Member, A. Agrawal, S. Member, M. Singh, S. Member, and S. G. Srivani, “Protection Challenges Under Bulk Penetration of Renewable Energy Resources in Power Systems: A Review,” *CSEE Journal of Power and Energy Systems*, vol. 3, no. 4, pp. 365–379, 2017.
- [14] IEEE Standards Coordinating Committee, *IEEE Guide for Design, Operation, and Integration of Distributed Resource Island Systems with Electric Power Systems*, 2011, no. July. [Online]. Available: <http://ieeexplore.ieee.org/servlet/opac?punumber=5960749>
- [15] A. C. Zambroni de Souza and M. Castilla, *Microgrids design and implementation*, 2018.

## Chapter 2

# The Evolution of Electrical Power Systems

Typically, microgrids are considered as a complete independent electrical power system of relatively lower capacity than national systems, where multiple generation units and loads are connected close to each other in a small geographical area. Microgrids often have the flexibility to connect with larger power systems (for example, national transmission network or interconnection) or operate independently. It is difficult to give an exact definition of a microgrid since it might vary depending on the geographical size, generation capacity and types of generation. However, in this research, AC microgrids are considered to have a generation capacity of 2 - 5 MW, are dominated by power electronics inverter-interfaced generation and typically located at the remote and rural locations of developing countries with limited access to the grid (predominantly operated in islanded mode). Although microgrids are small in size and capacity, they can provide significant levels of reliability and resilience in an economic manner by ensuring uninterrupted high quality of power to the consumer. Microgrids may become ever more popular in developing nations where renewable energy is the main source of power; for example, a substantial amount of solar panels are installed

in the rural and remote areas of Bangladesh and India, and with large integration of these sources, microgrids will gain popularity, since large interconnected transmission systems were historically required to transfer large amounts of power over long distances from very large individual generators, and this may not be required for future power systems in nations where power is not widely available and/or a transmission system is not yet built. This chapter will illustrate the details of conventional power systems along with an overview of the microgrids, and will describe the evolution of microgrids from traditional electrical power system configurations. Furthermore, the chapter will provide technical details of the traditional protection system that are used in power systems, with details on protection challenges and potential solutions contained in Chapter 3.

## 2.1 Power System Structure and Evolution

In the late nineteenth century, electrical power systems originated with Pearl Street Station in New York, USA. At that time, electricity was produced using DC generators, often referred to as dynamos, and only used to light up the street lamps. The Pearl Street Station began generating on 4 September 1882 with six dynamos using coal as a fuel source, and providing electricity to 400 lamps with a combined total load of 30 kW [1, 2]. Around the same time, the first British power generating station, Holborn Viaduct began its operation with a 60 kW generator driven by a horizontal steam engine [3]. Although Thomas Alva Edison proposed his concept of a central power station in 1878, the first long distance transmission of electrical energy took place in Germany with the installation of a 59 km transmission line [4]. In this regard, it is important to mention that Werner Von Siemens's invention of modern electric dynamo made it possible to generate electricity economically and contributed greatly to the global expansion of power systems [5].

At that time, several challenges are introduced in DC power system. For instance, increase of load size and power transmission to the distant consumer poses problem of power losses. A short-time solution to the problem was addition of three-wire 220 V DC system but again, it was very expensive and did not solve the issue of voltage regulation. Therefore, extensive research has been carried out in alternative current (AC) field that eventually, replaced the DC system.

William Stanley proposed the concept of practical transformer in 1885 that can achieve different AC voltage levels [6]. In 1888, Nicola Tesla developed AC generator and two-phase induction and synchronous motor of 50 Hz, and the first three-phase, 179 km long ac transmission line of 12 kV was installed in Germany in 1891 [2]. In UK, the first electrical power system project started at Bradford, Yorkshire in 1889 [4].

In modern age, power system network is considered as a complex structure to transfer electricity to its end user (domestic, commercial and industry) from the generation sides through electrical wires or other means. Historically, electric power system is structured in a way that it tended towards large-scale generation in some particular locations with different natural resources, and to transfer the produced electrical energy to the consumers, transmission and distribution networks are used. A typical power system is shown in Figure 2.1 which is divided into three major sections. The first section is “Generation”, where electricity is produced through different natural resources (for example, coal and oil) in large power plants. The generators at the power plants produces electricity at a specific voltage level but to transmit the power over long distance the voltage is increased through step-up power transformers. The second section is called “Transmission Networks”, where electricity is transferred through long cables in high levels of system voltage. To distribute electricity to the consumers in a suitable voltage, the third section of the power system is used which is called “Distribution Networks”.

In order to analyse the electric power system as presented physically in Figure

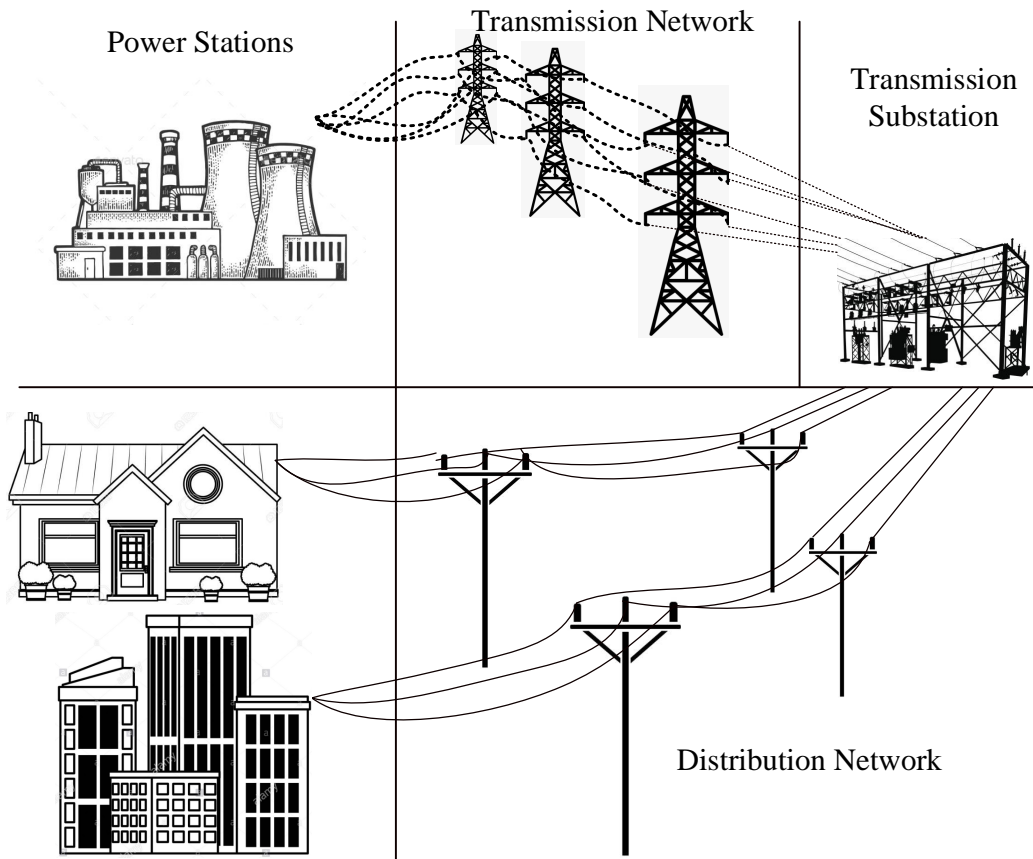


Figure 2.1: A typical electrical power system adapted from [7].

2.1, the system need to be presented in a schematic diagram called as Single Line Diagram (SLD). The SLD of a typical power system is shown in Figure 2.2. As can be seen from Figure 2.2, power stations can be represented as generators that produce electricity. The transmission network can be represented as a line with resistor and reactance where impedance value is varied with length of the line and type of conductors. However, there are different models available to present and analyse the transmission and distribution network. The transmission substation is presented as step-down transformer to reduce the voltage level to distribution level. Breakers in the line are generally used to isolate a particular section during the faults or other emergencies.

Currently, in UK, the electricity market is flourishing very swiftly with a sustainable economic growth and it can be considered as one of the largest and

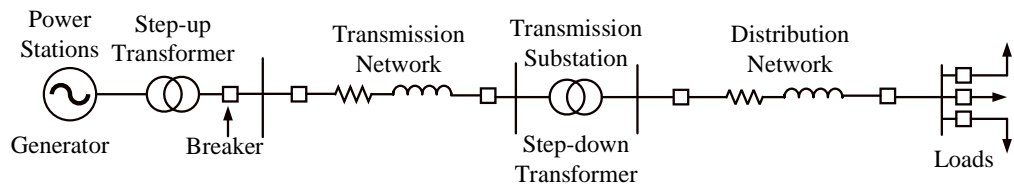


Figure 2.2: Single line diagram of a typical power system.

wealthiest industries with rapid increase of demand. After World War II, around 560 electrical power companies were established in UK, and different private companies own one third of them [8]. However, the electricity industries in North and South of Scotland, Wales and England were nationalised and reformed under the act of 1943 and 1947 [8]. Before the privatisation era, the electricity market was mostly vertically integrated, meaning the generation, transmission, distribution and supply companies were under the same unit [9]. In many countries, the public-owned companies are given the overall charge of supplying services to the consumers in vertically integrated utility. However, in 1990, the British Electricity Supply Industry was privatised [3]. Similar trends of changes of ownership and regulation have been followed by some European countries [10]. This requires a substantial amount of capital and operating expense to meet the commitment to the consumer, and governments guarantee a fair return to the companies in return for a fair and stable energy price to the consumers. This requires close government regulation to observe and control prices and various other factors associated with operating the industry and system [11].

Nevertheless, the regulator faced a challenge to keep the price within acceptable range that can satisfy both utilities to provide reasonable profit and a fair price to the customers with improved quality of electricity at the same time [12]. Furthermore, cost allocation in a vertical structured system is neither accurate nor transparent. Therefore, regulation cannot ensure economically efficient system with marginal cost. As solution to the challenge, deregulation of power industry

in UK took place and competitive markets strategy has been introduced.

In competitive market, the monopoly is removed from generators, transmission companies, system operators, distribution network owners/operators and others, and theoretically this should offer competitive prices and choices to the consumers with good services. A mechanism known as “Electricity Pool” has been introduced for trading electricity as commodity in wholesale price between generation and system supplier. In electricity pool, generation companies compete with each other to sell the electricity to the pool. In this system, generators set the bid for half hour of the day, and the selection of generators that meet the electricity demand for particular time is done based on the forecast. However, a key disadvantages of the pool is volatile price structure [9]. However, it has been replaced by New Electricity trading Arrangement in 2001, where generators and suppliers can buy electricity from each other [13].

## 2.2 Generation

Generation units are typically represented by the power plants that produce electricity in a large quantity and generally owned by different generation companies. The prime target of the generation companies is to maximise the profit with minimum down time of the generation units. Electricity production from the generation units may vary significantly depending on the demand from the customers side. Variation in demand can take place based on weather condition, hourly activities around the day; for example, off-peak time in UK is in between 10 pm to 8 am, when the demands are at lowest [14].

It can be observed from Figure 2.3, the electricity consumption around the world has increased remarkably over the last 50 years [15]. In 2018, final consumption of electrical energy around the world was more than 22000 TWh. However, a small decrease in energy consumption can be observed in between 2007 – 2009 due to

economic crisis [15], and it is possible to predict the similar trends after 2019 due to COVID19 situation when most of the industries and business were closed due to nationwide lockdown.

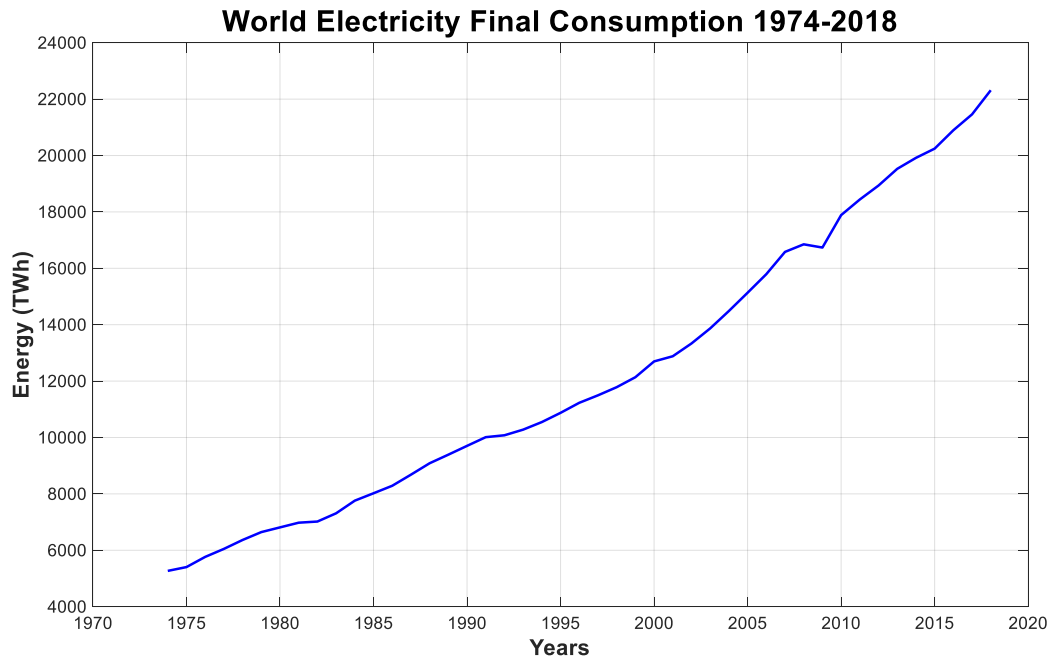


Figure 2.3: Electricity energy consumption around the world between 1974 and 2018 [15].

Electricity production generally refers to utilising different natural resources to convert one form of energy into electrical energy, and different generation technologies are available to achieve that, for example, combined cycle gas turbines (CCGT), conventional steam stations and upon the types of fuels used that are coal, gas, hydro, solar, wind or geothermal, bio-mass or waste and wood-chips. Most of the generation units in the vertically integrated power system are synchronous generator with large production capacity. A summary of different types of generation units that are available is provided in Table 2.1.

All power stations with different types of generation units are considered as the starting point for the vertically integrated power system as can be seen from Figure 2.1 and Figure 2.2, and then connected to large power transformers so

Table 2.1: Different types of power generation technologies [16].

<b>Generation Type</b>	<b>Description</b>
Fossil fuel power station	Generate electricity by burning fossil fuels (coal, stations petroleum oil or natural gas) to convert water into steam, which then powers the steam turbines.
Nuclear power station	Similar to fossil fuel-based power station, nuclear power station uses steam turbines but, in this case, nuclear fission reaction is utilised in place of fossil fuels to thermal energy needed for steam turbines.
Open cycle gas turbines (OCGT)	OCGT also uses natural gases as source but in place of producing steam, it uses pressurised combustion gases heat through a turbine to produce electricity.
Combined cycle gas turbines (CCGT)	As the name suggests, CCGT stations produce electricity using the combination of both gas turbine (used in OCGT) and steam turbine. The hot exhaust gases from the gas turbine are sent to the steam engine, and the heat from exhaust gases is used to generate steam.
Solar thermal power station	Heat from the sun is utilised to create the steam which then rotate the turbines to produce electricity.
Hydro-electric power stations	To produce electricity, generator's turbine is rotated through falling water in rivers and reservoirs.
Other stations	There are other renewable-based converter interfaced generation that can typically produce electricity in small-scale such as wind turbines, photovoltaic (PV), energy storage and bio-energy. Furthermore, many power stations burn bio-mass or waste and wood-chips to replace the use of coal.

that the voltage output can be increased to transmit electrical energy over the transmission and distribution networks. Also, it can be observed from Table 2.1, the power plants are dependent upon different natural resources, and therefore, generally designed in such a way that plants were located close to where the fuel resources were located, and were often far from load centres due to safety and pollution concerns. However, it is necessary to mention that the location of power plants depends on many factors, therefore, these requirements of health and safety and resource availability may not be true for all power plants and in some cases, raw materials are transported over long distances to power stations.

Most of the large power stations produce carbon dioxide which is posing threat

to the environment. In case of safety hazards, nuclear power plants pose potentially the greatest threats in terms of health and safety, since the nuclear radiation could be very harmful. Chernobyl and Fukushima Daiichi nuclear disasters are examples for this case, but in general the nuclear industry has a very good safety record overall, but continues to attract debate and differences of opinions between different nations, governments and individuals [17, 18, 19].

In UK, nuclear, coal and gas power stations produce almost 73% of the all electrical energy consumed [20]. However, targeting the net-zero carbon emission [21], Scotland has decided to integrate more renewable energy resources to the power system and replace existing large conventional fossil-nuclear-fuelled power stations. Therefore, the power system is changing drastically and this is having a significant impact on the system which will be discussed in later sections of the thesis. A chart showing the contribution of different plants to the total electricity supply for UK is presented in Figure 2.4, where it can be observed that most of the electricity is produced by gas-based power stations, around 36%, while wind turbines contribute around 24%. Contributions from nuclear power stations are around 16%, coal is around 2%, hydro generation is around 2%, solar is around 4%, oil and pumped storages are less than 1%, and other renewables and fuel generation (for example, bioenergy, thermal sources including non-biodegradable waste, coke oven gas and waste production) are around 16%.

## 2.3 Transmission Network

The transmission networks make sure that a bulk of electrical energy can be transmitted from generation to throughout the country in various range of voltages in an efficient manner. In many countries, transmission companies own and operate the transmission network, and situations in terms of ownership and operation vary from country to country. However, in GB, different transmission companies can

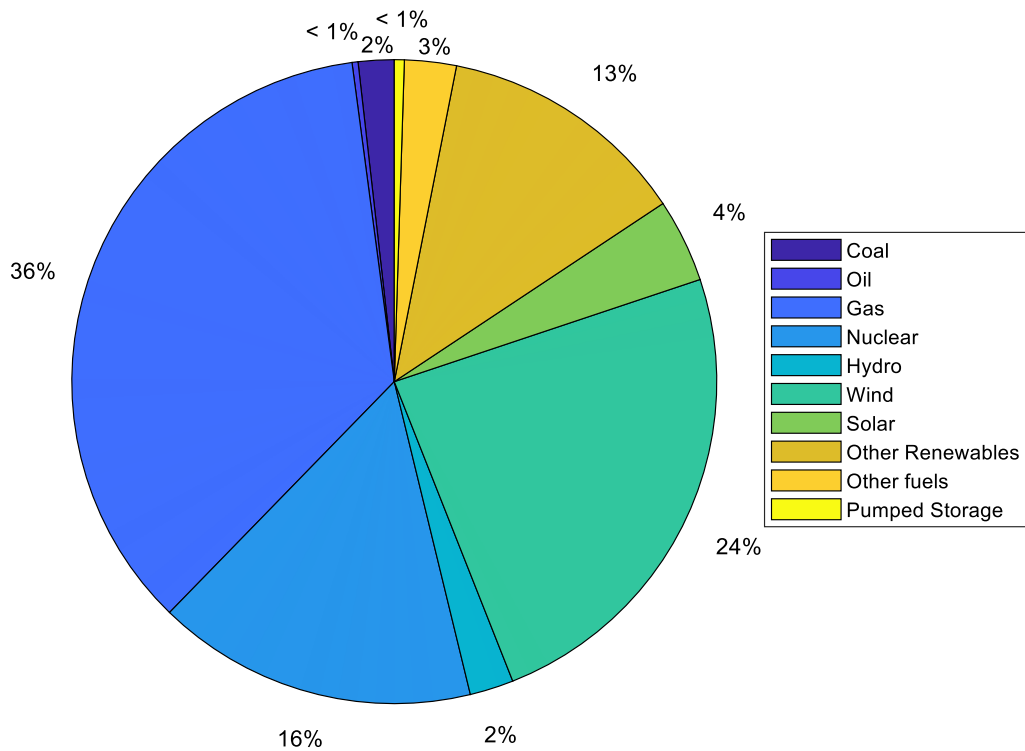


Figure 2.4: Electricity production by different types of generation units in 2020 at UK [22].

own the assets of transmission network but they are not entitled to operate them. System operators generally control transmission network, where transmission owners build the network according to the plan provided by the system operators and look after the maintenance of the transmission assets to ensure reliable operation of the power system.

In GB, the system operator is charged with ensuring that the transmission network is available to all users (e.g. new generators or large loads) and modifications to the network could be made to facilitate connection to new users - although investment (and sometime co-investment) may be required to facilitate this. The objective of ensuring equitable access to the transmission network is intended to maximise the participation with and access to the power network and markets in GB - similar situations existing in some, but not all, other countries in the world

and are influenced by policy and socio-economic factors. Generally, overhead lines are used to connect the transmission network to distribution network through the transmission substations.

Different countries have different levels of transmission voltage levels. For example, in GB, the minimum voltage level of the sub-transmission network for Scotland is 132 kV and Scotland also has both 400 kV and 275 kV transmission lines; whereas, in England and Wales, 132 kV is considered as a distribution network and transmission network voltages are 400 kV and 275 kV [9]. There are three transmission owners in GB [23], and they are responsible for the development and maintenance of the transmission networks. The three owners are:

1. Scottish and Southern Electricity (SSE Network) [24].
2. ScottishPower (SP) Energy Networks [25].
3. National Grid (NG) [26].

Figure 2.4 shows the map of UK along with the owner of the transmission network and their operating regions. Transmission networks in Scotland are divided into north and south regions owned by Scottish and Southern Electricity (SSE) Networks and Scottish Power (SP) Energy Networks respectively. National Grid (NG) owns the transmission networks in Wales and England, and Northern Ireland Electricity owns the transmission network in Northern Ireland.

## 2.4 Distribution Network

Distribution networks transport electrical energy from the transmission network to industrial, commercial and domestic customers. The distribution networks carry electricity in the form of medium and low voltage through either overhead line or underground cable. The regulatory agency who own and operate the distribution

## Electricity Transmission

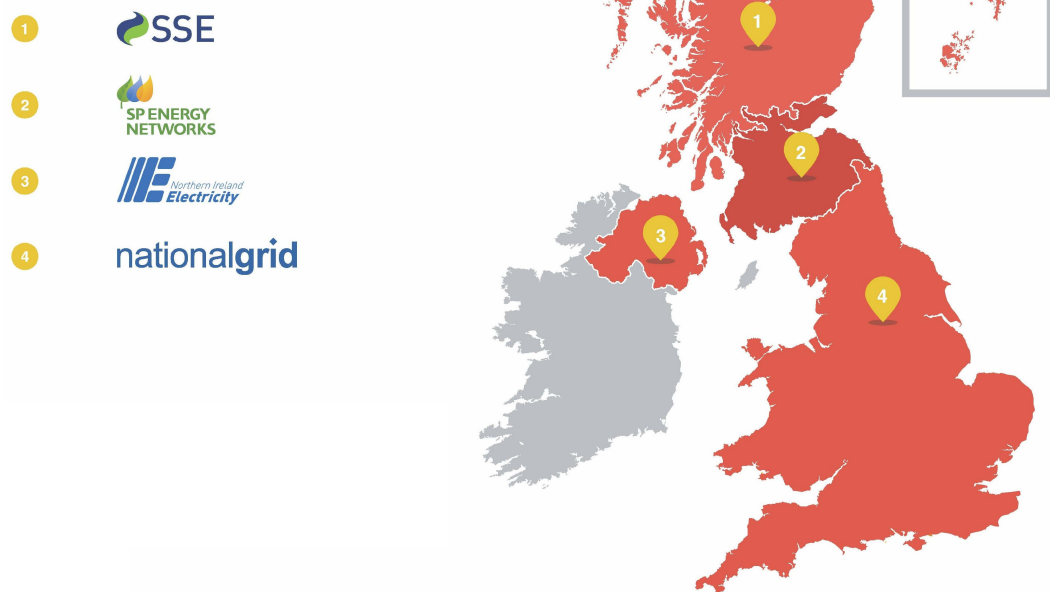


Figure 2.5: UK transmission network owners by regions [23].

network are known distribution network operator (DNO). Their prime work is to coordinate distribution services, i.e. making sure of energy to be reached to the customers in the adequate quantity with proper reliability and quality.

In GB, the voltage levels for medium voltage (MV) distribution networks are 132 kV (England and Wales only), 33 kV and 11 kV, and 400 V is considered as low voltage [27]. In some DNOs, 33 kV is known as extra high voltage (EHV), 11 kV (and 6.6 kV in some cases) is termed MV, and 400/415 V is LV. According to international standard, IEC60038 [28], any voltage between 1 kV to 35 kV is considered as MV, whereas, any voltage lower than 1 kV is LV. A few large industries and commercial buildings are generally connected to the MV distribution networks, for example, most universities receive power from multiple dedicated 11 kV feeders supplied from 33/11 kV substations. However, the majority of the residential and commercial consumers are connected to the 400 V distribution networks.

There are total 14 licensed DNOs in GB - 12 in England and Wales, and 2 in

Scotland, and these DNOs are owned by 7 different network companies [29, 30].

Figure 2.6 shows the distribution network map for GB with DNOs and each DNO's operating regions.

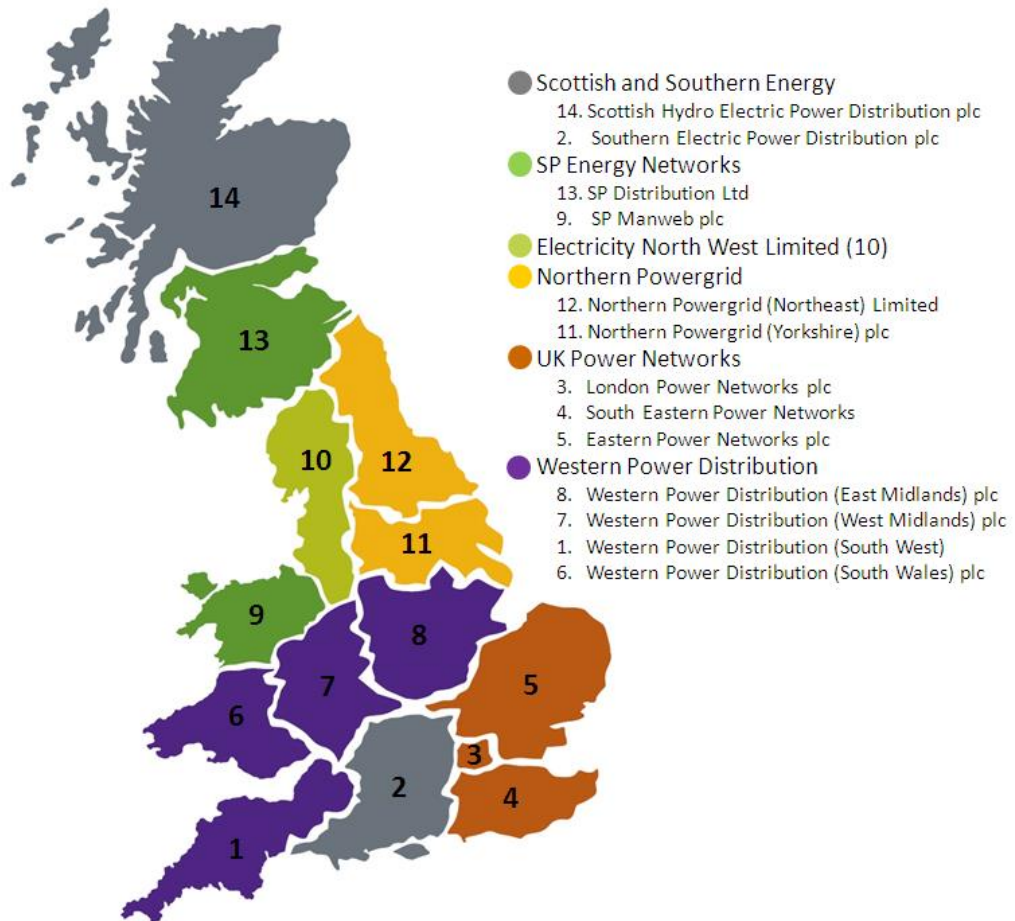


Figure 2.6: Map of GB with DNOs and their operating regions as of September 2021 [31].

As time has progressed, various new and advanced technologies are becoming integrated within electrical systems; for example, interconnection of DGs in distribution networks. This has the potential to enhance overall efficiency, reduces operating costs and improve reliability and resilience of the system (detailed advantages are discussed in Section 2.6.2). However, with new types of loads and generation technologies, the system is becoming complex and new challenges are

arising. Therefore, power system is expected to be affected highly due to these new challenges.

## 2.5 Integration of Distributed Generation

It is difficult to provide an exact and globally-accepted definition of a distributed generator (DG), however, as a general view, DGs are considered as electric power generators that produce electricity at a relatively small scale to provide electricity to loads in their neighbourhood. They are also termed as embedded or dispersed generators, and they can also be specified by generation technology (for example, wind, PV and energy storage), rating, voltage level, and connecting point to the network [32]. According to [33, 34], the main features of these types of generation can be categorised as follows:

1. DGs are generally installed in the distribution networks with typical voltage levels of 230/415 V to 145 kV.
2. There is no central plan from the power utility and small-scale DGs are not dispatched centrally.
3. The maximum power ratings of the DGs are typically lower than 50 MW.

The maximum size of the DGs depends upon the distribution network capacity and voltage level to which the DG is connected [35]. Ackermann in [36] classified the DGs as follows:

- Micro DGs: range - 1 W to 5 kW; connected to single phase domestic LV systems;
- Small DGs: range - 5 kW to 5 MW; connected to three phase distribution network LV systems;

- Medium DGs: range - 5 MW to 50 MW; connected to three phase distribution network MV systems.

In recent years, the DGs have become an integral part of the power system network and replacing the traditional large synchronous generation. A simple difference between traditional and future power system network due to DGs integration can be observed from Figure 2.7.

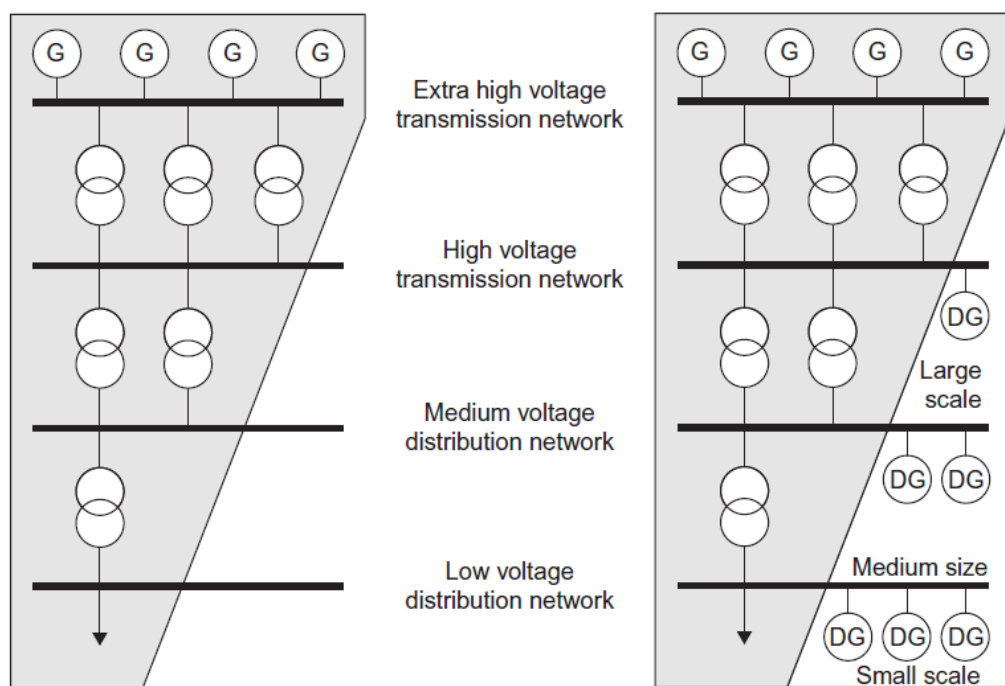


Figure 2.7: Difference between traditional and future power system with the connection of DGs [32].

There are different types DGs that either supply power through conventional generation; for example, small diesel and gas generators or non-conventional generation systems; for example, small hydro using run-of-the-river technology, wind energy with microturbines, PV, energy storage, and other generation units that utilises renewable energy resources. Considering the harmful environmental effects of the fossil-fueled power sources, small-scaled DGs are an effective solution to reduce carbon emission and meet the target of net-zero. Furthermore, since

most of the DGs use renewable energy resources, they are not exhaustible. From the financial perspective, investing in the DGs is very desirable due to lower capital cost, lower risk and no large infrastructure being required. There is also the benefit of reducing losses in the system as the energy sources in systems with lots of DG are typically physically very close to the loads that are consuming the generated power. The costs benefits of DGs are discussed in [37].

Moreover, power electronics plays an important role to integrate non-synchronous DGs to an ac power system. Owing to the variation in types of DGs, the produced electrical power/current could be either DC or AC; for example, PV, batteries energy storage and fuel cell produce the DC power and it is required to convert the power to AC using power electronics converter. Wind turbine, micro turbine and biomass deliver the AC power, but typically this may not be synchronous. Therefore, power electronics is often used to convert this to synchronous AC power, and to facilitate voltage and frequency regulation [38]. Furthermore, in recent years, advancements in power electronics devices facilitated power converters to improve their performance, which in turn enhances the use of converter-interfaced DGs in the power system.

## **2.6 Introduction to Microgrids**

Due to massive connections of DGs in the distribution networks, power flow in the network no longer is unidirectional instead it becomes bidirectional as can be seen from 2.7. Electrical power generated by DGs in the active distribution networks or microgrids (microgrids are essentially active distribution networks) can be higher than the required power by the loads connected to that particular networks. In such cases, the additional electrical energy produced by the DGs is exported to the transmission networks from the distribution system. As a result, distribution networks are becoming active in nature, whereas, according to

previous definition, distribution networks without DGs were unidirectional, that is power flows from upstream generation and transmission to distribution networks are known as passive distribution networks [33].

Active distribution networks require different components such as control, supervision, and effective communication between different equipment to ensure a safe, secure and reliable operation. One way of achieving these requirements is to introduce the smart grids concept. Different researches defined the smart grids in different ways; for example, according to [39] smart-grid is not just a specific technology or equipment, but a concept that interconnects and intensively uses information and communication technology in the power system. In GB, there is a requirement for an electrical system that can support an efficient, timely transition to an economy transition to a low/net-zero carbon system that ensures energy security and wider energy goals while minimising costs to consumers [40].

Active distribution networks with different converter interfaced DGs in combination with smart grid technologies introduce the microgrids concept. Microgrids are considered as part of large power system networks that composed of DGs and a cluster of loads connected in close proximity [41]. Microgrids are generally connected to the grid through a point of common coupling (PCC). Also, microgrids can import or export electrical energy to/from the main grid by controlling active and reactive power contribution from the DGs [42].

### **2.6.1 Modes of Operation**

The operation of independent isolated network with local generation and loads is not a novel concept. It has been a common practice for remote areas to operate within a small network without any grid due to lack of technical knowledge and economical support [43]. Furthermore, microgrids have been operated for many years in industrial complexes and in critical commercial facilities. The current concept of microgrid was first introduced in [41], where microgrids are presented

as part of larger system, for example, distribution network with connection of converter interfaced DGs.

A microgrid can contain both dispatchable and non-dispatchable generation units, and can produce electricity in both AC and DC form. However, since majority of the microgrids are to transmit electricity through AC, power electronic converters are required to convert DC to AC quantity. As mentioned earlier microgrids made the connection to the main grid through PCC, therefore, a circuit breaker at the PCC is used to disconnect the microgrid from the main grid in cases of disturbances, and/or to allow the operation in islanded mode. A typical model of microgrid is shown in Figure 2.8.

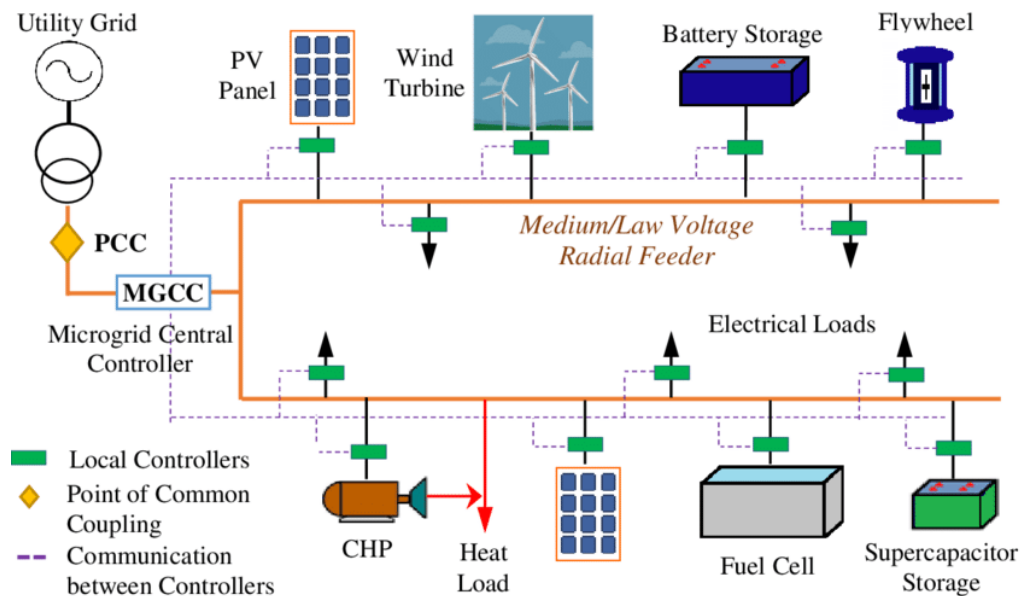


Figure 2.8: A typical schematics of microgrid [44]

There could be several controllers in the a microgrid, and they are performed hierarchically. For example, converter controller (CC), and load controller (LC) can be used for connecting and controlling DGs and controllable loads in the microgrid. While, CCs and LCs operate at the local level, the microgrid central controller (MCC) can manage the overall control and operation of the devices

centrally. To coordinate all the controllers within the microgrid and central controller, communication channels are necessary to exchange information. The functions of the controllers are listed below [33, 45, 46]:

- ***Microgrid Central Controller (MCC)***: This central controller coordinates operation of other local controllers, ensures overall performance of the microgrid remain within acceptable range, maximise the efficiency of the microgrid and controls the islanding logic. Also, the controller ensures that the voltage and frequency of the microgrid remain with a range of specified limits.
- ***Converter Controller (CC)***: There are different types of CCs and their functions and operating strategies could be significantly different from each other. Different types of CCs can exist in the same microgrid. CCs can control the power flow and voltage of the microgrid using local information such as voltage and current magnitude, frequency, load change and disturbances. CCs can also respond quickly and has the ability to adjust the DGs to operate in certain ways.
- ***Load Controller (LC)***: LCs can connect and disconnect certain constant loads or can change the magnitude of variable loads depending on the generation capacity and commands from the central controller.

The controllers in the microgrids ensure safe and flexible operation. Furthermore, microgrids can perform in a manner that either it can be operated in islanded mode or in the grid connected mode. To make sure that electricity is supplied to the customers in the safe and uninterrupted manner in both mode of operation, microgrids certainly require some additional equipment and controls. The details of the main features of the microgrids' operating modes are listed below:

- ***Grid-Connected Mode:*** During grid connected mode of operation of microgrid, the main grid controls or determines the voltage and frequency of the system. The advantage of the grid connected operation is, while there is shortage of supply from the local generation to local loads, main grid can provide the deficit of energy. Similarly, excess power generation from the microgrids can be exported to the main grid. Therefore, it is possible to operate power system most efficiently and reliably. Furthermore, microgrids can provide ancillary services while necessary such as voltage regulation and reserve power.
- ***Islanded Mode:*** Islanding can be either intentional or unintentional [43]. While unintentional islanding may take place due to faults or any other disturbance in the main grid, intentional islanding occurs in a planned manner that may occur due to scheduled maintenance in the main grid. In any case, islanded mode of operation allows microgrids to supply electricity continuously that enhances the reliability of the system. To operate in the islanded mode of operation, generation capacity in the microgrids must have to higher than or equal (minimum) to the critical loads. Also, it may be necessary to shed some non-priority loads during the transition from grid connected mode to islanded mode. Voltage and frequency of the islanded microgrid is controlled by the DGs in the network.

### 2.6.2 Advantages and Disadvantages of Microgrids

As it can be understood from the aforementioned discussion that microgrids have unique features of integrating both renewable, non-renewable and converter-based small-scale DGs close to loads, and can be operated in grid connected or islanded mode. Therefore, developments of microgrids can be a promising and cost-effective solution for the future power system network. However, microgrids have some

advantages and disadvantages both. In this section both merits and demerits of the microgrids will be discussed. Starting with the advantages, some of the key positive aspects of the microgrids are listed below:

- ***Reliable Power Supply:*** Since microgrids can operate in both grid-connected and islanded mode, power can be delivered to the customers without any interruption, and can continue even when there is a disturbance or maintenance in the grid side. In such cases, microgrids can continue to supply electricity in islanded mode (as long as there is enough supply to meet demand – in cases, load shedding could be used to ensure supply to critical loads continues) [47]. Therefore, microgrids are more reliable in terms of power supply.
- ***Reduction in Line Losses:*** Power losses due to transmission over a long distance can be reduced significantly due to short electrical distance between load and generation [48].
- ***Reactive Power Support:*** Depending of the design of the CCs, DGs in the microgrid can provide improve voltage profile, frequency support and fault ride through services [49].
- ***Integration of Renewable Power Sources:*** Microgrids can effectively integrate and control different renewable sources with low nominal capacities and intermittent generation [50]. Therefore, microgrids can help to increase number of renewable generators in the power system.
- ***Reduction of Carbon Emission:*** Targeting net-zero carbon emission [21], Paris climate change agreement [51] and Kyoto Protocol [52], all the industrialised developed countries in the world has agreed to reduce the greenhouse gas emission. Microgrids with renewable DGs can reduce carbon

and greenhouse gases emission by replacing other sources such as gas, coal, oil, diesel, or any other fossil fuel-based electricity generation.

- **Lower Capital Cost:** Formation of microgrids can reduce substantial investments on further development of large power stations and longer transmission lines. Furthermore, the capital cost for small-scale renewable generation is comparatively very low than the conventional generation, and does not require large space or infrastructure costs, for example: PVs can be installed on the roof top of the existing buildings, therefore, does not need to purchase additional land for electricity generation [50].
- **Cost Reduction:** With increased reliability of power delivery in microgrids, price of electrical energy can be reduced significantly with less power system outage, and that can also reduce fines paid by the operator to the customers due to loss of connection. Operation costs of large power plants can also reduce since renewable generation is replacing large synchronous generators. Furthermore, overall price of the energy in the power market will be reduced due to plug and play connection of the renewable resources [50].
- **Provision of Ancillary Services:** When connected to the main grid, microgrids can provide ancillary services like power reserve, inertial power supply - fast power injection to reduced the magnitude and RoCoF excursions following disturbances that impact upon frequency, voltage control, frequency support and other services [53].

Despite many advantages, microgrids have several technical and operational challenges. Some of the disadvantages of microgrids that needs to be addressed and solved are also listed below.

- **Stability Issue:** Voltage and frequency of the microgrid during grid connected mode remain constant due to support from the grid. However,

during islanded mode, since there is no swing bus in the system, controlling the frequency can be a critical issue. Frequency and voltage requirements need to be taken into consideration to ensure proper stability between the transition of operating modes [54].

- ***Require Custom Designing:*** From the technical point of view to operate microgrids optimally, several elements need to be taken into consideration; for example, location of DGs and network topology. If small capacity DGs are connected to a weak part of the system voltage fluctuation and stability issue may arise. Furthermore, inadequate analysis, tuning of CCs, and loss of communication can cause active and reactive power flow issue in microgrid [55].
- ***Protection Issues:*** Fault current magnitude can change significantly with the change of mode of operation. During islanded mode of operation fault current magnitude can be very low to detect any fault. Also, bidirectional power flow in the microgrid can cause coordination issues [56, 57].
- ***Communication Channels:*** Proper operation and management of microgrids largely depends upon the communication between the controllers (CC, LC and MCC). Therefore, it may cause additional costs for the system and unexpected loss of communication may create serious issue with the operation of DGs [58].

## 2.7 Overview of Protection Schemes

Electrical faults and disturbances, the majority of which are due to short circuits, but may also be caused by, or lead to, unbalance, overloads, open-circuits, loss of connections to main grid systems, islanded situations, out-of-step conditions, or other phenomena, may occur at any time and are usually not anticipated. Short

circuit faults are the most common types of faults that may take place in the power system. These types of faults can cause heavy thermal and mechanical damage to the power system components. Short circuits faults can be categorised in to balanced fault (for example, three-phase to earth short circuit) and unbalanced faults (for example, single-phase to earth fault, phase to phase fault and phase to phase to earth fault). It is not possible to stop the occurrence of the faults in the power system networks; however, it is possible to limit the damage to the power system equipment and other consequences faults through appropriate use of power system protection. Therefore, protection against the electrical faults is considered one of the most crucial and essential components of the power system.

Protection equipment in the power system isolates only the faulty sections from the rest of the healthy sections of the network. Hence, the main philosophy of the protection is not stopping the occurrences of the fault in the network but isolate the fault from the network so that rest of the network can work properly and minimise the effect of the fault in the network. To carry out the protection requirements, there are four distinct parameters: discrimination (ability to detect whether to operate or not), stability (ability to remain inoperative when it does not require), sensitivity (ability to detect the fault) and operating time (how fast it can operate).

To detect and isolate faults from the network, protection system requires several equipment as shown in Figure 2.9 [59]. Measuring devices are required to measure and monitor different power system parameters such as current and voltage. The measurements are then fed to the relay to discriminate healthy and faulted condition. Current transformer (CT) and voltage transformer (VT) are the mostly used measuring devices in the network. Relays are the brain for the protection that can detect any fault events based on the measurements, and finally to isolate the fault relays send tripping signal to circuit breaker (CB). CB works as switch and has two mode, open and close. Generally, in normal condition CBs

are in close position, but if there is a fault and relay send the tripping signal, the associated CBs change its mode to open and isolate a particular section from the network. Communication between the relays may require depending on the protection strategies. To avoid the unnecessary tripping, relays can communicate with each other through communication channels.

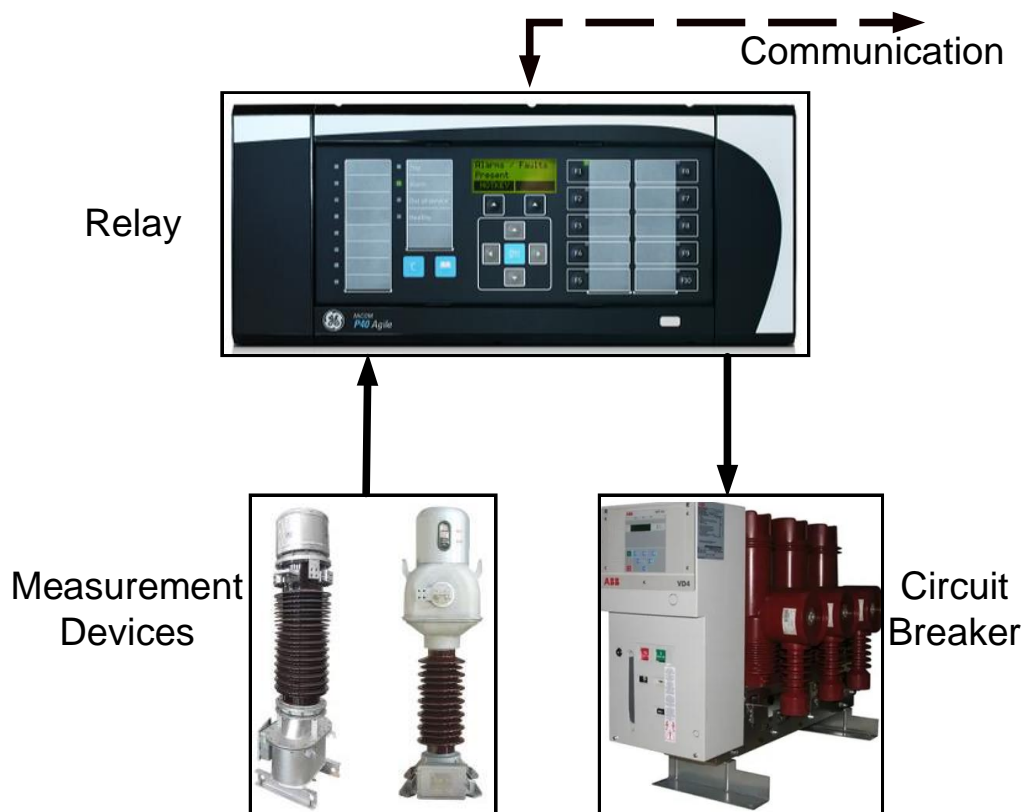


Figure 2.9: Main components of power system protection.

There are two ideologies of protection system unit scheme and non-unit scheme. The schemes are explained through Figure 2.10 and Figure 2.11. Unit scheme provides protection to a particular zone/section/equipment of the power system network. As can be seen in Figure 2.10, when there is a fault between Bus A and Bus B (Fault 1), the protection relays will issue tripping signals, and isolate the fault from both side of the network. However, if fault is outside of the protection zone (Fault 2), relay will consider it as an external fault and will not issue any

tripping signal.

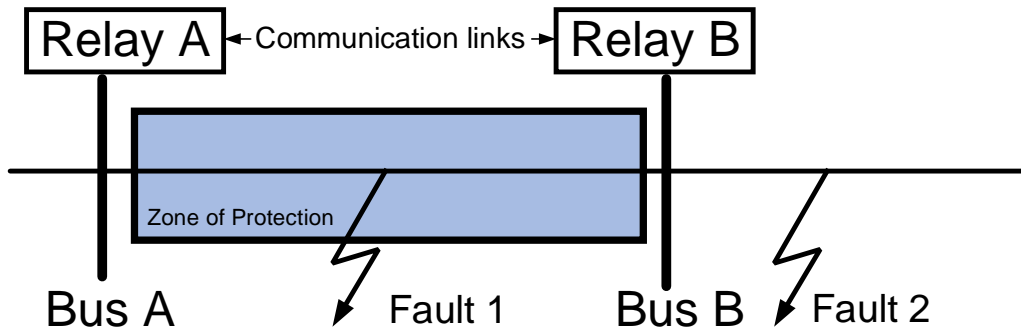


Figure 2.10: Unit protection scheme.

However, non-unit protection scheme can provide protection beyond its protection zone. As can be seen in Figure 2.11, non-unit protection can operate for both faults, Fault 1 and Fault 2. The protection relay, Relay A operate as the main protection scheme for Fault 1 and operate as backup for Fault 2. Both schemes have their own benefits and shortcomings, for example, unit scheme is much more discriminative and sensitive compared to the non-unit scheme, but, the non-unit scheme has inherent backup property which unit scheme does not have.

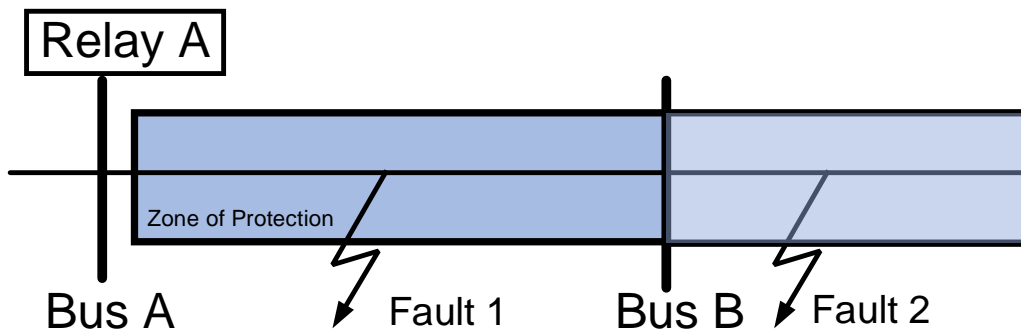


Figure 2.11: Non-unit protection scheme.

Both unit and non-unit schemes are required in transmission networks to provide high level of discrimination and stability. Unit protection work as the main protection in the transmission network and non-unit protection provides

backup. However, in the distribution networks, non-unit scheme provides both main and backup protection. Three main protection strategies are widely used in the power system networks. The operation and characteristics for all three types of strategies are described in details below.

### 2.7.1 Differential Protection

Differential protection scheme is part of unit scheme. This protection scheme continuously monitors and compares the current measurement from the both end of a section of the network to detect the fault. The scheme requires communication between the relays.

The operation of differential protection scheme can be explained with Figure 2.12 and Figure 2.13. Figure 2.12 shows the operation of one relay differential scheme and Figure 2.13 shows the dual relay differential relay operation. Generally, in most of the longer line section, dual relay differential scheme is used.

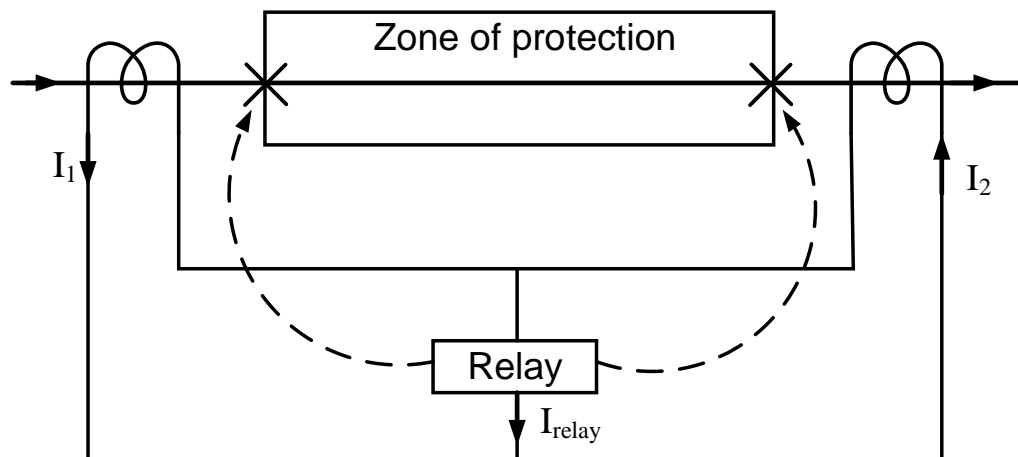


Figure 2.12: One-relay differential protection scheme.

As can be seen from the figures, if there is no fault or if fault is outside of the protected zone, the current flowing through each end,  $I_1$  and  $I_2$  will be equal in magnitude, and therefore, vector sum of the current  $I_{relay}$  will be zero. As a result, relays will not detect any faults, and hence, will not issue any trip.

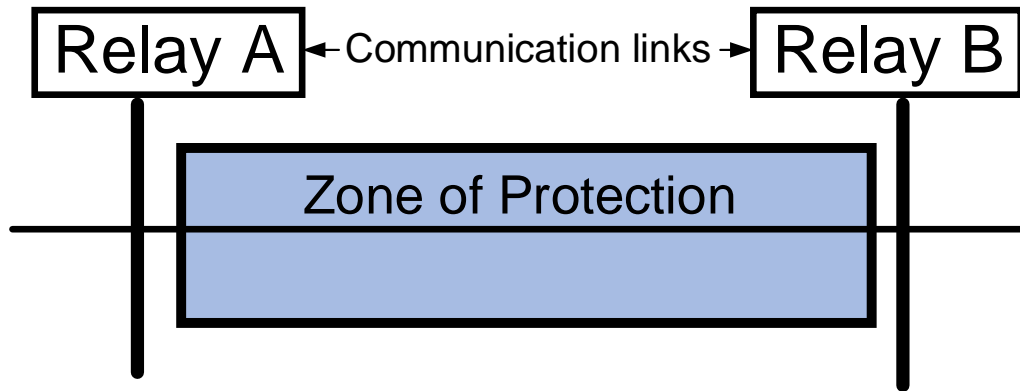


Figure 2.13: Double-relay differential protection scheme.

However, if there is fault in the zone of protection, the currents  $I_1$  and  $I_2$  will not be equal in magnitude, and that will cause  $I_{relay}$  to be non-zero. As a result, the relays can detect any fault between the protection section. Some differential relays also take current phase differences of both ends into consideration along with magnitude to detect the faults.

Overall, differential protection can provide better discrimination and stability. However, this scheme requires communication between the relays, and can be very expensive for the protection. Therefore, differential protection is used the power transformers, generation and transmission network protection, not for the protection of distribution level or microgrids.

### 2.7.2 Distance Protection

Distance protection detects fault based on the measurements of impedance, i.e. voltage and current both. Hence, distance protection is also known as impedance protection. The key principle of distance protection is to estimate the positive sequence impedance from the voltage and current measurements. To measure both voltage and current, CTs and VTs need to be installed at one end of the network where the distance relay is located. Since the positive sequence

impedance is distributed uniformly along the line, one of the positive aspects of this scheme is, the measure impedance can provide an estimated location of the fault in the network. The measured impedance is then mapped on the operational characteristic to make the decision, if the fault is within the range of protection zone or outside of the zone.

This protection scheme is classed as non-unit scheme, i.e. can provide inherent backup protection. Communication links between the distance relays may not be essential; however, to enhance the performance of the relays, communication between the relays to send blocking and inter-tripping signals are required.

In three-phase system, distance relays generally have 6 elements and each measure positive sequence impedance of different types of faults -

- i Phase A to earth fault,
- ii Phase B to earth fault,
- iii Phase C to earth fault,
- iv Phase A to Phase B fault,
- v Phase B to Phase C fault,
- vi Phase C to Phase A fault,

Distance relays will operate if any the of the comparators detect any of the above types of faults.

There are different characteristics available for the distance protection; for example, directional, non-directional, Mho, offset Mho, resistive, reactive, quadrilateral. Settings of the distance relay can be setup through different zones. Protection zones for distance relay can be explained through Figure 2.14 and Figure 2.15, where Mho characteristics has been used.

Zone 1 is designed to protect the nearest section of the line. It is not possible to detect all the faults in the network through zone 1 only, but, to ensure relay

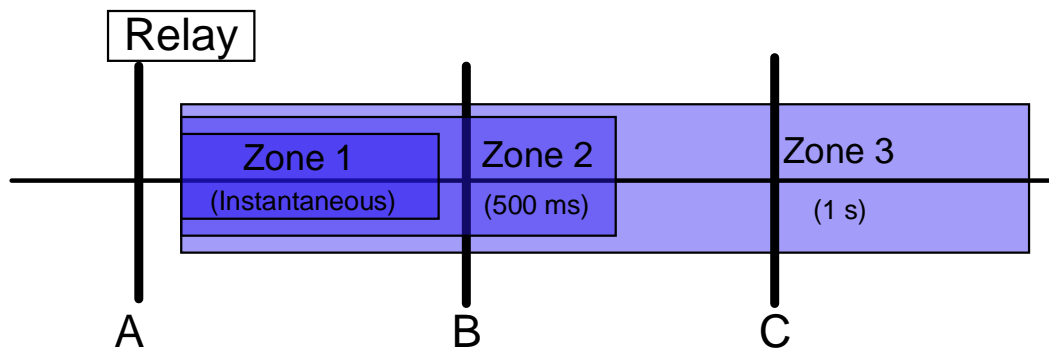


Figure 2.14: Distance protection relay's zones.

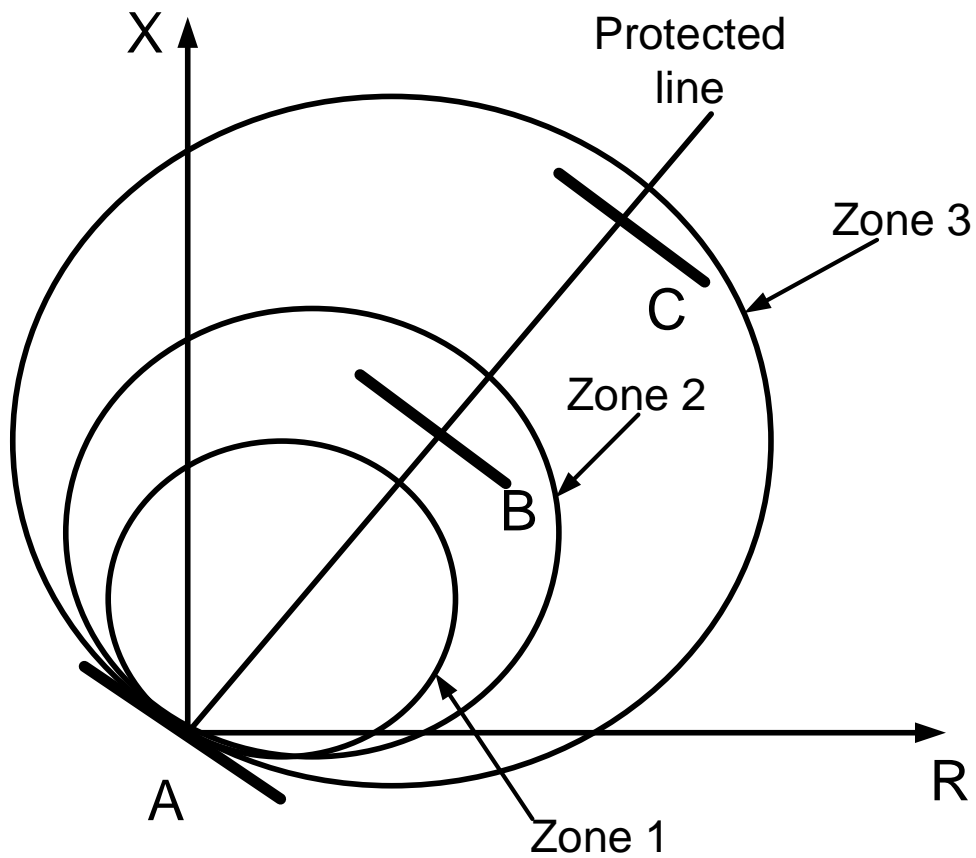


Figure 2.15: Boundary for each zone with Mho distance relay.

security zone 1 reach/setting is set as the 80% of protected line impedance. A margin of 20% is give so that due to measurement and other errors such as overreaching issues can be avoided. Zone 2 makes sure that the relay operated for

the fault for an end of the zone. Adding the previous errors onto the impedance, zone 2 setting is set as 120% of the protect line impedance. Relays operates with delay of 500 ms for zone 2 faults. Zone 3 is set as 200% – 250% of line impedance, and both zone 2 and zone 3 of the distance relays are generally used for the backup protection. Therefore, an additional 500 ms delay with zone 2 (total 1 s) is added for operation zone 3.

Distance protection scheme generally used as main or backup protection for transmission network and used as a backup for transformers and generators. Sometimes, it is used as only protection scheme for long distance distribution networks (MV) with its inherent backup.

### **2.7.3 Overcurrent Protection**

Another example of non-unit scheme is overcurrent protection. The scheme detects fault based on the magnitude of fault current supplied by the generation units in the network. Therefore, overcurrent protection is directly dependent upon the short circuit levels of the network, and most suitable for strong power system with large fault current capacity.

Overcurrent relay detects fault if the magnitude of the current is higher than the predetermined threshold current value, and the operation time for the relays are also dependent on the magnitude of the current. If the magnitude of the fault current is high then the relay will operate fast but if the fault current magnitude is low than it will operate with predetermined delay.

This inverse relationship between current and operating time known as inverse definite minimum time (IDMT). The delays in operation helps the IDMT relays to coordinate so that relays closer to the fault operate first and other upstream relays can operate as backup protection. The operation of overcurrent protection and coordination of the relays can be explained through Figure 2.16 and Figure 2.17.

Relay A and B, shown in Figure 2.16 are assumed to be standard inverse IDMT overcurrent relay. The characteristic graphs for both relays are shown in Figure 2.17. If we assume during normal condition, power is flowing from Bus A to Bus B, for a fault after Bus B, (Fault 2), the fault current will be  $I_{fault2}$ , and with that fault current the operating time for relay B is  $t_{Bfault2}$  and for relay A, the operating time is  $t_{Afault2}$ . So, it can be observed that there is a margin of delay between relay A and relay B for the fault, Fault 2. In case of fault, Fault 1, the fault current will be  $I_{fault1}$ , and only Relay A will detect the fault and issue a tripping signal around  $t_{Afault1}$ .

According to IEC 60255 standard [60], IDMT has four different characteristics: standard inverse, very inverse, extremely inverse and definite inverse. Table 2.2 presents the difference in operation time in seconds for each characteristic. The term used in Table 2.2 are,  $I_r = \frac{I}{I_s}$ ,  $I$  = Measured current of the line (A),  $I_s$  = Relay setting current (A), and  $TMS$  = Time multiplier setting of the relay.

Table 2.2: Definition of IDMT relay characteristics [61].

Relay Characteristics	Equation
Standard Inverse	$t = TMS \times \left( \frac{0.14}{I_r^{0.02-1}} \right)$
Very Inverse	$t = TMS \times \left( \frac{13.5}{I_r-1} \right)$
Extremely Inverse	$t = TMS \times \left( \frac{80}{I_r^2-1} \right)$
Long-time standard earth fault	$t = TMS \times \left( \frac{120}{I_r-1} \right)$

To operate the overcurrent relays, two settings need to be provided for each relay pickup or plug setting (PS) and time multiplier settings (TMS). Plug setting changes the level of operation by changing the characteristic curve in the horizontal plane and TMS controls the time of operation by changing the vertical position of the characteristic curve.

Generally, the relay begins to operate when current is greater than 125-150% of the rating with the fast operation as possible. The major benefit of the scheme is that it can provide fast clearance for fault. The major drawback for the over-

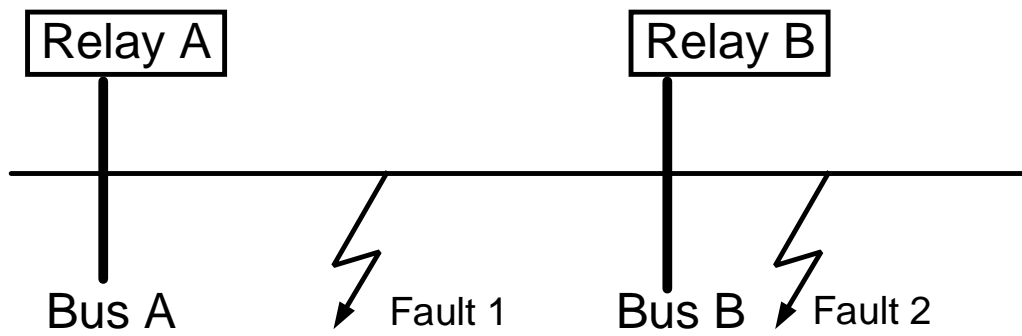


Figure 2.16: Protection with overcurrent relays.

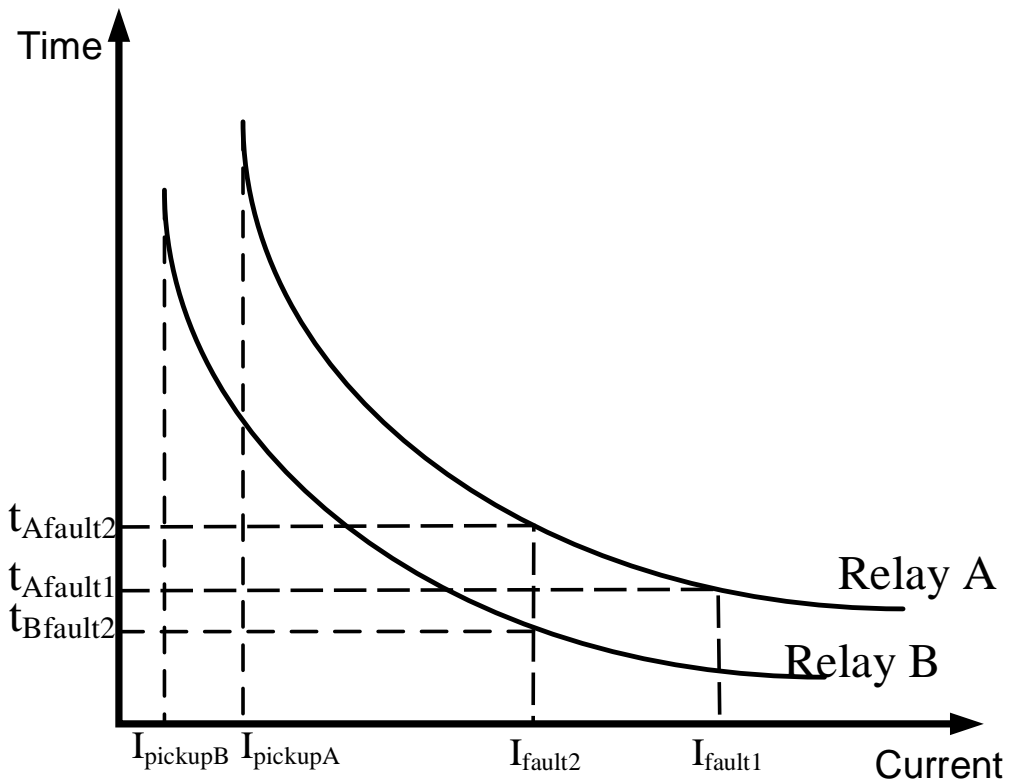


Figure 2.17: Standard inverse IDMT characteristics of overcurrent relays shown in Figure 2.16.

current protection is, in multi section feeders with multiple relays, operating time increase as fault current moves closer to the source. As a result, a fault closer to the source will remain longer time in the system which can be destructive for the

rest of the healthy system.

Instantaneous or high set protection is used along with inverse characteristic of the IDMT relay to mitigate the problem. The pickup setting for the instantaneous element is set in a way such that it operates with 130% of the fault current of the downstream relay location.

#### 2.7.4 Loss of Mains Protection

Islanding or loss of mains (LOM) occurs while a single or multiple of DGs continuously energise a particular section of the distribution network that has been separated from the main utility system [62]. The phenomena can be described more clearly by Figure 2.18, where the grid get disconnected from the network (through disconnecting the CB connecting the grid and distribution network) but DG connected to the network is continuously supplying to the connected loads.

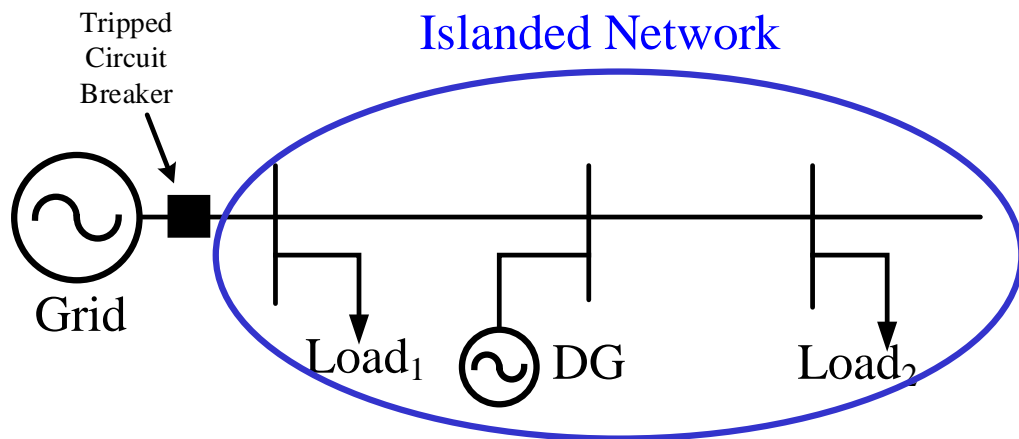


Figure 2.18: Example of islanding

Islanding scenarios can be divided into two categories, one is intentional islanding and the other is unintentional islanding. The unintentional islanding can take place in the network when DGs in the islanded network continue to supply electricity to the local loads and protection systems of the DGs do not identify the islanded condition. Various problems can take place and risks may

be introduced within the network during unintentional islanding [63]. The most important issues are listed here.

- Damage of the connected loads due to electromechanical torques generated by DGs.
- Creation of transient overvoltage surge on the feeder.
- Risk of life for the maintenance crews during maintenance.

Intentional islanding is achieved in a controlled fashion and is often proposed as being used in microgrid systems which typically can operate in either grid connected or islanded modes, where the local generation has enough capacity to provide energy to supply the demand. However, a number of prerequisite conditions must be met before implementation of intentional islanding can be considered [64]. For examples:

- i. DGs must be capable of maintaining the standard limit of voltage and frequency in the network.
- ii. Stability must be achieved.
- iii. The protection system of the islanded network must be able to detect and isolate the faults through the system.

The first two conditions can be achieved through the control of the generators and converter assuming local DGs has sufficient capacity to provide power to local loads or otherwise planned load shedding scheme needs to be implanted. However, the third one requires possible fault studies with different fault scenarios since the existing overcurrent protection is not sufficient to provide the protection towards the islanded section with variation of different parameters [64, 65, 66].

## 2.8 Summary

This chapter presented an overview of the power systems and its historical evolution with the development and introduction of new technologies. A general description and definition of microgrids, and their advantages and disadvantages were discussed. Finally, a technical overview of conventional protection systems was included to complete the necessary background information relating to the research reported in this thesis.

## References

- [1] M. Josephson, *Edison : a biography*. New York: J. Wiley, 1992.
- [2] H. M. Rustelbakke, *Electric Utility Systems and Practices*. Wiley, 1983.
- [3] B. M. Weedy, *Electric power systems*. Wiley-Blackwell, jul 2012.
- [4] S. Butler, “The nature of UK electricity transmission and distribution networks in an intermittent renewable and embedded electricity generation future,” Ph.D. dissertation, Imperial College of Science, Technology and Medicine, 2001. [Online]. Available: <https://www.parliament.uk/globalassets/documents/post/e5.pdf>
- [5] W. Feldenkirchen, *Werner Von Siemens: Inventor and International Entrepreneur*, ser. Historical perspectives on business enterprise series. Ohio State University Press, 1994. [Online]. Available: <https://books.google.co.uk/books?id=tDJtAXTxkTUC>
- [6] J. D. Glover, M. S. Sarma, and T. Overbye, *Power System Analysis and Design*. Cengage Learning, 2011. [Online]. Available: <https://books.google.co.uk/books?id=uQcJAAAAQBAJ>

- [7] A. A. Sallam and O. P. Malik, *Electric Distribution Systems*, 2nd ed. John Wiley and Sons, 2018.
- [8] M. Hassan and D. Majumder-Russell, “Electricity regulation in the UK: overview,” 2014. [Online]. Available: [https://uk.practicallaw.thomsonreuters.com/1-523-9996?transitionType=Default&contextData=\(sc.Default\)](https://uk.practicallaw.thomsonreuters.com/1-523-9996?transitionType=Default&contextData=(sc.Default))
- [9] G. Simmonds, “Regulation of the UK Electricity Industry,” University of Bath, Bath, Tech. Rep., 2002. [Online]. Available: [https://archive.uea.ac.uk/~e680/energy/energy\\_links/electricity/Electricity\\_Gillian\\_Simmonds.pdf](https://archive.uea.ac.uk/~e680/energy/energy_links/electricity/Electricity_Gillian_Simmonds.pdf)
- [10] M. Heddenhausen, “Privatisations in europe’s liberalised electricity markets—the cases of the united kingdom, sweden, germany, and france,” *Stiftung Wissenschaft und Politik, Research Unit EU Integration*, 2007. [Online]. Available: [http://swpberlin.org/fileadmin/contents/products/projekt\\_papiere/Electricity\\_paper\\_KS\\_IIformatiert.pdf](http://swpberlin.org/fileadmin/contents/products/projekt_papiere/Electricity_paper_KS_IIformatiert.pdf)
- [11] S. Stoft, “Power System Economics Designing Markets for Electricity,” *Wiley & Sons*, vol. 79, no. 5, pp. 402–406, 1973.
- [12] K. Kidokoro, “Price-based and cost-based regulations for a monopoly with quality choice,” University of Tokyo, Tokyo, Tech. Rep., 1996. [Online]. Available: <http://www.csis.u-tokyo.ac.jp/%0Adp/14.pdf>
- [13] Practical Law Energy, “New Electricity Trading Arrangements (NETA).” [Online]. Available: [https://uk.practicallaw.thomsonreuters.com/w-001-6354?transitionType=Default&contextData=\(sc.Default\)](https://uk.practicallaw.thomsonreuters.com/w-001-6354?transitionType=Default&contextData=(sc.Default))
- [14] S. Hutson, “Peak and off-peak electricity times,” 2021. [Online]. Available: <https://www.comparethemarket.com/energy/content/is-energy-cheaper-at-night/>

- [15] International Energy Agency (IEA), “Electricity Information: Overview,” International Energy Agency (IEA), Paris, Tech. Rep., 2020. [Online]. Available: <https://www.iea.org/reports/electricity-information-overview>
- [16] B. Afework, J. Hanania, K. Stenhouse, and J. Donev, “Energy Education - Power plant,” 2020. [Online]. Available: [https://energyeducation.ca/encyclopedia/Power\\_plant#Types\\_of\\_Power\\_Plants](https://energyeducation.ca/encyclopedia/Power_plant#Types_of_Power_Plants)
- [17] C. Lane, “Nuclear Energy Pros and Cons,” 2021. [Online]. Available: <https://www.solarreviews.com/blog/nuclear-energy-pros-and-cons>
- [18] K. Bickerstaff, I. Lorenzoni, N. Pidgeon, W. Poortinga, and P. Simmons, “Reframing nuclear power in the uk energy debate: nuclear power, climate change mitigation and radioactive waste,” *Public Understanding of Science*, vol. 17, no. 2, pp. 145–169, 2008, pMID: 19391376. [Online]. Available: <https://doi.org/10.1177/0963662506066719>
- [19] F. Beaudouin, “Implementing a Multiple Criteria Model to Debate About Nuclear Power Plants Safety Choices,” *Group Decision and Negotiation*, vol. 24, no. 6, pp. 1035–1063, 2015. [Online]. Available: <https://doi.org/10.1007/s10726-015-9428-8>
- [20] Department for Business Energy and Industrial Strategy, “DIGEST of United Kingdom Energy Statistics 2017,” *Digest of UK Energy Statistics (DUKES)*, 2017. [Online]. Available: [www.nationalarchives.gov.uk/doc/](http://www.nationalarchives.gov.uk/doc/open-government-)open-government-
- [21] Committee on Climate Change, “Net Zero: The UK’s contribution to stopping global warming,” London, United Kingdom, Tech. Rep., 2019. [Online]. Available: <https://www.theccc.org.uk/wp-content/uploads/2019/05/Net-Zero-The-UKs-contribution-to-stopping-global-warming.pdf>.

- [22] F. Mitschke, “DIGEST of United Kingdom Energy Statistics 2020: Chapter 5 Electricity,” Digest of United Kingdom Energy Statistics (DUKES), London, Tech. Rep., 2019. [Online]. Available: [https://assets.publishing.service.gov.uk/government/uploads/system/uploads/attachment\\_data/file/904805/DUKES\\_2020\\_Chapter\\_5.pdf](https://assets.publishing.service.gov.uk/government/uploads/system/uploads/attachment_data/file/904805/DUKES_2020_Chapter_5.pdf)
- [23] Jointing Tech, “Power Transmission,” 2020. [Online]. Available: <https://www.jointingtech.co.uk/Power-Transmission>
- [24] SSEN, “Scottish and Southern Electricity Networks - Who we are and what we do.” [Online]. Available: <https://www.ssen-transmission.co.uk/about-us/>
- [25] SP Energy Network, “Our Transmission Network - SP Energy Networks.” [Online]. Available: [https://www.spenergynetworks.co.uk/pages/our\\_transmission\\_network.aspx](https://www.spenergynetworks.co.uk/pages/our_transmission_network.aspx)
- [26] Nation Grid, “National Grid Electricity Transmission — National Grid ET.” [Online]. Available: <https://www.nationalgrid.com/electricity-transmission/>
- [27] C. K. Gan, N. Silva, D. Pudjianto, G. Strbac, R. Ferris, I. Foster, and M. Aten, “Evaluation of alternative distribution network design strategies,” *IET Conference Publications*, no. 550 CP, 2009.
- [28] Eco Power Supplies, “UK Electricity Voltages - EcoPowerSupplies.” [Online]. Available: <https://www.ecopowersupplies.com/uk-electricity-voltages>
- [29] Energy Solutions, “DNO - Distribution Network Operators.” [Online]. Available: <https://www.energybrokers.co.uk/electricity/dno-distribution-network-operators>
- [30] Parliamentary Office of Science and Technology, “UK Electricity Networks,” Parliamentary Office of Science and Technology, London, Tech. Rep., 2001.

- [Online]. Available: <https://www.parliament.uk/globalassets/documents/post/pn163.pdf>
- [31] Transparent, “New home - How do I find out my energy supplier?” 2021. [Online]. Available: <https://forum.ovoenergy.com/switching-suppliers-and-moving-home-144/new-home-how-do-i-find-out-my-energy-supplier-7083>
- [32] N. Jenkins, J. B. Ekanayake, and G. Strbac, *Distributed generation*, 2010.
- [33] P. Crossley, *Microgrids and Active Distribution Networks*, ser. Energy Engineering. Institution of Engineering and Technology, 2009. [Online]. Available: <https://digital-library.theiet.org/content/books/po/pbrn006e>
- [34] P. Salmerón Revuelta, S. Pérez Litrán, and J. Prieto Thomas, “Distributed Generation,” *Active Power Line Conditioners*, pp. 285–322, jan 2016. [Online]. Available: <https://linkinghub.elsevier.com/retrieve/pii/B9780128032169000080>
- [35] T. Funabashi, “Integration of Distributed Energy Resources in Power Systems: Implementation, Operation and Control,” *Integration of Distributed Energy Resources in Power Systems: Implementation, Operation and Control*, pp. 1–309, mar 2016.
- [36] T. Ackermann, G. Ran Andersson, and L. Sö Der A, “Distributed generation: a definition,” *Electric Power Systems Research*, vol. 57, pp. 195–204, 2001. [Online]. Available: [www.elsevier.com/locate/epsr](http://www.elsevier.com/locate/epsr)
- [37] G. Allan, I. Eromenko, M. Gilmartin, I. Kockar, and P. McGregor, “The economics of distributed energy generation: A literature review,” *Renewable and Sustainable Energy Reviews*, vol. 42, pp. 543–556, 2015. [Online]. Available: <https://www.sciencedirect.com/science/article/pii/S1364032114005164>

- [38] W. El-Khattam and M. M. Salama, “Distributed generation technologies, definitions and benefits,” *Electric Power Systems Research*, 2004.
- [39] O. Majeed Butt, M. Zulqarnain, and T. Majeed Butt, “Recent advancement in smart grid technology: Future prospects in the electrical power network,” *Ain Shams Engineering Journal*, vol. 12, no. 1, pp. 687–695, mar 2021.
- [40] OFGEM, DECC, and Smart Grid Forum, “Smart Grid Vision and Routemap Smart Grid Forum,” *Report Number: URN 14D / 056*, no. February, 2014. [Online]. Available: [www.nationalarchives.gov.uk/doc/open-government-licence/](http://www.nationalarchives.gov.uk/doc/open-government-licence/)
- [41] R. H. Lasseter, “MicroGrids,” *2002 IEEE Power Engineering Society Winter Meeting, Vols 1 and 2, Conference Proceedings*, pp. 305–308, 2002.
- [42] J. M. Guerrero, J. C. Vásquez, J. Matas, M. Castilla, and L. García de Vicuna, “Control strategy for flexible microgrid based on parallel line-interactive UPS systems,” *IEEE Transactions on Industrial Electronics*, vol. 56, no. 3, pp. 726–736, 2009.
- [43] D. E. Olivares, A. Mehrizi-Sani, A. H. Etemadi, C. A. Cañizares, R. Iravani, M. Kazerani, A. H. Hajimiragha, O. Gomis-Bellmunt, M. Saeedifard, R. Palma-Behnke, G. A. Jiménez-Estévez, and N. D. Hatziargyriou, “Trends in microgrid control,” *IEEE Transactions on Smart Grid*, vol. 5, no. 4, pp. 1905–1919, 2014.
- [44] C. Phurailatpam, B. S. Rajpurohit, and N. Pindoriya, “Embracing Microgrids : Applications for Rural and Urban India,” *10th National Conference on Synergy with Energy*, no. May, pp. 49–54, 2015.

- [45] N. Hatziargyriou, *Microgrids Architectures and Control*. New York: Wiley and Sons, 2014, vol. 51, no. 3. [Online]. Available: <https://www.amazon.com/Microgrids-Architectures-Control-Wiley-IEEE/dp/1118720687>
- [46] Z. A. Arfeen, “Control of distributed generation systems for microgrid applications : A technological review,” *International Transactions on Electrical Energy Systems*, no. January, pp. 1–26, 2019.
- [47] A. Haun, “Microgrids: Achieving Reliable Power for Our Most Critical Facilities,” 2019. [Online]. Available: <https://microgridknowledge.com/healthcare-microgrids-reliable-power/>
- [48] M. Rengasamy, S. Gangatharan, R. M. Elavarasan, and L. Mihet-Popa, “Incorporation of microgrid technology solutions to reduce power loss in a distribution network with elimination of inefficient power conversion strategies,” *Sustainability*, vol. 13, no. 24, 2021. [Online]. Available: <https://www.mdpi.com/2071-1050/13/24/13882>
- [49] V. Kekatos, G. Wang, A. J. Conejo, and G. B. Giannakis, “Stochastic reactive power management in microgrids with renewables,” *IEEE Transactions on Power Systems*, vol. 30, no. 6, pp. 3386–3395, 2015.
- [50] F. Farzan, S. Lahiri, M. Kleinberg, K. Ghariéh, F. Farzan, and M. Jafari, “Microgrids for Fun and Profit,” *IEEE Power & Energy Magazine*, vol. 11, no. 4, pp. 52–58, 2013.
- [51] United Nations Framework Convention on Climate Change, “Paris Agreement,” United Nation, Paris, France, Tech. Rep., 2015.
- [52] D. French, “Kyoto Protocol to the United Nations Framework Convention on Climate Change,” *Journal of Environmental Law*, vol. 10, no. 1, pp. 215–224, 1998.

- [53] A. Majzoubi and A. Khodaei, “Application of microgrids in providing ancillary services to the utility grid,” *Energy*, vol. 123, pp. 555–563, 2017. [Online]. Available: <https://www.sciencedirect.com/science/article/pii/S0360544217301202>
- [54] M. Farrokhhabadi, C. A. Cañizares, J. W. Simpson-Porco, E. Nasr, L. Fan, P. A. Mendoza-Araya, R. Tonkoski, U. Tamrakar, N. Hatziargyriou, D. Lagos, R. W. Wies, M. Paolone, M. Liserre, L. Meegahapola, M. Kabalan, A. H. Hajimiragha, D. Peralta, M. A. Elizondo, K. P. Schneider, F. K. Tuffner, and J. Reilly, “Microgrid stability definitions, analysis, and examples,” *IEEE Transactions on Power Systems*, vol. 35, no. 1, pp. 13–29, 2020.
- [55] M. Stadler and A. Naslé, “Planning and implementation of bankable microgrids,” *The Electricity Journal*, vol. 32, no. 5, pp. 24–29, 2019. [Online]. Available: <https://www.sciencedirect.com/science/article/pii/S1040619019301216>
- [56] A. Dagar, P. Gupta, and V. Niranjana, “Microgrid protection: A comprehensive review,” *Renewable and Sustainable Energy Reviews*, vol. 149, p. 111401, 2021. [Online]. Available: <https://www.sciencedirect.com/science/article/pii/S1364032121006869>
- [57] S. C. Vegunta, M. J. Higginson, Y. E. Kenarangui, G. T. Li, D. W. Zabel, M. Tasdighi, and A. Shadman, “AC microgrid protection system design challenges—a practical experience,” *Energies*, vol. 14, no. 7, 2021. [Online]. Available: <https://www.mdpi.com/1996-1073/14/7/2016>
- [58] A. C. Zambroni de Souza and M. Castilla, *Microgrids design and implementation*, 2019.

- [59] C. Booth and K. Bell, “Protection of transmission and distribution (T&D) networks,” in *Electricity Transmission, Distribution and Storage Systems*. Woodhead Publishing, jan 2013, pp. 75–107.
- [60] IEC, *International Standard Norme Internationale Measuring relays and protection equipment-Part 121: Functional requirements for distance protection Relais de mesure et dispositifs de protection-Partie 121: Exigences fonctionnelles pour protection de distance*, 2014.
- [61] ALSTOM, *Network Protection & Automation Guide*. Alstom Grid, 2011. [Online]. Available: <http://rpa.energy.mn/wp-content/uploads/2016/07/network-protection-and-automation-guide-book.pdf>
- [62] P. Barker and R. De Mello, “Determining the impact of distributed generation on power systems. i. radial distribution systems,” in *2000 Power Engineering Society Summer Meeting (Cat. No.00CH37134)*, vol. 3, 2000, pp. 1645–1656 vol. 3.
- [63] “IEEE draft standard for interconnecting distributed resources with electric power systems - amendment 1,” *IEEE P1547a/D3*, December 2013, pp. 1–12, 2014.
- [64] F. Pilo, G. Celli, and S. Mocci, “Improvement of reliability in active networks with intentional islanding,” in *2004 IEEE International Conference on Electric Utility Deregulation, Restructuring and Power Technologies. Proceedings*, vol. 2, 2004, pp. 474–479 Vol.2.
- [65] H. Mohamad, S. Sahdan, N. N. Y. Dahlan, and N. M. Sapari, “Under-frequency load shedding technique considering response based for islanding distribution network connected with mini hydro,” in *2014 IEEE 8th International Power Engineering and Optimization Conference (PEOCO2014)*, 2014, pp. 488–493.

- [66] M. A. Zamani, T. S. Sidhu, and A. Yazdani, “Investigations into the control and protection of an existing distribution network to operate as a microgrid: A case study,” *IEEE Transactions on Industrial Electronics*, vol. 61, no. 4, pp. 1904–1915, 2014.

## **Chapter 3**

# **Literature Review: Microgrid Protection Challenges and Solutions**

Researchers are studying and analysing protection related problems that may arise or already been raised in power system due to different incidents. Also, numerous control and protection schemes are suggested in the literature to face those future challenges due to increased number of new technologies that are expected to be integrated with power system. However, this research findings suggest those proposed solutions have certain limitations. Hence, this chapter will first present microgrids/active distribution networks' protection related issues, then will discuss about the solutions that are suggested in the literature, and finally will critically review those solutions highlighting potential limitations that can be challenging for protection of microgrids that are dominated with power electronics inverter-interfaced renewable generation.

### 3.1 Protection Issues due to Integration of Distributed Generation

Several challenges in the future GB's power system network due to integration of the distributed generation (DG) are discussed in the [1, 2, 3], among them reduced system inertia, rate of change of frequency (RoCoF), frequency containment, voltage management, protection and stability are the main concern. From the protection perspective, reduction of overall short circuit level (SCL) and system inertia are the two most concerning parameters with the reduction of conventional synchronous generation in the power system.

One of the major reasons behind the reduction of SCL and system inertia is the use of power electronics-based inverters to interface DC sources (for example, solar PV and energy storage) in the AC distribution networks. At the transmission level, interconnection of other power systems (import and export through HVDC lines) and with major renewable generation installation (for example, offshore wind farms) can reduce the overall SCL and inertia of the existing power system network. These sources cannot provide the same SCL as the rotating conventional synchronous generators can provide. Similarly, many non-synchronous generators cannot supply inertial support to the power system as they are interfaced via power electronic converters (although many control schemes providing "synthetic inertia" have been researched and developed [4]). As a result, during an event of fault or any other disturbance in a low inertia system, there is a large frequency deviation which can cause large RoCoF and that can disconnect generators and connected loads causing further frequency disturbance and eventually a black-out in the worst-case scenario where frequency is not managed properly. In recent years, many coal-fired and nuclear power stations around the UK have been decommissioned and that has significantly reduced the number and capacity of rotational synchronous generators. Therefore, it is expected that SCL and inertia

of the power system will reduce significantly in future with further integration of renewable DERs [1].

Typically, protection issues of microgrids and low voltage distribution networks are classified into two main categories. The first category is related to the loss of coordination and issues with settings and responses across the various protection relays, reclosers and fuses during grid connected operation, and the protection issues during islanded mode of operation. The second category related to loss of mains (LOM) protection – however, this is not addressed further in this thesis as it is outside of the scope of this research. In this research, several protection issues with relays, reclosers and fuses that are addressed by different researchers are covered and presented. A number of these issues with illustrative examples are presented in this section. For each of the identified challenges, comments are made as to the relevance of the work reported in this thesis and how it may address or resolve the identified issues and challenges.

### **3.1.1 Sympathetic Tripping**

If healthy section(s) of a network get disconnected by the protection device(s) due to fault in another section, then this is known as sympathetic tripping of that protection device(s). Sympathetic tripping can be caused by network relays tripping due to changes in fault current magnitude/direction for remote faults (that they should not trip for), and sympathetic tripping can also be experienced when DG (or DG interface) protection trips on undervoltage as a remote fault (for which it should not operate) is on the system for a long enough time such that the undervoltage protection may operate. This particular form of sympathetic tripping is covered in more detail in Section 3.1.4. The remainder of this section covers the overcurrent-based sympathetic tripping phenomenon.

Sympathetic tripping can also be termed as false tripping. This type of tripping compromises the discrimination, selectivity and stability criteria of a protection

system and is highly undesirable since it causes unnecessary loss of loads and losses to the utility provider in turn.

The protection of conventional distribution network is designed based on the assumption that the network has a unidirectional power flow during normal and fault condition [5]. However, presence of DGs in the distribution network can result in bidirectional currents under certain circumstances both under normal and fault condition. Therefore, current with high enough magnitude, opposite to the regular direction may cause a trip and opening of the corresponding CBs although there is no fault on the downstream line.

Sympathetic tripping can be explained properly by an example shown in Figure 3.1, where, a radial distribution network with five different buses and loads are connected to bus 2, bus 3 and bus 5. Overcurrent relays are installed at different sections of the network. Relay,  $R_1$  is connected between bus 1 and 2,  $R_2$  is connected between bus 2 and 3,  $R_3$  is connected between bus 1 and 4 and  $R_4$  is connected between bus 4 and 5. The settings for the overcurrent relays are pre-specified based on the grid's fault level calculations. After that let us assume,  $DG_1, DG_2$  and  $DG_3$  are getting connected at bus 3, bus 4 and bus 5 respectively.

For a fault between bus 2 and 3 as shown in Figure 3.1,  $DG_1, DG_2$  and  $DG_3$  will contribute large currents towards the fault (shown in Figure 3.1 with blue line) along with the grid. For this fault, relay  $R_2$  is the main protection relay and relay,  $R_1$  is backup protection. However, if the fault currents contribution from the  $DG_2$  and  $DG_3$  are large enough then there is a possibility of unnecessary tripping of relay  $R_3$  and  $R_4$  depending on their settings although there is no fault in the related sections of the relay  $R_3$  and  $R_4$ . This type of sympathetic tripping causes stability and sensitivity characteristic of the protection relays to reduce.

Again, there is a possibility of sympathetic tripping for relay  $R_3$  and  $R_4$  even there is no fault in the line. For example, if the power supply from grid is low, and  $Load_1$  and  $Load_2$  consumes additional power, then both the  $DG_2$  and  $DG_3$

will supply that additional power (depending on their ratings). In this process depending on the settings of  $R_3$  and  $R_4$  there is a possibility of either one of them or both relays will operate unnecessarily. This situation will severely decrease the discrimination characteristic of the protection system.

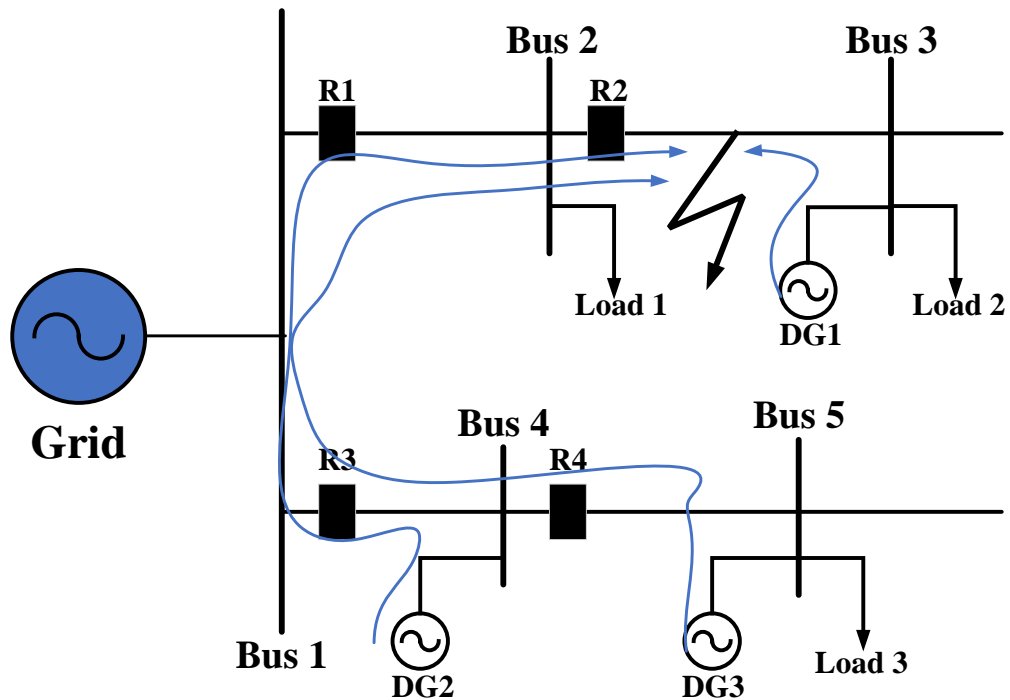


Figure 3.1: An example of radial distribution network with multiple DG units contributing to a fault.

The problem of sympathetic tripping is more severe in case of synchronous based DGs, but in case of IIDGs, fault current contribution is limited and hence, the problem may not be so acute. Also, use of directional characteristic in the relay may solve this problem. In case of directional overcurrent relays, there are two different settings for two different direction which can avoid sympathetic tripping [6]. However, for the fault in Figure 3.1,  $DG_1$  is also contributing to the fault, now even if  $R_2$  clears the fault,  $DG_1$  will continuously supply fault currents (until protection of  $DG_1$  activates).

The methods developed in this research and reported in the thesis would

overcome this issue as detection of fault would be based on harmonic component rather than measuring fault current magnitude. The tripping times for the scheme reported in this thesis range from 0.1 – 0.3 s, and this would further reduce risks of any sympathetic tripping (which is more likely for faults where the overcurrent protection takes a relatively long time to operate – main protection fault clearance times of up to 1 s can be experienced in time-graded overcurrent-based systems). Therefore, the risk sympathetic tripping of other network protection and/or DG interface protection in the vicinity would be reduced significantly. Furthermore, the use of overcurrent relays may not be required (perhaps only as a second line of backup protection), further reducing the possibility of sympathetic tripping on overcurrent.

### 3.1.2 Blinding of Protection Relays

When a DG is connected between a relay and fault position, DG increases its output current due to fault while decreasing the fault current measured by the upstream relay (upstream from DG) simultaneously, which may cause the protection relay to operate slowly or in the worst situation, theoretically the protection relay may not operate at all. This mal-operation of the relay termed as blinding of the relay [7, 8] or protection under reach [9, 10]. This protection challenge can be explained properly with the help of Figure 3.2.

As can be seen from Figure 3.2, a DG is connected between a bolted fault and protection relay. The direction of fault current supplied by DG,  $I_{F,DG}$  is from Bus 2 to fault, and voltage at Bus 2 and Bus 1 will increase (compared to the fault situation when DG is not connected). Subsequently, the current supplied by the grid,  $I_{F,Grid}$  towards the fault and relay decreases, which might cause relay to operated slowly.

The proposed protection relay does not depend upon the current magnitude supplied by the generators in the system. Therefore, blinding of protection relay

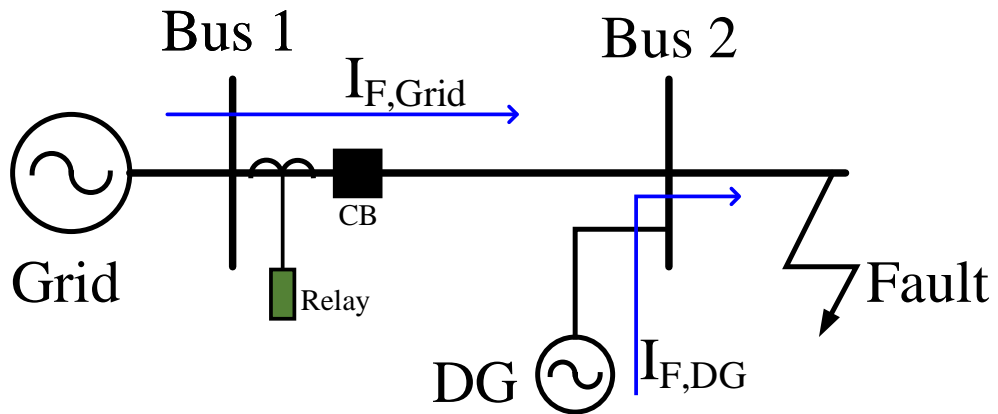


Figure 3.2: Example of protection blinding.

can successfully overcome by the proposed solution.

### 3.1.3 Coordination Issues with Backup Protection

Impact of DGs on the protection system largely depends upon its number, capacity and location. Reference [11] discusses the issue of loss of grading or loss of coordination of overcurrent relay and [12] simulates different scenarios by varying multiple DGs' location and capacity. It is shown in [12] that with certain conditions of DG's capacity and location there is a possibility of operation of backup or secondary protection before the operation of primary protection (loss of coordination between primary and backup protection).

The plug setting (PS) and time multiplier setting (TMS) of overcurrent relays are calculated through fault current levels of the network and remain constant during the operation of the distribution network. However, due to additional fault currents supplied by any synchronous machine-based DG units during grid connected mode of operation, the existing protection with fixed settings can operate faster than it should, which may lead to tripping of backup protection before primary protection and ultimately loss of coordination between the relays.

For example, in Figure 3.1, relay  $R_1$  provides backup protection for relay  $R_2$ .

Thus, for any fault between bus 2 and bus 3,  $R_2$  should operate first and then  $R_1$  should operate if necessary. However, this expected behaviour deviates due to additional fault current supply from  $DG_2$  and  $DG_3$  (assuming the relays,  $R_3$  and  $R_4$  will not operate). This problem can cause serious issues in case relays in the network use instantaneous element for fast tripping. A case from [12] is demonstrated here in Figure 3.3, which is an IDMT characteristic graph of relay  $R_1$  with instantaneous element. The green cross on the Figure 3.3 indicates the operating time without DG, while the red cross indicates the operating time and fault current with DGs connected to bus 4 and bus 5. So, for fault between bus 2 and bus 3,  $R_1$  may operate instantaneously due to additional fault current supply from DGs and ultimately will cause loss of coordination between relay  $R_1$  and  $R_2$ .

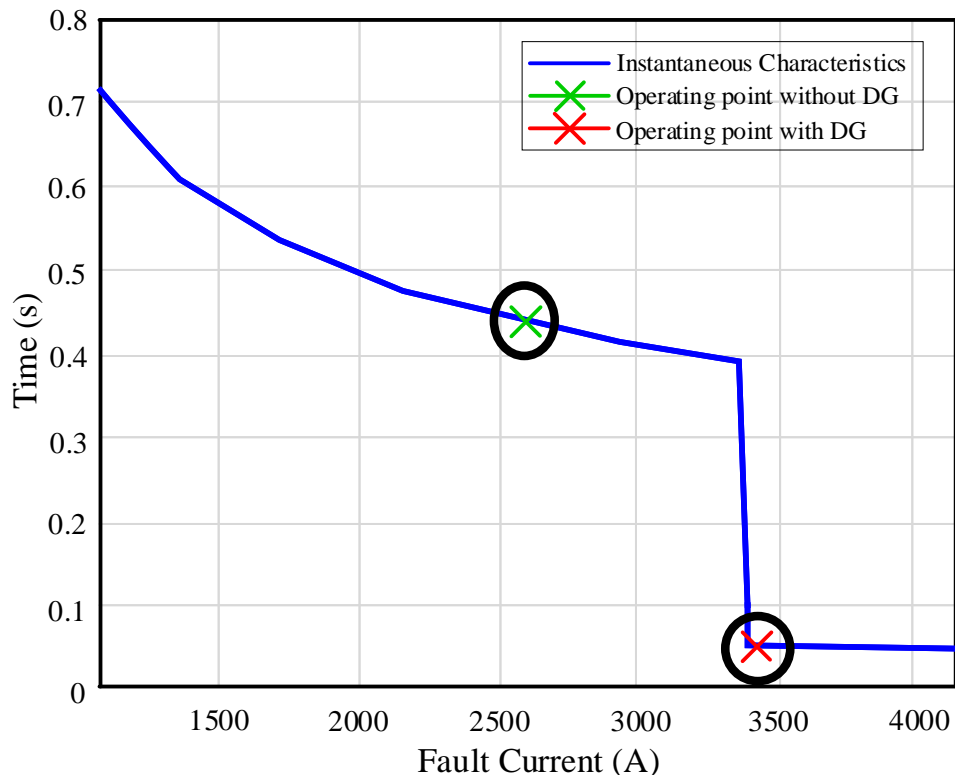


Figure 3.3: Instantaneous protection characteristic showing with and without DG fault current contribution [12].

To address the coordination issue among the relays, the proposed protection scheme reported in this thesis uses definite time settings in lieu of inverse definite minimum time (IDMT) settings. IDMT characteristic for the protection relays are most common and popular since it provides an inverse relation between operating time and current magnitude. The scheme reported in this thesis is effectively a unit-based scheme with incorporated backup, based on definite time settings which are shown to be advantageous for microgrid protection, as outlined in Chapter 5. This means that the use of IDMT systems, and the backup coordination problems that may occur as explained in this section can be solved easily with the use of definite time settings (details in Chapter 5).

### **3.1.4 Nuisance Tripping of Undervoltage Protection**

One of the solutions for loss of coordination problem can be changing the time settings of the overcurrent relays. However, change of settings; for example, increase in time grading, might cause delay in relay operation, which in turn creates more challenges such as nuisance tripping of DG units' under voltage protection.

According to settings policy/guidelines document G59/3 [13], two stages of undervoltage protection should be imposed to facilitated appropriate fault ride through capability and according to stage 2 of the undervoltage protection policy, the undervoltage protection of DG in the distribution network shall trip after 0.5 s if the measured network voltage at the DG location is less than 80% of nominal. However, overall reduction of fault level in the distribution network due to addition of DGs with limited short circuit current might cause installed overcurrent relays to operate slowly than it should (more than 0.5 s). Also, overcurrent relays may operate slowly due to the coordination intervals between the primary and backup relays. As a result, there is a possibility of unnecessary tripping of the DG's undervoltage protection.

Again, the developed protection algorithm in this research would overcome this issue as faults would be cleared quickly (100 ms) and the possibility of sustained faults and therefore, nuisance tripping of DGs due to undervoltage can be significantly reduced.

### 3.1.5 Out of Phase Reclose Issue

Most of the faults in the distribution network are temporary in nature. So, to resolve the issue of the temporary faults, the combination of the reclosers, fuse and sectionalisers are used. Generally, reclosers open the line during temporary fault for few hundreds of milliseconds (referred as reclosers dead time) before closing and recheck the fault exists or not [14]. If fault exists, then reclosers open the line again and attempt 3 or 4 times before permanently opening the line.

During the deadtime of the reclosers operating sequence (i.e. when the recloser is open) in the islanded condition, there is a chance of developing a different phased voltage across the open terminals of recloser and causes out-of-phase reclosing, which could eventually cause damage to the network infrastructure [15]. Furthermore, during the deadtime, the deionised arc may actually be ionised by the sustaining arc from DGs, which could cause a temporary fault to become permanent [14].

This issue would not necessarily be resolved by the protection scheme reported in this thesis. However, the scheme is able to identify faulted sections with a higher degree of certainty than non-communicating overcurrent/recloser-based schemes, and perhaps this could be used to enhance or change the logic relating to auto-reclose schemes in the future. However, the issue with system angular drift during periods of system separation may remain in the future if DG is widely used, but solving the issue of temporary faults is outside of the remit of this research.

### 3.1.6 Recloser and Fuse Coordination

There are two types of techniques to coordinate reclosers and fuses in distribution networks: fuse sacrificing and fuse saving. Fuse saving is the most widely used technique in practice [16]. Reclosers clear temporary faults by tripping relatively faster than fuses (that is, faster than the time at which fuse will blow) in the “fuse saving” mode. On contrary, fuse picks up the fault current and blow before the upstream reclosers attempt in the fuse sacrificing scheme [16].

Placement of DG (for example, between the recloser location and the fuse, for a fault downstream of the fuse) could act to increase fault current (or cause fault current to persist) for a fault beyond the fuse, resulting in fuse blowing, and potentially resulting in slower recloser operation due to reduced “upstream” fault current. These coordination problems are discussed further in [11, 17, 18]. The coordination between recloser and fuse can also be explained by Figure 3.4.

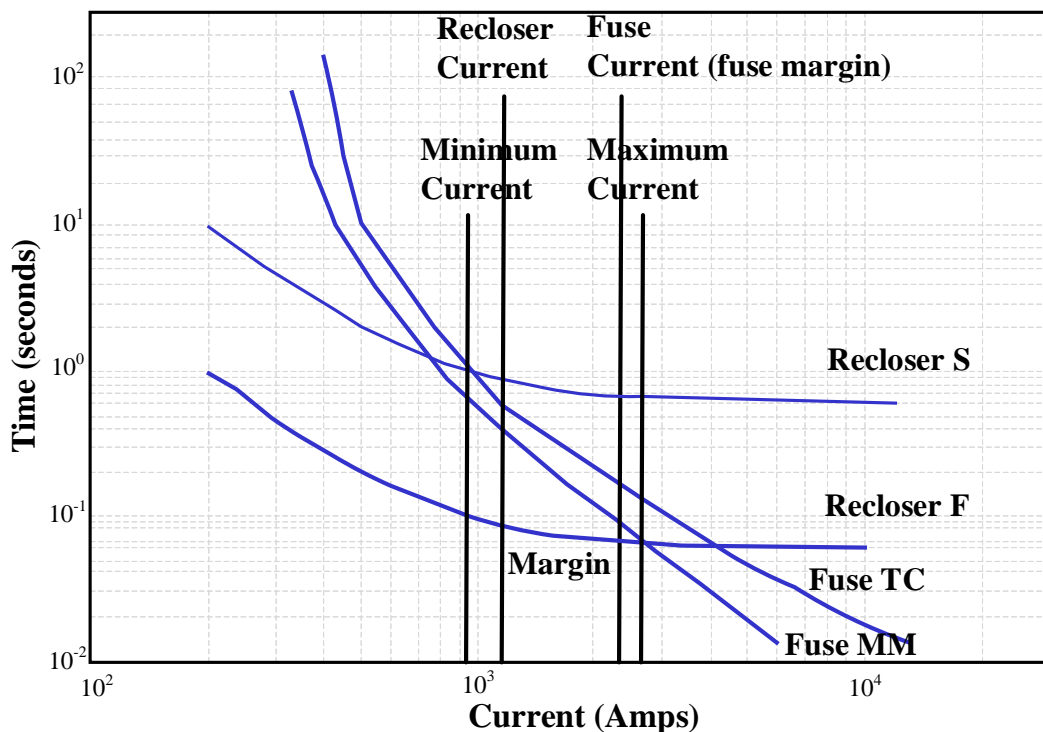


Figure 3.4: Coordination between fuse and recloser [18].

Two characteristic curves for each reclosers and fuses can be observed in Figure 3.4, Recloser has fast (denoted as F) and slow (denoted as S) curves and similarly, the fuse also has two curves TC and MM curve. TC indicates total clearing and MM indicates melting margin. The operation sequence for the reclosers is F-F-S-S so that fuse has ample time to operate during temporary fault. However, when there is a DG connected to the distribution network, it will supply additional current to the system and as a result, the grading coordination between fuse and reclosers will be lost. During a temporary fault, fuse will blow fast due to lower recloser current margin after addition of DG which is undesirable for fuse saving approach.

The system reported in this thesis is effectively a unit-based scheme and can identify the fault location with greater accuracy than convention schemes. Accordingly, the coordination issues here may not be experienced in a system equipped with the protection scheme outlined in this thesis. The solutions to the issues of temporary faults as explained in Section 3.1.5 and 3.1.6 are not the focus of this research. These two sections are provided only for knowledge purpose.

### **3.1.7 High Impedance Faults**

High impedance faults (HIFs) generally occurs while an energised conductor touches quasi-insulated materials, for example, a tree, pole with high grounding, or even the ground in case of conductor breaking and falling [19]. Increase or addition of DGs in the active distribution network neither has impact on the HIFs nor its occurrence in the network. However, this type of fault has been concerned for the distribution and transmission networks operators for many years [19]. The characteristics of HIFs can vary significantly; however, in this research, HIFs are simulated as high resistance faults between phases and earth.

During the calculation and setting of parameters for the relays, fault in the distribution network generally assumed to have negligible or almost zero impedance.

However, due to HIFs, the fault current in the network reduces than the expected value and reduction of voltage is also not so significant compare to a fault condition. Therefore, the conventional overcurrent protection scheme may not be able to detect this type of fault [20] since it is cannot distinguish difference between load variation and fault scenario.

Reference [21] calculates the possible resistance value during line to earth fault and [12] simulates different scenarios by changing fault resistance and observed that the operating time of the overcurrent relay increases as the fault resistance increases. So, there is a possibility of slow operation or mal operation of the protection scheme when fault resistance increases.

The operation of the scheme in this research has been validated for HIFs. Fault at different location of the network have been simulated with different values of fault resistance and successful tripping from the relays verifies its effectiveness, with a maximum fault resistance of  $60 \Omega$  being able to be identified. The details of the validation against HIFs are described in Chapter 6.

## **3.2 Critical Literature Review of Proposed Protection Solutions**

It can be understood from the above discussion that, under certain circumstances, conventional overcurrent protection scheme for active distribution networks/microgrids may no longer suitable or sufficient for future applications due to significant addition of the DGs. To mitigate and address protection issues, several solutions have been proposed by different researchers. This section of the paper outlines and analyses various protection solutions from the appropriate literature. The schemes are classified into three categories and critical descriptions for different protection solutions are described in the following subsections.

### 3.2.1 Adaptive Protection Scheme

Adaptive schemes are the most popular and widely researched form of flexible protective solution. Different methods and algorithms are carried out and discussed in [22, 23, 24, 25, 26]. A good definition of adaptive protection scheme is provided in the [27] which is,

“Adaptive protection is a protection philosophy which permits and seeks to make adjustments to various protection functions in order to make them more attuned to prevailing power system condition”

From the definition it is clear that the scheme can change the various protection settings such as plug settings (PS) and time multiplier settings (TMS) for the overcurrent relays according to the prevailing fault levels in the network.

Reference [28] presents an adaptive protection scheme that can protect active distribution network with high penetration levels of DG. In this solution, active distribution network is divided into several zones and each zone has sufficient amount of load(s) and DG units. Again, these zones are separated by individual breakers as shown in Figure 3.5. All the breakers and DG relays are controlled by a central controller and has the capacity to communicate with each relay and breaker. During fault, the main relay detects and locates the fault and isolate the appropriate section with the help of central controller.

The problems with the scheme are, in addition to extra sets of equipment to operate and coordinate the protective relays properly, practically it is difficult divide the zones based on the balance of load and DG capacity. Also, there is a possibility of islanding after opening of a breaker due to fault and the paper neither discussed islanded network’s frequency and voltage stability and control (for example, operation of the islanded network with the sets of DGs and loads) nor protection of individual zone of the islanded network while fault current is significantly low. Therefore, suggested scheme may not operate properly during

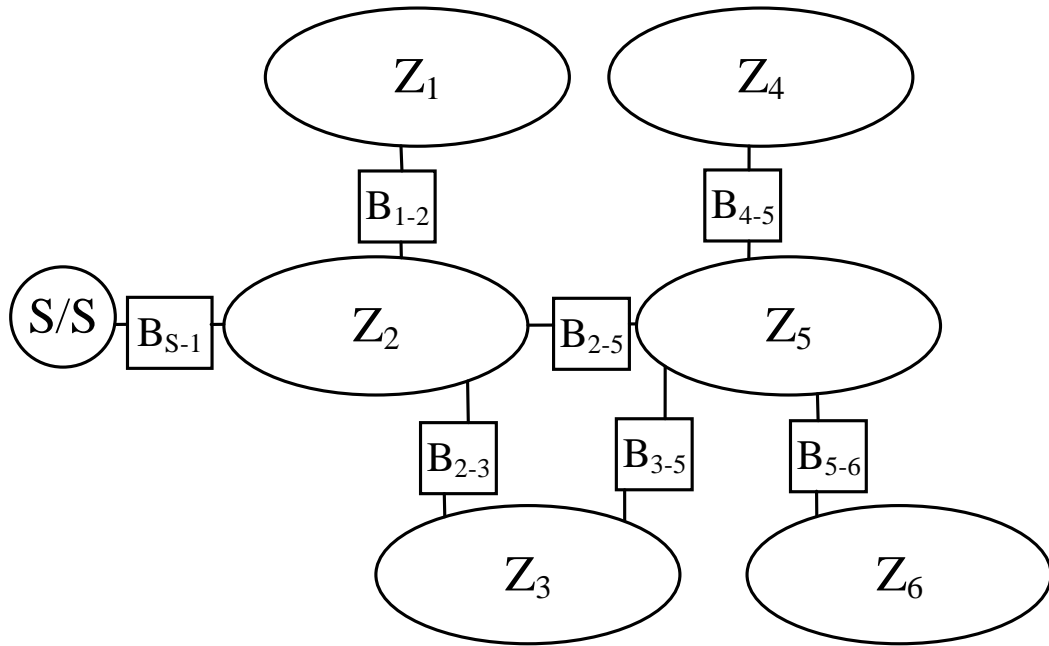


Figure 3.5: Zonal division of distribution network according to [28].

the islanded operation. The solution presented in this thesis capable of successfully operating in islanded modes under a wide a range of fault situations, as discussed and presented in Chapter 6.

A three-layer architecture based adaptive overcurrent protection scheme is proposed in [22]. The layers of the scheme are shown in Figure 3.6, where at the bottom it has primary system containing lines, transformer, DG and circuit breaker. The first layer is execution layer which contains intelligent electronic devices (IEDs), the second layer is coordination layer which maintains the monitoring and coordination. Finally, at the top, the scheme has energy management layer which is responsible for managing overall network. All the layers can communicate with each other through communication protocols. This scheme changes existing overcurrent protection settings based on the reading from continuous monitoring block in the coordination layer.

Positive aspect of the scheme is it can manage to alter overcurrent relay settings by monitoring different topologies of the distribution network such as

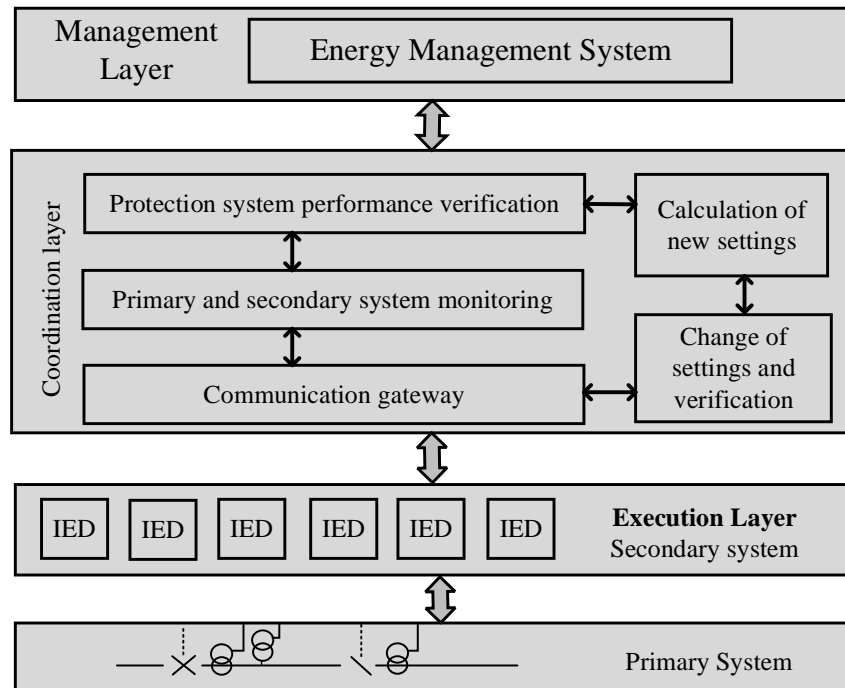


Figure 3.6: Three-layer architecture of the adaptive protection scheme suggested in [22].

connection and disconnection of DGs (for example, by assessing corresponding CBs' status information), change of modes (grid connect to island, vice versa), and active network management. However, the scheme is too much dependent upon the communication and managing all the scenarios of the network might be complicated due to large amount of data. Again, the solution presented in this thesis does not require communications and is not overly complicated to configure or set up, as shown in Chapter 5.

The adaptive system suggested in [25], has two blocks to operate the scheme as shown in the flowchart of Figure 3.7. The operation of real time block is like traditional adaptive protection system- tripping decision and settings are updated based on the measurements units. However, non-real time block decides whether to change the protection settings based on the prediction of the data of DG availability. However, exactly how the settings can be changed, based upon

predicted DG status and availability, is not discussed in detail in this publication. The proposed approach of adaptive scheme is suitable for grid-connected operation assuming prediction of data from DG are accurate and communication is reliable but during islanded mode it might not work properly. Also, the scheme may not operate properly for the IIDG dominated microgrid, which is addressed by the solution proposed in this thesis.

Two groups of pre-calculated overcurrent settings, one for grid connected mode and one for islanded mode are used by [29, 30]. The scheme is relatively simple but how to maintain coordination between the relays are not discussed in this research. Also, DG connection and disconnection might cause serious issues since it requires additional calculation and needs update the settings (though update of the settings is not discussed in the research). In the proposed solution, the settings do not need to be changed with change of the connection of the generation and load since detection of fault depends upon the harmonics in the network and coordination is achieved by definite time settings.

The proposed scheme of [24] is validated by hardware-in-the-loop (HIL) simulations. In this scheme several settings groups for the OC relays are calculated in real time by considering fault contribution from the different sources. To maintain the coordination between the relays, the optimisation technique is used. Complex implementation of the algorithm is the main challenge of this scheme. As shown in the Chapter 5, the proposed solution is independent of fault level of the system and therefore, solution does not need to carry out extensive calculation as required for the adaptive based protection schemes.

A short summary of above-mentioned adaptive protection schemes is presented in Table 3.1. The various shortcomings of each method are summarised in the table; and it is proposed that many of these shortcomings are addressed by the scheme proposed in this thesis.

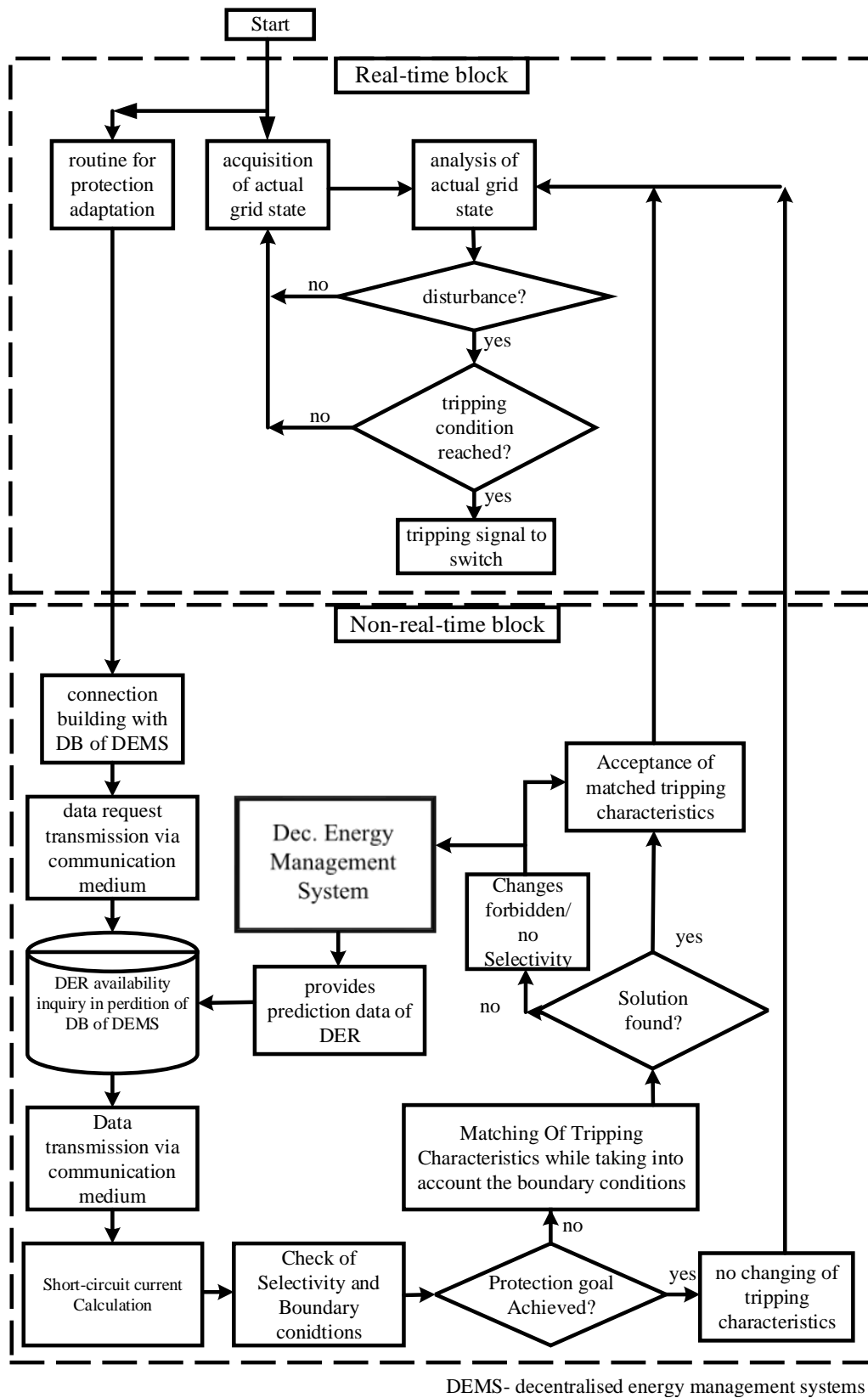


Figure 3.7: Flowchart of the adaptive scheme suggested in [25].

Table 3.1: Summary of the adaptive protection schemes.

Referenced Article	Description of the Method	Positive Impacts	Shortcomings
[28]	Central controller based adaptive protection compares fault current with total generation contribution during normal condition.	The paper discussed the relay's settings along with its coordination with CBs and the scheme is suitable for large integration of DGs.	Differentiating excessive load current with fault condition, and the offline calculations needed to be run with each addition of DGs and load variations.
[22, 25]	Communication based adaptive over-current protection scheme.	Can be operated in both grid-connected and islanded mode, and can maintain coordination between main and backup relays.	Dependent on communication channels, requires additional devices and therefore, expensive.
[29, 30]	Settings are modified based on detection of islanding.	The proposed scheme is relatively simple.	Coordination with backup relays could be challenging.
[24]	Online fault level calculation and optimisation approach is used for calculation of settings.	Validated through the HIL simulations. Addresses impact of DGs on coordination of the relays.	Expensive due to communication and additional devices. Complex due to lots of online calculation.
[31]	Settings are modified based on fault current ratio between reclosers and fuse.	Validated against high impedance fault.	Require more validation with different scenarios with different DG locations.
[32]	The adaptive approach is achieved through real-time calculation of the Thevenin equivalent parameters.	Economical since modifications are based on local measurements.	Accuracy of the measurements. Requires lots of rigorous calculation and if the network size increases, the scheme might not work properly.

### 3.2.2 New Protection Algorithm

To acknowledge future distribution network protection requirements, various studies suggest novel protection methods that replace conventional method of mea-

suring overcurrent to detect fault. Specifically, inverter-interfaced source/storage installation typically do not produce significantly large currents when faults occur close to them as converters are designed and controlled in such a way that they cannot carry large fault currents due to their rated thermal capacity [33]. This typical limit of fault currents may not be sufficient to activate IDMT overcurrent relays. Various types of protection schemes are suggested, including protection based on voltage measurement, harmonic content and travelling waves. Each produces different techniques to locate and identify the faults.

Several researchers [34, 35, 36, 37, 38, 39, 40] suggest existing protection scheme from the transmission networks such as distance protection and differential protection, to be utilised as the main protection for low voltage distribution networks and microgrids.

Distance protection analyses the line impedance through the measurements of both current and voltage to detect and locate the fault in the transmission line. There are different characteristics distance relays (for example, mho, quad), but mho type distance relays are most widely used relays for transmission protection.

Distance protection may consider to be a suitable protection solution for protection of microgrids and systems with high penetrations for distributed generation since it has been tested and practically been used in transmission networks for a long time. However, different real-time simulation based results [41, 42, 43] verifies that the distance protection scheme may not operate accurately due to large interconnection of distribution generation. Furthermore, [44] explains different scenarios of where distance protection either operates slowly or does not operate due to power-electronics based converter's connection with the explanation of distance protection's overreach and underreach protection. Moreover, distance protection requires communication between relays to facilitate accelerate and blocking scheme. As mentioned earlier distance relay makes decision based on the measurement of voltage and current and therefore, require additional measurement

which can increase the expense with addition of communication channels. The proposed relay as explained in Chapter 5 only requires current measurements to detect the harmonic component, hence, does not require additional measuring devices. Also, this solution is suggested by carefully analysing the fault behaviour of both short and long-distance distribution networks/microgrids while distance protection is more suitable for long distanced transmission network.

Differential protection algorithm is based on the Kirchhoff's current law (summation of the currents entering a node and leaving the node must be zero) and therefore, differential relays compare the current magnitude at the both ends of a protection equipment. Differential protection can detect the fault most accurately with proper selectivity and sensitivity. Therefore, differential protection scheme can be most suitable solution for the protection of microgrids.

However, differential protection requires dedicated (and expensive) communication channels with relays at both end of a protected element and does not provide any inherent backup protection like other non-unit protection scheme i.e. distance and overcurrent protection. Hence, this scheme can be very expensive for microgrid protection – often separate communication channels, and backup channels are required, and there can be issues experienced with latency and/or jitter, and timing synchronisation of measurements is required (which could involve the use of GPS timing systems). All of this could further add to costs and complexity. Finally, use of dedicated communications may also lead to risks associated with cyber security and attack [45, 46]. As shown in Chapter 5, the suggested scheme in this thesis does not require any communication and provide inherent backup protection, therefore, the proposed scheme can be cheaper than the differential protection.

The scheme proposed in [47] utilises total harmonic distortion (THD) to identify and locate a fault in microgrid. The relay in this scheme observes the THD at the inverter's terminal voltage. The protection algorithm of the scheme

is shown in Figure 3.8.

The scheme has two stages: the first stage detects the fault and identifies the fault type, and second stage provides fault location/coordination between the relays of different sections of the line. Fault is identified by measuring total harmonic distortion (THD) from the three-phase voltage. The THD for each phase are calculated separately. According to the scheme, the fundamental frequency amplitude of the voltage will reduce significantly for the faulted phase(s) compared to healthy phase(s). In the second stage, for coordination and locating the fault, communication link is used and summation of THD the both ends relays of the network are compared to detect the location of the fault which is quite similar to the differential protection scheme.

The coordination among the relays are not demonstrated comprehensively using a range of different case scenarios. Therefore, there is a chance that the scheme might not work properly if the fault location is changed or additional DGs in the network are added or remove one of them from the network. This scheme requires more validation with different fault cases while the proposed scheme has been validated against a wide range of simulated cases. Also, the proposed solution demonstrated coordination among the relays with different cases by changing fault and IIDG locations in the network, and does not require communication to isolate the faulted section.

The same authors from [47] proposed different voltage-based protection scheme in [48]. The scheme requires to convert ‘*abc*’ phase domain voltage signals into the ‘*dq*’ frame. The scheme can be illustrated with the aid of following figure, Figure 3.9. The ‘*dq*’ voltage values are compared to reference voltage value to extract disturbance signal which is then compared with threshold to detect fault. However, communication is required to locate the fault and isolate the fault section only. The suggested scheme in Chapter 5 of this thesis can isolate the faulted section without the support from communication channels.

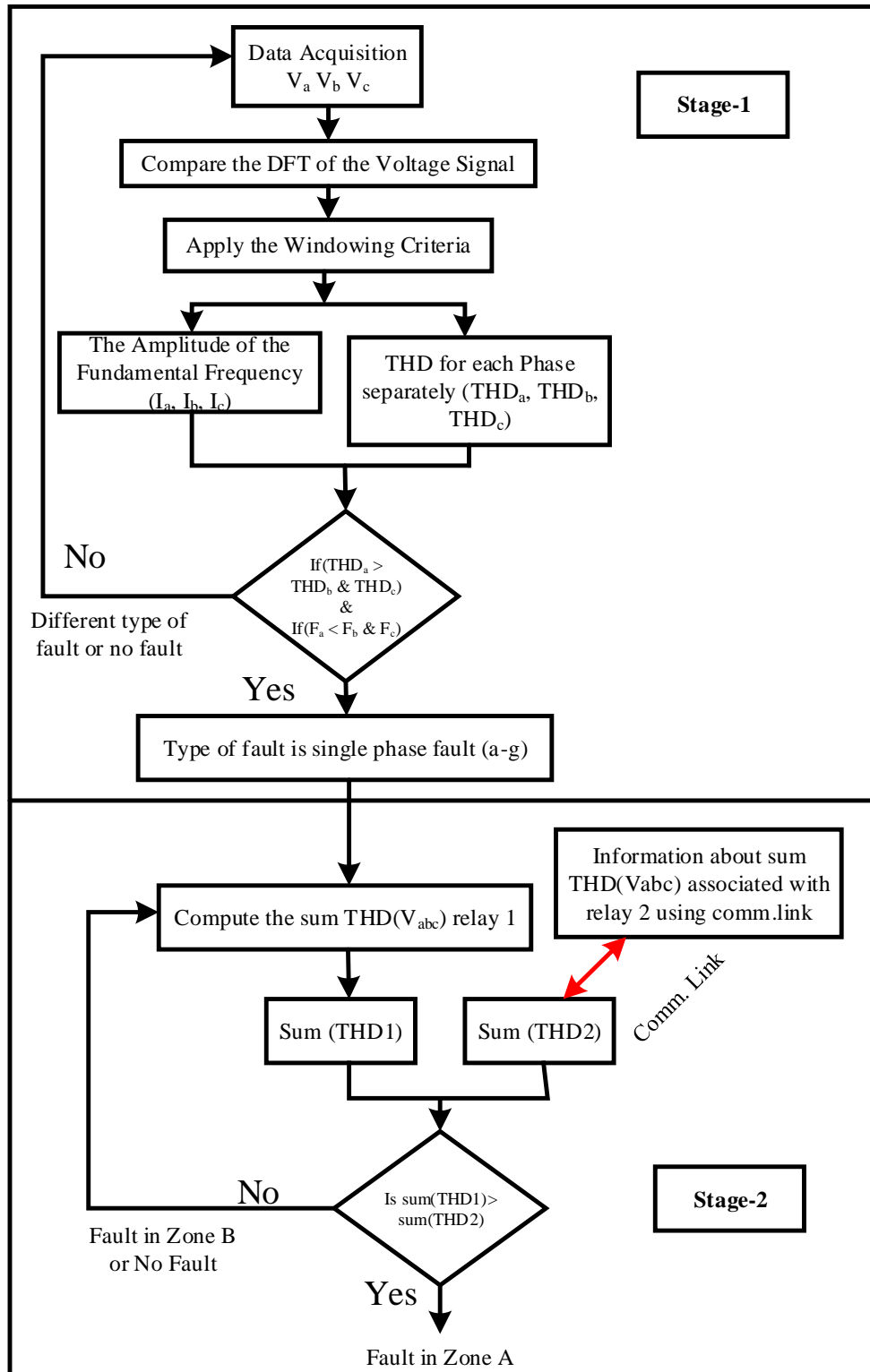


Figure 3.8: Block diagram of the protection scheme proposed in [47].

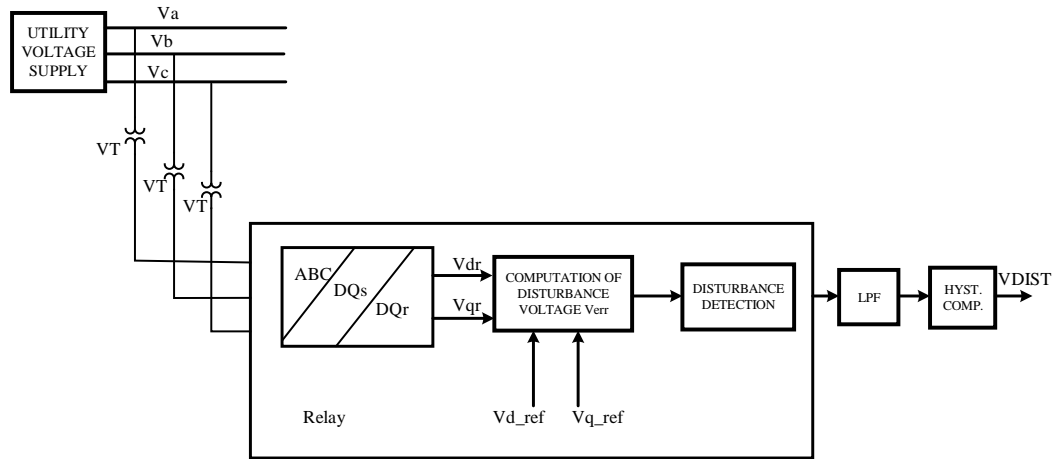


Figure 3.9: Proposed scheme in [48].

The solution suggested in [36] measures current phase jump to detect fault. The phase jump is compared with the pre-fault condition and rate changes so that direction of the current can be measured. The calculation of the phase jump can be explained by Figure 3.10, where, phase jump  $\Delta\phi$  is the difference between phase angle between pre-fault and post-fault current. A phase jump of  $180^\circ$  means change of current direction. By estimating the detection of the fault current the scheme can locate the faulted section. The implementation of the scheme is shown in Figure 3.11. Again, a communication link is necessary to maintain coordination among the relays. The scheme may not operate properly in the active distribution network where power flow is bidirectional, while the proposed solution in this thesis has been tested for both bidirectional normal and fault conditioned.

Utilising the phase difference between positive sequence voltage and current, a new fault detection scheme for the grid connected IIDGs is suggested by [49]. The paper mainly focuses fault models of grid connected PQ controllers, analyses the positive sequence phase components of both voltage and current, and describes the controllers design with low voltage ride-through (LVRT) capability. The fault detection and locating algorithm for the solution is presented in Figure 3.12

The scheme starts the fault detection through calculating the value of  $R$  and

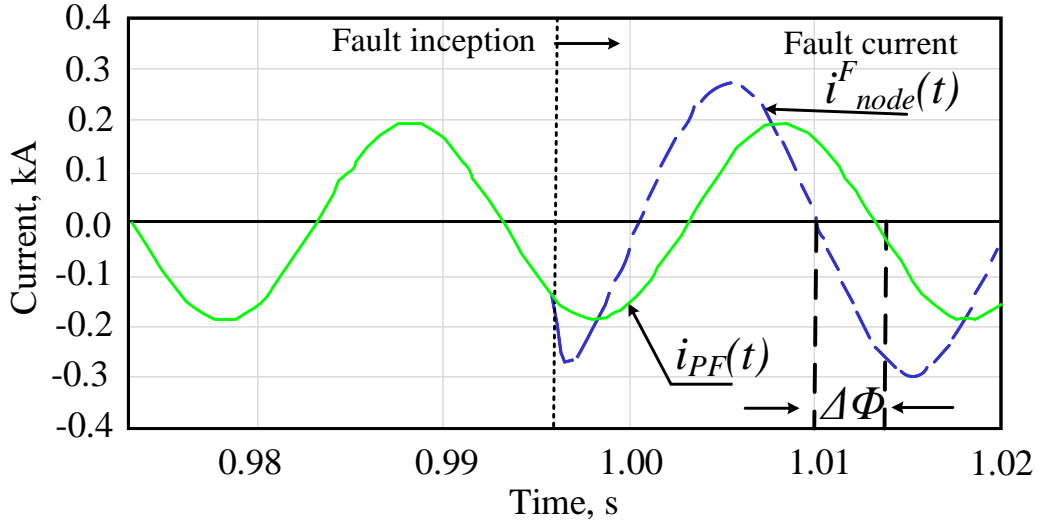


Figure 3.10: Phase jump calculation in [36].

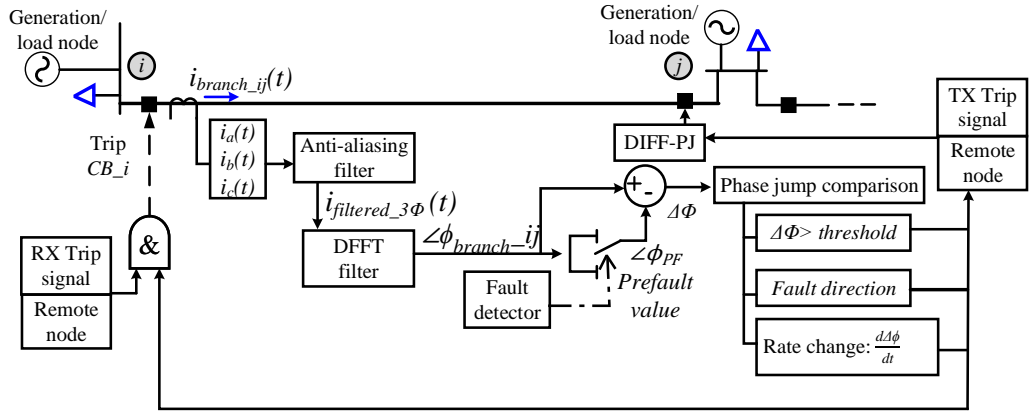


Figure 3.11: Implementation of proposed differential scheme in [36].

the equation of  $R$  is provided in (3.1), where  $F_i = \frac{\Delta I_0 + \Delta I_2}{\Delta I_1}$ ,  $F_n = \frac{I_0 + I_2}{I_1}$  and  $R_{set}$  is the starting threshold and assumed as 1.2 in the paper.  $I_1$ ,  $I_2$  and  $I_0$  are the positive, negative and zero sequence RMS current respectively. Then measures the phase difference between voltage and current during the fault condition for each feeder,  $\phi_{ij}$ . If both  $\phi_{1j}$  and  $\phi_{2j}$  are in the range, fault is in main feeder otherwise fault is in the branch feeder.

$$R = \frac{F_i}{F_n} > R_{set} \quad (3.1)$$

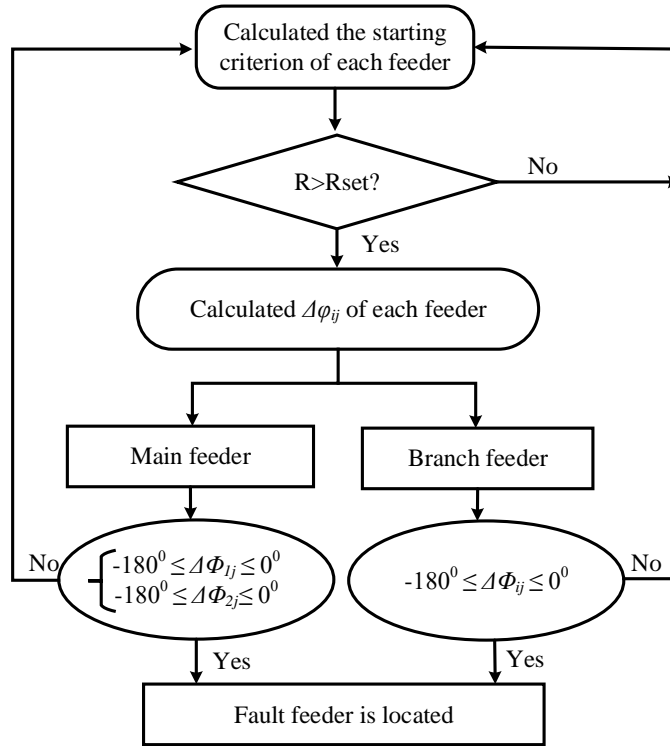


Figure 3.12: Fault detection algorithm proposed in [49].

Now during normal condition, it is assumed that distribution network will be unbalanced and hence,  $F_n$  is not zero but imbalance will be comparatively low. With a fault  $F_n$  changes significantly. However, fault detection through this ratio may not be very accurate since during normal condition, due to load change, this ratio can be high and may cross the threshold. Even depending on the type of fault,  $F_i$  can change differently and hence, may not detect all the faults (for example, fault with high impedance) in the network. Again, this algorithm requires communication channels and central controller to coordinate the relay which can be a big disadvantage of the scheme. The presented solution in Chapter 5 of this thesis has discussed protection strategy for both radial and meshed network, and does not require communication between the relays to detect and isolate the faults.

Active protection scheme is suggested by [50, 51] to protect microgrids with

high proliferation of IIDGs. In both schemes the control of the inverter is modified so that during fault, the inverter can inject a specific signal to detect the fault. In [50] off-nominal frequency is injected by one of the connected IIDG during fault, and relays in the network detect those harmonic components and compare with the other end relay's frequency component. If both relays in a single section detect same frequency components then fault is external otherwise fault is internal. The relay diagram is shown in Figure 3.13. The paper verifies that it is possible to inject different frequency components, other than harmonic and fundamental frequency through the controller of inverters.

However, communication between the relays are required to coordinate the relays as well as to detect the fault. Also, the research did not provide any explanation of choosing such non-fundamental components. The scheme does not have significant difference from existing differential protection other than differentiating off-nominal components in place of currents. Therefore, proposed solution can be expensive for the protection of islanded microgrids. The suggested scheme in this thesis also utilises similar methodology of harmonic injection but do not require any communication link to coordinate the relays in the network.

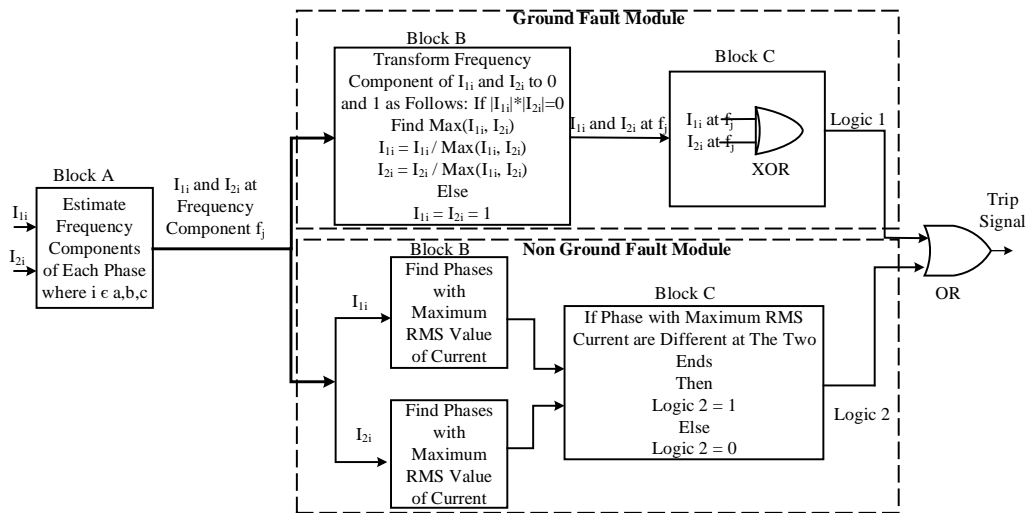


Figure 3.13: Proposed relay diagram in [50].

Similarly, [51] also proposes an active protection scheme for islanded microgrid that injects fifth harmonic through the controller of the IIDG after detecting fault. The scheme not only coordinate the relays in the network without any communication link but also suggest a novel current limiting strategy through controlling DC current of the inverter with addition of limiting current at the AC side of the network through conventional limiter. After limiting fault current contribution from the IIDG, the scheme adds a portion of fifth harmonics (although, it has been mentioned that any harmonics can be injected as long as it is not creating any resonance with filter impedance) with fundamental current. To coordinate the relays in the network, conventional IDMT characteristic has been utilised and to differentiate the value of the injected fifth harmonics, a droop between impedance and magnitude of fifth harmonic injection has been made. Hence, while fault is closer to the relay and IIDG, higher magnitudes of fifth harmonic will be injected so that grading throughout the network is maintained. The most advantage of the scheme is, it can operate without any requirements of communication. Therefore, relatively cheaper than other communication-based solutions. The overall algorithm of the proposed scheme is shown in the flowchart Figure 3.14.

However, this scheme also has some flaws associated with it. Starting with the fault current limiter, the solution includes an additional limiter through DC side current, which can be additional cost and compatibility of this new limiter has not been tested through the practical demonstration. Again, in the scheme, only one IIDG is injecting harmonic components, hence, the scheme will not work absence of that particular IIDG (may also be dependent upon the size of that particular IIDG) and may also not operate properly with the connection of IIDGs in different location. Most importantly, if only one IIDG injecting specifically only one harmonic component, the IDMT relays may face the similar coordination issue as the typical overcurrent relays face, only difference in this case will be

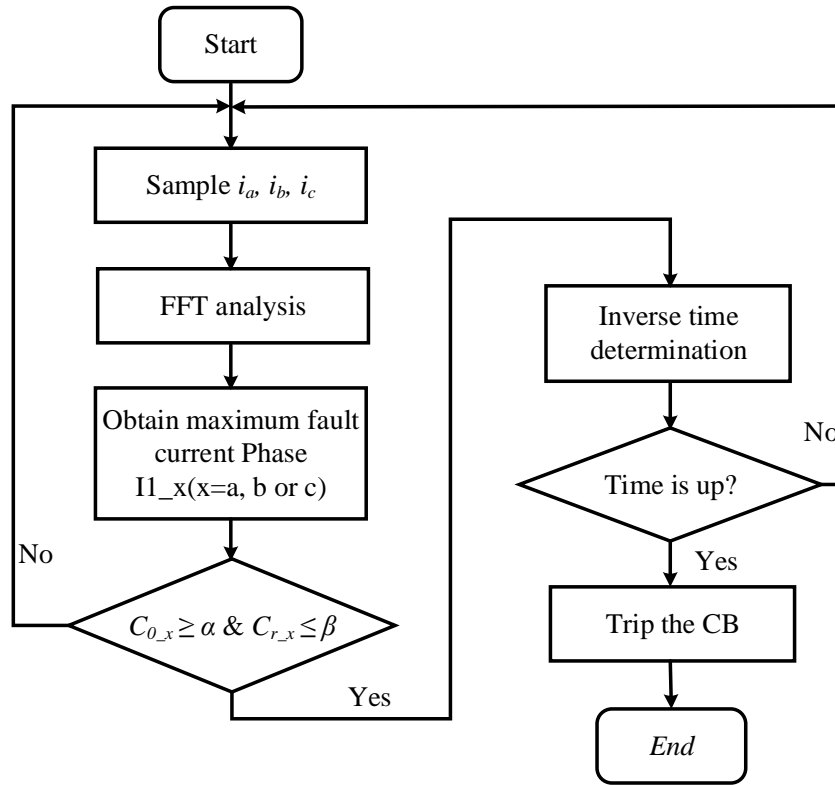


Figure 3.14: Proposed algorithm in [51].

instead of current magnitude, the relays will be dependent upon the fifth harmonic component. Finally, injecting components based on the line (or fault) impedance might create several new challenges of overreach and underreach conditions which might not be suitable for the operation of the islanded microgrids. The proposed scheme as presented in Chapter 5, injects harmonics through all the IIDGs to make the scheme more robust and it has been demonstrated that the scheme can operate properly with different location of IIDGs in the network.

Another similar injection based active protection scheme is proposed in [52]. In this solution rather than using IIDGs connected with the network, a separate unit is used for the injection during fault. Now, this provides a good support while there is no IIDG is connected to the network or different combination of connection and can operate during both grid-connected and islanded mode. However, an additional unit for injection will be costly and unnecessary loss of a power source

which will be used only during fault. Furthermore, the paper does not discuss how to coordinate the relays in the network.

Commercially, protection manufacturers use sub-harmonic (20 Hz voltage) injection to detect 100% stator earth faults near the neutral of large generators [53].

A summary of the new algorithm-based protection schemes for the distribution network is listed in Table 3.2 with critical evaluation included. Again, shortcomings which can be largely overcome by the scheme proposed in this thesis are included.

Table 3.2: Summary of the new protection algorithm-based schemes.

Referenced Article	Description of the Method	Positive Impacts	Shortcomings
[35, 36, 37, 38, 39, 40]	Traditional differential and distance protection schemes used in the transmission network.	Widely used in the transmission network and commercially available. Therefore, most reliable and tested protection scheme.	May not be suitable due to short line lengths of the microgrid. Require additional measurement devices and communication between the relays. May not be very economical option for the microgrids.
[47]	Total harmonic distortion (THD) is utilised to detect the faults.	The scheme can detect type of fault along with location of the fault with the presence of appropriate communication channels.	May not be reliable due to communication.

Table 3.2: Summary of the new protection algorithm-based schemes.

Referenced Article	Description of the Method	Positive Impacts	Shortcomings
[48]	Fault is detected through measuring voltage in d-q frame.	Can be used in the grid-connected mode and islanded operation.	Do not provide protection against the HIF and sensitive to voltage condition. So, small change grid voltage can activate the system's protection. Furthermore, coordination among the relays are not possible without communication.
[36]	Detects fault based on the different between the current phase jump of post and pre-fault condition.	Can be used in the islanded mode of operation and can detects the faults with high impedance.	Since the scheme differentiate the current angle of the two ends current of a feeder, reliable communication is required for the scheme.
[49]	Analyses the positive sequence phase difference between voltage and current to detect the fault.	Fault analysis is carried for inverter-based generation in the microgrid. Detection of the fault is independent of current magnitude.	It is difficult to differentiate the external and internal fault through this scheme without the aid of communication.

Table 3.2: Summary of the new protection algorithm-based schemes.

Referenced Article	Description of the Method	Positive Impacts	Shortcomings
[50, 51, 52]	Active protection scheme- fault is initially detected by the IIDGs and then modify the controllers' action to detect and locate the fault in the network.	Most suitable option to detect the fault in the islanded mode with several IIDGs connection.	Require communication to coordinate the relays in the network.

### 3.2.3 Managing Fault Contribution from DGs

As synchronous based DGs may typically contribute fault currents more than 5 to 6 times of the rated output current [2], the motivation of the methods presented in this section is to limit the fault current contribution from the DGs during grid connected mode of operation so that the original coordination settings of the pre-installed overcurrent relays do not need to change. However, these type of protection solutions are not necessary for small DG or DG interfaced via power electronics converters since fault current contribution from those sources will be limited. The limitations of the reviewed solutions in this section are not applicable to the protection scheme proposed in this thesis. The solution explained in Chapter 5 is utilising IIDGs' controller action and a current limiter is used in each of the IIDG control. It has been already shown in Section 3.1 that overcurrent relays may not be suitable for the protection of the converter dominated microgrids.

Reference [54] introduces the technique of Fault Current Limiters (FCL) in the radial distribution system. Low impedance is maintained by the FCL during

normal operating condition but during a fault, it increases the impedance value to a level that can limit DG fault current contribution to almost zero. The method removes the complexity of changing or modifying the protection settings along with control of the DGs operation during the fault conditions. As a result, the connection of FCLs can provide flexibility on the control operation of DGs and centralised monitoring unit. However, the scheme has serious issues associated with losses, size, reliability, operation speed and cost.

A protection technique based on the measurement of the voltage at the point of common coupling (PCC) is proposed in [55]. The scheme controls the normal condition current by using (3.2) and fault current contribution from the DGs by using (3.3), where,  $k$  and  $n$  are constants (can be modified so that the thermal ratings of the power electronics devices do not exceed) and  $I_{max}$  is the maximum allowable current in the system.

$$I_{DG} = \frac{P_{desired}}{V_{PCC}}; \quad \text{when, } V_{PCC} \geq 0.88p.u. \quad (3.2)$$

$$I_{F,DG} = k \cdot V_{PCC}^n \cdot I_{max}; \quad \text{when, } V_{PCC} < 0.88p.u. \quad (3.3)$$

The scheme is relatively very simple and current contribution during normal operation remain sustained. However, the scheme cannot discriminate the voltage variation due to faults and loads variation and if the fault is far from PCC, the scheme will not be able to detect the fault.

A fuzzy logic decision-making module is designed in [56] to monitor the DGs contribution in the network and modify the penetration level of DGs during the fault. Also, a digital numerical algorithm is developed through fast recursive discrete Fourier transformation to control the operation of DGs. The scheme has both control and adaptive protection functions, but the algorithm is very complex and difficult to implement in practice.

Reference [57] suggested an approach where location, size and penetration level of DGs are optimised through the measurement of Protection Coordination Index (PCI). PCI is the ratio between the change of penetration power in the distribution network by DGs and change in the coordination time interval. However, limiting the DGs capacity is not desirable during intentional islanding operation.

### 3.3 Summary

Various protection challenges that already been faced by the utility or may face in future due to excessive interconnection of renewable based IIDGs are discussed. Also, different solutions from the literature are discussed along with their positive and negative aspects. In this research the solutions are categorised into three groups- adaptive protection scheme, new protection algorithm and managing fault contribution from DGs. From the discussion, it is clear that a potential contribution is required in respect of suggesting a novel and effective protection scheme to overcome the protection challenges of the islanded microgrid. To summarise this chapter a comparison between three solutions are drawn and presented in Table 3.3, which presents three types of protection scheme.

Table 3.3 present three types of protection schemes, issues and each schemes' requirements through mapping them so that a better understanding of various schemes' capabilities can be provided. This can facilitate the development of future protection schemes that can be more flexible, cost-effective and capable of addressing a wider range of issues more effectively. The ratings provided in Table 3.3 for each scheme is based on the performance of the schemes and are of course, somewhat subjective. The criteria of this rating are based upon addressing the stated protection issues, practical applications in the real world, complexity of the algorithm and cost.

Table 3.3: Comparison of the solutions

Protection Schemes	Protection Issues			Additional Requirements and Feasibility				
	Sensitivity & selectivity	Coordination with backup	Operating time	HIFs detection	Islanded operation	Communication	Cost	Complexity
Adaptive Protection Scheme	Medium	Possible	Depend on the Communication	Not Effective	Possible	Require	Expensive	Relatively Simple
New Protection Algorithm	High	Possible	Depend on the Communication	Effective	Possible	Require	Moderate	Relatively Complex
Controlling DGs Fault Contribution	Low	N/A	Fast	N/A	Possible	Not Required	Expensive	Simple

## References

- [1] National Grid, “System Operability Framework 2016,” no. November, 2016. [Online]. Available: <https://www.nationalgrideso.com/sites/eso/files/documents/8589937803-SOF2016-FullInteractiveDocument.pdf>
- [2] —, “System Operability Framework 2015,” no. NOVEMBER, 2015. [Online]. Available: <https://www.nationalgrideso.com/sites/eso/files/documents/44046-SOF2015FullDocument.pdf>
- [3] —, “System Operability Framework 2014,” no. September, 2014. [Online]. Available: <https://www.nationalgrideso.com/sites/eso/files/documents/35435-SOF2014Final.pdf>
- [4] X. Liu and A. Lindemann, “Control of vsc-hvdc connected offshore windfarms for providing synthetic inertia,” *IEEE Journal of Emerging and Selected Topics in Power Electronics*, vol. 6, no. 3, pp. 1407–1417, 2018.
- [5] A. Darlington, K. Birt, S. Boutilier, W. Hartmann, D. Sevcik, and S. S. Venkata, “Impact of Distributed Resources on Distribution Relay Protection,” no. August, 2004.
- [6] T. Amraee, “Coordination of directional overcurrent relays using seeker algorithm,” *IEEE Transactions on Power Delivery*, vol. 27, no. 3, pp. 1415–1422, 2012.
- [7] J. Morren, “Impact of distributed generation units with power electronic converters on distribution network protection,” *IET Conference Proceedings*, pp. 663–668(5), January 2008. [Online]. Available: [https://digital-library.theiet.org/content/conferences/10.1049/cp\\_20080118](https://digital-library.theiet.org/content/conferences/10.1049/cp_20080118)
- [8] K. Kauhaniemi, “Impact of distributed generation on the protection of distribution networks,” *IET Conference Proceedings*, pp. 315–318(3),

- January 2004. [Online]. Available: [https://digital-library.theiet.org/content/conferences/10.1049/cp\\_20040126](https://digital-library.theiet.org/content/conferences/10.1049/cp_20040126)
- [9] R. Dugan and T. McDermott, “Distributed generation,” *IEEE Industry Applications Magazine*, vol. 8, no. 2, pp. 19–25, 2002.
- [10] T. Gallery, L. Martinez, and D. Klopota, “Impact of distributed generation on distribution network protection,” *ESBI Engineering & Facility Management, Ireland*, 2005.
- [11] A. Girgis and S. Brahma, “Effect of distributed generation on protective device coordination in distribution system,” in *2001 Large Engineering Systems Conference on Power Engineering*, 2001, pp. 115–119.
- [12] M. A. U. Khan and C. D. Booth, “Detailed analysis of the future distribution network protection issues,” *The Journal of Engineering*, vol. 2018, no. 15, pp. 1150–1154, 2018. [Online]. Available: <https://ietresearch.onlinelibrary.wiley.com/doi/abs/10.1049/joe.2018.0218>
- [13] Energy Networks Association (ENA), “Recommendation for the connection of generating plant to the distributed systems of licensed distribution network operators,” London, Tech. Rep., 2019. [Online]. Available: [http://www.energynetworks.org/assets/files/electricity/engineering/engineeringdocuments/ENA\\_EREC\\_G59\\_Issue\\_3\\_Amendment\\_7\\_\(2019\).pdf](http://www.energynetworks.org/assets/files/electricity/engineering/engineeringdocuments/ENA_EREC_G59_Issue_3_Amendment_7_(2019).pdf)
- [14] L. Kumpulainen and K. Kauhaniemi, “Analysis of the impact of distributed generation on automatic reclosing,” in *IEEE PES Power Systems Conference and Exposition, 2004.*, 2004, pp. 603–608 vol.1.
- [15] J. Kennedy, P. Ciufu, and A. Agalgaonkar, “A review of protection systems for distribution networks embedded with renewable generation,” *Renewable*

- and Sustainable Energy Reviews*, vol. 58, pp. 1308–1317, 2016. [Online]. Available: <http://dx.doi.org/10.1016/j.rser.2015.12.258>
- [16] A. R. Haron, A. Mohamed, and H. Shareef, “A review on protection schemes and coordination techniques in microgrid system,” *Journal of Applied Science*, vol. 12, no. 2, pp. 101–112, 2012.
- [17] A. Fazanehrafat, “Maintaining the recloser-fuse coordination in distribution systems in presence of dg by determining dgapos;s size,” *IET Conference Proceedings*, pp. 132–137(5), January 2008. [Online]. Available: [https://digital-library.theiet.org/content/conferences/10.1049/cp\\_20080024](https://digital-library.theiet.org/content/conferences/10.1049/cp_20080024)
- [18] S. Chaitusaney and A. Yokoyama, “Prevention of Reliability Degradation from Recloser-Fuse Miscoordination Due to Distributed Generation,” *IEEE Transactions on Power Delivery*, vol. 23, no. 4, pp. 2545–2554, 2008.
- [19] I. Ojangueren, *High Impedance Faults*. Paris: CIGRE, 2009, no. December.
- [20] A. Ghaderi, H. L. Ginn, and H. Ali, “High impedance fault detection : A review,” *Electric Power Systems Research*, vol. 143, pp. 376–388, 2017. [Online]. Available: <http://dx.doi.org/10.1016/j.epsr.2016.10.021>
- [21] V. D. Andrade and E. Sorrentino, “Typical expected values of the fault resistance in power systems,” in *2010 IEEE/PES Transmission and Distribution Conference and Exposition: Latin America (T D-LA)*, 2010, pp. 602–609.
- [22] F. Coffele, C. Booth, and A. Dysko, “An Adaptive Overcurrent Protection Scheme for Distribution Networks,” *IEEE Transactions on Power Delivery*, vol. 30, no. 2, pp. 561–568, 2015.
- [23] M. Baran and I. El-Markabi, “Adaptive over current protection for distribution feeders with distributed generators,” *2004 IEEE PES Power Systems Conference and Exposition*, vol. 2, no. figure 2, pp. 715–719, 2004.

- [24] V. A. Papaspiliotopoulos, G. N. Korres, V. A. Kleftakis, and N. D. Hatziargyriou, “Hardware-In-the-Loop Design and Optimal Setting of Adaptive Protection Schemes for Distribution Systems with Distributed Generation,” *IEEE Transactions on Power Delivery*, vol. 32, no. 1, pp. 393–400, 2017.
- [25] N. Schaefer, T. Degner, A. Shustov, T. Keil, and J. Jaeger, “Adaptive protection system for distribution networks with distributed energy resources,” in *IET Conference Publications*, vol. 2010, no. 558 CP, Manchester, 2010.
- [26] M. K. Singh and P. N. Reddy, “A fast adaptive protection scheme for distributed generation connected networks with necessary relay coordination,” *2013 Students Conference on Engineering and Systems, SCES 2013*, 2013.
- [27] A. G. Phadke, M. Ibrahim, and T. Hlibka, “Fundamental Basis for Distance Relaying with Symmetrical Components,” *IEEE Transactions on Power Apparatus and Systems*, vol. PAS-96, no. 2, pp. 635–646, 1977.
- [28] S. M. Brahma and A. A. Girgis, “Development of Adaptive Protection Scheme for Distribution Systems with High Penetration of Distributed Generation,” *IEEE Transaction on Power Delivery*, vol. 19, no. 1, pp. 56–63, 2004.
- [29] A. Oudalov and A. Fidigatti, “Adaptive Network Protection in Microgrids,” *ABB International Journal of Distributed Energy Resources*, vol. 5, pp. 201–227, 2009.
- [30] P. Mahat, Z. Chen, B. Bak-Jensen, and C. L. Bak, “A simple adaptive overcurrent protection of distribution systems with distributed generation,” *IEEE Transactions on Smart Grid*, vol. 2, no. 3, pp. 428–437, 2011.
- [31] P. H. Shah and B. R. Bhalja, “New adaptive digital relaying scheme to tackle recloser-fuse miscoordination during distributed generation interconnections,”

- IET Generation, Transmission and Distribution*, vol. 8, no. 4, pp. 682–688, 2014.
- [32] S. Shen, D. Lin, H. Wang, P. Hu, K. Jiang, D. Lin, and B. He, “An Adaptive Protection Scheme for Distribution Systems with DGs Based on Optimized Thevenin Equivalent Parameters Estimation,” *IEEE Transactions on Power Delivery*, vol. 32, no. 1, pp. 411–419, 2017.
- [33] V. Telukunta, S. Member, J. Pradhan, S. Member, A. Agrawal, S. Member, M. Singh, S. Member, and S. G. Srivani, “Protection Challenges Under Bulk Penetration of Renewable Energy Resources in Power Systems: A Review,” *CSEE Journal of Power and Energy Systems*, vol. 3, no. 4, pp. 365–379, 2017.
- [34] K. Pandakov and H. K. Høidalen, “Distance Protection with Fault Impedance Compensation for Distribution Network with DG,” in *2017 IEEE PES Innovation Smart Grid Technology Conference Europe*, 2017.
- [35] F. Zhao, “Pilot Protection Scheme for Distribution Network Considering Low Voltage Ride-Through of Inverter-Interfaced Distributed Generators,” *IEEE Transactions on Electrical and Electronic Engineering*, pp. 1613–1621, 2020.
- [36] N. E. Halabi, M. García-gracia, J. Borroy, and J. L. Villa, “Current phase comparison pilot scheme for distributed generation networks protection,” *Applied Energy*, vol. 88, no. 12, pp. 4563–4569, 2011. [Online]. Available: <http://dx.doi.org/10.1016/j.apenergy.2011.05.048>
- [37] B. W. Han, H. F. Li, G. Wang, D. H. Zeng, and Y. S. Liang, “A Virtual Multi-Terminal Current Differential Protection Scheme for Distribution Networks With Inverter-Interfaced Distributed Generators,” *IEEE Transactions on Smart Grid*, vol. 9, no. 5, pp. 5418–5431, 2018.

- [38] H. Gao, J. Li, and B. Xu, “Principle and Implementation of Current Differential Protection in Distribution Networks With High Penetration of DGs,” *IEEE Transactions on Power Delivery*, vol. 32, no. 1, pp. 565–574, 2017.
- [39] A. Gururani, S. R. Mohanty, and J. C. Mohanta, “Microgrid protection using Hilbert-Huang transform based-differential scheme,” *IET Generation Transmission Distribution*, vol. 10, no. 15, pp. 3707–3716, 2016.
- [40] M. Dewadasa, A. Ghosh, G. Ledwich, and S. Member, “Protection of Microgrids Using Differential Relays,” in *2011 Australas. University Power Engineering Conference*. IEEE, 2011, pp. 1–6.
- [41] R. Li, J. Zhu, Q. Hong, C. Booth, A. Dysko, A. Roscoe, and H. Urdal, “Impact of low (zero) carbon power systems on power system protection: A new evaluation approach based on a flexible modelling and hardware testing platform,” *IET Renewable Power Generation*, 2020.
- [42] J. J. Chavez, M. Popov, A. Novikov, S. Azizi, and V. Terzija, “Protection function assessment of present relays for wind generator applications’,” in *International Conf. on Power Systems Transients (IPST2019), Perpignan, France*, 2019, pp. 1–6.
- [43] V. P. Mahadanaarachchi and R. Ramakumar, “Impact of Distributed Generation on Distance Protection Performance - A Review,” *2008 IEEE Power Energy Society General Meeting, Vols 1-11*, pp. 3745–3751, 2008.
- [44] B. D. José, P. A. Cavalcante, F. C. Trindade, and M. C. De Almeida, “Analysis of distance based fault location methods for Smart Grids with distributed generation,” *2013 4th IEEE/PES Innovative Smart Grid Technologies Europe, ISGT Europe 2013*, pp. 1–5, 2013.

- [45] Y. Xu, “A review of cyber security risks of power systems: from static to dynamic false data attacks,” *Protection and Control of Modern Power Systems*, vol. 5, no. 1, pp. 1–12, dec 2020. [Online]. Available: <https://pcmp.springeropen.com/articles/10.1186/s41601-020-00164-w>
- [46] L. Che, X. Liu, Z. Li, and Y. Wen, “False data injection attacks induced sequential outages in power systems,” *IEEE Transactions on Power Systems*, vol. 34, no. 2, pp. 1513–1523, 2019.
- [47] H. Al-Nasseri and M. A. Redfern, “Harmonics content based protection scheme for micro-grids dominated by soled state converters,” *2008 12th International Middle East Power System Conference, Vols 1 and 2*, pp. 371–+, 2008.
- [48] H. Al-Nasseri, M. A. Redfern, and F. Li, “A voltage based protection for micro-grids containing power electronic converters,” *2006 Power Engineering Society General Meeting, Vols 1-9*, pp. 3786–+, 2006.
- [49] F. Zhang, “A Fault Detection Method of Microgrids With Grid-Connected Inverter Interfaced Distributed Generators Based on the PQ Control Strategy,” vol. 10, no. 5, pp. 4816–4826, 2019.
- [50] A. Soleimanisardoo, H. K. Karegar, and H. Zeineldin, “Differential Frequency Protection Scheme Based on Off-Nominal Frequency Injections for Inverter-Based Islanded Microgrids,” *IEEE Transactions on Smart Grid*, vol. 10, no. 2, pp. 2107–2114, 2019.
- [51] Z. Chen, X. J. Pei, M. Yang, L. Peng, and P. X. Shi, “A Novel Protection Scheme for Inverter-Interfaced Microgrid (IIM) Operated in Islanded Mode,” *IEEE Transactions on Power Electronics*, vol. 33, no. 9, pp. 7684–7697, 2018.
- [52] H. K. Karegar, “Alleviating the impact of DGs and network operation modes on the protection system,” *IET Generation, Transmission Distribution*,

- vol. 14, no. 1, pp. 21–28(7), jan 2020. [Online]. Available: <https://digital-library.theiet.org/content/journals/10.1049/iet-gtd.2019.0831>
- [53] R. J. Alcantara and F. G. Garcia, “100% Stator Ground Fault Protection - a Comparison of Two Protection Methods.” pp. 1–112, 2006.
- [54] W. El-Khattam and T. S. Sidhu, “Restoration of directional overcurrent relay coordination in distributed generation systems utilizing fault current limiter,” *IEEE Transactions on Power Delivery*, 2008.
- [55] H. Yazdanpanahi, Y. W. Li, and W. Xu, “A new control strategy to mitigate the impact of inverter-based DGs on protection system,” *IEEE Transactions on Smart Grid*, 2012.
- [56] D. S. Kumar, D. Srinivasan, and T. Reindl, “A Fast and Scalable Protection Scheme for Distribution Networks with Distributed Generation,” *IEEE Transactions on Power Delivery*, 2016.
- [57] H. H. Zeineldin, Y. A. R. I. Mohamed, V. Khadkikar, and V. Ravikumar Pandi, “A protection coordination index for evaluating distributed generation impacts on protection for meshed distribution systems,” *IEEE Transactions on Smart Grid*, vol. 4, no. 3, pp. 1523–1532, 2013.

# Chapter 4

## Power Electronics Inverter Control in Microgrids and Analysis of their Dynamic Behaviour

In this chapter, basic concepts of power electronics inverter control, including different designs and operation in microgrids, will be discussed. Firstly, the key functions and classification of inverter controller will be illustrated, with a complete description of different control loops implemented within the controllers. Secondly, a comprehensive study will be presented to evaluate the dynamic performance of IIDG in comparison with a Synchronous Generator (SG) and a Synchronous Compensator (SC), under a range of grid contingency events.

### 4.1 Classification of Inverter Controllers

Extensive research and a literature review have been carried to ascertain and evaluate the different designs, modes of operation and range of functionality of

controllers for IIDGs in microgrids. In a broad context, inverter control can be categorised into two types: grid-forming inverters (GFR); and grid-following (GFL).

It should also be noted that some researchers refer inverters as converters, for example, grid-forming inverters are often also known as grid-forming converters (GFC). Typically, converter is used as a more generic term (covering all forms of converter – inverters, rectifiers, DC/DC voltage converters, frequency converters). In this thesis, only DC/AC converters are considered, and hence the term inverter is used.

GFR can set and control voltage magnitude and frequency within an islanded microgrid through its controller, and can be represented as an ideal voltage source with an impedance as shown in Figure 4.1. The controller maintains the microgrid voltage and frequency according to reference voltage and frequency values assigned by an MCC as explained Section 2.

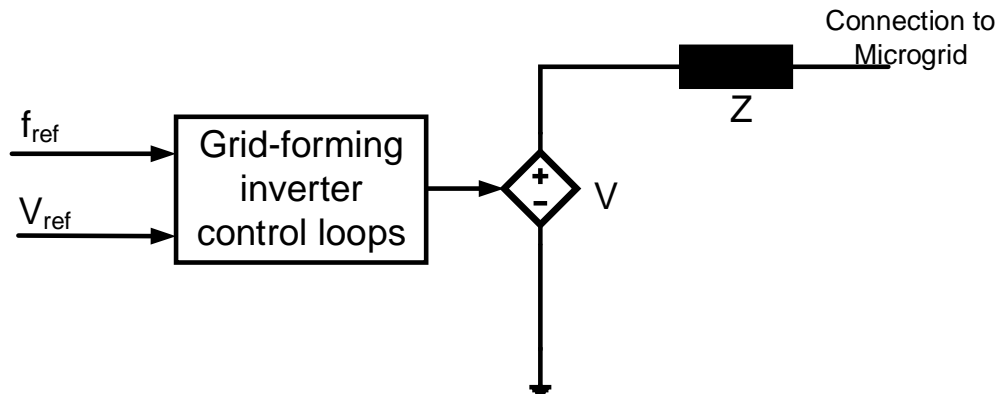


Figure 4.1: Simplified diagram of a GFR.

To operate the GFLs, frequency and voltage are defined by the grid to which GFL is connected. The GFLs are designed such that they can only deliver a fixed amount of real or reactive power to an energised grid. This controller produces a constant amount of real and reactive power according to a reference value set by the MCC. The GFL can be represented as an ideal current source with parallel

impedance to the connected network as shown in Figure 4.2. Since the controller is not responsible for defining the frequency and voltage of the system (but reacts to changes from the grid), it is necessary for the controller to be synchronised with the AC voltage at the PCC, in order to operate properly and accurately supply the desired quantities of the levels of real and reactive power required.

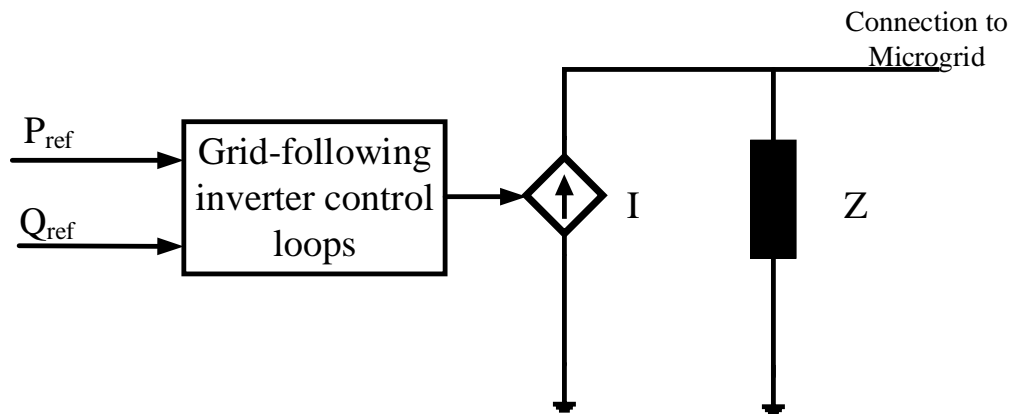


Figure 4.2: Simplified diagram of a GFL.

Other researchers [1, 2] categorised inverter controllers into three types, i.e., in addition with GFR and GFL, they introduce grid-supporting inverter control. The grid-supporting inverters can be represented either as an ideal AC-controlled current source in parallel with an impedance or as an ideal AC voltage source in series with an impedance, as shown in Figure 4.3 (a & b), respectively. This type of inverter controller can regulate its output power (by varying current) and/or voltage so that overall frequency and voltage magnitude of the microgrid remain close to the rated values [3]. Therefore, grid-supporting inverter can be considered as either GFL (while operating as current source) or GFR (while operating as voltage source). In this section, the design and operating strategy of the controller will be discussed in detail.

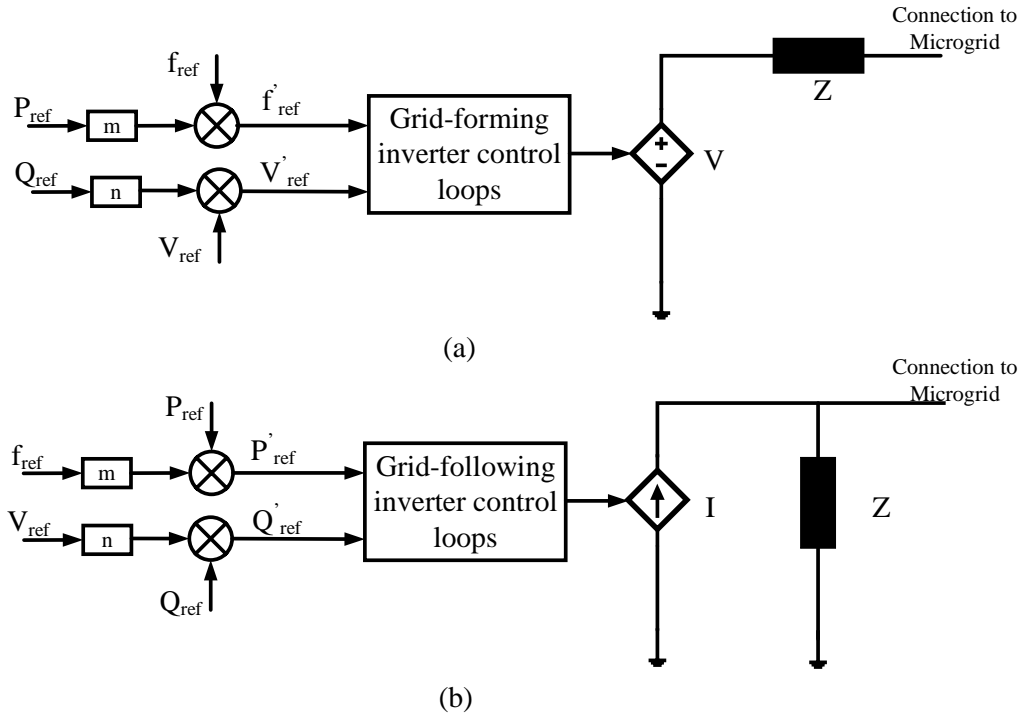


Figure 4.3: Simplified diagram of a grid-supporting controller (a) when behaves like a GFR (b) when behaves like a GFL.

#### 4.1.1 Grid-forming Inverter Control (GFR)

The key attribute of a GFR is the ability to maintaining the microgrid voltage and frequency through regulating its terminal voltage. These inverters are controlled via closed loops to behave as ideal AC voltage sources with a given voltage magnitude,  $V_{ref}$  and frequency,  $f_{ref}$  [1]. The load connected to the microgrid generally determines the output current or power delivered by the GFRs. One practical example of a GFR is a standby UPS, which monitors certain conditions and remain disconnected from the system until those conditions are met. However, during a grid outage, the UPS maintains the voltage within the safe operating region for the system [1]. Therefore, the GFRs can only be used during islanded mode of operation to regulate the voltage and frequency. In an islanded microgrid, the rest of the GFLs utilise the AC voltage (generated by the GFR) as reference and synchronise with other IIDGs parallelly connected to the network.

Figure 4.4 presents the overall configuration of a GFR. The controller is typically fed by a reliable and stable DC voltage source that is supplied by primary sources, for example, batteries and fuel cells. The control system is implemented using two cascaded synchronous controllers and one voltage reference block, with all operating in the synchronous reference (or ‘dq’ reference) frame. The synchronous reference frame uses the Park transformation to convert the three-phase voltage and current signal into a synchronously rotating frame so that time-varying ac signals can be transformed to dc signals. The controller can also be implemented in other reference frames such as stationary (‘ $\alpha\beta$ ’) reference frame and natural (‘ $abc$ ’) reference frame [4, 5]; however, in this research synchronous reference frame has been used to implement the controller since it is commonly used in the industrial application [6].

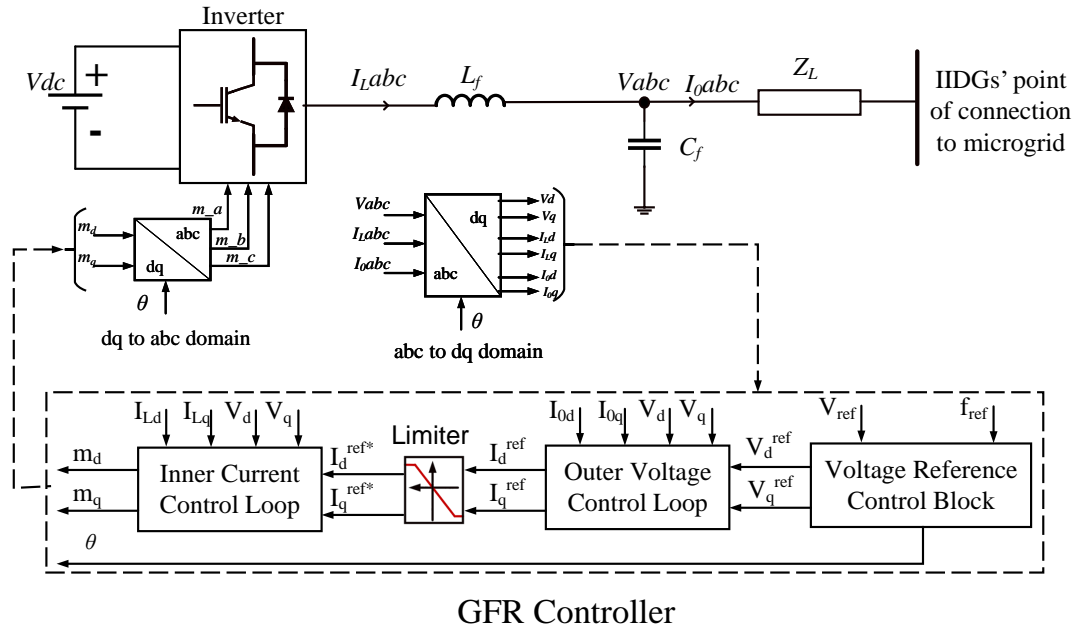


Figure 4.4: Basic control structure of a GFR.

The voltage reference block takes its input from the MCC of the microgrid in the form of a reference voltage magnitude,  $V_{ref}$ , and reference frequency value,  $f_{ref}$ . The outer voltage control loop regulates the microgrid voltage according to the reference voltage magnitude and generates the current reference for the

inner current control loop. The inner current control loop then regulates the current supplied by the inverter. The regulated signals are then fed to the inverter switches. The capacitance and inductance are included to filter out any higher order harmonics and other high frequency noise from the generated output.

### Voltage Reference Control Block

The basic function of the voltage reference control block is to provide a modified reference voltage in the form of ‘ $dq$ ’ rotational frame, that is,  $V_d^{ref}$  and  $V_q^{ref}$  and a voltage angle,  $\theta$  to the voltage control loop. It also takes input from the central controller of the microgrid in the form of desired reference voltage,  $V_{ref}$  and desired reference frequency,  $f_{ref}$ .

There are four different methods available for voltage reference control block. The detailed control structure of the voltage reference control block is presented in Figure 4.5. The first method is the simplest structure where output voltage magnitude is formed from the input reference voltage directly and the angle is formed from the input reference frequency through mathematical integration. The main challenge associated with this method is the fact that an extremely accurate synchronisation system is required if there are multiple GFRs incorporated in the system.

The second method is known as the droop control method, where a voltage reference control block requires reference active and reactive power along with reference frequency and voltage parameters. The output voltage and angle is then formed based on droop control. The equations for the droop control modified reference voltage and frequency are provided below in (4.1) and (4.2) respectively, where  $P_{ref}$  and  $Q_{ref}$  are the reference value of the active and reactive power respectively,  $P_{meas}$  and  $Q_{meas}$  are the measured active and reactive power delivered by the inverter respectively,  $m$  is the droop coefficient between active power and frequency,  $n$  is the droop coefficient between reactive power and voltage.

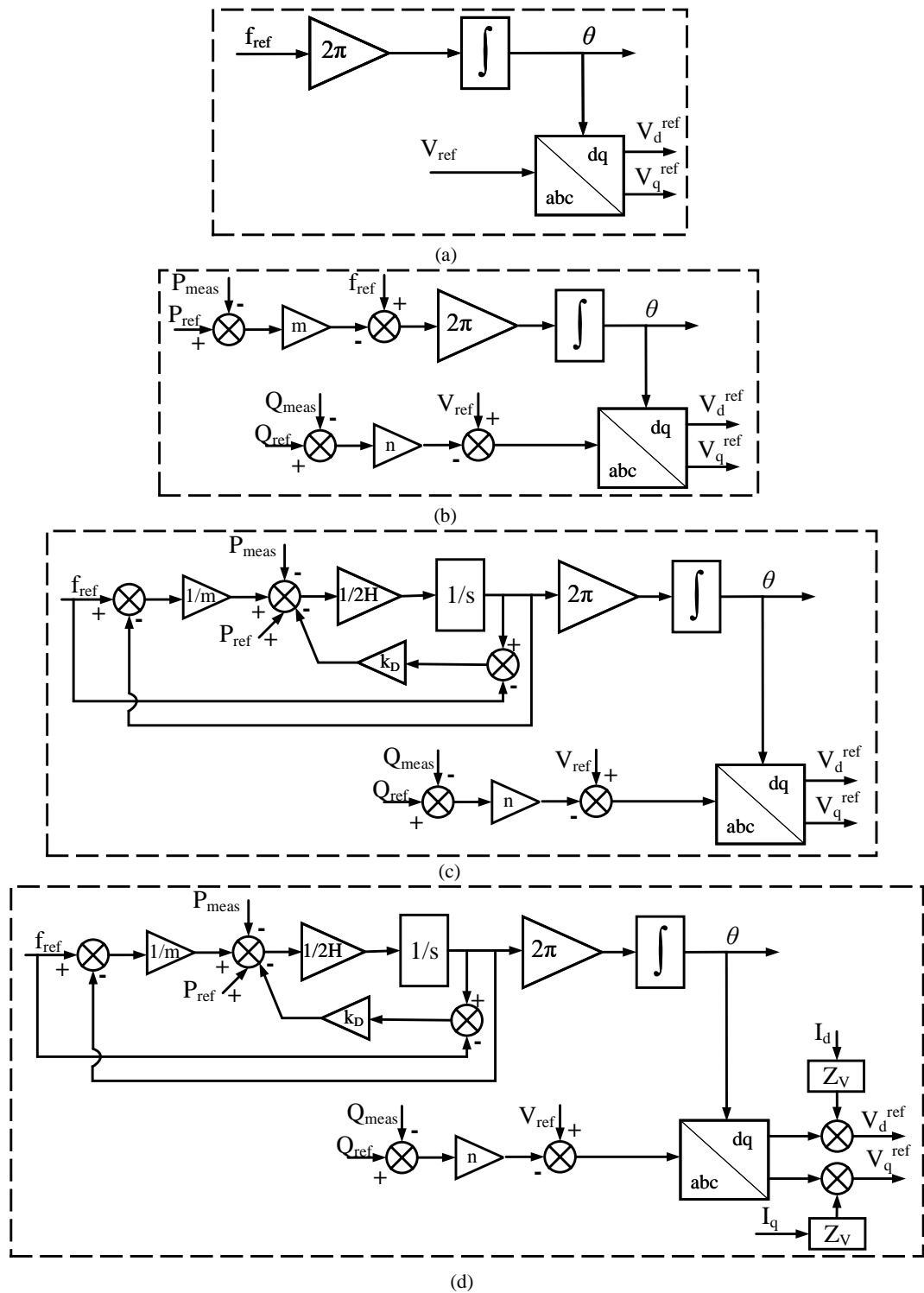


Figure 4.5: Block diagram of different voltage formations, (a) general grid forming; (b) droop control; (c) inertia emulation with droop control; and (d) virtual impedance with inertia emulation and droop control.

$$f'_{ref} = f_{ref} - m(P_{ref} - P_{meas}) \quad (4.1)$$

$$V'_{ref} = V_{ref} - n(Q_{ref} - Q_{meas}) \quad (4.2)$$

The third method is similar to the second method, but it adds an extra inertia control feature to the main droop control (sometimes, droop is deactivated) in the voltage reference control block [1]. Inertia emulation with droop control is implemented based on the swing equation. The implemented equation in the voltage reference block for this third method is provided in (4.3), where,  $H$  is the inertia constant,  $f'_{ref}$  is the output frequency,  $f_{ref}$  is the reference frequency,  $P_{ref}$  is the reference power,  $P_{meas}$  is the measured output power by the GFR,  $k_D$  is the damping coefficient, and  $m$  is the droop coefficient.

$$P_{ref} - P_{meas} = 2 \cdot H \cdot s \cdot f'_{ref} + k_D \cdot (f'_{ref} - f_{ref}) - \frac{1}{m} \cdot (f_{ref} - f'_{ref}) \quad (4.3)$$

In the fourth and final method, an extra voltage is added (this extra voltage represent voltage drop across the virtual impedance) to the final modified voltage reference through implementing the concept of virtual impedance (i.e. impedance,  $Z_V$  that can also be modified) to emulate the role of the impedance of a synchronous generator [7].

### Voltage Control Loop

The voltage control loop is the outer control loop of the GFR and operates as a tracking controller, being responsible for ensuring that the inverter output voltage can accurately tracks the modified reference voltage in the 'dq' domain ( $V_d^{ref}$  and  $V_q^{ref}$ ) provided by the voltage reference control block [8] as shown in Figure 4.5. A block diagram of the voltage control loop of a GRF is shown in Figure 4.6.

This external control loop strives to regulate the output voltage of the inverter

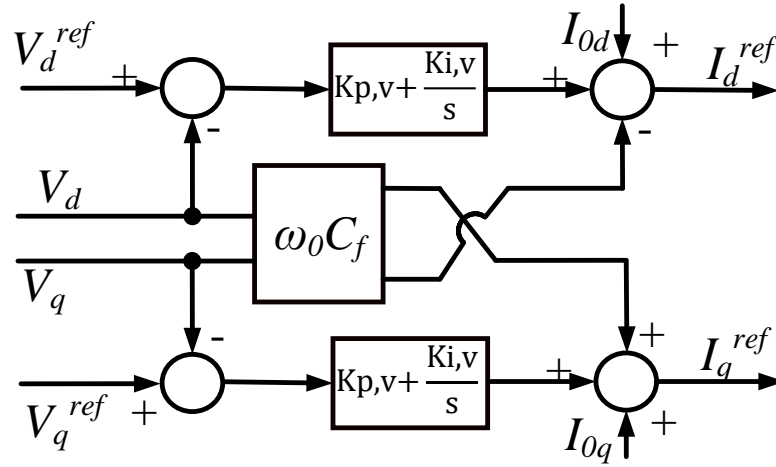


Figure 4.6: Block diagram of the voltage control loop of a GFR.

based upon the input provided by the voltage reference block. It should be noted that the voltage control loop of the GFR will be only enabled during islanded mode, since the voltage will be controlled by grid during grid-connected operation. In the voltage control loop, the error between the reference (both  $V_d^{ref}$  and  $V_q^{ref}$ ) and the measured voltages ( $V_d$  and  $V_q$ ) are fed to the PI controllers and used to produce the reference current inputs ( $i_d^{ref}$  and  $i_q^{ref}$ ) for the current control loop of the GFR. The reference current can be expressed using the following equation, where  $k_{p,v}$  and  $k_{i,v}$  are the PI controllers gain.

$$i_{dq}^{ref} = \left( k_{p,v} + \frac{k_{i,v}}{s} \right) (V_{ref} - V_{meas}) \quad (4.4)$$

### Fault Current Limiter

There are different approaches available for limiting the fault current magnitude provided by the IIDGs during faults and excessive external voltage depressions. One method entails the use of saturation on the current reference [9]. Prior to the current control loop, a current limiter is used so that the reference current input to the current control loop does not exceed the limit of 1.2 pu of the maximum nominal current. In this research, q-axis priority-based fault current limitation

has been used [10]. This method can be explained via the following equations.

$$i_q^{ref*} = \min(1, i_q^{ref}) \quad (4.5)$$

$$i_d^{ref*} = \min\left(\sqrt{I_{max}^2 - (i_q^{ref})^2}, i_d^{ref}\right) \quad (4.6)$$

$I_{max}$  is the maximum allowable current magnitude the IIDG can supply, which is 1.2 times of the nominal capacity. It can be seen from the equations above that if the current magnitude is lower than  $I_{max}$ , the modified reference currents in ‘dq’ domain will remain unsaturated, i.e.,  $i_d^{ref*} = i_d^{ref}$  and  $i_q^{ref*} = i_q^{ref}$ . During fault conditions, the current will increase but will be limited to  $I_{max}$ .

### Current Control Loop

The inner current control loop of the GFR is also a tracking controller in the synchronous reference (‘dq’) frame and similar to the voltage control loop as explained in Section 4.1.1. The responsibility of this control loop is to ensure the inverter current output accurately tracks the reference current ( $i_d^{ref*}$  and  $i_q^{ref*}$ ) provided by the voltage control loop and fault current limiter.

The structure of the inner current control loop is shown in Figure 4.7. The current control loop supplies the error between the reference current and measured current (for both ‘d’ and ‘q’ domain) to the PI regulator to regulate the inverter current in accordance with the reference current input. The output equation for the current control loop is provided in (4.7). The output signals of the current control loop are then sent to the inverter switches through pulse width modulator (PWM).

$$m_{dq} = \left(k_{p,i} + \frac{k_{i,i}}{s}\right) (i_{dq}^{ref*} - i_{dq}^{meas}) + V_{dq} \quad (4.7)$$

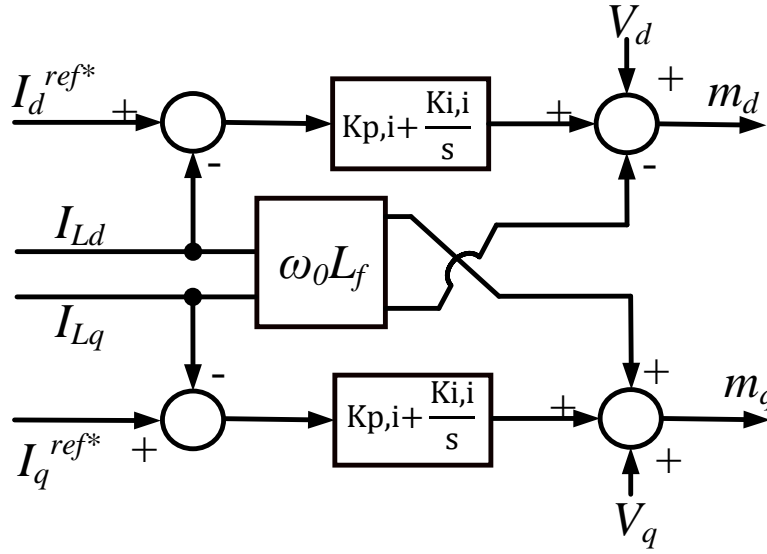


Figure 4.7: Block diagram of the current control loop of a GFR.

#### 4.1.2 Grid-following Inverter Control (GFL)

Grid-following power inverter is also known as a grid-feeding inverter [11]. The controller acts as a controlled current source connected to the system via a parallel output impedance and requires a GFR or other generator that can form the microgrid voltage. Hence, during islanded mode of operation of microgrid, this inverter type cannot operate independently without any support from a GFR. However, this inverter control method is most suitable for grid-connected operation when the main grid's AC voltage is formed by conventional synchronous generation [12]. The majority of power inverters use renewable DG systems operate with GFL, such as PV or wind power systems [13].

The output current provided by the GFL is generally controlled by a higher-level control layer, which supplies the active and reactive powers reference values,  $P_{ref}$  and  $Q_{ref}$ , to be delivered [14, 15]. A typical control structure of a GFL is shown in Figure 4.8. Typically, the operation of a GFL is regulated by a high-level controller; for example, maximum power point tracking (MPPT) controller, that can modify the reference values of active and reactive power that GFL will provide.

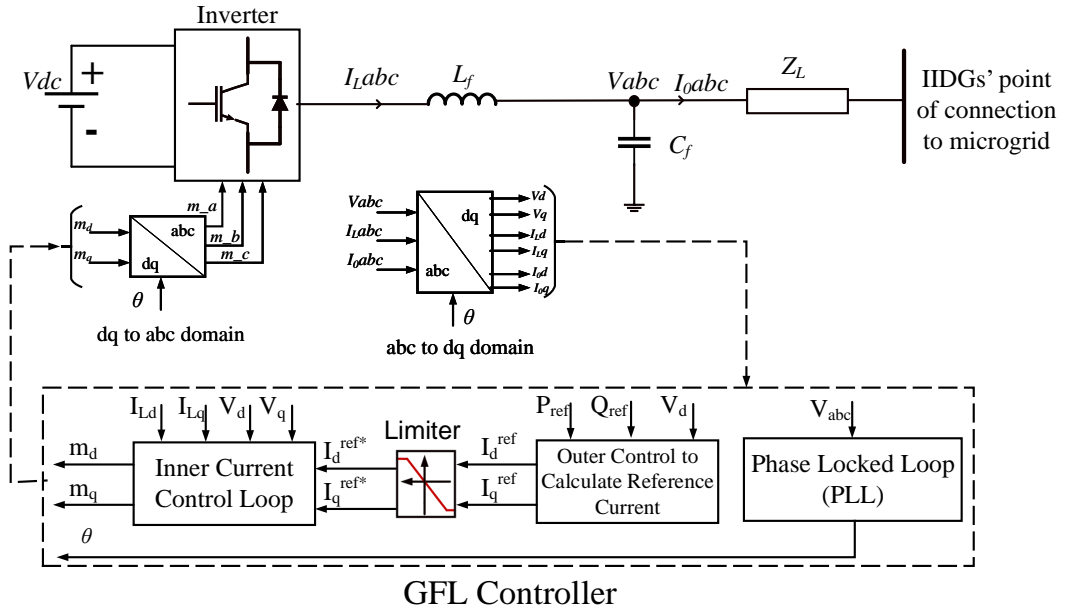


Figure 4.8: Basic control structure of a GFL.

The output current from the inverter and microgrid voltage are measured and transformed to ‘dq’ domain using a Park transformation. To synchronise the operation of the GFL, the angle of the system is measured and controlled by a phase-locked loop (PLL). The inner current control loop regulates the current provided by the GFL and maintains the current value to be close to the reference current input. An outer controller is used to generate the reference current value based on the active and reactive power output. The details for each control loop are explained in the following subsections.

### Phase-Locked Loop (PLL)

The overall performance of a GFL is greatly influenced by the accuracy in the estimation of the AC voltage parameters of the microgrid. Hence, an accurate synchronisation algorithm is required to estimate the microgrid’s voltage parameters, that is, voltage magnitude, frequency and phase angle. The estimation of voltage parameters is necessary to execute accurate control of the active and reactive power delivered by the GFL. The overall structure of a PLL in GFL is

shown in Figure 4.9.

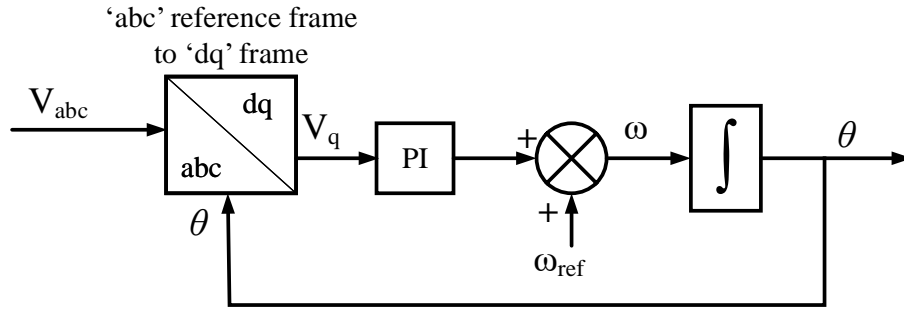


Figure 4.9: Block diagram of the PLL in a GFL.

Firstly, the PLL converts the three-phase instantaneous voltage waveforms from the ‘*abc*’ reference frame into the synchronous reference frame (or ‘*dq*’ reference frame), through the Park transformation. The angular position of this ‘*dq*’ reference frame is controlled by a feedback control loop. Therefore, in the second step, the ‘*q*’ component of the voltage,  $V_q$  equates to zero. Thirdly, the value of the rated angular frequency,  $\omega_{ref}$  is included as a feed forward to the output of the PI controller to improve the dynamics of the phase angle estimation. Finally, the phase angle,  $\theta$  is obtained through integrating the calculated phase angle,  $\omega$  [16, 17]. One of the shortcomings of the PLL is that its performance deteriorates (that is, it is incapable of tracking frequency and voltage angle effectively) significantly when it is presented with unbalanced or distorted three-phase input signals [18, 19].

### Outer Control to Calculate Reference Current of a GFL

The outer control of the GFL sets the reference current that will be regulated in the inner current control loop. The reference current is usually calculated from the reference active and reactive power. Typically, the active and reactive power delivered to the microgrid through the GFL can be calculated using (4.8) and (4.9) respectively.

$$P_{GFL} = \frac{3}{2} (V_d I_d + V_q I_q) \quad (4.8)$$

$$Q_{GFL} = \frac{3}{2} (-V_d I_q + V_q I_d) \quad (4.9)$$

As mentioned earlier, if the PLL is in a steady state, the ‘ $q$ ’ component of the voltage,  $V_q$  is equal to zero, equations (4.8) and (4.9) can be rewritten as,

$$P_{GFL} = \frac{3}{2} V_d I_d \quad (4.10)$$

$$Q_{GFL} = -\frac{3}{2} V_d I_q \quad (4.11)$$

As a result, based on equations (4.10) and (4.11), it can be concluded that  $P_{GFL}$  and  $Q_{GFL}$  can be controlled by  $I_d$  and  $I_q$ . Therefore, the reference current for the GFL can be calculated through (4.12) and (4.13). The implementation of the outer control of the GFL is shown in Figure 4.10.

$$I_d^{ref} = \frac{2}{3 \cdot V_d} P_{ref} \quad (4.12)$$

$$I_q^{ref} = -\frac{2}{3 \cdot V_d} Q_{ref} \quad (4.13)$$

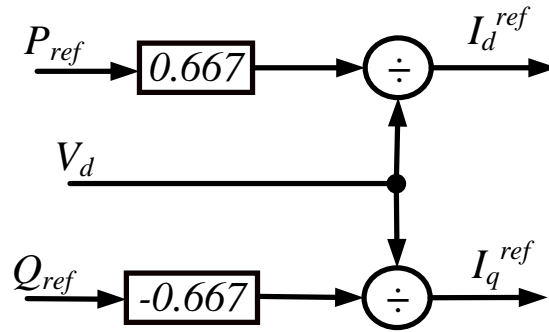


Figure 4.10: Block diagram of the outer control of a GFL.

As can be seen from Figure 4.8, a GFL has two additional components within its controller, i.e., the fault current limiter and the current control loop. The process of implementing those two components are similar to the control sections of the GFR as discussed in Section 4.1.1 of this thesis. Therefore, the process for

implementing the fault current limiter and inner current control loop for the GFL is not repeated here.

## 4.2 Dynamic Behaviour Comparison between IIDG and Synchronous Machines

Following the process explained in Section 4.1, both GFR and GFL controlled IIDGs are implemented in MATLAB Simulink and RTDS, and the implemented IIDG models are used in the microgrid for the validation of the proposed protection solution as explained in Chapter 6. To validate the performance of the developed IIDG models, a comprehensive simulation studies has been carried out under a range of grid contingency events including short circuit faults and voltage depressions. The dynamic behaviours of the IIDGs under these events are compared with the behaviours of SG and SC in order to understand different characteristics and capabilities of IIDGs to maintain the requirements provided in GB grid code [20].

This section presents the results and analysis of a number of technical criteria selected for evaluating the dynamic performance and capability of IIDGs when compared with SCs and SGs. The criteria have been selected based on the technical performance requirements as specified by the “stability path-finder”, which is an approach initiated by National Grid ESO to seek potential solutions to support the stable operation of the future system with increasing integration of renewable generation [21]. This research focuses on the following aspects:

- i Short circuit faults;
- ii Fault ride through capability; and
- iii Voltage depression events.

### 4.2.1 Simulation Setup

To analyse the dynamic behaviour of SG, SC and IIDG, a radial microgrid model as shown in Figure 4.11 has been developed in MATLAB Simulink. The electrical parameters of the three units have been set to be the same or equivalent to each other so that a fair comparison of the performance can be drawn. The values of the associated parameters of the distribution network model, SG, SC and IIDG are presented in Table 4.1. A brief description of the modelling of SG and SC are also provided in this section while the details of the implementation of IIDG model has been discussed in Section 4.1.

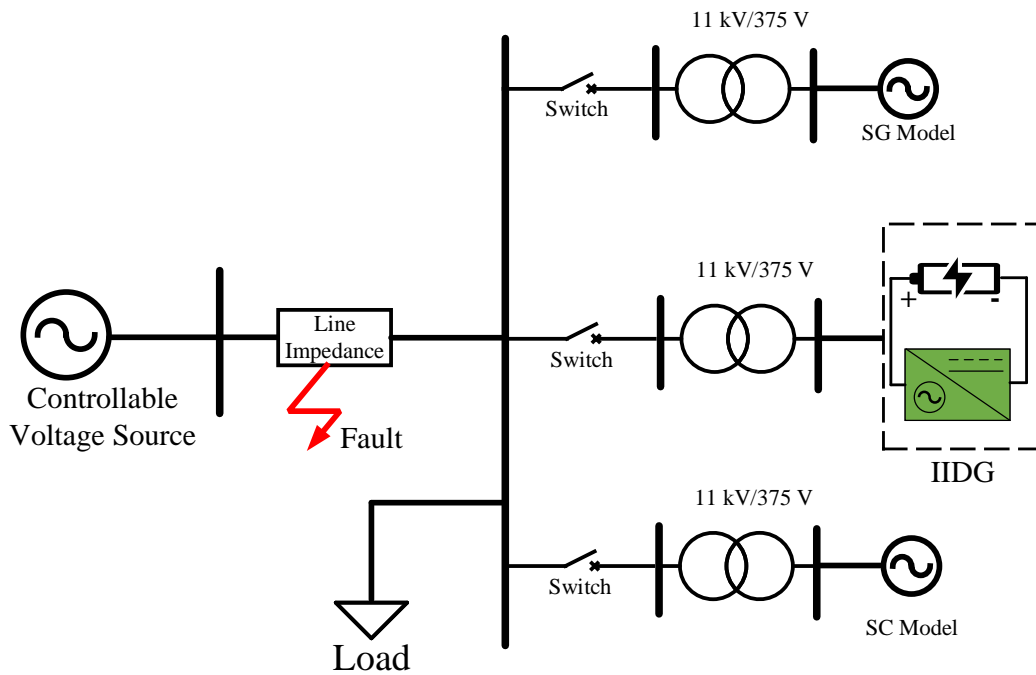


Figure 4.11: Simulation setup for dynamic behaviour study of IIDG and synchronous machines.

The modelling and dynamic behaviour of SGs is well understood and information widely available in the literature [22]. For the purpose of study and analysis, a general model of a SG is developed and used, and the block diagram of the implemented SG is shown in Figure 4.12. There are two main controllers used for the SG, that are, the excitation system for voltage and reactive power control,

Table 4.1: Simulation and generators' parameters.

Parameter Name	Symbol	Value
Frequency	$f_0$	50 Hz
Grid voltage	$V_{grid}$	11 kV
Line impedance	$Z_{Line}$	$0.5765 + j1.7\Omega$
Rated capacity	$S_{rated}$	246 kVA (for all generation units)
Reference active power	$P_{ref}$	100 kW (for SG and IIDG); and 0 kW (for SC)
Inertia constant	$H$	2 s (same for all generation units)
Damping	$D$	1 (same for all generation units)
Load size	$S_{Load}$	10 kVA

and the turbine governor for regulating active power. For the excitation system, the model from [23] is used in this work, and for the governor, the GAST model is developed based on [24] that represents the dynamics of a gas turbine. Since the droop control in the governor is not applicable for the SC [25], the droop in the SG's governor has also been disabled, where the similar setup was also adopted for the IIDG.

SC is a special type of SG without a prime mover, and an SC cannot provide sustained active power to the system. Hence, a governor is not used within an SC. In this research, it is assumed that the implementation of the SC is similar to the SG as presented in Figure 4.12, and uses the same excitation system; the main difference is that there is no governor for the SC model, and the mechanical power fed to the SC is zero.

#### 4.2.2 Studies of Short Circuit Faults

With a decrease in the overall amount of SGs in the power system, the overall short circuit level of the system is also decreasing, and it could compromise both the stability of inverters and the reliability of protection systems. As reported in [26], when the SCL decreases to a certain level, the PLL may experience stability issues, thus resulting in overall instability of inverters. For the protection system,

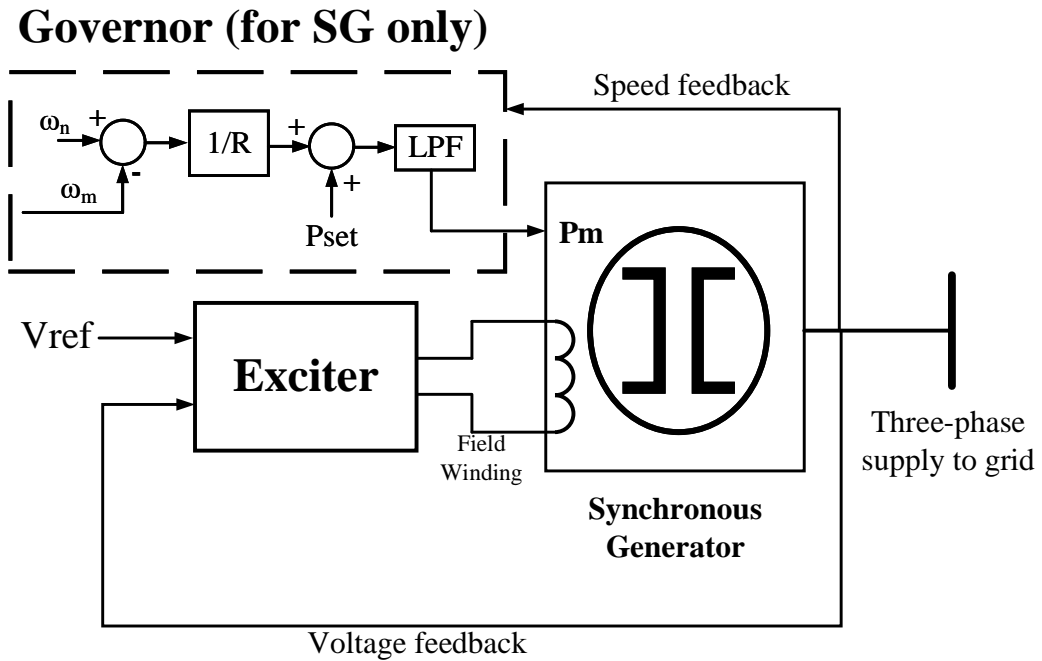


Figure 4.12: Schematic of the simulation model of SG and SC.

conventional overcurrent protection relies on sufficient fault current to detect faults and react within the required time and it may be necessary to replace or supplement the existing overcurrent protection with novel protection strategy to ensure the effective protection of microgrids in the future, particularly those operating in islanded mode. The details of the shortcomings of existing protection schemes is discussed in Chapter 3 and operation issues of overcurrent relays in microgrid is discussed in Chapter 5 of this thesis. Therefore, it is critical to assess the short circuit contribution and the fault characteristics of IIDGs during short circuit events as compared with SCs and SGs.

In this study, three types of fault cases are simulated: (1) a three-phase; (2) a single-phase to earth fault; and (3) a phase to phase fault, to evaluate the capability of IIDG, SC and SG in providing fault current contribution and their more general fault current characteristics. The fault is located between the controlled voltage source and the tested models as shown in Figure 4.11. The

fault impedance is assumed to be  $0.1 \Omega$  (which, as can be seen from Figure 4.13, Figure 4.14 and Figure 4.15, introduces a significant disturbance and voltage drop to the system), and the fault duration is 1 s, starting at 5 s in the simulations. The three-phase instantaneous currents for all three units are shown in Figure 4.13. Similarly, the instantaneous voltages and currents for the single-phase to earth fault and phase to phase fault are shown in Figure 4.14 and Figure 4.15 respectively.

Note that in the figures, per-unit values are used for the Y axes. That is, the peak values of the sinusoidal wave shown (for example, 1.2 pu during a fault) would be using the peak value of rated current as the per unit base value.

It can be observed from Figure 4.13 that, the fault currents from the SG and SC are similar in characteristics and magnitudes, (approximately 8 pu for transient period and 3.8 pu for steady state) during the three-phase fault, which is significantly higher than the fault current contribution from IIDG unit (only 1.2 pu). This is due to their stored energy, their strong overloading capability and the electro-magnetic and mechanical characteristics. In the case of IIDG, a fast reaction to the fault is observed with fault current injection within 1 cycle of the fault. According to the technical criteria included in [21, 20], both SC and IIDG fulfil the conditions of fast current injection. However, the current magnitude from IIDG during fault is intentionally limited to 1.2 pu through the control of IIDG unit due to the physical thermal limit of power electronics components and the economic barriers to providing overload capabilities.

For a single-phase to earth (phase A to earth) unbalanced fault as shown in Figure 4.14, the fault current characteristics and magnitude for both SG and SC are the same. It can be seen from Figure 4.14 that due to phase A to earth (A-E) fault, only phase A voltage decreases significantly and other two phases are close to the normal operating voltage. A considerable increase in phase A and phase C current can be observed from SG and SC during the A-E fault and fault

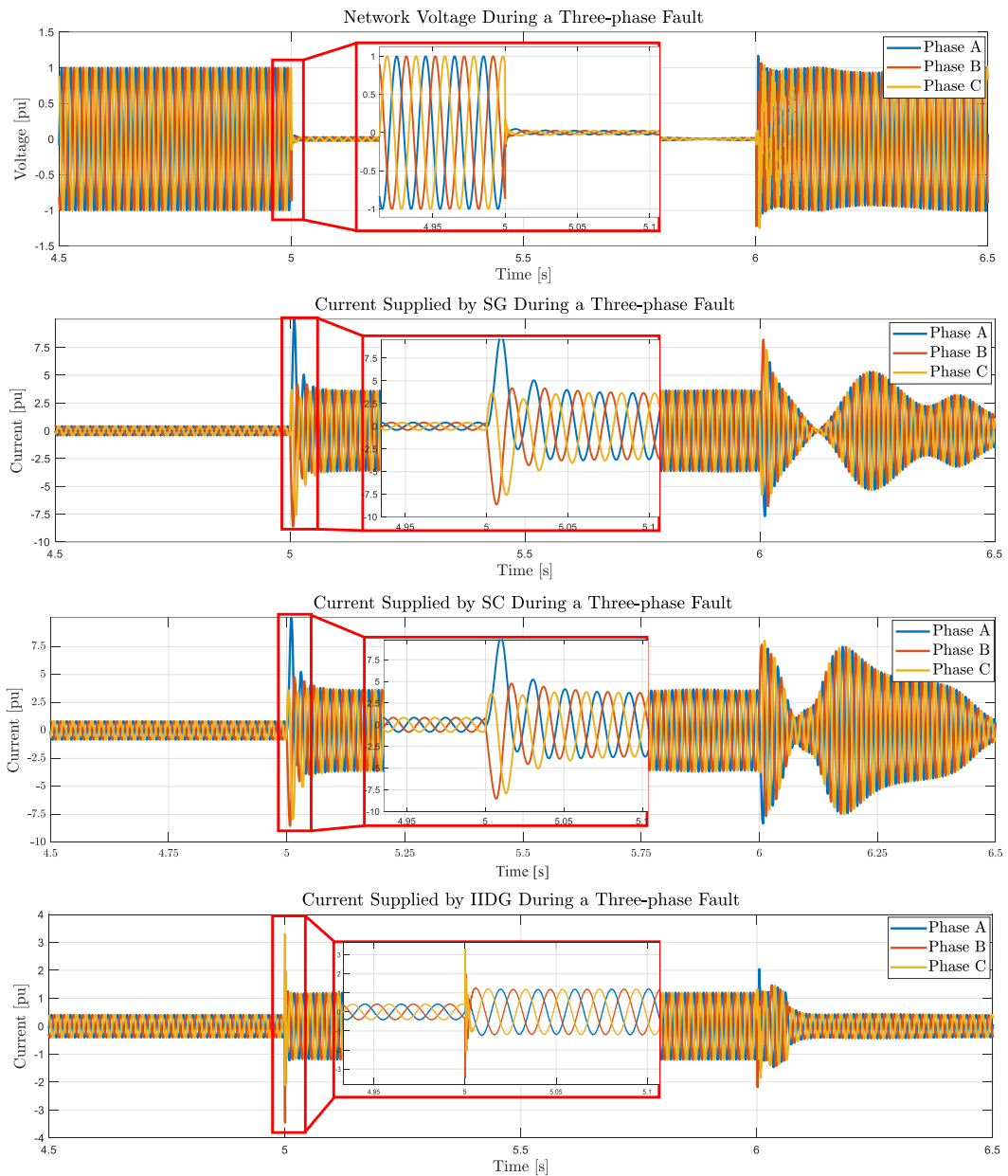


Figure 4.13: Grid voltage and current from all generation units during a three-phase fault.

current magnitudes for both SG and SC are 5 pu for transient period and 4.5 pu for steady state fault condition. However, fault characteristic and magnitude provided by IIDG is significantly different from SG and SC. As can be observed from Figure 4.14, fault current supplied by IIDG is limited to 1.2 pu as designed by the controller and current magnitudes for all three phases have been increased

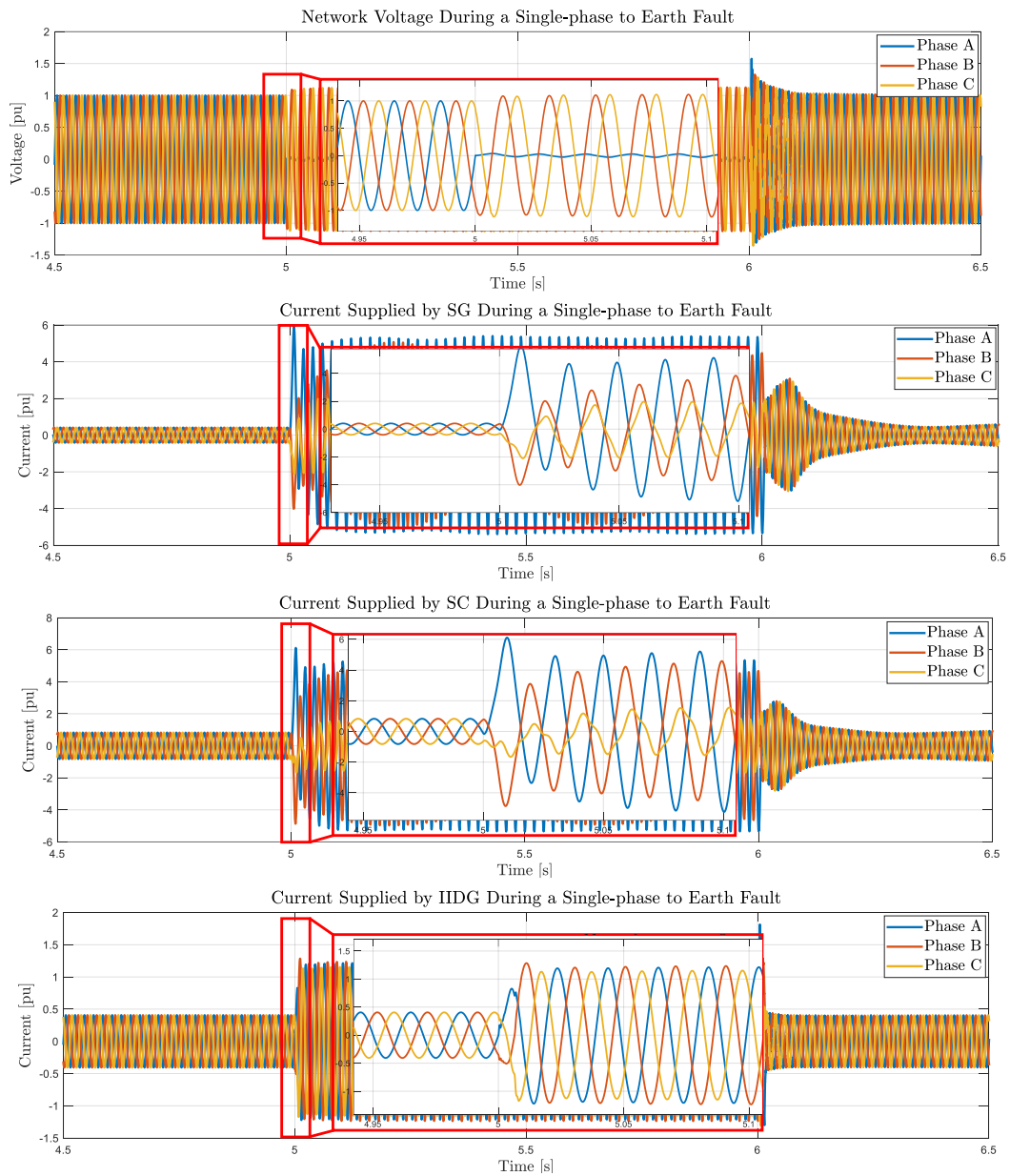


Figure 4.14: Grid voltage and current from all generation units during a single-phase fault.

(due to the internal current control of the inverter with zero sequence components removed) where, in case of SG and SC, phase A and phase C current have been increased. This different characteristic of IIDG's fault current can have significant impact on the existing protection devices; for example, distance protection as explained in [27].

It is necessary to mention that the fault currents of both phases A and C (for

SG and SC) increased during the phase A to earth fault is due to the earthing transformer winding configurations. The currents shown for SC and SG are measured at the generator outputs, which are supplying a delta-star step-up transformer, which is earthed on the HV side. Accordingly, while the transformer will supply phase A current with minimal phase B and C currents, the delta side will be supplied with significant currents on all three phases.

The results for a phase to phase fault (phase A to phase B (A-B)) is shown in Figure 4.15. A reduction in voltage of phase A and phase B can be observed due to the A-B fault. For SG and SC, a significant increase in phase A and phase B fault current can be observed, which is approximately 6 pu. The phase C fault current of both SG and SC are out of phase compared to normal condition and aligned with the phase A fault current. However, in case of IIDG, no changes in all three phases fault currents can be observed compared to single-phase to earth fault and three-phase fault, i.e. fault current for all three phases increases during A-B fault and limited to 1.2 pu.

Overall, it can be observed that IIDG fault current characteristic and magnitude do not vary depending on the type of fault since fault current magnitude is controlled by the internal current control loop of the IIDG and can be limited to a certain value. In this research, fault current from IIDG has been limited to 1.2 pu by maintaining the criteria mentioned in IEEE standard 1547.4-2011 [28]. It is necessary to mention that several other researchers use different magnitude of fault current limitation [29, 30] and there is no specific requirement in GB grid code regarding fault current limitation of IIDG.

Furthermore, from the analysis it can be concluded that fault current provided by SG and SC are similar in characteristics and magnitude while a significant difference can be observed between IIDG and synchronous machines. Inverters normally act to limit unbalance (negative and zero sequence) output currents – this can sometimes adversely affect conventional protection as the detection

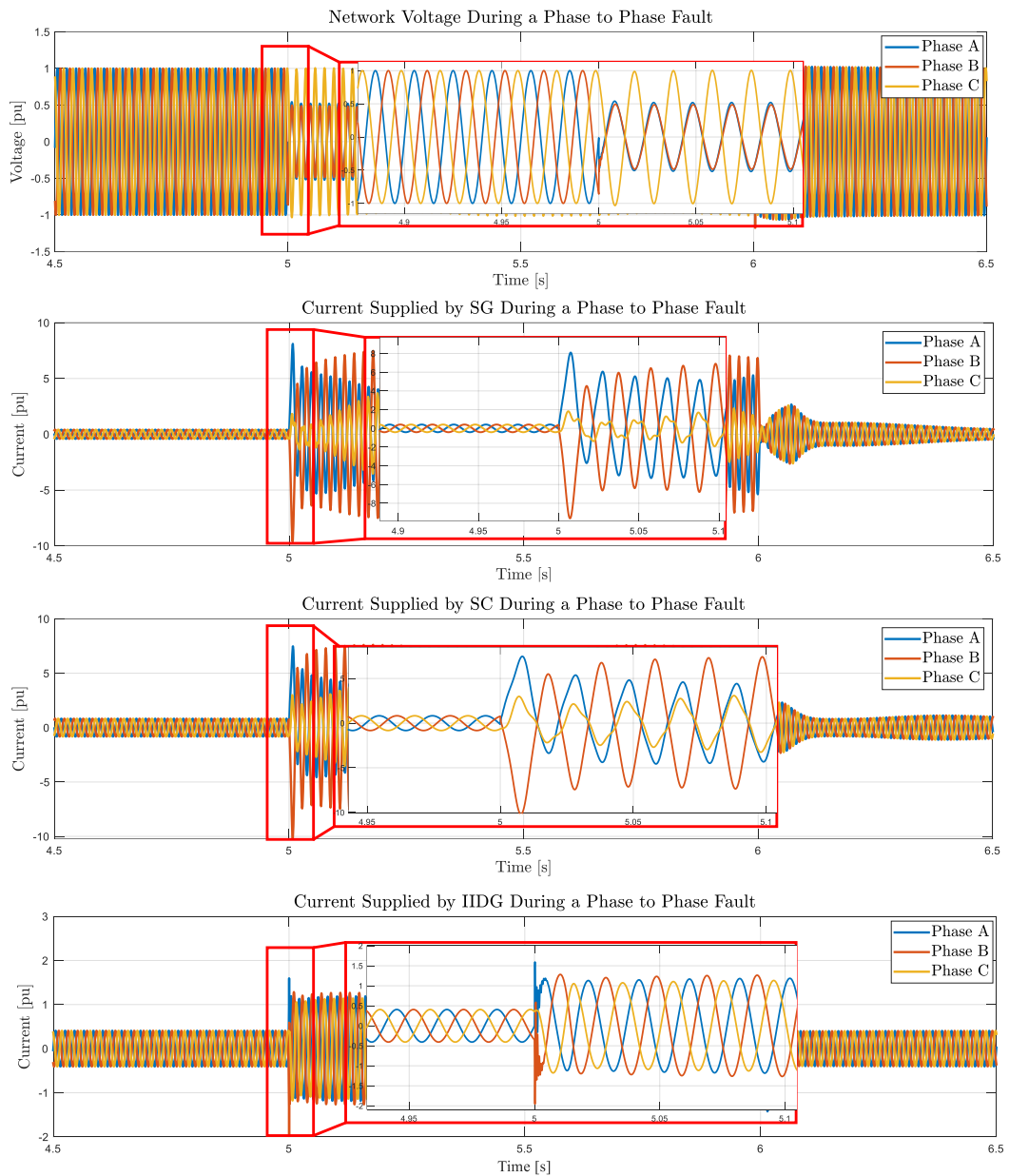


Figure 4.15: Grid voltage and current from all generation units during a phase to phase fault.

of negative and zero sequence current is sometimes used to trigger or “start” protection operation. It is preferable for conventional protection to have inverters that behave “like” synchronous machines, and efforts to achieve this have been made via “virtual synchronous machines”. However, there will still be significantly different behaviour [31], which is why alternative protection solutions (such as the solution reported in this thesis) will be required in many situations.

### 4.2.3 Fault Ride Through (FRT)

For any generator or energy source aiming to provide support to the grid during external fault/undervoltage conditions (for which the unit should not trip instantly), the capability to remain connected to the system in order to provide voltage support is crucial. Based on [21], the IIDG unit must ride through a voltage depression down to a level of 0.3 pu for a duration of at least 140 ms. However, there are different FRT requirements mentioned in the GB grid code [20] for different types of power generating modules (for example, synchronous power generating module, power park module) connected at different voltage levels. Therefore, in this research, a similar voltage profile matching the FRT requirements for power park generating modules for onshore transmission network as specified in the grid code [20] have been simulated to evaluate the IIDG's FRT capability and same voltage profile is utilised to compare performance with SC and SG.

A similar voltage profile of FRT for power park generating modules connected at onshore transmission network according to the GB's grid code [20] is shown in Figure 4.16, which is applied at the controllable voltage source as shown in Figure 4.11 for emulating a severe fault event. According to the FRT requirement mention in [20], the generation units must need to be connected for 3 minutes (after 2.5 s) at 0.85 pu voltage. It is difficult to demonstrate the voltage graph and generation connection for that significant long time through simulation. Therefore, the voltage profile after 2.5 s (starting from the occurrence of the event) has not been shown in Figure 4.16. However, several voltage step simulations have been carried out in Section 4.2.4. The results from the voltage step will verify the effectiveness of the implemented IIDG model. The reactive current and total current magnitude provided by each of the generation unit (IIDG, SG and SC) during FRT voltage profile are shown in Figure 4.16.

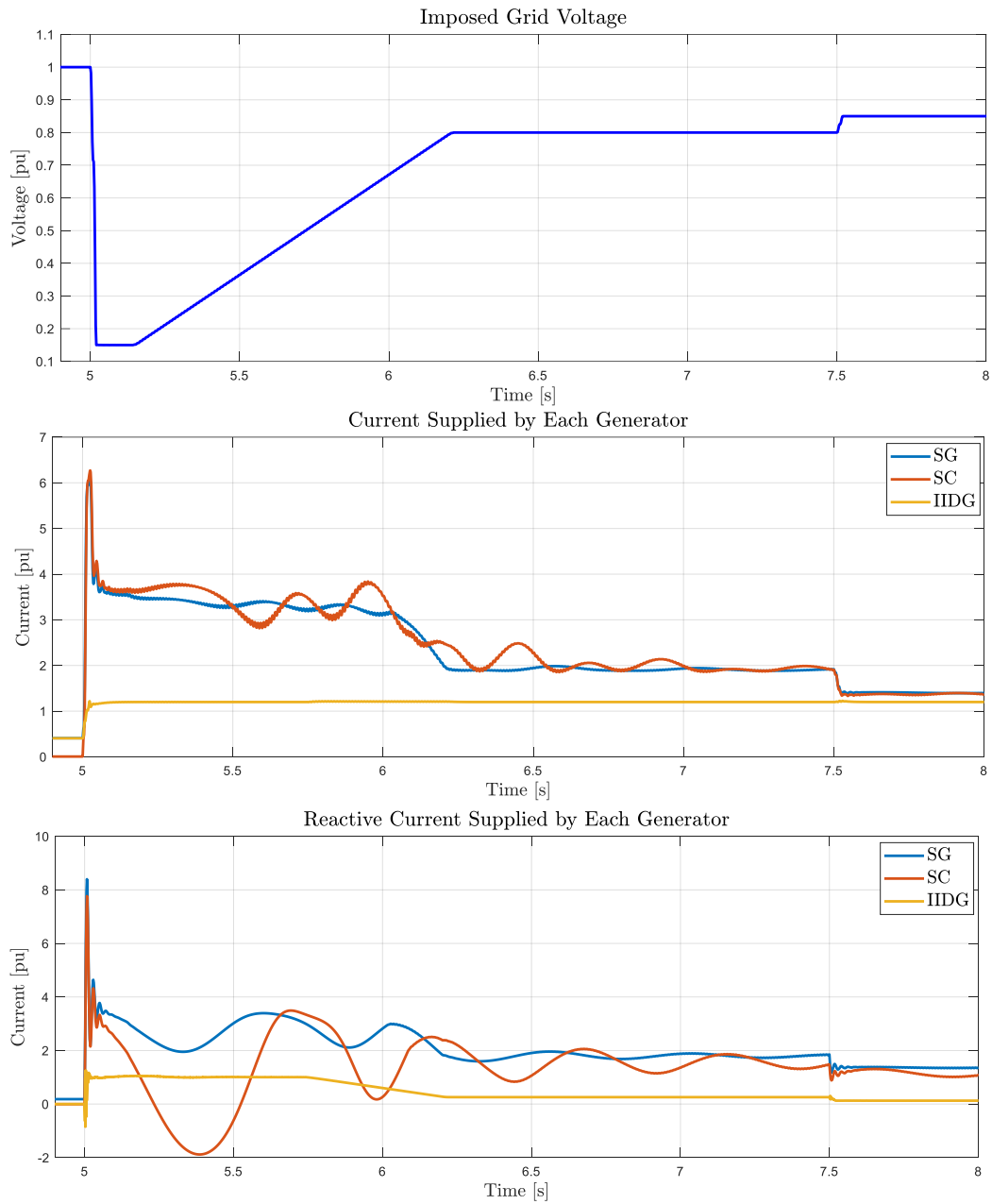


Figure 4.16: Simulation results for FRT.

From Figure 4.16, it can be observed that the IIDG can successfully remain connected to the system throughout the FRT profile specified in the current GB grid code for the onshore transmission network. The IIDG unit started to provide reactive current to the network while grid voltage is less than 0.9 pu and by following the GB grid code, the IIDG unit provides the maximum reactive current of 1 pu when grid voltage is less than 0.5 pu. However, as can be seen from Figure

4.16, the total current supplied by IIDG is always 1.2 pu when voltage drops at or lower than 0.9 pu. This is due to fault current limiter of the IIDG unit. Whenever, voltage is less than 0.9 pu, the IIDG controller detects that as a fault and limit the IIDG output current within 1.2 pu. Therefore, it can be concluded that fault current supply from IIDG unit is independent of fault location (assuming voltage magnitude does not change significantly in short line length microgrids, although may not be true for the long transmission network) and always will be limited whenever, there is a fault in the network. This behaviour of the IIDG unit is significantly different than the conventional synchronous machines. Furthermore, the IIDG unit is capable of remaining connected for 140 ms during the severe voltage depression of 0.15 pu, meeting the requirements as specified in [21].

The behaviour of both SG and SC are almost similar with a large amount of current and reactive current injected to the system due to their large overloading capability. However, a stability issue can be observed during FRT voltage profile for SC unit as the reactive current supplied by the SC unit oscillates significantly, due to the aforementioned absence of a governor in the SC, and a sharp decrease in reactive current can be observed during voltage slope increasing from 0.15 pu.

#### 4.2.4 Voltage Steps

The case studies of this section will evaluate the capability of IIDG's remaining connected during severe voltage depression for certain period and compared with SC and SG in terms of providing reactive power support to the grid when a voltage disturbance occurs. According to GB grid code [20], the IIDG units (power park module) are expected to remain connected under several severe voltage reduction for certain period while providing reactive power support to the grid. Therefore, three different simulations with different voltage depression (i.e. voltage is reduced to 0.3 pu, 0.5 pu and 0.85 pu from 1 pu) has been carried out and the results are shown in Figure 4.17, Figure 4.18 and Figure 4.19 along with imposed depressed

grid voltage, total and reactive current provided by each generation unit.

According to GB grid code, the IIDG units must remain connected during a severe voltage drop of 0.7 pu for 384 ms. Therefore, a simulation has been carried out that can replicate the similar condition as can be seen from Figure 4.17, where a grid voltage drops to 0.3 pu and the designed IIDG unit remain connected throughout the disturbance and provided maximum reactive current of 1 pu. The current supplied by the IIDG unit is smaller than the reactive current supplied by SG and SC units.

In the second simulation of the voltage step, a voltage reduction of 50% (of nominal value) has been carried out for 710 ms. The IIDG units must remain connected for 710 ms and inject maximum reactive current to support to the grid during voltage reduction of 0.5 pu as specified in the GB grid code. The implemented IIDG successfully maintain the condition as can be observed in Figure 4.18. The behaviour for SC and SG units are very similar to each other and providing comparatively higher reactive power than IIDG.

According to GB grid code, the power park modules need to provide reactive power to the grid when there is a voltage drop of 0.1 pu and remain connected to the system when voltage is 0.85 pu for a duration of 3 minutes. Therefore, in the third simulation of the voltage step, voltage step at 0.85 pu has been simulated for 5 s instead of 3 minutes because simulation of more than 180 s is difficult to present and carry out in a non-real time simulation. However, the implemented IIDG unit remain connected to the simulated grid in this simulation and provided reactive power as can be seen from Figure 4.19.

It can be observed from all the voltage step simulations (as shown in Figure 4.17, Figure 4.18 and Figure 4.19) that both SC and SG units provide better reactive power support to the grid during a voltage disturbance or voltage reduction in comparison to the IIDG unit due their large overloading capability. However, as it is evident from Figure 4.19, SG can provide slightly higher reactive current

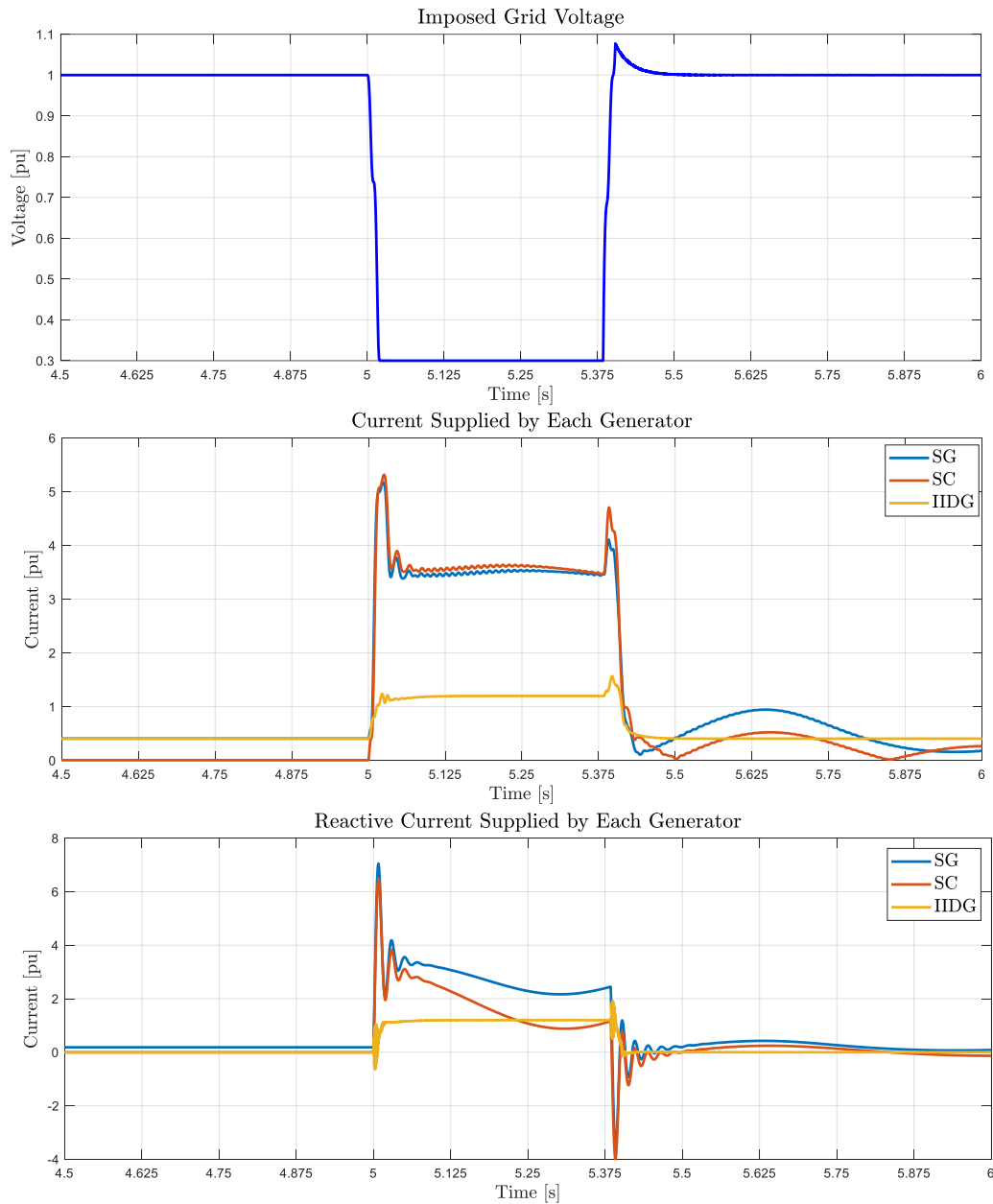


Figure 4.17: Grid voltage, total and reactive power supplied by all generation units during voltage step to 0.3 pu simulation.

support in comparison to the SC when voltage reduction is not severe; for example, when voltage is higher than 0.8 pu. Also, SG unit may provide better stability due to the governor which is not available in the case of SC unit.

Overall, the developed IIDG unit meets all the requirements as specified in the GB grid code and stability-pathfinder document. Therefore, it can be concluded

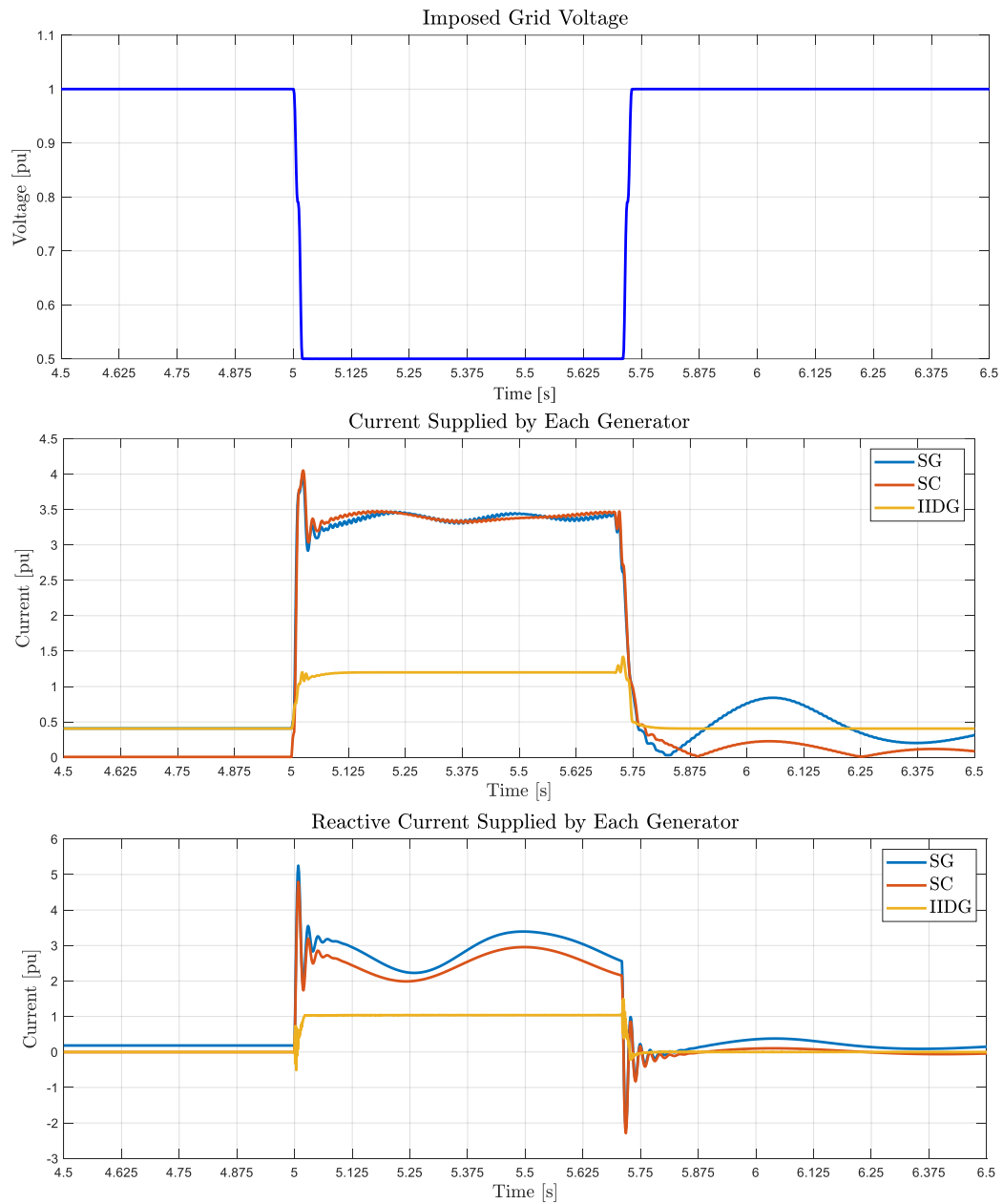


Figure 4.18: Grid voltage, total and reactive power supplied by all generation units during voltage step to 0.5 pu simulation.

that the developed IIDG model is ready to carry out further simulations to validate the proposed protection scheme which is the prime objective of this thesis.

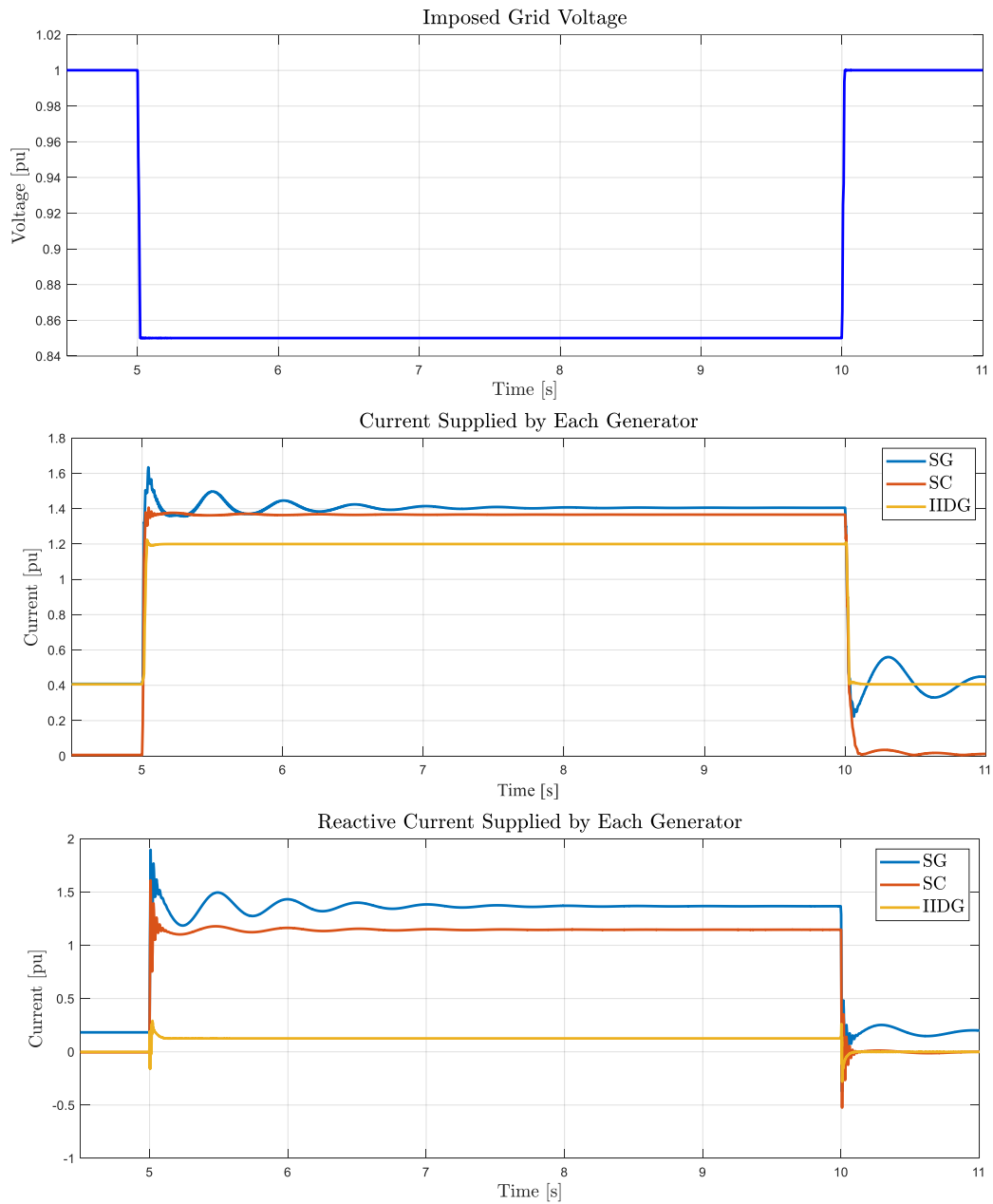


Figure 4.19: Grid voltage, total and reactive power supplied by all generation units during voltage step to 0.85 pu simulation.

### 4.3 Summary

In this chapter, design, modelling, implementation and internal construction of the control loops of two types of inverter control scheme have been discussed. A wide range of simulation studies have been carried out to evaluate the capabilities of the developed IIDG unit. Furthermore, the dynamic behaviours of the SG, SC

and IIDG during various contingency events are compared.

It can be observed that the behaviour of SG and SC are very similar for all studied cases. For short circuit faults, while the IIDG can potentially provide a fast fault current injection, a key limitation is on the magnitude of fault currents, so it is unlikely to be capable of offer the same level of short circuit contribution compared to SCs and SGs. In terms of unbalanced fault characteristics, the IIDG's fault characteristic is similar to the balanced fault characteristic where all three phase currents increase equally. Therefore, IIDG units' fault characteristic is significantly different compared to one provided by SCs and SGs.

A substantial difference in reactive power supply during FRT and voltage steps can also be observed between IIDG and synchronous machines. Due to higher overloading capacity, SC and SG units can provide a large reactive current during the voltage disturbances. In case of IIDG unit, although it provides limited reactive current during voltage disturbances, it can remain connected during the FRT and voltage steps, and can provide required amount of reactive power with specified voltage levels as stated in the GB grid code.

## References

- [1] J. Rocabert, A. Luna, F. Blaabjerg, and P. Rodríguez, "Control of power converters in ac microgrids," *IEEE Transactions on Power Electronics*, vol. 27, no. 11, pp. 4734–4749, 2012.
- [2] K. De Brabandere, B. Bolsens, J. Van den Keybus, A. Woyte, J. Driesen, and R. Belmans, "A voltage and frequency droop control method for parallel inverters," *IEEE Transactions on Power Electronics*, vol. 22, no. 4, pp. 1107–1115, 2007.

- [3] J. C. Vasquez, J. M. Guerrero, A. Luna, P. Rodriguez, and R. Teodorescu, “Adaptive droop control applied to voltage-source inverters operating in grid-connected and islanded modes,” *IEEE Transactions on Industrial Electronics*, vol. 56, no. 10, pp. 4088–4096, 2009.
- [4] F. Blaabjerg, R. Teodorescu, M. Liserre, and A. Timbus, “Overview of control and grid synchronization for distributed power generation systems,” *IEEE Transactions on Industrial Electronics*, vol. 53, no. 5, pp. 1398–1409, 2006.
- [5] A. Timbus, M. Liserre, R. Teodorescu, P. Rodriguez, and F. Blaabjerg, “Evaluation of current controllers for distributed power generation systems,” *IEEE Transactions on Power Electronics*, vol. 24, no. 3, pp. 654–664, 2009.
- [6] M. Reyes, P. Rodriguez, S. Vazquez, A. Luna, R. Teodorescu, and J. M. Carrasco, “Enhanced decoupled double synchronous reference frame current controller for unbalanced grid-voltage conditions,” *IEEE Transactions on Power Electronics*, vol. 27, no. 9, pp. 3934–3943, 2012.
- [7] J. M. Guerrero, L. Hang, and J. Uceda, “Control of distributed uninterruptible power supply systems,” *IEEE Transactions on Industrial Electronics*, vol. 55, no. 8, pp. 2845–2859, 2008.
- [8] J. C. Vasquez, J. M. Guerrero, M. Savaghebi, J. Eloy-Garcia, and R. Teodorescu, “Modeling, analysis, and design of stationary-reference-frame droop-controlled parallel three-phase voltage source inverters,” *IEEE Transactions on Industrial Electronics*, vol. 60, no. 4, pp. 1271–1280, 2013.
- [9] T. Qoria, F. Gruson, F. Colas, X. Kestelyn, and X. Guillaud, “Current limiting algorithms and transient stability analysis of grid-forming vscs,” *Electric Power Systems Research*, vol. 189, p. 106726, 2020. [Online]. Available: <https://www.sciencedirect.com/science/article/pii/S0378779620305290>

- [10] L. Huang, H. Xin, Z. Wang, L. Zhang, K. Wu, and J. Hu, “Transient stability analysis and control design of droop-controlled voltage source converters considering current limitation,” *IEEE Transactions on Smart Grid*, vol. 10, no. 1, pp. 578–591, 2019.
- [11] T. Qoria, T. Prevost, G. Denis, F. Gruson, F. Colas, and X. Guillaud, “Power converters classification and characterization in power transmission systems,” in *2019 21st European Conference on Power Electronics and Applications (EPE '19 ECCE Europe)*, 2019, pp. P.1–P.9.
- [12] T. Green and M. Prodanović, “Control of inverter-based micro-grids,” *Electric Power Systems Research*, vol. 77, no. 9, pp. 1204–1213, 2007, distributed Generation. [Online]. Available: <https://www.sciencedirect.com/science/article/pii/S037877960600191X>
- [13] J. T. Bialasiewicz, “Renewable energy systems with photovoltaic power generators: Operation and modeling,” *IEEE Transactions on Industrial Electronics*, vol. 55, no. 7, pp. 2752–2758, 2008.
- [14] H. H. Zeineldin, “A  $q-f$  droop curve for facilitating islanding detection of inverter-based distributed generation,” *IEEE Transactions on Power Electronics*, vol. 24, no. 3, pp. 665–673, 2009.
- [15] H. H. Zeineldin, E. F. El-saadany, and M. M. A. Salama, “Distributed generation micro-grid operation: Control and protection,” in *2006 Power Systems Conference: Advanced Metering, Protection, Control, Communication, and Distributed Resources*, 2006, pp. 105–111.
- [16] P. Rodriguez, A. Lunar, R. Teodorescu, F. Iov, and F. Blaabjerg, “Fault ride-through capability implementation in wind turbine converters using a decoupled double synchronous reference frame pll,” in *2007 European Conference on Power Electronics and Applications*, 2007, pp. 1–10.

- [17] S.-K. Chung, “A phase tracking system for three phase utility interface inverters,” *IEEE Transactions on Power Electronics*, vol. 15, no. 3, pp. 431–438, 2000.
- [18] R. M. Santos Filho, P. F. Seixas, P. C. Cortizo, L. A. B. Torres, and A. F. Souza, “Comparison of three single-phase pll algorithms for ups applications,” *IEEE Transactions on Industrial Electronics*, vol. 55, no. 8, pp. 2923–2932, 2008.
- [19] S. Shinnaka, “A robust single-phase pll system with stable and fast tracking,” *IEEE Transactions on Industry Applications*, vol. 44, no. 2, pp. 624–633, 2008.
- [20] National Grid, “The Grid Code- Issue 6 Revision 11,” National Grid ESO, Warwick, UK, Tech. Rep. 6, 2022. [Online]. Available: <https://www.nationalgrideso.com/document/162271/download>
- [21] National Grid ESO, “Stability Pathfinder RFI Technical Performance and Assessment Criteria,” no. Attachment 1, p. Report, 2019. [Online]. Available: <https://www.nationalgrideso.com/document/148341/download>
- [22] K. R. Padiyar and A. M. Kulkarni, *Modeling and Simulation of Synchronous Generator Dynamics*, 2019, pp. 59–113.
- [23] “Ieee recommended practice for excitation system models for power system stability studies,” *IEEE Std 421.5-2016 (Revision of IEEE Std 421.5-2005)*, pp. 1–207, 2016.
- [24] M. Nagpal, A. Moshref, G. Morison, and P. Kundur, “Experience with testing and modeling of gas turbines,” in *2001 IEEE Power Engineering Society Winter Meeting. Conference Proceedings (Cat. No.01CH37194)*, vol. 2, 2001, pp. 652–656 vol.2.

- [25] E. Bompard, A. Mazza, and L. Toma, “Chapter 3 - classical grid control: Frequency and voltage stability,” in *Converter-Based Dynamics and Control of Modern Power Systems*, A. Monti, F. Milano, E. Bompard, and X. Guillaud, Eds. Academic Press, 2021, pp. 31–65. [Online]. Available: <https://www.sciencedirect.com/science/article/pii/B9780128184912000031>
- [26] National Grid ESO, “System operability framework Impact of declining short circuit levels,” *report*, p. 8, 2018.
- [27] J. Jia, G. Yang, A. H. Nielsen, and P. Rønne-Hansen, “Impact of vsc control strategies and incorporation of synchronous condensers on distance protection under unbalanced faults,” *IEEE Transactions on Industrial Electronics*, vol. 66, no. 2, pp. 1108–1118, 2019.
- [28] “IEEE guide for design, operation, and integration of distributed resource island systems with electric power systems,” *IEEE Std 1547.4-2011*, pp. 1–54, 2011.
- [29] M. Haj-Ahmed and M. Illindala, “The influence of inverter-based dgs and their controllers on distribution network protection,” *IEEE Transactions on Industry Applications*, vol. 50, no. 4, pp. 2928–2937, 2014, cited By 112. [Online]. Available: <https://www.scopus.com/inward/record.uri?eid=2-s2.0-84904662097&doi=10.1109%2fTIA.2013.2297452&partnerID=40&md5=f6b3c443438762287e42f923277a32e6>
- [30] B. Mahamedi, M. Eskandari, J. E. Fletcher, and J. Zhu, “Sequence-based control strategy with current limiting for the fault ride-through of inverter-interfaced distributed generators,” *IEEE Transactions on Sustainable Energy*, vol. 11, no. 1, pp. 165–174, 2020.
- [31] D. Liu, Q. Hong, M. Khan, A. Dyśko, A. Egea Alvarez, and C. Booth, “Evaluation of grid-forming converter’s impact on distance

protection performance,” Mar. 2022, the 16th International Conference on Developments in Power System Protection ; Conference date: 07-03-2022 Through 10-03-2022. [Online]. Available: <https://dpsp.theiet.org/>

## Chapter 5

# Demonstration of Practical Challenges Associated with Overcurrent Protection and Proposed Protection Scheme

After reviewing the protection challenges and shortcomings of the available solutions in Chapter 3, this chapter presents the practical shortcomings of the traditional overcurrent relays by simulating different fault scenarios by varying location of the faults and generation units in a microgrid. Furthermore, this chapter suggests a unique protection scheme for islanded microgrids. The details implementations of the proposed protection scheme will also be illustrated with appropriate examples, diagrams and practical consideration.

## 5.1 Performance Analysis of Overcurrent Protection

Overcurrent (OC) protection scheme is universally used in low voltage active distribution networks/microgrids and popular due to cost, reliability, inherent provision of backup and other factors. However large-scale integration of IIDGs, and islanded operation, present many challenges to conventional OC schemes, as presented in detail in Chapter 3. In this section, those challenges will be studied and demonstrated on the test network used for demonstration of the proposed novel scheme. Several fault cases are simulated with different locations and for different combinations of IIDGs on the network.

### 5.1.1 Simulation Model of Micorgrid and Overcurrent Relays

To understand the protection challenges and to observe the performance of the overcurrent scheme on the microgrid, a simple and realistic model of a microgrid is designed in the MATLAB Simulink and is shown in Figure 5.1. It is necessary to mention that the same microgrid model has been utilised to validate the proposed protection scheme, which will be illustrated with details in Chapter 6. From the figure, it can be seen that there are three buses and each bus can contain IIDG and load. The connections of each IIDG in the buses are flexible, that is, they can be connected or disconnected from the network based on the simulation cases which will be discussed later in Section 5.1.2. A controllable switch at the point of interconnection (POI) (in this thesis, POI and PCC are used interchangeably) can enable connection of an 11 kV distribution grid.

The OC relays,  $R_1$ ,  $R_2$  and  $R_3$  are installed at the end of Bus 1, Bus 2 and Bus 3 respectively as can be seen from Figure 5.1. The operating characteristics

CHAPTER 5. DEMONSTRATION OF PRACTICAL CHALLENGES  
ASSOCIATED WITH OVERCURRENT PROTECTION AND PROPOSED  
PROTECTION SCHEME

---

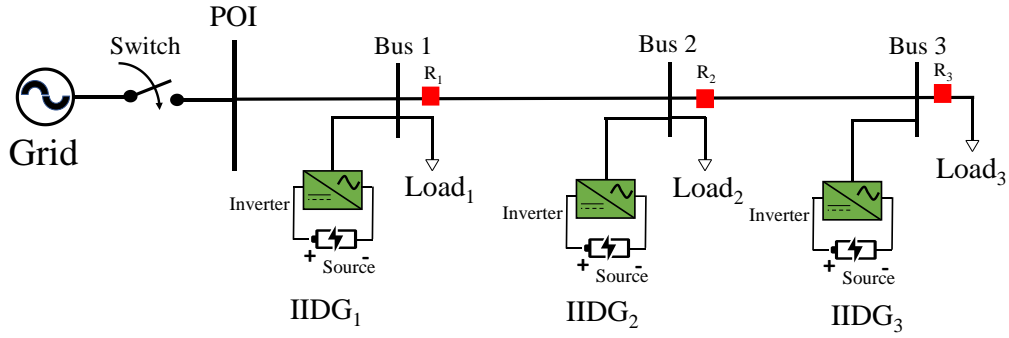


Figure 5.1: Designed microgrid to test the overcurrent relays.

of the relays are inverse definite minimum time (IDMT) and the operating time of each relay can be calculated using (5.1), where TMS is the time multiple setting and PSM is the plug setting multiplier (which effectively defines the multiple of the rated measured primary/secondary current that will cause the relay to begin operating [1]). The characteristic curves of all three IDMT overcurrent relays are shown in Figure 5.2. From the characteristic graph of Figure 5.2, it can be seen that for a three-phase to earth balanced fault after Bus 3 (the fault current is around 1.9 kA), relay  $R_3$  operates as the primary protection relay (with a time delay of around 0.07 s) while relay  $R_2$  works as backup protection (around 0.37 s, if necessary), maintaining a coordination interval of 0.3 s. Similarly, for a fault between Bus 2 and Bus 3, the fault current is around 3.3 kA and  $R_2$  acts as primary protection, operating with a time delay of approximately 0.32 s and  $R_1$  is the backup, operating at around 0.62 s if  $R_2$  or its controlled circuit breaker fails to operate. Assuming the grid fault level is 250 MVA (the system is operating in grid connected mode), the settings of each relay for the network configuration shown in Figure 5.1 are calculated and are presented in Table 5.1. The calculation of load currents and the relay settings are presented in Appendix A, along with analysis and discussion of performance and associated issues.

$$OT = \frac{0.14}{PSM^{0.02} - 1} \quad (5.1)$$

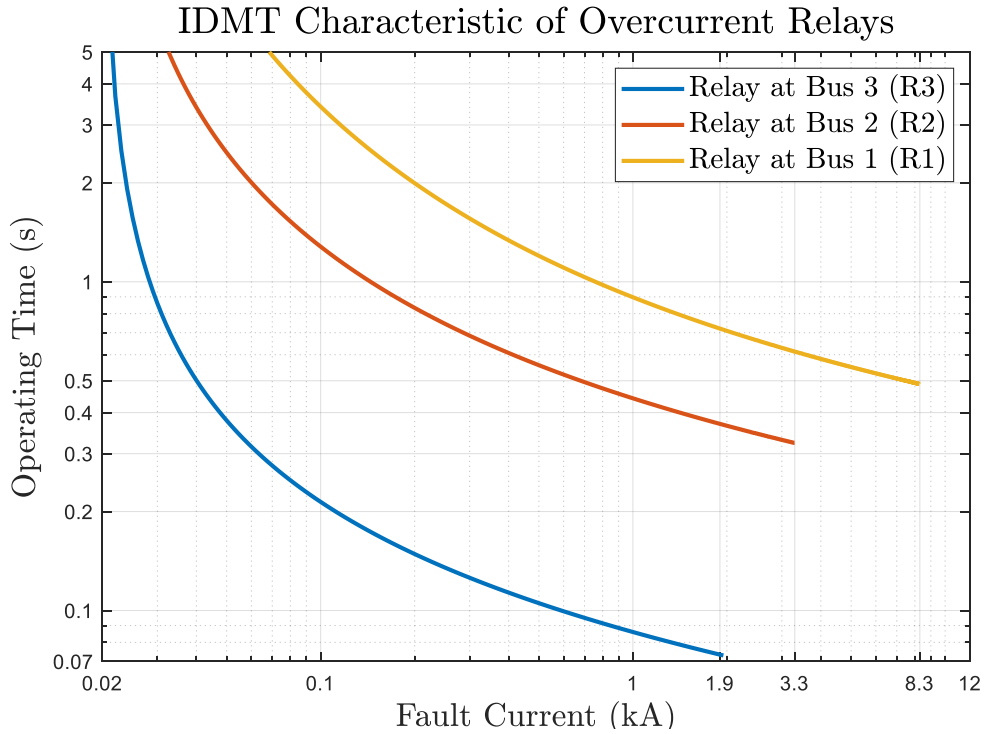


Figure 5.2: IDMT characteristics for all three overcurrent relays used for simulations.

Table 5.1: Settings of the relays used for the simulations.

Relays	CT Ratio	PS	TMS
$R_1$	40	200%	0.34
$R_2$	20	175%	0.22
$R_3$	20	100%	0.05

### 5.1.2 Simulation Results with Demonstration of OC Relays Performance Under Different Scenarios

The results from simulations considering a range of scenarios, including variations in fault level, islanded mode operation, and cases where IIDGs are present throughout the system, are analysed in this section. Using the results, demonstration and explanation of protection challenges (with respect to conventional OC protection) are also provided.

CHAPTER 5. DEMONSTRATION OF PRACTICAL CHALLENGES  
ASSOCIATED WITH OVERCURRENT PROTECTION AND PROPOSED  
PROTECTION SCHEME

---

**Scenario 1: Variation of Grid Fault Levels**

In this scenario, the fault current level from the grid is decreased from 250 MVA to 2 MVA (effectively approaching islanded mode operation), and the impact of progressively “weaker” grid infeed on protection performance is ascertained. Table 5.2 presents the operating time (OT) of the relays after faults at different locations of the network with the aforementioned progressively decreasing fault levels.

Table 5.2: Operating time (OT) of the relays during different faults with variation of grid fault level.

Grid Fault Level (MVA)	Fault After Bus 3 ( $F_3$ )		Fault between Bus 2 and Bus 3 ( $F_2$ )		Fault before Bus 2 ( $F_1$ )
	OT of $R_3$ (s)	OT of $R_2$ (s)	OT of $R_2$ (s)	OT of $R_1$ (s)	OT of $R_1$ (s)
250	0.07	0.37	0.32	0.62	0.49
225	0.07	0.37	0.33	0.62	0.50
200	0.07	0.37	0.33	0.62	0.51
150	0.07	0.38	0.33	0.64	0.53
100	0.08	0.38	0.35	0.67	0.57
50	0.08	0.41	0.38	0.75	0.68
25	0.09	0.46	0.44	0.90	0.85
20	0.09	0.49	0.46	0.97	0.92
10	0.11	0.59	0.58	1.31	1.26
5	0.14	0.79	0.77	2.08	2.01
2	0.21	1.45	1.43	9.83	9.21

A significant change in the operating time of the relays can be observed when the grid fault level reduces to less than 50 MVA. Furthermore, for 10 MVA grid fault level,  $R_2$  operates with a delay of 0.58 s for fault  $F_2$  (fault between Bus 2 and Bus 3), which is significantly high. Generally, undervoltage protection (if the voltage is less than 50% of the nominal value during a fault) of the generators is activated at 0.5 s. Therefore, it is expected that the main line protection of the network must operate before 0.5 s. However, from the simulation results, it has been observed that there is a possibility of slow operation for  $R_2$  for fault,  $F_2$

while the grid fault level is 10 MVA or while power system is weak.

Similar results are also observed for the relay  $R_1$  for fault,  $F_1$  (fault between Bus 1 and Bus 2). From Table 5.2, it can be seen that OT of  $R_1$  is relatively high because of the high TMS (the value is set in this way to maintain coordination between the relays). To solve this issue, an instantaneous element can be used in conjunction with the IDMT element. The IDMT characteristic including an appropriately-set instantaneous element for  $R_1$  for fault  $F_1$  is shown in Figure 5.3. However, for a fault level of 10 MVA, the maximum fault current for fault,  $F_1$  is around 0.51 kA and from Figure 5.3 it can be seen that OT for  $R_1$  is still higher than 0.5 s.

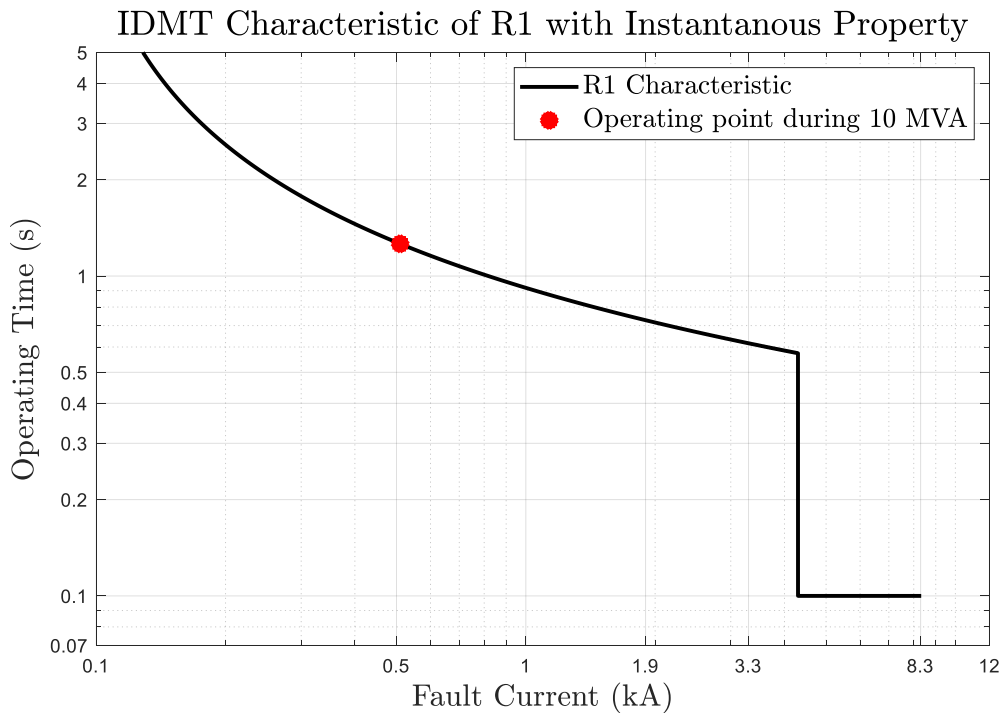


Figure 5.3: IDMT characteristic of  $R_1$  with the instantaneous property.

Thus, based on the simulation results for this case, it can be concluded that overcurrent protection for a microgrid, using settings calculated based on maximum fault levels, will operate progressively more slowly for weakened grid system. While this could be resolved with multiple setting groups, or adaptive protection, the

complexity and perhaps costs (and possibility of incorrect settings being applied when the fault level is different from that anticipated) of protection will increase substantially.

### Scenario 2: Miscoordination of the Relays

Two examples of miscoordination of the relays due to variation of fault locations and/or IIDGs locations are analysed using simulations in this section. The first example is presented in Figure 5.4, where one IIDG is connected at Bus 3 and the fault is located between Bus 1 and Bus 2 ( $F_1$ ). In this case, the relay at Bus 1,  $R_1$  should operate to isolate the faulty section from the grid and to disconnect the fault current being supplied from the IIDG; the relay at Bus 2,  $R_2$ , should also operate in this case (in fact, a relay/circuit breaker to the left hand side of Bus 2 would ideally be required in order to preserve supply to Load<sub>2</sub> from any IIDGs connected downstream of this location for this particular fault example).

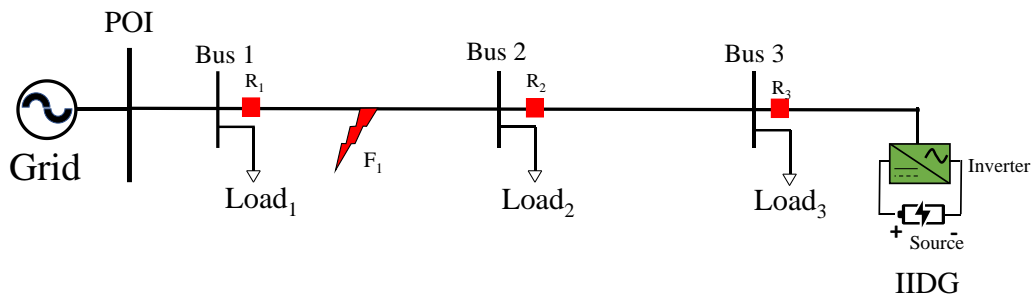


Figure 5.4: Example of Miscoordination of the relays.

However, according to the settings of the relays, as shown in Table 5.1, for fault at  $F_1$ , the operating times of  $R_1$ ,  $R_2$ , and  $R_3$  are respectively 0.49 s, 1.45 s and 0.21 s; while the fault current contribution from IIDG has not been limited. As mentioned earlier, for fault  $F_1$ , only relays  $R_1$  and  $R_2$  should isolate the faulted section. However, from the results of the simulation, it can be observed that  $R_3$  is operating faster than  $R_2$ , which is effectively unwanted and unnecessary

CHAPTER 5. DEMONSTRATION OF PRACTICAL CHALLENGES  
ASSOCIATED WITH OVERCURRENT PROTECTION AND PROPOSED  
PROTECTION SCHEME

---

sympathetic tripping of relay  $R_3$ . Furthermore, it is also evident that while fault current contribution of the IIDG is limited to 30 A, relay  $R_2$  does not operate and relay  $R_3$  operates after a delay at 1.39 s.

Therefore, from this simulation, it can be concluded that there is the potential for sympathetic tripping and miscoordination of relays due to the addition of IIDG (with and without fault current limitation). The remedy to this situation could involve the use of directional overcurrent protection where the relays will detect the direction of fault current and settings will be different based on direction. Again, the directional overcurrent relays could be expensive compared to nondirectional overcurrent relays and require additional voltage measurements, again adding to expense.

The second example is shown in Figure 5.5, where IIDG is connected to Bus 1 and fault is between Bus 2 and Bus 3 ( $F_2$ ). In this case, relay  $R_2$  should clear the fault and  $R_1$  should operate as a backup (if necessary). However, from the simulation results, it can be seen that the relay  $R_1$  operates faster (with its instantaneous element tripping- operating after a delay of 0.1 s) than relay  $R_2$ , which operates with a delay of 0.31 s. The operating times of relay  $R_1$  with and without IIDG are shown in Figure 5.6.

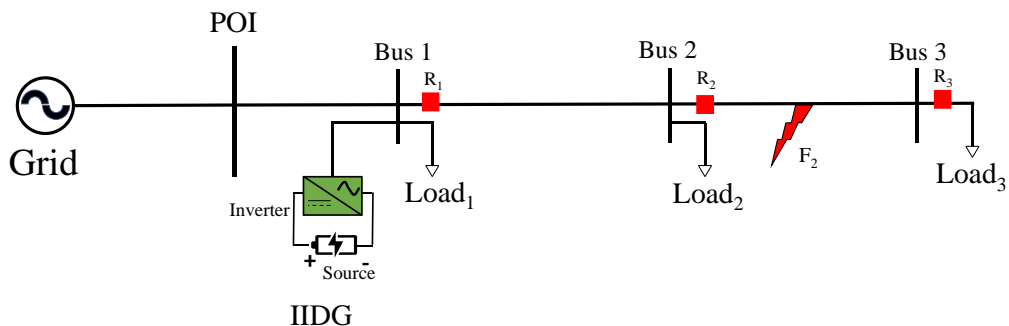


Figure 5.5: Miscoordination of relay  $R_1$  due to fault  $F_2$  with the instantaneous element.

The green point indicates the operating point when IIDG is not connected

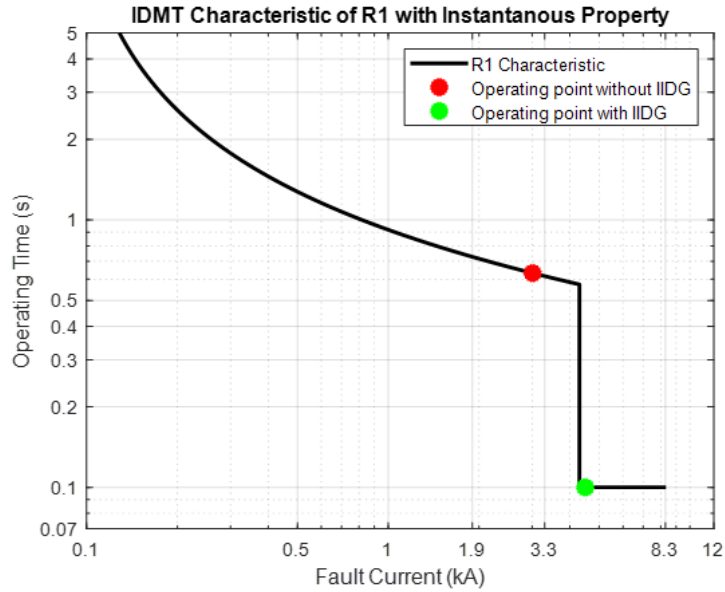


Figure 5.6: Characteristics of relay  $R_1$  with and without IIDG.

and  $R_1$  operates as backup protection for relay  $R_2$ . The red point indicates the operation for  $R_1$  while IIDG is connected, which is in the instantaneous part. As a result,  $R_1$  operates faster than  $R_2$  for fault  $F_2$ , which represents loss of coordination between relays  $R_1$  and  $R_2$ . However, this challenge largely depends on the capacity/fault level capability of the connected IIDG and may not be an issue for relatively small-scale IIDG with relatively lower fault current capabilities.

### Scenario 3: Islanded Network

In this simulation, the grid has been disconnected and the system operates in island mode. In order to maintain stability, and voltage and frequency within standard limits, a GFR is used in the  $IIDG_1$  as shown in Figure 5.1 and all other IIDG units are GFLs. The setup for this simulation is the same as shown in Figure 5.1 except in this case grid is not connected. Faults are simulated at three different locations in the network, between Bus 1 and Bus 2 ( $F_1$ ), between Bus 2 and Bus 3 ( $F_2$ ) and after Bus 3 ( $F_3$ ). The operating times of the relays for each

CHAPTER 5. DEMONSTRATION OF PRACTICAL CHALLENGES ASSOCIATED WITH OVERCURRENT PROTECTION AND PROPOSED PROTECTION SCHEME

fault are represented in Table 5.3.

Table 5.3: Operating time of the relays during islanded mode grid-connected operation modes.

Fault Location	Operating time during islanded mode		Operating time during grid connected mode (250 MVA)	
	Primary Protection (s)	Backup Protection (s)	Primary Protection (s)	Backup Protection (s)
$F_3$	0.25	3.54	0.07	0.37
$F_2$	3.45	Fault Not Detected	0.32	0.62
$F_1$	Fault Not Detected	N/A	0.49	N/A

As can be seen from Table 5.3, a significant change in the operating time of the overcurrent relays can be observed from grid-connected mode. In the worst-case situation, relay  $R_1$  does not detect the fault. Furthermore, detection of faults now depends on the number and fault current capabilities of the IIDGs.

#### Scenario 4: Bidirectional Power Flow

A case scenario is demonstrated in this section, where elements of the microgrid might not be protected due to bidirectional power flow. This scenario can be explained with the aid of Figure 5.7.

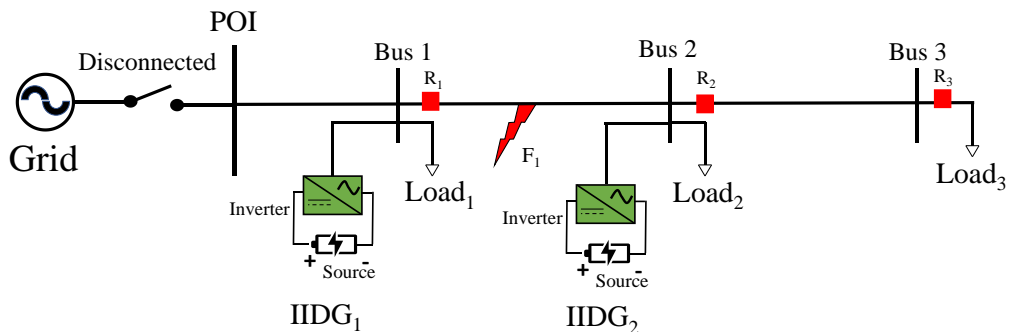


Figure 5.7: Microgrid protection challenge due to bidirectional power flow during fault.

In this case, due to fault  $F_1$ , both IIDGs will contribute fault current into the fault. Now, relay  $R_1$  might detect the fault depending on the fault current contribution from  $IIDG_1$  and the settings of the relay (although there is less possibility for that as described earlier). However, there is no relay/breaker in the network which can isolate the fault current contribution from  $IIDG_2$  towards the faulted section unless the IIDG's internal protection detects the fault and activates. Again, disconnection of  $IIDG_2$  may disrupt the power supply to the rest of the consumers and loads, which is not desirable.

## 5.2 Fundamental Principle of Operation of the Proposed Scheme

The proposed protection scheme is active in nature. That is, following fault inception, all connected IIDGs in the microgrid detect the fault, then intentionally limit their output currents and inject a specific harmonic component along with the fundamental frequency current. Based on analysis of the combination of injected and subsequently measured harmonic components, the relays in the network can identify the faulted line section and then take appropriate action (either in main and/or backup modes).

The scheme consists of four main steps that are involved in the protection of the islanded microgrid. The first step is the fault detection, when the scheme is initiated. The fault detection is achieved through analysis of the symmetrical components of the terminal voltage on each IIDG (explained in detail in Section 5.4). The second step is active harmonic components injection. Upon the detection of a fault by IIDGs, all connected IIDGs in the microgrid intentionally reduce output current and inject a specific predefined harmonic component which is superimposed on the output current (details of this process are discussed in Section 5.5). In the third step, all protection relays in the network analyse the

harmonic content of their locally measured currents, and based on the detected harmonics, identify the faulty line in the network (refer to Section 5.6). Finally, in the fourth step, the relays in the network take appropriate actions to isolate the fault in a time coordinated manner, i.e. operating either in main or backup mode (details are discussed in Section 5.7).

### 5.3 IIDG Control Strategies

To better understand the proposed protection approach, it is helpful to talk first about the control strategies of IIDGs, as the fault behaviour of an IIDG is largely determined by its control actions and for this scheme, harmonic injection after detection of fault is also dependent on the controllers of IIDGs. It is assumed that each generation unit in the microgrid is interfaced by a three-phase two level inverter with an LC filter as shown in Figure 5.8. Several different control strategies are available for the inverter, among those PQ (real and reactive power), V/F (voltage and frequency) and droop controllers are the most widely adopted and proposed control schemes for microgrids [2]. Depending on their contribution to system stability, the IIDGs can be categorised either as GFR or GFL as mentioned earlier in Chapter 4. GFL provides a specific amount of power/current to the grid depending upon the set-point provided by the operator. GFR, on the other hand, acts as a voltage source and plays an important role in controlling voltage and frequency of the system.

Therefore, when a microgrid operates in an islanded mode, it is necessary to have at least one GFR. In this research, only one of the generating units is assumed to be GFR, and the rest of the generators are using GFLs. Representative diagrams for both controllers along with the proposed method for harmonic injection and fault detection are shown in Figure 5.8.

The power source behind the inverter is represented by an ideal DC voltage

CHAPTER 5. DEMONSTRATION OF PRACTICAL CHALLENGES ASSOCIATED WITH OVERCURRENT PROTECTION AND PROPOSED PROTECTION SCHEME

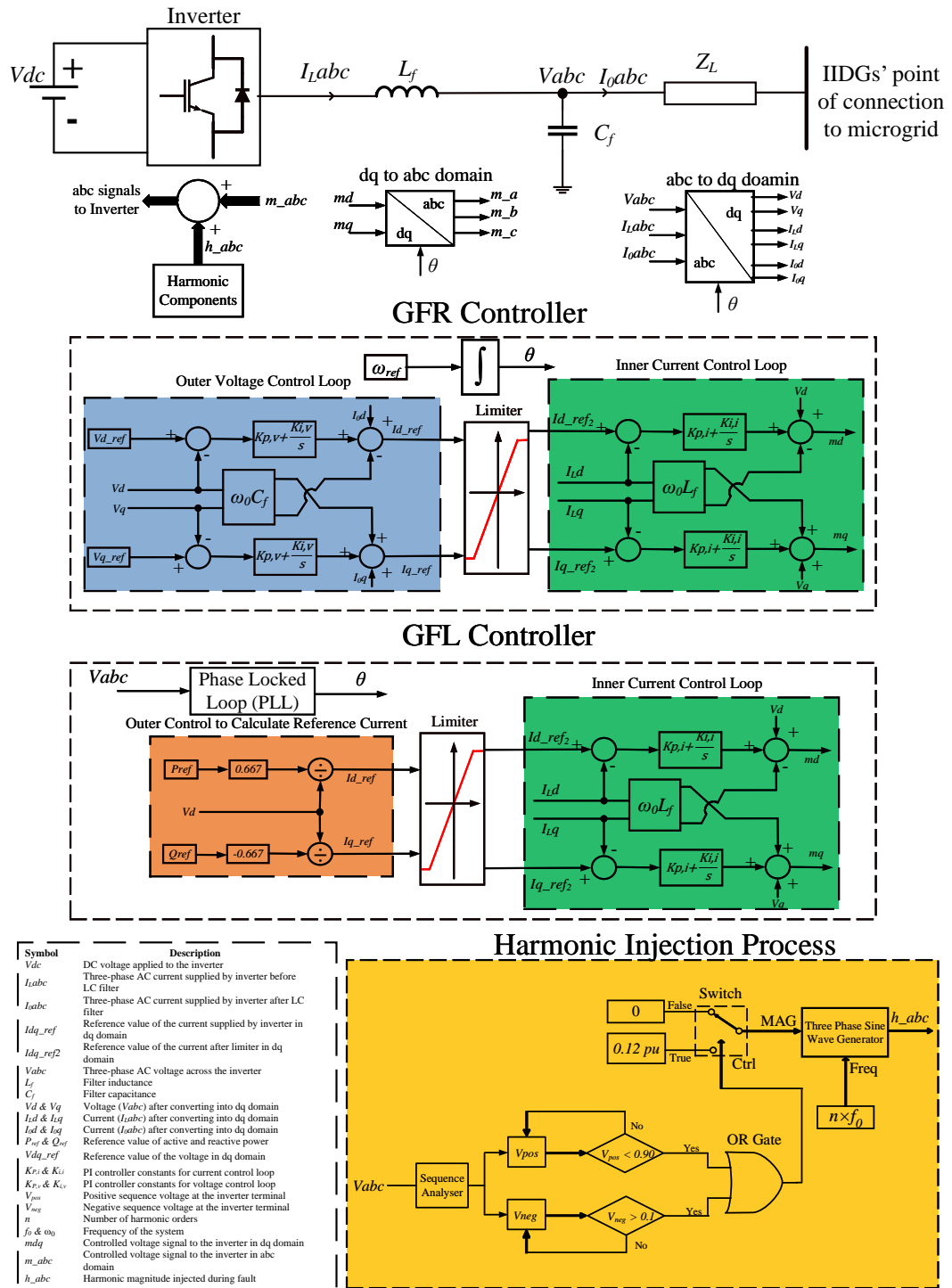


Figure 5.8: Block Diagram of the Controllers of IIDGs including fault detection and harmonic injection process.

source, and the dynamics of the different buck/boost converters and their controls (before the inverter) are not considered since the emphasis of this work is on

protection of the AC side. It is assumed that the dynamics on the DC side should not have a significant impact on the AC side protection, therefore, only inverter characterisation during the fault has been taken into consideration. A detailed review of the implementation of different controllers during normal operating conditions can be found in Chapter 4 of this thesis. The units controlled with GFL have a current loop that provides independent control of active and reactive power (green controller in Figure 5.8), a PLL, and a PQ outer loop that provides the current references to the inner loop (marked orange in Figure 5.8).

As mentioned earlier, to maintain voltage and frequency stability in the islanded microgrid, a GFR controller is used in this research. The GFR controller has an internal current controller (marked green in Figure 5.8) and a voltage controller (marked blue in Figure 5.8). As the proposed protection scheme requires a fast harmonic voltage injection, a controller is added at the output of the current loop. It is worth mentioning that it is also possible to inject harmonics through ‘*dq*’ current control, however, using that method of injection would be relatively slower. A detailed description of the harmonic injection controller is provided in Section 5.5. During a fault, as there will typically be a significant network voltage reduction, a large reference current will be presented to the current controller. Hence, to limit the output current of the inverter, a current limiter is used in front of the current control loop for both types of control schemes so that the reference current does not exceed the threshold. This threshold will be defined by the inverter’s maximum sustained current output, which is usually around 110-120% of its nominal output [3]. In this paper, the limit for the fundamental fault current is set to 108% after detection of a fault, leaving a margin of 12% to cater for harmonic injection and to ensure that the overall peak current remains within the 120% range. As a result, during the fault, both types of controllers and all IIDGs in the network will behave as current control sources with limited output current.

## 5.4 Fault Detection Method by IIDG

Before the injection of harmonic components from the IIDGs, the fault must initially be detected. To achieve reliable fault detection, both positive and negative sequence voltages are measured at the terminal of the IIDGs through the controller of the inverter. The process can be explained with reference to Figure 5.8 (harmonic injection process). The threshold for positive sequence under-voltage element is set to 0.9 pu (i.e. the voltage lower than the threshold sets the output state to high) and the negative sequence over-voltage threshold is 0.1 pu (i.e. the voltage above the threshold triggers the element). Balanced faults will be detected by the positive sequence voltage, while negative sequence element will indicate unbalanced faults. Either threshold being violated will trigger subsequent steps of the scheme. The positive and negative sequence thresholds can both be varied.

To cater for non-fault transient undervoltage or phase imbalance conditions, an intentional time delay of 100 ms is included in each of the relays before any operation is initiated. This delay results in longer protection operating times, but it needs to be noted that fault clearance time requirements in an islanded microgrid are typically not very stringent due to the relatively low fault levels and thus limited impact on electrical equipment. Also, since the most faults on microgrids are unbalanced in nature, negative sequence voltage analysis may improve the scheme's stability during non-faulted conditions. Furthermore, to coordinate the scheme's setting in accordance with the prevailing GB grid code [4], where the minimum voltage level for normal operation is 0.9 pu, the relay threshold is set accordingly. Finally, the undervoltage and unbalance threshold settings and time delays, can all be configured to take specific system conditions and/or regulation into account.

It has been demonstrated through systematic simulation that with the assumed voltage settings, the scheme can provide very good sensitivity to high impedance

faults. A number of resistive faults with increasing value of fault resistance have been applied at different locations and, through sensitivity analysis, it has been established that the scheme can operate correctly with fault resistances up to a limit of  $60 \Omega$ , which can be considered as high fault impedance in a practical 11 kV system.

Upon the detection of fault or triggering of the scheme, harmonic components are injected. It should be noted that in normal operation (when there is no fault) no harmonics are injected and hence ' $h_{abc}$ ' is set to zero. When a fault is detected a specific magnitude of a specific harmonic component will be injected by each generator- the magnitude and nature of the harmonics injected will be clearly discernible from normal background noise and power quality related harmonics.

## 5.5 IIDG Injection of Harmonic Components

Two main criteria, i.e. the order and the magnitude of the harmonics, must be addressed to ensure appropriate injection of harmonic components during fault conditions. Theoretically, it is possible to inject any order of harmonics. However, considering the practical aspects, in the proposed scheme, lower-order harmonics ( $2^{nd}$ ,  $3^{rd}$  and  $4^{th}$ ) are used. Harmonic components higher than 10 are not typically considered, as the resonant frequency of the LC filter is typically between 10 times of the grid frequency and half of the converter switching frequency [5]. Therefore, limiting the injected harmonics to the  $10^{th}$  order ensures that no unnecessary filtering of the protection related frequencies occurs. It should also be noted that it is not essential for all the IIDGs in the network to inject harmonics. Injection from IIDGs with relatively high capacity is sufficient as discussed in detail in Section 5.8. Therefore, in the proposed scheme, injection of harmonics higher than 10 can be realistically avoided. Finally, inter-harmonics or other specific frequencies could be used (below the  $10^{th}$  harmonic) if a relatively high number

of protected lines/circuits with IIDGs are present in a particular microgrid.

In terms of harmonic magnitude, currently, there is no requirement or limitation on the magnitude of harmonics during faults from a regulatory/ system operation perspective. However, according to IEEE standard 519 [6], during the normal operating condition, the maximum allowable magnitude of harmonics (low order) is 4% of the maximum load current. Therefore, to differentiate harmonics during normal and fault conditions, in this proposed scheme, the magnitude of harmonics is set to be 10% of the fault current (i.e. 0.12 pu in terms of rated current as fault current magnitude is assumed to be 1.2 pu). Again, it is important to mention that the proposed scheme will not inject harmonic components continuously, but only for a short time, when a fault is detected by the inverters' controllers. Therefore, the harmonic injection will not have a large impact on the loads, transformers, fault ride-through (FRT) requirements of the IIDGs, or power quality. Regarding FRT, it is assumed that the inverters will remain connected during a fault following grid code requirements. The fundamental output current will be reduced only marginally, that is, by 12% of the rated current. This 12% headroom is then used for harmonic injection. Therefore, the proposed solution will not be detrimental to the FRT requirements of inverters. During faults, loads in the vicinity of the fault may be experiencing significant under-voltages anyway, so any relatively small harmonic distortion of the current will not have a significant impact.

## **5.6 Detection and Identification of Faulted Line Section by Relays**

In this research, two circuit breakers (CBs) for each section of the line is used and hence, in this protection scheme, there are two relays; one at each end of every section of the line. These relays are categorised into two groups - forward group relay (FGR) and backward group relay (BGR). The relays upstream of each line

CHAPTER 5. DEMONSTRATION OF PRACTICAL CHALLENGES  
ASSOCIATED WITH OVERCURRENT PROTECTION AND PROPOSED  
PROTECTION SCHEME

---

(left hand side) are FGRs, and the relays downstream of each line (right hand side) are BGRs.

For traditional passive grid connected radial systems, normally only one CB at the upstream end (i.e. the end that would be supplying fault current) of the line is used since there is no contribution of fault current from the downstream system. However, in future microgrids relying solely on distributed generation at many locations throughout the network, it will be necessary to use two CBs in a single interconnecting line due to the presence of multiple IIDGs in the microgrid and bidirectional power flow during both normal and fault conditions. Therefore, even if a fault is detected by a relay at one end, there is a chance that current will be fed to the fault from the downstream position. In that case, generation will be lost and supply to the other connected loads may also be compromised. It is important to note that, in the proposed scheme, no communication between the relays (FGRs and BGRs) is required to achieve protection coordination among the relays, which is beneficial. In grid connected mode, conventional protection and CB arrangements may be sufficient (but this protection scheme could still also be in operation to interrupt/isolate IIDGs).

To identify the faulted line section, FGRs analyse the injected harmonic components from the upstream IIDGs, while the BGRs analyse harmonic components injected by the downstream IIDGs. The algorithm for fault detection of the proposed solution is presented in Figure 5.9. The harmonic component threshold for relay operation must be greater than 0.04 pu since as mentioned earlier, during normal operating conditions, the accepted range of lower-order harmonic presence in an 11 kV system is 4% [6]. Therefore, in this research, the threshold for the relays in the network is set to 0.08 pu which provides sufficient headroom to detect a fault and non-faulted situation. Relays can analyse the harmonics of the current through (5.2), where,  $k$  is the harmonic number (for example,  $k = 1$  means fundamental;  $k = 2$  is  $2^{nd}$  harmonic, and other harmonics.),  $I_k$  is calculated

CHAPTER 5. DEMONSTRATION OF PRACTICAL CHALLENGES ASSOCIATED WITH OVERCURRENT PROTECTION AND PROPOSED PROTECTION SCHEME

---

harmonic current magnitude,  $I(t)$  is the measured current fed to the relay,  $f_0$  is the fundamental frequency of 50 Hz, and  $T$  is the period of the input current (inverse of the fundamental frequency,  $f_0$ ). The block diagram of the implementation of the relay is shown in Figure 5.10, where, measured current,  $I(t)$ , fundamental frequency,  $f_0$ , a matrix of harmonics,  $k = 2; 3; 4;$ , and threshold of the harmonic magnitude,  $I_{th}$  will be given as input and the relay will provide the tripping signal as output.

$$I_k = 2f_0 \sqrt{\left( \int_{t-T}^t I(t) \sin(2\pi k f_0 t) dt \right)^2 + \left( \int_{t-T}^t I(t) \cos(2\pi k f_0 t) dt \right)^2} \quad (5.2)$$

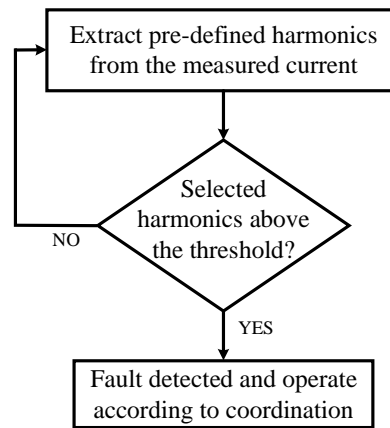


Figure 5.9: Fault detection algorithm.

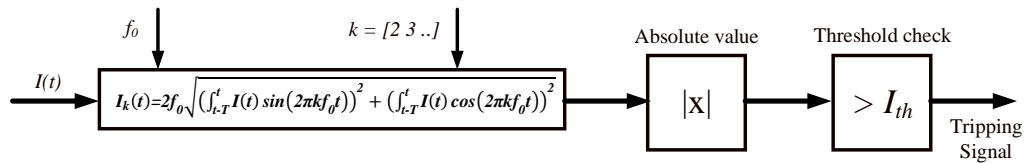


Figure 5.10: Generic block diagram of the proposed scheme's relay

## 5.7 Relay Coordination

The proposed method utilises definite time characteristics to coordinate the relays. The operating time settings for the FGRs are set in a way that the most downstream relays operate faster and the most upstream relays operate slower, with a constant time grading being applied between two consecutive relays. On the contrary, the BGRs are set opposite to the FGRs, i.e. the most upstream relays will operate the fastest, and downstream will operate slower with a constant time difference.

Inherently longer operating times for certain faults is the major drawback of using definite time delay coordination, especially in the case of grid-connected operation where fault current is relatively high and the potential for damage with sustained faults on the system increases. However, fault currents are significantly lower during islanded mode; accordingly, the slow operation should be more tolerable. Furthermore, during an upstream fault, the current contribution from the majority of the IIDGs is quickly eliminated due to the fast operation of the BGRs. Also, due to restricted output currents of IIDGs during fault, the fault current magnitudes in the islanded microgrid will be limited and is not expected to vary significantly with the variation of fault location. Therefore, the use of IDMT characteristic is unlikely to provide a reduction in protection operation times, as it would otherwise be the case in a distribution system with higher fault level (that is, grid-connected). Additionally, the use of communication to coordinate the relays can be costly and may prove unreliable. Thus, in the case of islanded microgrid protection, definite time characteristic was considered most suitable. An additional benefit of such time grading approach is the inherent provision of backup protection functionality.

## 5.8 Protection Operation Example and Practical Consideration

To better understand the operation of the proposed scheme a simple fault scenario is presented in this section. Figure 5.11 represents a small section of a microgrid with IIDG connected at each end of the line, where both IIDGs, that are,  $IIDG_1$  and  $IIDG_2$  inject different order harmonics  $I_{H1}$  and  $I_{H2}$  respectively, after detecting the presence of a fault. Faults are initially identified by IIDGs using the sequence components of the measured terminal voltage. According to the proposed scheme, during a fault inside the protected section ( $F_1$ ), relay  $R_1$  will detect  $I_{H1}$ , and relay  $R_2$  will detect  $I_{H2}$ , and both relays operate accordingly to isolate the faulted section. In the case of a fault outside the protected section; for example, fault  $F_2$  as shown in Figure 5.11,  $IIDG_1$  and  $IIDG_2$  both will inject harmonic components towards the relay  $R_3$ . Therefore, relay  $R_2$  will not detect the harmonic component  $I_{H2}$  and will not issue a trip, however, relay  $R_1$  can still detect the fault and can be operated as backup protection; that is,  $R_3$  operating fast and  $R_1$  with a time delay.

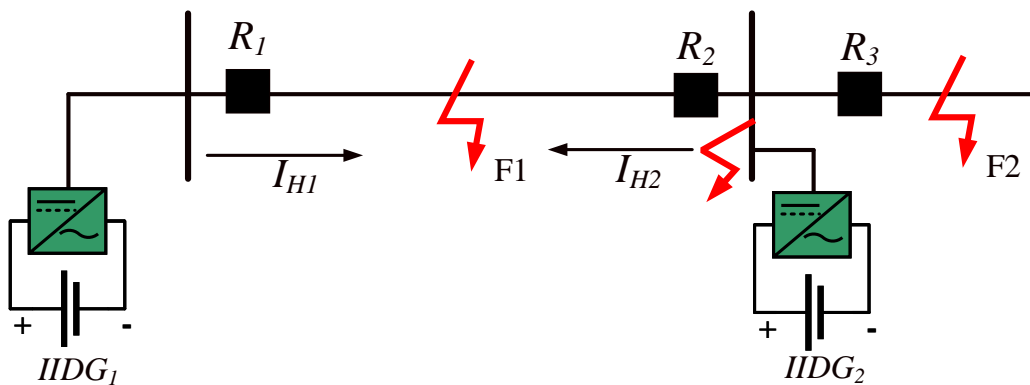


Figure 5.11: Single section of a microgrid with two IIDGs.

To further clarify the key assumptions and additional practical considerations of the proposed scheme the following points are included:

1. All of the connected IIDGs in the network inject harmonic components during a fault, with IIDGs connected to neighbouring buses injecting different order harmonics. However, it is also possible to coordinate the relays (both detecting and identifying the faulted section) through the harmonic injection from a single IIDG, i.e. injection of only one harmonic component as shown in the results of the different combination of IIDG location (refer to Section 6). Injection of harmonic components from all IIDGs makes the scheme more reliable in case any IIDG(s) in the network being out of service. Also, in circumstances where multiple IIDGs connected to a single bus, all of them might inject the same harmonic component into the system, or a single IIDG could be selected for harmonic injection during the fault. Typically, a relatively large-rated generator, expected to be constantly connected to the network, would be most suitable for this. In the future, large scale storage units may become widely accessible in microgrids, and it could be convenient to inject harmonic components using these units (assuming they are never at zero state of charge) with the proposed solution since they should always remain connected to the network, whether in charging/discharging or “floating” mode.
2. The proposed solution is suitable for the protection of microgrids with both radial and meshed architectures. However, to protect meshed networks an additional arrangement is needed. It is proposed that the scheme would be equipped with fast-acting sectionalisers/isolators (which could be triggered by overcurrent or under-voltage element), connected to a suitable point in the network (for example, the “mid-point” or where a normally open point would be located in typical distribution networks). When a fault occurs on the network (at any location), the isolator would operate quickly (with a delay of around 0.05 s), thereby separating the network into radial sub-

networks, and then the relays can operate on the faulted section of the radial networks as explained earlier. An example arrangement of the proposed scheme to protect a meshed network can be explained with the aid of Figure 5.12. A sectionaliser,  $R_{sec}$  is installed at the interconnection point between Busses 1 and 3. When there is a fault in the network (at any location),  $R_{sec}$  is tripped very quickly (with a delay of around 0.05 s) and other relays will operate as they would for a radial network, as the network will have been split rapidly following initial fault detection. Paper [7] presents a fast mechanical switch that operates very quickly within only a few milliseconds and this could be utilised in conjunction with the proposed scheme. Even if the sectionaliser/isolator is not capable of operating extremely quickly, the operating times of the proposed scheme could be extended to cater for this. Given that fault levels in islanded microgrids may be relatively low, it is probable that a relatively low interrupting rating would be sufficient for such sectionaliser/isolator (not suitable for grid connected operation). It is also worth noting that many distribution networks and microgrids are not operated in a meshed fashion [8] due to the complexity of protection and the requirement to isolate more customers for every fault, so it is anticipated that the proposed scheme would mainly be implemented in radial networks.

3. The scheme is proposed for islanded microgrids (which is assumed to be the predominant mode of operation) where the relays do not need to communicate with each other to detect a fault and coordinate properly, and it has been assumed that a separate method of detecting islanding is in place; that is, this scheme does not detect islanded mode but is assumed to be operational only when the system is islanded. Therefore, it has been assumed that an overall microgrid management system (which would only require very simple non-continuous signalling-based communications) is available,

which is typically the case in existing microgrids, to activate/disconnect the protection scheme depending on the microgrid's mode of operation.

4. A fault between FGR and BGR, for example, fault between relay,  $R_2$  and  $R_3$  in Figure 5.11 is assumed to be an internal busbar fault. Therefore, to clear the fault at such a location, it is assumed that a separate protection unit is already available at ring main unit (RMU)/busbar. If the fault is not cleared by the RMU/busbar protection, the proposed protection scheme still can detect such faults; for example, in the case shown in Figure 5.11, relay  $R_1$  will detect the fault and operate accordingly as a backup.

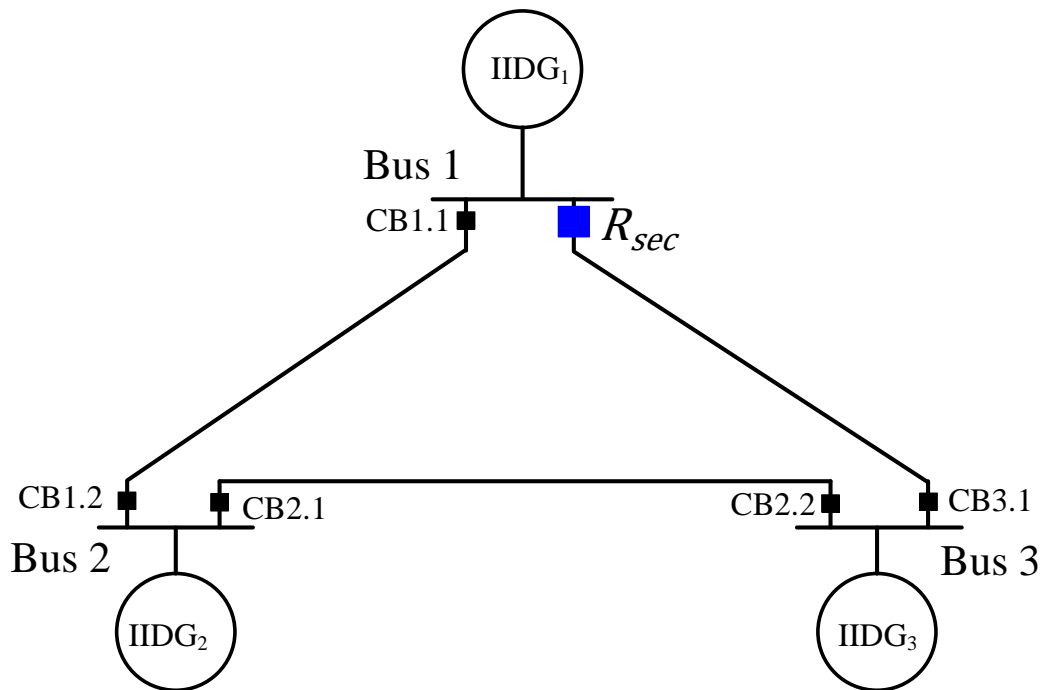


Figure 5.12: Meshed network protection.

## 5.9 Summary

Several different simulation cases have been presented in this section to illustrate the protection challenges in microgrids under a range of scenarios, with a particular

focus on analysing the performance of the overcurrent relays, under scenarios including high penetrations of renewable-based generation and islanded operating states. It can be concluded from the simulation results as presented show that conventional overcurrent schemes might not provide adequate protection for future active and islanded distribution networks. In the worst-case scenario, the protection might not be able to detect faults, this applies particularly to islanded modes of operation.

A protection solution has been suggested in this chapter that incorporates control action of the IIDGs with microgrids protection. The faults in the network first detected by the IIDGs connected to the microgrid by analysing the positive and negative sequence voltage. Upon detection of a fault, all the IIDGs in the network modify the control action and injects specific order and magnitude of harmonic with the fault current. Afterwards relays in the network analyse the harmonic components to identify and isolate the faulted section.

## References

- [1] ALSTOM, *Network Protection & Automation Guide*. Alstom Grid, 2011. [Online]. Available: <http://rpa.energy.mn/wp-content/uploads/2016/07/network-protection-and-automation-guide-book.pdf>
- [2] A. Nisar and M. S. Thomas, “Comprehensive control for microgrid autonomous operation with demand response,” *IEEE Transactions on Smart Grid*, vol. 8, no. 5, pp. 2081–2089, 2017.
- [3] “IEEE Standard for the Specification of Microgrid Controllers,” *IEEE Std 2030.7-2017*, pp. 1–43, 2018.

CHAPTER 5. DEMONSTRATION OF PRACTICAL CHALLENGES  
ASSOCIATED WITH OVERCURRENT PROTECTION AND PROPOSED  
PROTECTION SCHEME

---

- [4] National Grid, “The Grid Code- Issue 6 Revision 11,” National Grid ESO, Warwick, UK, Tech. Rep. 6, 2022. [Online]. Available: <https://www.nationalgrideso.com/document/162271/download>
- [5] M. Liserre, F. Blaabjerg, and S. Hansen, “Design and control of an LCL-filter-based three-phase active rectifier,” *IEEE Transactions on Industry Applications*, vol. 41, no. 5, pp. 1281–1291, 2005.
- [6] “IEEE Recommended Practice and Requirements for Harmonic Control in Electric Power Systems,” *IEEE Std 519-2014 (Revision of IEEE Std 519-1992)*, pp. 1–29, 2014.
- [7] C. Peng, I. Husain, A. Q. Huang, B. Lequesne, and R. Briggs, “A Fast Mechanical Switch for Medium-Voltage Hybrid DC and AC Circuit Breakers,” *IEEE Transactions on Industry Applications*, vol. 52, no. 4, pp. 2911–2918, 2016.
- [8] M. Barnes, T. Green, R. Lasseter, and N. Hatziargyriou, “Real-World MicroGrids- An Overview,” in *2007 IEEE International Conference on System of Systems Engineering*, 2007, pp. 1–8.

## Chapter 6

# Demonstration and Validation of the Developed Protection Scheme and Analyses of Results

This chapter presents the simulation models and results that demonstrate and validate the developed protection schemes. This chapter is divided into two main sections. The first section presents the MATLAB Simulink models of the microgrid that are used to simulate primary system faults, the settings applied to the protection relays at the various locations and the simulation results for various case studies that are used to demonstrate and validate the operation and advantages of the proposed protection scheme under a wide variety of scenarios. The second section illustrates the Hardware-in-the-Loop (HiL) laboratory configuration, consisting of a microgrid model developed in RSCAD and executed on the RTDS, and the validation results for the developed scheme with faults at different locations of the microgrid.

## 6.1 Simulation based Performance Demonstration and Validation of the Proposed Scheme

To verify the effectiveness and analyse the performance of the developed scheme that addresses various protection-related issues as outlined earlier in the thesis, several fault scenarios have been simulated using a realistic microgrid model developed in MATLAB Simulink in accordance with IEEE2030.7 [1]. In the following subsections, the model is described and presented, along with the settings of the relays (for example, the specific harmonics injected by each relay during faults, the threshold values for fault detection and initiation of operation), and the simulation results for the validation of the protection scheme are also presented.

### 6.1.1 Overview of the Microgrid Model

The developed microgrid model is shown in Figure 6.1, and it is designed in a way that it can be operated either in grid-connected mode or islanded mode (which is the main mode considered in this research), through a controllable switch at the point of interconnection (POI) to the 11 kV external distribution grid. However, as stated, since this research focuses only on the protection of islanded microgrids, the external grid always remains disconnected.

There are three loads and three IIDGs connected to the network; each bus has one load and one IIDG. The rating of each IIDG is assumed to be 500 kVA. IIDG<sub>1</sub> is the GFR, and therefore, is responsible for the control of the islanded microgrid's voltage and frequency. IIDG<sub>2</sub> and IIDG<sub>3</sub> are both GFLs, and will provide a constant specified amount of active and reactive power to the microgrid. Line parameters for the simulated microgrid have been selected based on actual distribution lines as surveyed in [2]. Some of simulation parameters (line, load and IIDG models' parameters) along with their description, symbol and the values

CHAPTER 6. DEMONSTRATION AND VALIDATION OF THE DEVELOPED PROTECTION SCHEME AND ANALYSES OF RESULTS

used during simulations of are listed in Table 6.1. Full details of the IIDGs and transformers parameters are presented in Appendix B.

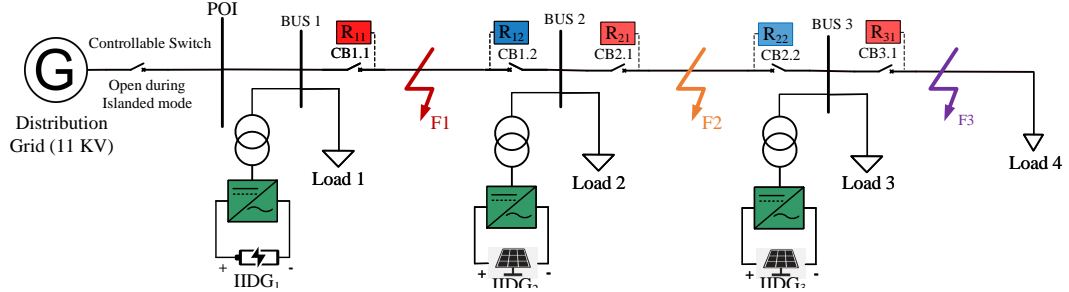


Figure 6.1: Model of the test microgrid used for demonstration and validation of the developed scheme's operation.

Table 6.1: Parameters for the microgrid model.

Simulation parameters	Description and symbol	Values
Frequency	$f_0$	50 Hz
AC grid and base voltage	$V$ or $V_{base}$	11 kV
Line impedance	$Z_{Line}$	$0.0543+j0.0495 \Omega/km$
Line length	Line between POI and Bus 1, $l_{01}$	0.5 km
	Line between Bus 1 and Bus 2, $l_{12}$	1.8 km
	Line between Bus 2 and Bus 3, $l_{23}$	2 km
	Line after Bus 3, $l_3$	1 km
IIDG rating and base power	For each generator, $S_{base}$	500 kVA
Reference value of IIDGs	IIDG <sub>1</sub>	400 kVA
	IIDG <sub>2</sub>	100 kVA
	IIDG <sub>3</sub>	50 kVA
LC filter	$L$ and $C$	43 $\mu$ H and 1.88 mF
Inverter's DC voltage	$V_{dc}$	500 V
Inner and outer control loop	Voltage loop proportional gain, $K_{p,v}$	2
	Voltage loop integral gain, $K_{i,v}$	20
	Current loop proportional gain, $K_{p,i}$	0.3
	Current loop integral gain, $K_{i,i}$	10
Load rating	Load <sub>1</sub>	200 kVA
	Load <sub>2</sub>	200 kVA
	Load <sub>3</sub>	100 kVA
	Load <sub>4</sub>	50 kVA
	Total Load	550 kVA

### 6.1.2 Selection of Harmonics

For the testing and validation of the scheme, and as described earlier, three individual and different order harmonics are injected into the network during fault conditions by each of the three IIDGs as presented in Figure 6.1. The injected order of harmonic components by the IIDGs for the microgrid shown in Figure 6.1 is presented in Table 6.2. As shown in Table 6.2, upon detection of a fault, IIDG<sub>1</sub> injects 2<sup>nd</sup> harmonic ( $I_{HC2}$ ), IIDG<sub>2</sub> injects 3<sup>rd</sup> harmonic ( $I_{HC3}$ ) and IIDG<sub>3</sub> injects 4<sup>th</sup> harmonic ( $I_{HC4}$ ). The harmonics injected can be specified when the system is initially configured. The current supplied by each IIDG during both normal and fault condition is presented in Figure 6.2. The magnitude of fundamental and harmonic components is also shown in the figure. As illustrated in Figure 6.2, after a three-phase bolted fault  $F_3$  (applied at 0.5 s) occurs, each IIDG injects its respective harmonic component and the peak value of fault current output remains within 120% of the rated capacity, therefore protecting the power electronics systems and components from thermal damage.

Table 6.2: Injected harmonic components from IIDGs.

Generator	Injected harmonic components
IIDG <sub>1</sub>	2 <sup>nd</sup> Harmonic ( $I_{HC2}$ )
IIDG <sub>2</sub>	3 <sup>rd</sup> Harmonic ( $I_{HC3}$ )
IIDG <sub>3</sub>	4 <sup>th</sup> Harmonic ( $I_{HC4}$ )

### 6.1.3 Relay Settings

To identify and isolate faults, CBs and relays are installed at both ends of each line section – this is more protective equipment than would be required in a traditional passive distribution system, but this level of protection and isolation capabilities are required when fault current infeeds are available at each busbar in the system, if preservation of the philosophy of only isolating a faulted line section is required. It should also be noted that fault levels are relatively much lower in this system

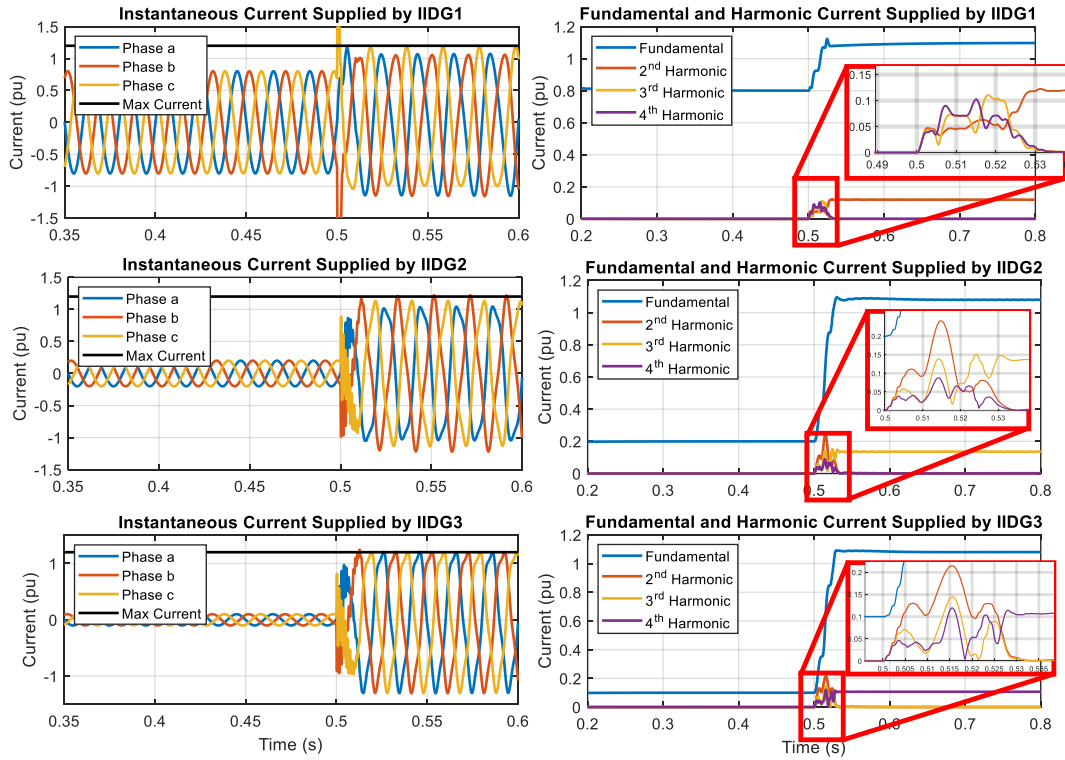


Figure 6.2: Harmonic and fundamental current measurements from the IIDGs for a fault,  $F_3$ .

compared to traditional distribution systems, and therefore relatively lower rated circuit breakers (during only islanded operation or grid connected operating mode with a significantly low SCL) would be required (in fact load breaking switches would probably be sufficient), reducing cost. The relays are split into two groups: FGRs ( $R_{11}$ ,  $R_{21}$  and  $R_{31}$ ) and BGRs ( $R_{12}$  and  $R_{22}$ ), with each relay having an associated CB

From Figure 6.1, it is evident that  $R_{11}$  analyses injected components from the IIDG<sub>1</sub> ( $I_{HC2}$ ),  $R_{21}$  analyses components from IIDG<sub>1</sub> ( $I_{HC2}$ ) and IIDG<sub>2</sub> ( $I_{HC3}$ ), and  $R_{31}$  checks the components of  $I_{HC2}$ ,  $I_{HC3}$  and  $I_{HC4}$ . In the case of BGRs,  $R_{21}$  analyses components injected by the downstream IIDGs, IIDG<sub>2</sub> ( $I_{HC3}$ ) and IIDG<sub>3</sub> ( $I_{HC4}$ ), and  $R_{22}$  analyses the injected component from IIDG<sub>3</sub> ( $I_{HC4}$ ). The decision making through analysed components and tripping time for all relays are summarised in Table 6.3.

Table 6.3: Relay settings.

Relay	Operating time (s)	Fault detection condition
$R_{11}$	0.3	$I_{HC2}$
$R_{21}$	0.2	$I_{HC2}$ or $I_{HC3}$
$R_{31}$	0.1	$I_{HC2}$ or $I_{HC3}$ or $I_{HC4}$
$R_{12}$	0.1	$I_{HC3}$ or $I_{HC4}$
$R_{22}$	0.2	$I_{HC4}$

#### 6.1.4 Balanced Faults

Balanced faults (three-phase to earth) have been simulated at locations  $F_1$ ,  $F_2$  and  $F_3$  of the microgrid shown in Figure 6.1, and the operation of the relays (in terms of tripping outputs) have been recorded, and measurements of fundamental and harmonic currents have also been captured. In order to observe the operation of backup protection functionality, none of the faults has been removed from the system and the CBs have not been opened in response to main protection signals so that a full picture of the subsequent (main and backup) response of the entire protection system can be observed and evaluated.

##### Results for Fault at Location $F_3$

As can be seen from Figure 6.1, for a fault after Bus 3, relay  $R_{31}$  should operate first and relay,  $R_{21}$  should operate as backup protection with a time delay. The results for both FGRs and BGRs are shown in Figure 6.3 and Figure 6.4 respectively.

The fault is initiated at 0.5 s, and all IIDGs inject their pre-specified harmonics as presented in Table 6.1. According to the relay settings as presented in Table 6.3, all FGRs should detect the fault, and the simulation results verifies the successful operation of all relays as anticipated.

It is clear from Figure 6.3 that relay  $R_{31}$  detects all of the harmonic components, and therefore issues a trip at time 0.6 s (with a delay of 0.1 s after the fault according to the settings). Relay,  $R_{21}$  detects 2<sup>nd</sup> and 3<sup>rd</sup> harmonic components and as a result, also issues a trip at 0.7 s (with a delay of 0.2 s after the fault

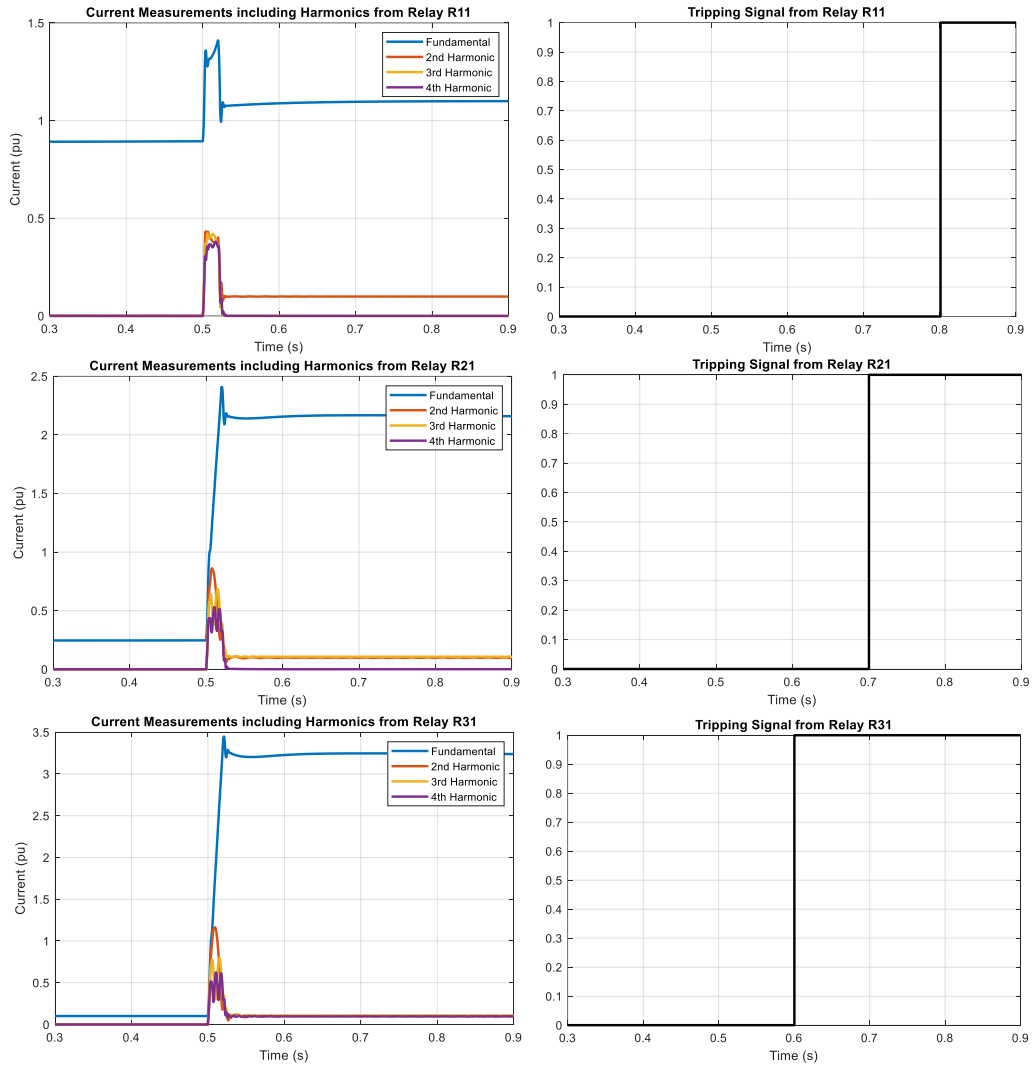


Figure 6.3: FGRs: fundamental current measurements, injected/measured harmonic output currents and tripping signals for a (non-cleared) three-phase balanced fault at  $F_3$ .

according to its settings) to provide backup protection if required. Finally, relay,  $R_{11}$  detects the 2<sup>nd</sup> harmonic injected by IIDG<sub>1</sub> and issues a trip at 0.8 s (with a delay of 0.3 s after the fault according to its settings) to provide backup protection for fault  $F_3$  if required.

The results for the BGRs for the same fault  $F_3$  are shown in Figure 6.4. According to the relay settings, the BGRs should not operate for this fault. Figure 6.4 shows that relay  $R_{12}$  detects the 2<sup>nd</sup> harmonic injected by IIDG<sub>1</sub>, but according

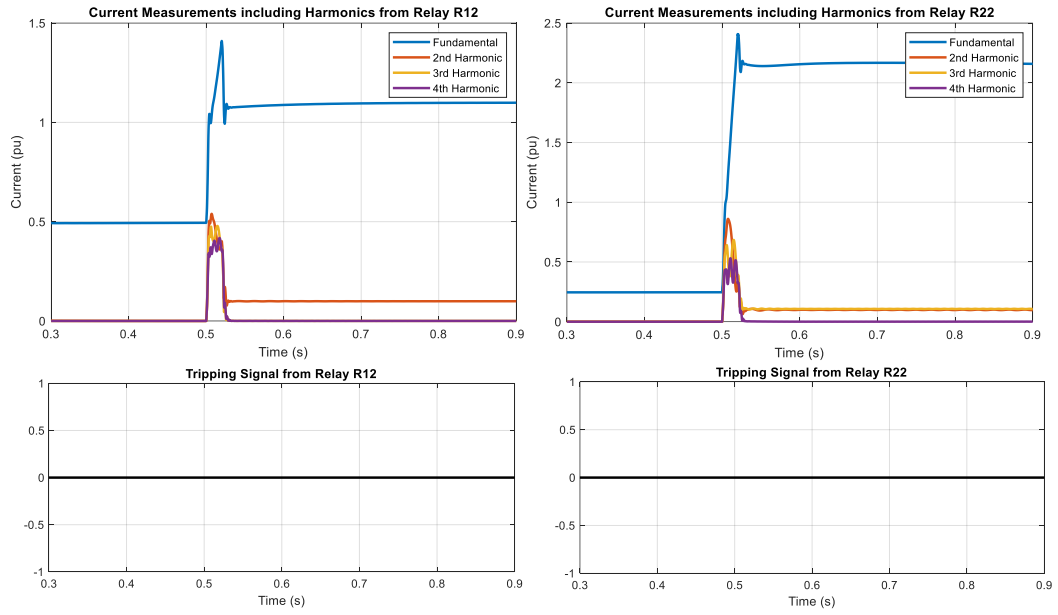


Figure 6.4: BGRs: fundamental current measurements, injected/measured harmonic output currents and tripping signals for a (non-cleared) three-phase balanced fault at  $F_3$ .

to settings shown in Table 6.3, relay,  $R_{12}$  will only issue tripping signals when it detects  $3^{rd}$  or  $4^{th}$  harmonics. Therefore, relay,  $R_{12}$  will not trip and this can also be verified from the simulation results. For relay,  $R_{22}$ , according to its settings, it must detect  $4^{th}$  harmonic in order for a trip to be issued, but upon inspection of Figure 6.4, it can be seen that it only detects  $2^{nd}$  and  $3^{rd}$  harmonics. As a result, relay  $R_{22}$  does not issue a trip for the fault  $F_3$ .

### Results for Fault at Location $F_2$

A three-phase balanced fault has been simulated at location,  $F_2$ . The simulation results for the relays can be explained using Figure 6.5 and Figure 6.6. Again, the fault has been initiated at 0.5 s and current inputs to the FGRs along with tripping signals are shown in Figure 6.5.

Figure 6.5 shows that relay  $R_{31}$  does not detect any harmonic components, and therefore remains inactive.  $R_{21}$  detects  $2^{nd}$  and  $3^{rd}$  harmonics ( $I_{HC2}$  and  $I_{HC3}$ ), and trips as expected at 0.7 s (i.e. 0.2 s after fault inception).  $R_{11}$  detects

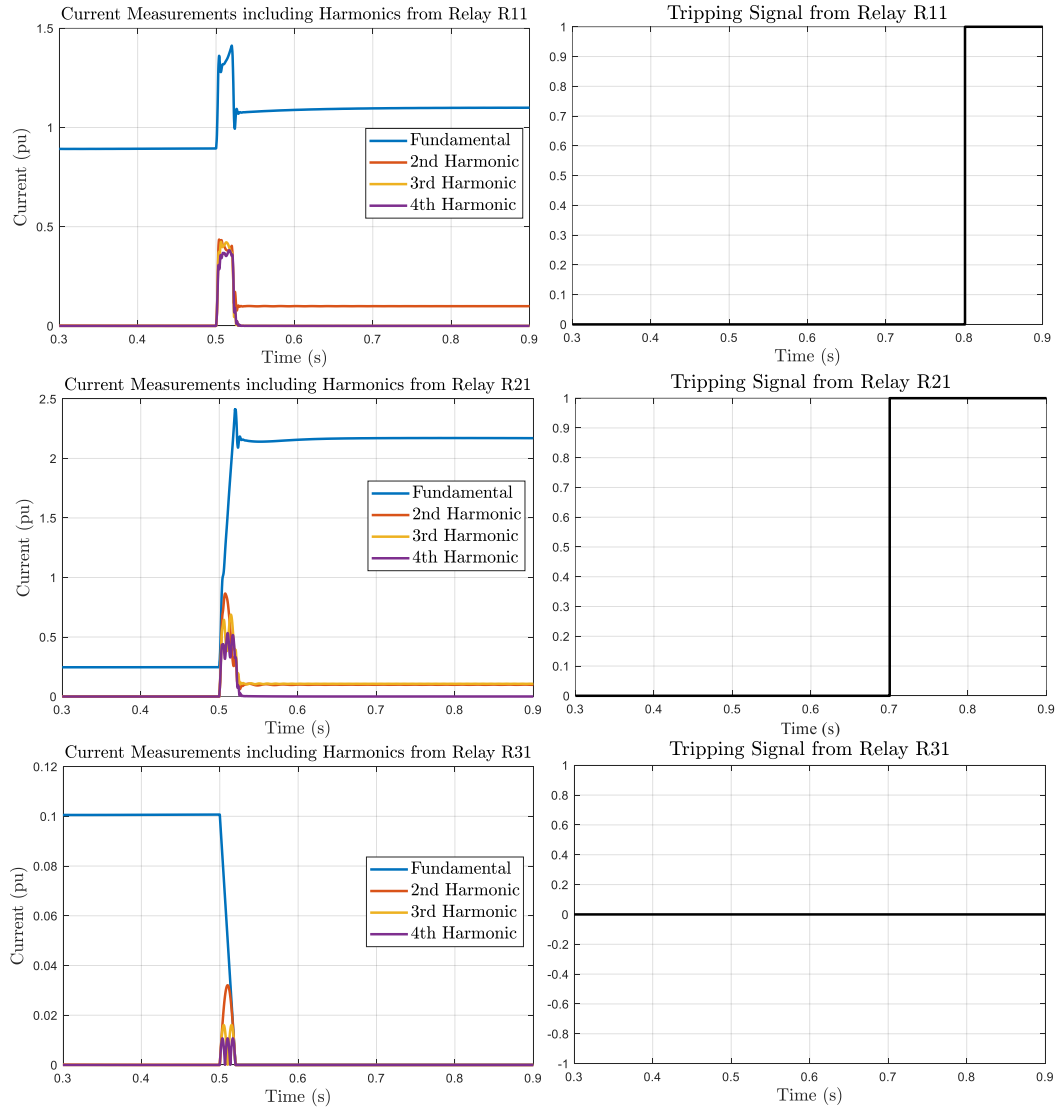


Figure 6.5: FGRs: fundamental current measurements, injected/measured harmonic output currents and tripping signals for a (non-cleared) three-phase balanced fault at  $F_2$ .

$2^{nd}$  harmonic ( $I_{HC2}$ ), so trips at 0.8 s (0.3 s after fault inception) as a backup.

The results for BGRs in terms of input current measurements and tripping signals are shown in Figure 6.6. From the figure it can be observed that relay  $R_{12}$  detects  $2^{nd}$  harmonic so remains inactive, and relay  $R_{22}$  detects  $4^{th}$  harmonic component ( $I_{HC4}$ ), so trips at 0.7 s (0.2 s after the fault). These responses are all correct and as expected.

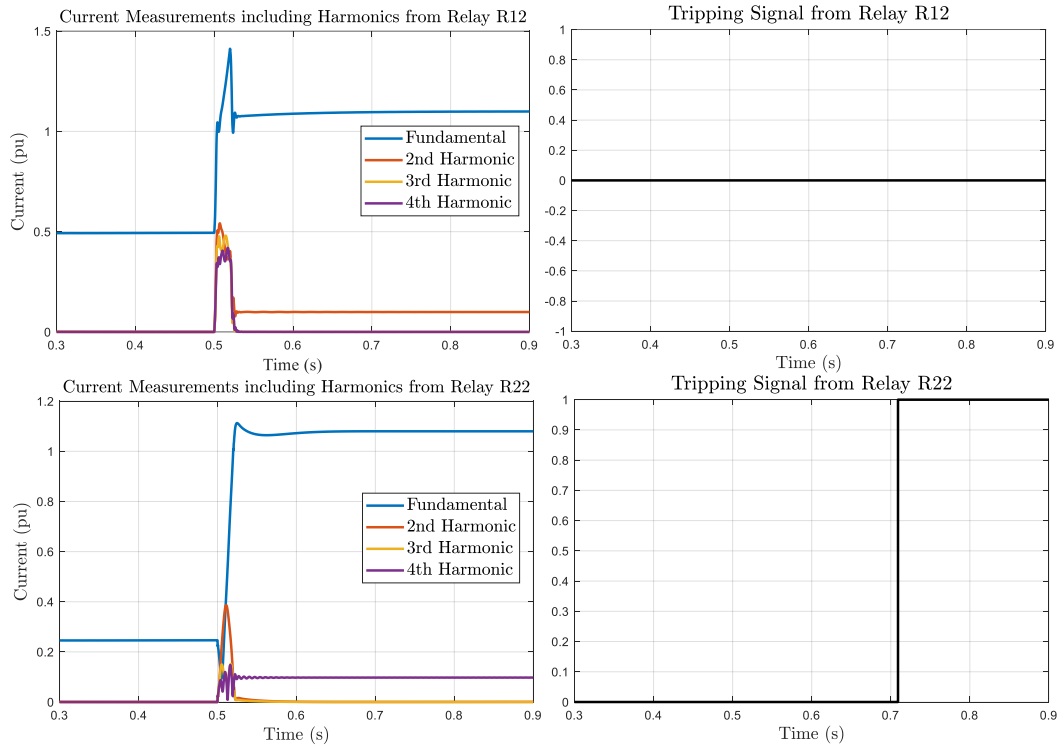


Figure 6.6: BGRs: fundamental current measurements, injected/measured harmonic output currents and tripping signals for a (non-cleared) three-phase balanced fault at  $F_2$ .

### Results for Fault at Location $F_1$

The responses of the system for fault  $F_1$  can be explained through inspection of the current measurements and tripping signals of all FGRs and BGRs as shown in Figure 6.7 and Figure 6.8. For this fault, only  $R_{11}$  should operate from the three FGRs, and both  $R_{12}$  and  $R_{22}$  should operate from the BGR set of relays.  $R_{12}$  should operate first as the main protection to isolate the fault and  $R_{22}$  should operate with a delay to provide backup if it is required.

It is clear from Figure 6.7 that  $R_{31}$  does not detect any harmonic components, so does not operate. Relay,  $R_{21}$  detects the 4<sup>th</sup> harmonic component ( $I_{HC4}$ ) injected by  $IIDG_3$ . However, according to the relay setting,  $R_{21}$  will operate when it detects 2<sup>nd</sup> or 3<sup>rd</sup> harmonic ( $I_{HC2}$  and  $I_{HC3}$ ), and hence, it does not issue a tripping signal for the fault at  $F_1$ .  $R_{11}$  detects 2<sup>nd</sup> harmonic, and issues a tripping

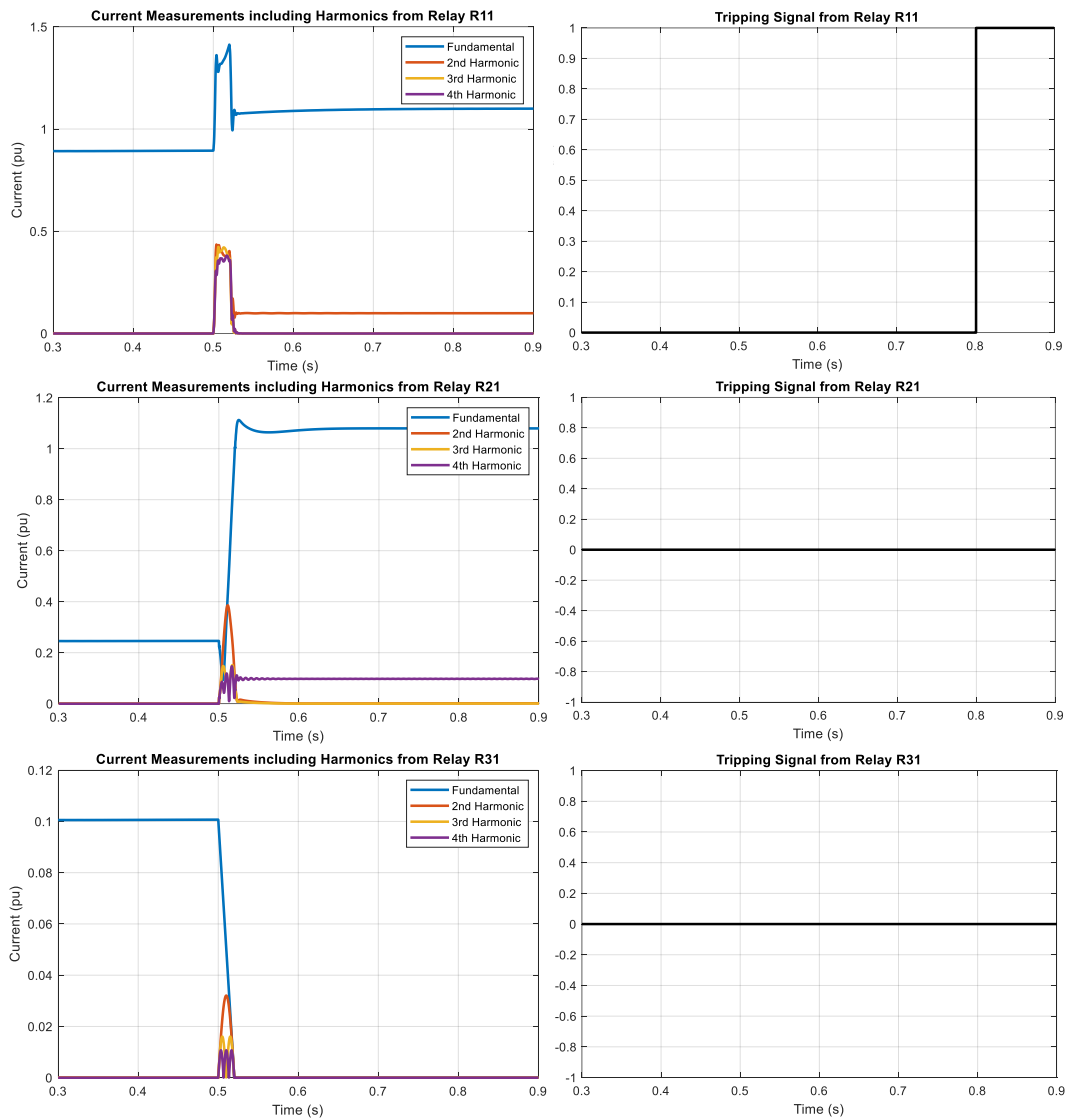


Figure 6.7: FGRs: fundamental current measurements, injected/measured harmonic output currents and tripping signals for a (non-cleared) three-phase balanced fault at  $F_1$ .

signal at 0.8 s (0.3 s after the fault inception) as desired.

The results for the BGRs are shown in Figure 6.8 and it is clear from the figure that both  $R_{12}$  and  $R_{22}$  detect the appropriate harmonic components in accordance with their settings, and both operate for the fault  $F_1$ , with  $R_{12}$  operating at 0.6 s (0.1 s after fault inception) and  $R_{22}$  operating as backup at 0.7 s (0.2 s after the fault inception).

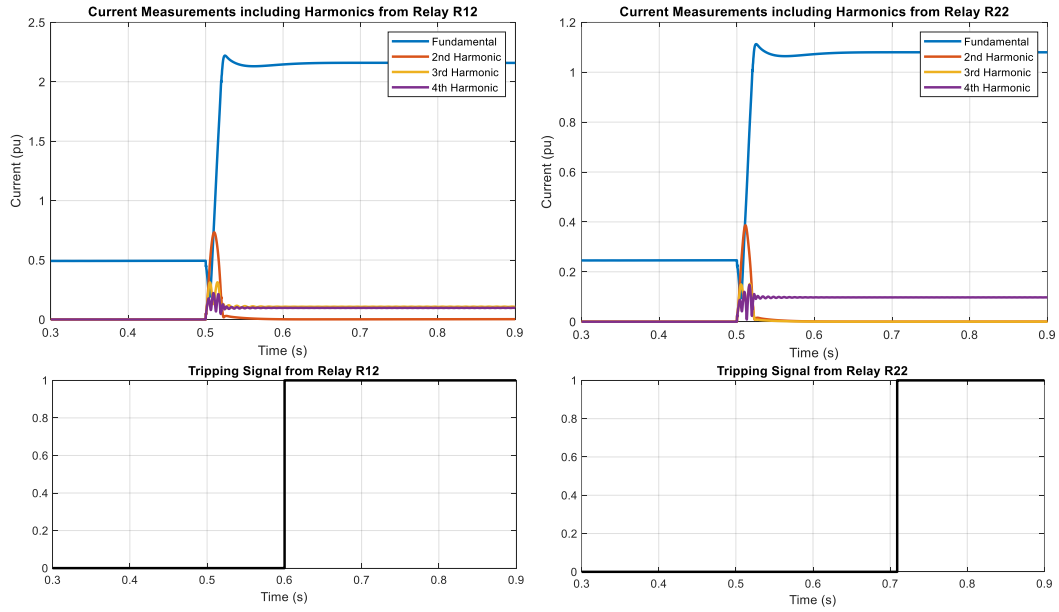


Figure 6.8: BGRs: fundamental current measurements, injected/measured harmonic output currents and tripping signals for a (non-cleared) three-phase balanced fault at  $F_1$ .

### 6.1.5 Unbalanced Faults

Unbalanced faults are the most commonly occurring faults in power systems, particularly in overhead systems and in phase-segregated underground cable systems. Unbalanced faults can be single phase to earth, phase to phase, or double phase to earth faults. There can even be circuit-circuit faults on double-circuit overhead lines but these are very uncommon and not considered here as this work is concerned with active distribution/microgrid systems.

During unbalanced faults, significant increases in negative and zero sequence components are present and can be readily measured and observed. In this research, the performance of the system for two types of unbalanced faults is reported: phase to earth and phase to phase faults. Similar to the previous case studies presented earlier in this chapter, faults have been applied at different locations of the microgrid and cases 4-21 in Table 6.4 show the successful operation of the proposed scheme for all unbalanced faults with low fault resistance. In

the interests of space and to avoid excessive repetition, the currents and tripping times for all possible faults at all locations are not shown graphically, but the table presents the outcomes of all scenarios, and the system operates correctly for all.

However, it has been observed from the simulation results that the scheme may not accurately isolate faulted sections during high resistive unbalanced faults as can be seen in case no 33 of Table 6.4. Therefore, the maximum fault resistance during unbalanced fault with the proposed protection scheme is  $20 \Omega$ . As can be seen from case 32 of Table 6.4 that with  $15 \Omega$  phase A to earth fault, the grading margin with the backup protection is significantly low, although the main protection can still operate within expected operating time. To avoid any unnecessary relay operation, the harmonics are injected in the faulted phases only so that injection does not affect the health phases. However, the simulation results (for example, case 33) reveals that with heavy loads connected close to generation unit, the healthy phases also carry harmonics during high resistive unbalanced faults.

### 6.1.6 High Impedance Faults (HIFs)

The fault resistance at  $F_3$  has been varied to test HIF performance. Two different types of faults have been simulated at this location, a balanced three-phase to earth fault and a single phase to earth fault (A-E). Cases 22-33 in Table 6.4 show the relay tripping times for different fault impedances. It can be observed that the scheme can properly detect and coordinate for HIFs with fault impedances of up to  $20 \Omega$  for single-phase to ground faults, and for three-phase faults, the maximum value of fault resistance that can be catered for is  $60 \Omega$ . Fault can be detected by the relays for resistances beyond the mentioned value for single-phase to ground faults, however, coordination between the relays may be compromised.

CHAPTER 6. DEMONSTRATION AND VALIDATION OF THE DEVELOPED PROTECTION SCHEME AND ANALYSES OF RESULTS

Table 6.4: Verification of the proposed solution under different fault simulations.

Case No.	Fault Location	Fault Type	Fault Imp ( $\Omega$ )	Distance from Grid (km)	Fault Clearing Time (s)					Correct Operation?
					CB 1.1	CB 1.2	CB 2.1	CB 2.2	CB 3.1	
1	$F_3$	ABC	0.1	5.3	0.8	-	0.7	-	0.6	Yes
2	$F_2$	ABC	0.1	3.3	0.8	-	0.7	0.7	-	Yes
3	$F_1$	ABC	0.1	1.4	0.8	0.6	-	0.7	-	Yes
4	$F_3$	A-G	0.1	5.3	0.77	-	0.7	-	0.6	Yes
5	$F_3$	B-G	0.1	5.3	0.81	-	0.7	-	0.6	Yes
6	$F_3$	C-G	0.1	5.3	0.81	-	0.7	-	0.6	Yes
7	$F_3$	A-B	0.1	5.3	0.77	-	0.7	-	0.6	Yes
8	$F_3$	B-C	0.1	5.3	0.84	-	0.7	-	0.6	Yes
9	$F_3$	C-A	0.1	5.3	0.83	-	0.7	-	0.6	Yes
10	$F_2$	A-G	0.1	3.3	0.77	-	0.7	0.71	-	Yes
11	$F_2$	B-G	0.1	3.3	0.81	-	0.7	0.74	-	Yes
12	$F_2$	C-G	0.1	3.3	0.81	-	0.7	0.71	-	Yes
13	$F_2$	A-B	0.1	3.3	0.77	-	0.7	0.74	-	Yes
14	$F_2$	B-C	0.1	3.3	0.84	-	0.7	0.75	-	Yes
15	$F_2$	C-A	0.1	3.3	0.83	-	0.7	0.73	-	Yes
16	$F_1$	A-G	0.1	1.4	0.83	0.64	-	0.72	-	Yes
17	$F_1$	B-G	0.1	1.4	0.82	0.61	-	0.71	-	Yes
18	$F_1$	C-G	0.1	1.4	0.77	0.62	-	0.71	-	Yes
19	$F_1$	A-B	0.1	1.4	0.77	0.62	-	0.73	-	Yes
20	$F_1$	B-C	0.1	1.4	0.77	0.66	-	0.76	-	Yes
21	$F_1$	C-A	0.1	1.4	0.77	0.64	-	0.74	-	Yes
22	$F_3$	ABC	1	5.3	0.8	-	0.7	-	0.6	Yes
23	$F_3$	ABC	5	5.3	0.79	-	0.72	-	0.62	Yes
24	$F_3$	ABC	10	5.3	0.79	-	0.72	-	0.62	Yes
25	$F_3$	ABC	15	5.3	0.79	-	0.72	-	0.64	Yes
26	$F_3$	ABC	20	5.3	0.79	-	0.72	-	0.64	Yes
27	$F_3$	ABC	30	5.3	0.79	-	0.72	-	0.64	Yes
28	$F_3$	ABC	50	5.3	0.79	-	0.73	-	0.64	Yes
29	$F_3$	ABC	66	5.3	0.79	-	0.73	-	0.73	No
30	$F_3$	A-G	1	5.3	0.81	-	0.7	-	0.6	Yes
31	$F_3$	A-G	10	5.3	0.81	-	0.7	-	0.6	Yes
32	$F_3$	A-G	15	5.3	0.78	-	0.75	-	0.64	Yes
33	$F_3$	A-G	20	5.3	0.81	0.76	0.92	-	0.64	No
34	$F_3$	ABC	0.1	14.3	0.8	-	0.7	-	0.6	Yes
35	$F_3$	ABC	0.1	24.3	0.8	-	0.7	-	0.6	Yes
36	$F_3$	ABC	0.1	34.3	0.8	-	0.71	-	0.6	Yes
37	$F_3$	ABC	0.1	44.3	0.8	-	0.71	-	0.6	Yes
38	$F_3$	ABC	0.1	54.3	0.8	-	0.71	-	0.62	Yes
39	$F_3$	ABC	0.1	64.3	0.8	-	0.71	-	0.62	Yes
40	$F_3$	ABC	0.1	144.3	0.82	-	0.71	-	0.62	No

### 6.1.7 Different Line Length/Impedance

The maximum overall line length within the tested microgrid is 5.3 km and the scheme can operate properly within this boundary. In this simulation, the capability of the scheme for longer line lengths is tested and the output is shown in Table 6.4. From the results for cases 34-40, it can be concluded that the scheme works perfectly for lines with lengths of more than 100 km (which is very high for microgrid and such lengths would almost certainly never be used in practice – losses and voltage drops would be unacceptably high). However, the injected components become highly unstable when line lengths are longer than 144.5 km, therefore, even though the scheme is working, it is been considered the scheme is limited up to this (unrealistically excessive) line length, so the system would be suited to all practical and realistic microgrids.

### 6.1.8 Different Combination of IIDG Locations

Three different scenarios have been tested for a three-phase fault at  $F_3$  to validate scheme operation for different IIDG locations. Initially, only  $IIDG_1$  is connected and the response, as shown in Table 6.5, verifies correct operation. Secondly,  $IIDG_1$  and  $IIDG_2$  are connected and finally,  $IIDG_1$  and  $IIDG_3$  are connected. For all cases, the scheme operates correctly in terms of both main and backup responses.

Table 6.5: Results of Different Combination of IIDG Location With a Three-Phase Fault at  $F_3$

Case No.	Connected Generators			Fault Clearing Time				
	$IIDG_1$	$IIDG_2$	$IIDG_3$	CB1.1	CB1.2	CB2.1	CB2.2	CB3.1
41	On	Off	Off	0.8 s	-	0.7 s	-	0.6 s
42	On	On	Off	0.8 s	-	0.7 s	-	0.6 s
43	On	Off	On	0.8 s	-	0.7 s	-	0.6 s

### 6.1.9 Combination of IIDGs and Synchronous Generator (SG)

In this simulation, IIDG<sub>2</sub> in Figure 6.1 is replaced with a conventional SG model with the same rated capacity of 500 kVA to verify the operation of the solution when mixed generation comprising SGs and IIDGs is used in the microgrid, which may be the case in practice. The fault current supplied by the SG during a fault at  $F_2$  is shown in Figure 6.9, along with the harmonic and fundamental currents measured by relays  $R_{21}$  and  $R_{22}$ . As can be seen in the figure, a fault is initiated at 0.5 s and in response, the SG injects a fault current that is 3.6 times the value of the rated current.

However, this high fault current does not have a negative impact on the harmonic injection through the IIDGs, nor does it limit the ability of the harmonics to be detected and measured by the relays. Therefore, the proposed scheme can successfully identify the faulted section and can take necessary actions to isolate the fault from the network.

However, it must be noted that, in order to identify the faulted section from both relays at each end of the system, harmonic injection is required from both “ends” of the network. Hence, the location of SGs would have to be between two IIDGs, which could limit applicability in some specific configurations.

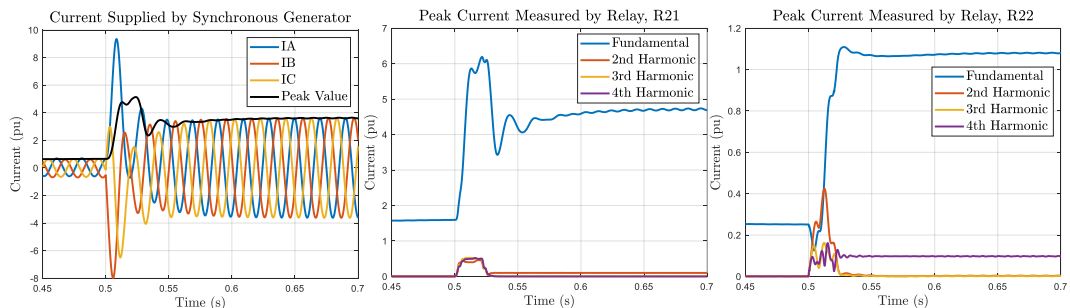


Figure 6.9: Simulation results for combination of IIDGs and SG.

## 6.2 Real Time Hardware-in-the-Loop (HiL) based Performance Demonstration and Validation of the Protection Scheme

### 6.2.1 Overview of the Test Configuration

To further validate the performance of the proposed protection scheme, an HiL experimental configuration has been set up, and case studies have been executed using this arrangement in the laboratory environment. An overview of the laboratory setup is presented in Figure 6.10. The microgrid shown in Figure 6.1 is implemented in the real-time digital simulator (RTDS) [3] to emulate the real-time dynamics of the microgrid during both normal and fault conditions. The output currents of the simulated CTs installed at Bus 2 and Bus 3 are sent to the OPAL-RT [4] through the Giga-Transceiver Analogue Output (GTAO) card within the RTDS.

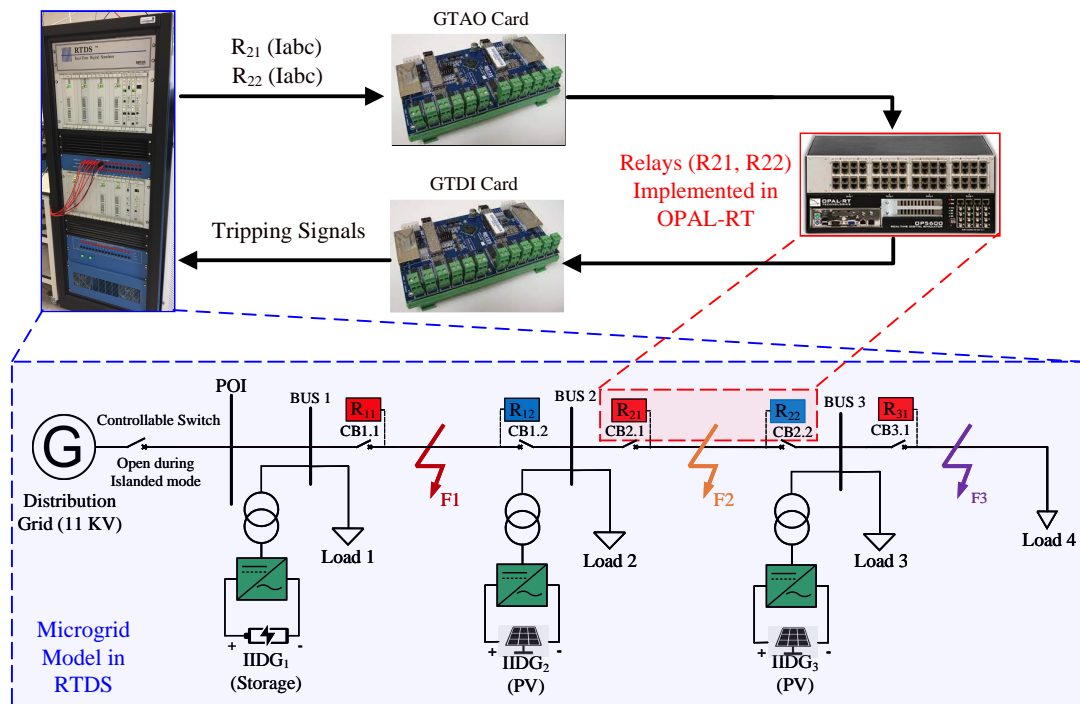


Figure 6.10: HiL Testing Setup in the Laboratory.

Within the OPAL-RT system, relays,  $R_{21}$  and  $R_{22}$  are implemented and the software operates in real time. Each relay requires total 3 signals (i.e. three phase current) through GATO from microgrid implemented in RTDS. Therefore, 2 relays implemented in OPAL-RT require total 6 signals from RTDS using GATAO. The relays analyse the measurement signals received from the RTDS using the algorithm and relay logic presented in Figure 5.2 and Figure 5.3.

Any tripping signals from the relays are sent to the RTDS using the Giga-Transceiver Digital Input (GTDI) card as the inputs to the simulation, closing the real-time simulation loop. Signals received from OPAL-RT through GTDI card are used to control the CB2.1 and CB2.2 of the microgrid as shown in Figure 6.1

### 6.2.2 Test Results for Three-Phase Balance Faults

As shown in Figure 6.1, three-phase faults have been simulated at different locations throughout the microgrid network. Since only relays  $R_{21}$  and  $R_{22}$  are implemented in OPAL-RT for HiL tests, it is assumed that other relays in the network will not operate for any fault occur on the microgrid. Following subsections describe the HiL test results with the aid of Figure 6.11, Figure 6.12 and Figure 6.13 for three phase balanced fault occur at different locations of the microgrid.

#### Results for Fault at Location $F_1$

The measured three phase current, harmonic components and tripping signals of the relays ( $R_{21}$  and  $R_{22}$ ) in response to simulated faults at  $F_1$  are shown in Figure 6.11. As can be seen from Figure 6.11, a fault at  $F_1$  has been initiated at 0.4 s and only relay  $R_{22}$  issues a tripping signal at 0.6 s (0.2 s after the fault inception), under the assumption that relay  $R_{12}$  (which is not included in the HiL arrangement) has not issued any tripping signal at 0.1 s after the fault inception. Also, it can be seen that relay  $R_{21}$  has not detected  $2^{nd}$  and  $3^{rd}$  order harmonic components but relay  $R_{22}$  has detected  $4^{th}$  order harmonic injected by the downstream  $IIDG_3$  (as

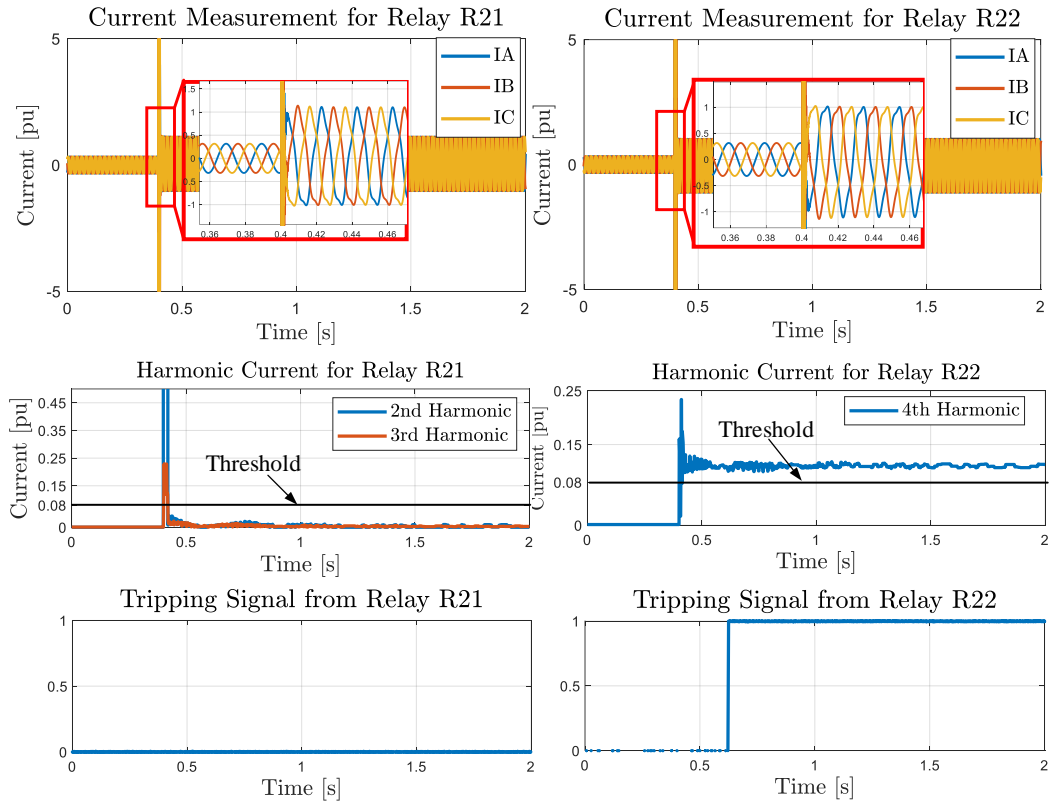


Figure 6.11: HiL Test Results for a Fault at  $F_1$ .

can be seen from Figure 6.1).

### Results for Fault at Location $F_2$

A fault has been simulated at location  $F_2$  in the microgrid shown in Figure 6.1 and the results for the simulated fault is shown in Figure 6.12. As can be seen from Figure 6.12, the fault has been initiated at 0.4 s and both relays issue a tripping signal at 0.6 s (0.2 s after the fault inception). Furthermore, relay  $R_{21}$  analysed the 2<sup>nd</sup> and 3<sup>rd</sup> harmonics injected by  $IIDG_1$  and  $IIDG_2$  from the upstream of the network and the magnitude of the harmonics are higher than the threshold used for the relay. Similarly, in case of relay  $R_{22}$ , it also detects the 4<sup>th</sup> harmonic component injected by  $IIDG_3$  and magnitude of the harmonic component is higher than the pre-set threshold. Therefore, both relays send the tripping signals at 0.2 s after the fault inception.

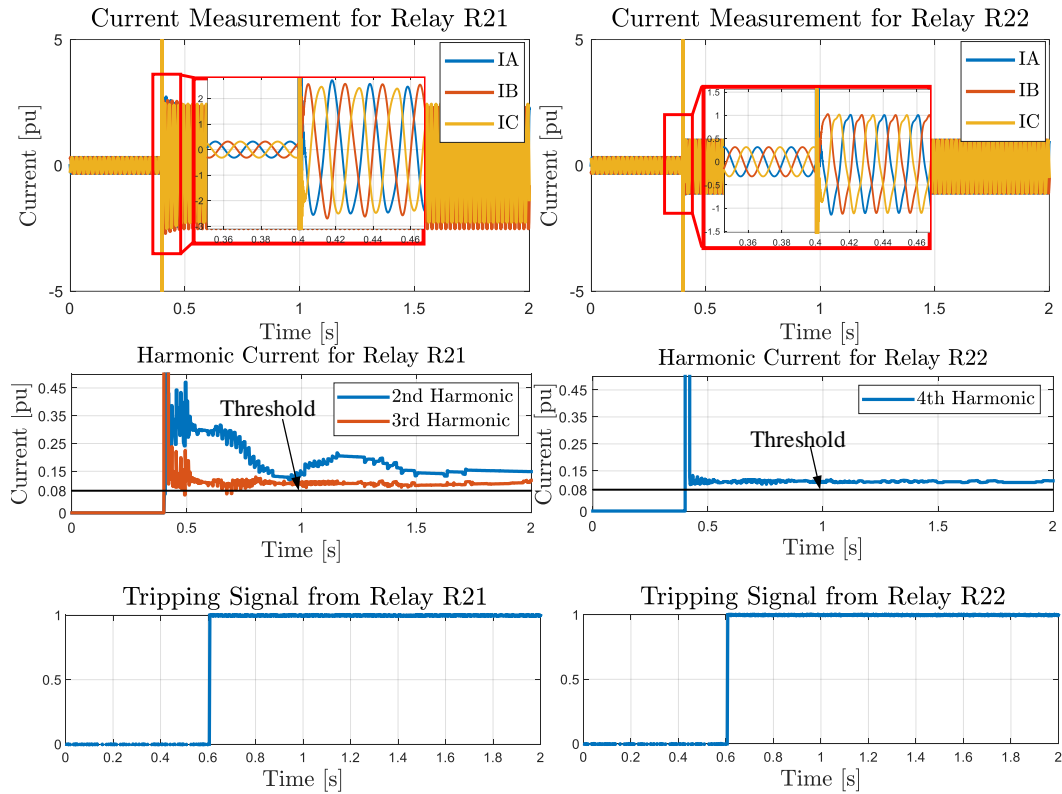


Figure 6.12: HiL Test Results for a Fault at  $F_2$ .

### Results for Fault at Location $F_3$

The current measurements, harmonic components and tripping signals by the relays  $R_{21}$  and  $R_{22}$  are shown in Figure 6.13 for a fault simulated at location  $F_3$  at 0.4 s. As can be seen from Figure 6.13, relay  $R_{21}$  can detect both  $2^{nd}$  and  $3^{rd}$  harmonic injected by  $IIDG_1$  and  $IIDG_2$  respectively. Therefore, issue a tripping signal at 0.6 s (0.2 s after the fault inception). The  $IIDG_3$  also inject the  $4^{th}$  harmonic during fault but since the fault position is downstream to the relay  $R_{22}$  position,  $R_{22}$  has not detected any harmonic component as can be seen from Figure 6.13 and therefore, remains inactive during the fault  $F_3$ .

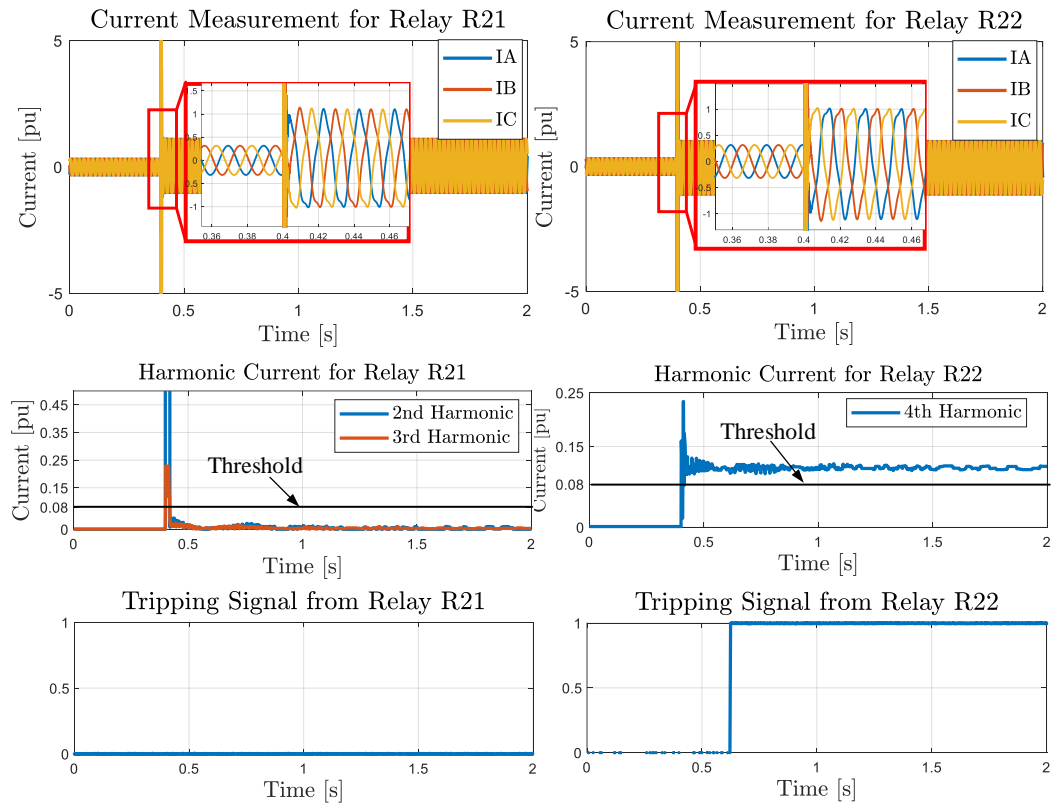


Figure 6.13: HiL Test Results for a Fault at  $F_3$ .

## References

- [1] “IEEE Standard for the Specification of Microgrid Controllers,” *IEEE Std 2030.7-2017*, pp. 1–43, 2018.
- [2] T. Haggis and EON, “Network Design Manual,” United Kingdom, Tech. Rep., 2006. [Online]. Available: <https://www.yumpu.com/en/document/read/8953808/network-design-manual-eon-uk>
- [3] RTDS Technologies, “RTDS Simulator Hardware,” Tech. Rep., 2011. [Online]. Available: <https://manualzz.com/doc/25744342/rtds-simulator-hardware>
- [4] OPAL-RT Technologies, “OPAL-RT OP5600 V3 Series Manuals,” Tech. Rep., 2018. [Online]. Available: <https://www.manualslib.com/products/Opal-Rt-Op5600-V3-Series-10349361.html>

# Chapter 7

## Conclusions and Future Work

### 7.1 Conclusions

This thesis has presented the findings of extensive analyses of the challenges associated with protection of islanded microgrids in low fault levels scenarios. A comprehensive literature review has been presented to assess and identify limitations of existing and proposed protection schemes. It has been demonstrated through a critical literature review, supported by simulations and investigations, that existing overcurrent protection relays may not detect and coordinate (and provide backup when required) properly to effectively isolate faults in all scenarios within islanded microgrids that are powered solely by IIDGs. Furthermore, since the behaviour of IIDGs are significantly different from that of SGs, particularly during network faults, they create several challenges for the protection system.

A comparison between IIDG and conventional SG and SC has been carried out to demonstrate their respective capabilities with respect to performance during faults in terms of voltage and current outputs. As a solution to the identified protection challenges, this research offers a novel protection system, which incorporates IIDG controllers. The novel protection solution analyses harmonic components that are deliberately injected by IIDGs during faults. The

scheme operates as a unit protection but does not require any communication between the relays and can provide inherent backup protection. The proposed scheme overcomes the issues associated with conventional overcurrent relays and can provide effective protection to islanded microgrids.

### **7.1.1 Analysis of the Dynamic Behaviours of IIDGs**

Design, control, modelling and implementation of two different types of controllers of inverters were presented in this thesis. The capabilities of the IIDGs in comparison to the SG and SC have been illustrated with a wide range of simulation studies in MATLAB Simulink.

It can be concluded that the developed IIDG can provide satisfactory dynamic performance in terms of reactive power support during voltage depression and FRT, and can also provide fast short circuit current during fault events. However, the fault current supplied by the IIDG is dependent on its controller, and on the physical thermal limitations of the power electronics converter system and components rather than fault type and location in the microgrid. It is possible to control the fault characteristics of the IIDGs through implementing a separate control strategy that is applied during faults.

The developed IIDG model can remain connected during severe voltage depression and FRT voltage profile as stated in GB grid code. Furthermore, the IIDG can provide reactive power with the voltage depression according the requirements of the GB grid code. However, in comparison to the synchronous machines, the contribution is limited due to IIDG controllers' thermal limit.

### **7.1.2 Protection Scheme**

To address the technical challenges regarding the need for communications, bidirectionality, and low fault current, a communications-free active protection method

has been developed, with uses control strategies within IIDGs to address the identified protection issues in islanded microgrids dominated by IIDGs.

In this proposed scheme, controllers of the IIDGs intentionally modify their injected fault current based on the presence of a fault in the network. After simulating various fault scenarios in a realistic microgrid, the following advantages of the proposed protection scheme are claimed:

- The proposed solution utilises multiple harmonic injections during a fault (with each of the individual IIDG units injecting a specific and assigned harmonic) to identify the faulted section of the network. Injection of multiple harmonics helps the scheme to be more sensitive and selective and can provide backup protection in networks with bidirectional power flow.
- Identification of the fault is independent of the fault current magnitude and the algorithm is relatively simple compared to other existing or proposed microgrid protection schemes in the literature.
- The proposed solution can operate with a combination of synchronous generators and IIDGs, as well as, when individual generators/IIDGs are out of service.
- The scheme does not require dedicated communication to operate, which increases the cost-effectiveness, reliability and practicality of implementing the scheme.

A wide range of simulations using both Simulink and HiL experimental arrangements have been carried out to validate the proposed scheme. It has been observed that the solution can overcome the vast majority of issues associated with the protection of islanded microgrids and can provide effective protection across a wide range of fault scenarios as evidenced through the simulated and demonstrated case studies. In terms of limitation of the scheme, it is not always

capable of identifying and isolating faulted sections effectively during unbalanced faults with very high fault resistances, and this is particularly evident if relatively large loads are connected close to the generation unit as discussed in Chapter 6. The established limits for fault resistance (that is, values above which the system may not always operate properly) are  $20 \Omega$  for single phase to earth faults and  $60 \Omega$  for three-phase faults. These values are relatively high and it is believed that such faults with high resistances are relatively uncommon [1]. Other forms of protection (for example, sensitive earth fault) could be added to the functionality of the system as future work to overcome this - as well as studying performance on systems with different earthing regimes. Another limitation relates to the fact that, while the scheme can operate successfully with combinations of SGs and IIDGs in the same system, it is only fully applicable in systems where the SGs are physically located between two IIDGs.

## 7.2 Future Research Work

Following on from the research, development and demonstration activities presented in this thesis, additional research work as listed below may be conducted.

- The tests and validation results presented in Chapter 6 can be expended further through integrating a physical inverter within the RTDS experimental arrangement. The inverter should be capable of providing active and reactive power in real-time. The proposed control method with harmonic injection during fault can be implemented to further research and test capabilities and limitations of actual inverter hardware to facilitate future practical scheme implementation.
- Compare the performance of the proposed solution with other existing and proposed schemes in response to different grid events and with other

microgrid models (perhaps assuming different regions of the GB network as self-sustaining microgrids) with larger amounts of renewable generation units and dynamic loads that are anticipated to be integrated with the network in future.

- Validating the proposed protection scheme under different fault types and scenarios along with a large mix of generation units using RTDS and Hardware-in-the-Loop (HiL) configuration.
- Implementation of the prototype of the proposed schemes for further validation of the solutions in a real microgrid network using large-scale test facilities, such as the Power Network Demonstration Centre (PNDC) at the University of Strathclyde.
- Compare the proposed protection scheme with other communication dependent protection solution and analyse the schemes in terms of sensitivity, selectivity, operation time and cost.
- The impact of IIDG controllers' parameters such as PID, filters and speed/bandwidth on the protection scheme will be studied.

## References

- [1] J. C. J. Theron, A. Pal, and A. Varghese, "Tutorial on high impedance fault detection," in *2018 71st Annual Conference for Protective Relay Engineers (CPRE)*, 2018, pp. 1–23.

# Appendix A

## Relay Setting Calculation

The performance of the overcurrent relays under different contingency events in a microgrid has been demonstrated in Chapter 5. In this chapter, different data related to line parameters, grid, loads and generation units are presented and effective way of calculating the overcurrent relays' settings are explained.

To calculate the relay settings, normal and fault current at different buses need to be calculate first. Therefore, it is necessary to redraw the implemented microgrid as shown in Figure 6.1 with different line parameters. As mentioned in the Chapter 6, the implemented microgrid's voltage is  $V_S = 11$  kV. The other parameters for grid are presented in Table A.1.

Table A.1: Grid parameters

Parameters	Symbol	Value
Frequency	$f_g$	50 Hz
Voltage (phase to phase)	$V_g$	11 kV
Phase A angle	$\theta_A$	$0^\circ$
Three-phase SCL	$S_g$	250 MVA
X/R ratio	X/R	7

From the data provided in Table A.1, the internal impedance of the grid can be calculated.

$$\text{Grid Impedance Magnitude, } |Z_S| = \frac{V_g^2}{S_g} = \frac{(11 \times 10^3)^2}{250 \times 10^6} = 0.484 \Omega$$

$$\text{Grid Impedance Angle, } \theta_g = \tan^{-1}(X/R) = \tan^{-1}(7) = 81.87^\circ$$

$$\text{Grid Impedance, } Z_g = |Z_g| (\cos(\theta_g) + j\sin(\theta_g)) = |0.484| (\cos(81.87^\circ) + j\sin(81.87^\circ))$$

$$Z_g = 0.06845 + j0.47914 \Omega$$

The line parameters of the microgrid are shown in Table A.2 and microgrid model with impedance values are shown in Figure A.1.

Table A.2: Line parameters

Parameters	Symbol	Value
Line Impedance	$Z_{Line}$	$0.295 + j0.595 \Omega/\text{km}$
Length between POI to Bus 1	$l_{01}$	0.5 km
Length between Bus 1 to Bus 2	$l_{12}$	1.8 km
Length between Bus 2 to Bus 3	$l_{23}$	2 km
Length after Bus 3	$l_3$	1 km

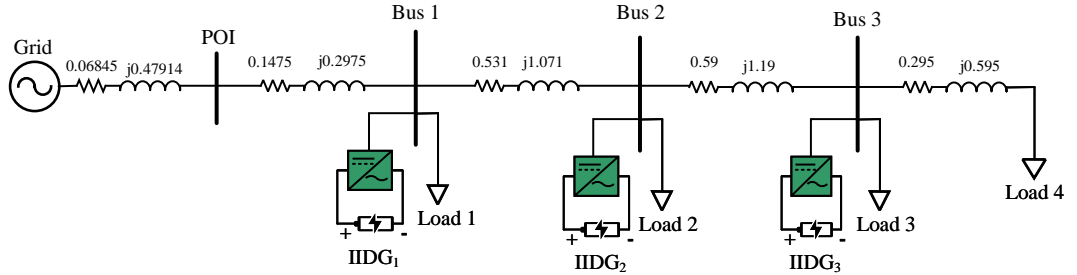


Figure A.1: One-line diagram of the microgrid.

The load size and CT ratio used for each bus are presented in Table A.3.

## A.1 Calculation of Load Current

During normal condition, following current magnitudes will be detected by the relays at each bus (at the primary side).

Table A.3: Load size and CT ratio.

Load Number	Size
$Load_1$	200 kVA
$Load_2$	200 kVA
$Load_3$	100 kVA
$Load_4$	50 kVA
Total Load	550 kVA
Bus Number	CT ratio
Bus 1	40
Bus 2	20
Bus 3	20

$$\text{Load current at Bus 1, } I_{L_{Bus1}} = \frac{TotalLoad}{\sqrt{3} \times V_S} = \frac{550 \times 10^3}{\sqrt{3} \times 11 \times 10^3}$$

$$I_{L_{Bus1}} = 28.87A$$

$$\text{Load current at Bus 2, } I_{L_{Bus2}} = \frac{TotalLoad - Load_1}{\sqrt{3} \times V_S} = \frac{350 \times 10^3}{\sqrt{3} \times 11 \times 10^3}$$

$$I_{L_{Bus2}} = 18.37A$$

$$\text{Load current at Bus 3, } I_{L_{Bus3}} = \frac{TotalLoad - Load_1 - Load_2}{\sqrt{3} \times V_S} = \frac{150 \times 10^3}{\sqrt{3} \times 11 \times 10^3}$$

$$I_{L_{Bus3}} = 7.87A$$

## A.2 Calculation of Fault Levels and Currents at Different Buses

### At POI:

$$\text{Fault level, } S_{POI} = \frac{V_S^2}{|0.06845+j0.47914|} = \frac{(11 \times 10^3)^2}{|0.06845+j0.47914|} = 249.998 \text{ MVA}$$

$$\text{Fault current, } I_{F,POI} = \frac{S_{POI}}{\sqrt{3} \times V_S} = \frac{249.998 \times 10^6}{\sqrt{3} \times 11 \times 10^3} = 13.12 \text{ kA}$$

### At Bus 1:

$$\text{Fault level, } S_{Bus1} = \frac{V_S^2}{|0.06845+j0.47914|+|0.1475+j0.2975|} = \frac{(11 \times 10^3)^2}{|0.21595+j0.77664|}$$

$$S_{Bus1} = 150.105 \text{ MVA}$$

$$\text{Fault current, } I_{F,Bus1} = \frac{S_{Bus1}}{\sqrt{3} \times V_S} = \frac{150.105 \times 10^6}{\sqrt{3} \times 11 \times 10^3} = 7.878 \text{ kA}$$

**At Bus 2:**

$$\text{Fault level, } S_{Bus2} = \frac{V_S^2}{|0.06845+j0.47914|+|0.1475+j0.2975|+|0.531+j1.071|} = \frac{(11 \times 10^3)^2}{|0.74695+j1.84764|}$$

$$S_{Bus2} = 60.72 \text{ MVA}$$

$$\text{Fault current, } I_{F,Bus2} = \frac{S_{Bus2}}{\sqrt{3} \times V_S} = \frac{60.72 \times 10^6}{\sqrt{3} \times 11 \times 10^3} = 3.187 \text{ kA}$$

**At Bus 3:**

$$\text{Fault level, } S_{Bus3} = \frac{V_S^2}{|0.06845+j0.47914|+|0.1475+j0.2975|+|0.531+j1.071|+|0.59+j1.19|} = \frac{(11 \times 10^3)^2}{|1.33695+j3.03764|}$$

$$S_{Bus3} = 36.46 \text{ MVA}$$

$$\text{Fault current, } I_{F,Bus3} = \frac{S_{Bus3}}{\sqrt{3} \times V_S} = \frac{36.46 \times 10^6}{\sqrt{3} \times 11 \times 10^3} = 1.914 \text{ kA}$$

## A.3 Relay Settings

**Relay at Bus 3:**

Plug Setting,  $PS = 1$  or 100% (assumed)

Time Multiple Setting,  $TMS = 0.05$  (assumed)

$$\text{Fault current at secondary side, } I_{F,Bus3sec} = \frac{I_{F,Bus3}}{\text{CT ratio at Bus 3}} = \frac{1.914 \times 10^3}{20} = 95.7 \text{ A}$$

$$\text{Operating Time, } OT = \frac{0.14}{\left(\frac{I_{F,Bus3sec}}{PS}\right)^{0.02} - 1} \times TMS = \frac{0.14}{\left(\frac{95.7}{1}\right)^{0.02} - 1} \times 0.05 = 0.07 \text{ s}$$

**Relay at Bus 2:**

Time grading between the relays are assumed to be 3 s.

Maximum plug setting multiplier (PSM) is assumed to be 100.

$$\text{Plug Setting, } PS = \frac{I_{F,Bus2}}{CTratio \times PSM} = \frac{3.187 \times 10^3}{20 \times 100} = 1.6$$

Since plug settings are generally set in 25% interval, considering next setting, PS is set as 175% or 1.75.

For a fault after Bus 3, operating time should be = OT relay at Bus 3 + coordination time delay = 0.37 s.

Fault current at secondary side for a fault after Bus 3,

$$I_{F,Bus2sec} = \frac{I_{F,Bus3}}{\text{CT ratio at Bus 2}} = \frac{1.914 \times 10^3}{20} = 95.7 \text{ A}$$

$$\text{Time Multiple Setting, } TMS = \frac{OT}{0.14} \times \left( \left( \frac{I_{F,Bus2sec}}{PS} \right)^{0.02} - 1 \right)$$

$$TMS = \frac{0.37}{0.14} \times \left( \left( \frac{95.7}{1.75} \right)^{0.02} - 1 \right)$$

$$TMS = 0.22$$

Fault current at secondary side for a fault between Bus 2 and Bus 3,

$$I_{F,Bus2sec} = \frac{I_{F,Bus2}}{\text{CT ratio at Bus 2}} = \frac{3.187 \times 10^3}{20} = 159.35 \text{ A}$$

$$\text{Operating Time, } OT = \frac{0.14}{\left( \frac{I_{F,Bus2sec}}{PS} \right)^{0.02} - 1} \times TMS = \frac{0.14}{\left( \frac{159.35}{1.75} \right)^{0.02} - 1} \times 0.22 = 0.32 \text{ s}$$

### Relay at Bus 1:

$$\text{Plug Setting, } PS = \frac{I_{F,Bus1}}{CTratio \times PSM} = \frac{7.878 \times 10^3}{40 \times 100} = 1.97$$

Since plug settings are generally set in 25% interval, considering next setting, PS is set as 200% or 2.

For a fault after Bus 2, operating time should be = OT relay at Bus 2 + coordination time delay = 0.62 s.

Fault current at secondary side for a fault between Bus 2 and Bus 3,

$$I_{F,Bus1sec} = \frac{I_{F,Bus2}}{\text{CT ratio at Bus 2}} = \frac{3.187 \times 10^3}{40} = 79.675 \text{ A}$$

$$\text{Time Multiple Setting, } TMS = \frac{OT}{0.14} \times \left( \left( \frac{I_{F,Bus2sec}}{PS} \right)^{0.02} - 1 \right)$$

$$TMS = \frac{0.62}{0.14} \times \left( \left( \frac{79.675}{2} \right)^{0.02} - 1 \right) = 0.34$$

Fault current at secondary side for a fault between Bus 1 and Bus 2,

$$I_{F,Bus1sec} = \frac{I_{F,Bus1}}{\text{CT ratio at Bus 1}} = \frac{7.878 \times 10^3}{40} = 196.95 \text{ A}$$

$$\text{Operating Time, } OT = \frac{0.14}{\left( \frac{I_{F,Bus1sec}}{PS} \right)^{0.02} - 1} \times TMS = \frac{0.14}{\left( \frac{196.95}{2} \right)^{0.02} - 1} \times 0.34 = 0.49 \text{ s}$$

The overall settings for three overcurrent relays at three different buses are summarised in Table A.4.

Table A.4: Overcurrent relay settings

Relays	PS	TMS
Relay 1 (at Bus 1)	200%	0.34
Relay 2 (at Bus 2)	175%	0.22
Relay 3 (at Bus 3)	100%	0.05

# Appendix B

## SG and IIDG Parameters for Chapter 6

### B.1 Parameters for IIDGs

As shown in Chapter 6, to validate the developed protection scheme's operation, three IIDG units are modelled and parameters for the IIDG units are presented in Table B.1.

Table B.1: Parameters for IIDG units

Parameter	Values	Comments
$S_n$	500 kVA	Nominal power
$f_n$	50 Hz	Nominal frequency
$V_n$	260 V	Nominal AC voltage (RMS L-L)
$V_{dc}$	500 V	Nominal DC voltage
$K_{p,v}$	2	Voltage loop proportional gain for GFR
$K_{i,v}$	20	Voltage loop integral gain for GFR
$K_{p,i}$	0.3	Current loop proportional gain
$K_{i,i}$	10	Current loop integral gain
$L_{filter}$	43 $\mu$ H	Filter inductance
$C_{filter}$	1.88 mF	Filter capacitance

## B.2 Parameters for Synchronous Generator

The parameters used for the SG model for the simulations in Chapter 6 are presented in Table B.2.

Table B.2: Parameters for SG unit

Parameter	Values	Comments
$S_n$	500 kVA	Nominal power
$f_n$	50 Hz	Nominal frequency
$V_n$	400 V	Nominal AC voltage (RMS L-L)
$R_S$	0.029 pu	Stator resistance
$X_l$	0.06 pu	Stator leakage inductance
$X_d$	2.2 pu	d-axis synchronous reactance
$X'_d$	0.17 pu	d-axis transient reactance
$X''_d$	0.12 pu	d-axis subtransient reactance
$X_q$	1.01 pu	q-axis synchronous reactance
$X'_q$	0.15 pu	q-axis subtransient reactance
$T'_d$	0.03 s	d-axis transient open-circuit time constant
$T''_d$	0.008 s	d-axis subtransient open-circuit time constant
$T''_q$	0.008 s	q-axis subtransient open-circuit time constant
$H$	2 s	Inertia coefficient
$F$	0.02032 pu	Friction factor
$p$	2	Pole pairs
$V_{to}$	1 pu	Initial value of terminal voltage
$V_{f0}$	1.07075 pu	Initial value of field voltage
$K_e$	1	Exciter gain
$T_e$	0.01	Exciter time constant
$P_{set}$	0.2215 pu	Initial value of reference power
$D$	0.05	Droop coefficient

### B.3 Parameters for Transformers

The parameters used for the transformers model for the simulations in Chapter 6 are presented in Table B.3.

Table B.3: Parameters for transformers

Parameter	Values	Comments
$S_n$	1 MVA	Nominal power
$f_n$	50 Hz	Nominal frequency
Configuration	Y-D1	Primary and secondary side's connection type
Core	Three single-phase	Core types
$V_1$	260 V	Primary side nominal AC voltage (RMS L-L)
$V_2$	11 kV	Secondary side nominal AC voltage (RMS L-L)
$R_1$	0.05 pu	Primary side resistance
$X_1$	0.05 pu	Primary side reactance
$R_2$	0.05 pu	Secondary side resistance
$X_2$	0.05 pu	Secondary side reactance
$R_M$	500 pu	Magnetisation resistance
$X_M$	500 pu	Magnetisation reactance